

PDF hosted at the Radboud Repository of the Radboud University Nijmegen

The following full text is a publisher's version.

For additional information about this publication click this link.

<http://hdl.handle.net/2066/100583>

Please be advised that this information was generated on 2017-12-06 and may be subject to change.

Bone Regeneration Using Calcium Phosphate Based Cement

Incorporation of additives
and performance in
osteoporotic conditions

COLOFON

Achterkant: kleur aangepaste SPECT/CT scans van ratten waarin calcium fosfaat cement met toegevoegd radioactief BMP-2 onder de huid geïmplantéerd is.

The research described in this thesis was financially supported by the Smart Mix Program of the Netherlands Ministry of Economic Affairs and the Netherlands Ministry of Education, Culture and Science

Het Anna Fonds | NOREF en de Nederlandse vereniging voor Biomaterialen en Tissue Engineering (NBTE) verschaften financiële ondersteuning voor het verschijnen van dit proefschrift.

Ontwerp: Floor CJ van de Watering

Druk: Ipskamp Drukkers, Enschede, Nederland

ISBN: 978-90-9026984-9

© Floor CJ van de Watering

Bone regeneration using calcium phosphate based cement

Incorporation of additives
and performance in
osteoporotic conditions

PROEFSCHRIFT

Ter verkrijging van de graad van doctor aan de Radboud Universiteit Nijmegen op gezag van de Rector Magnificus, prof. mr. SCJJ Kortmann, volgens besluit van het college van decanen in het openbaar te verdedigen op vrijdag 26 oktober 2012 om 13:00 uur precies door

Floor Cornelia Johanna van de Watering

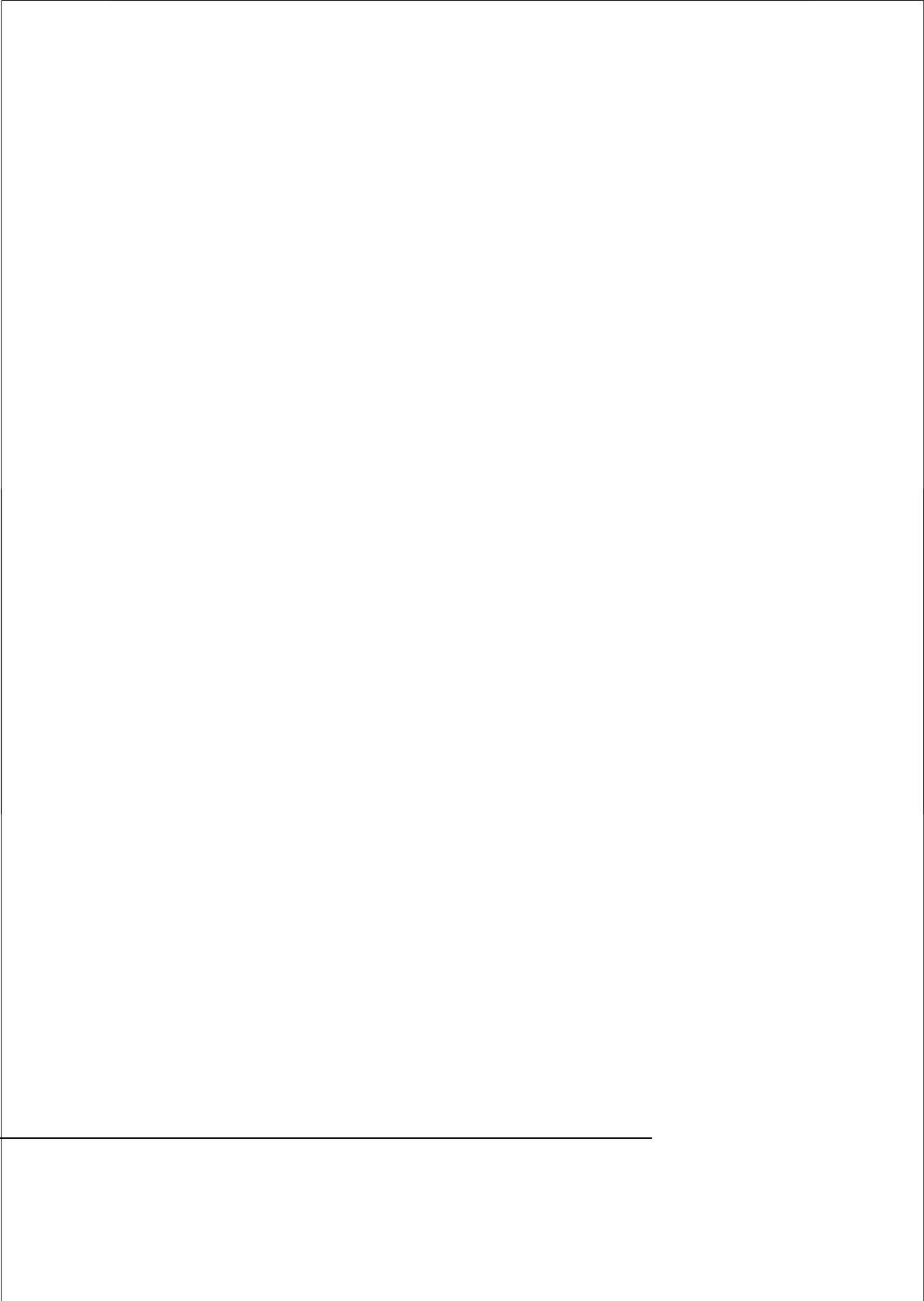
Geboren op 13 oktober 1983 te Bergen op Zoom

Promotor:
Prof. dr. JA Jansen

Copromotor:
Dr. JJJP van den Beucken

Manuscriptcommissie:
Prof. dr. GJ Meijer (Voorzitter)
Dr. TH van Kuppevelt
Prof. dr. H Weinans (Erasmus MC, Rotterdam)

Paranimfen:
Matilde Bongio
Rosa P Felix-Lanao



Voor mijn ouders

'Die mij de kans gaven door te blijven leren'

CONTENTS

CHAPTER 1	10
Introduction and objectives of this thesis	
CHAPTER 2	34
Calcium phosphate/PLGA composite bone substitute materials: evaluation of temporal degradation and bone ingrowth in a rat critical-sized cranial defect	
CHAPTER 3	56
Incorporation of bioactive glass in calcium phosphate cement Part II: Biological evaluation	
CHAPTER 4	80
Non-glycosylated BMP-2 can induce ectopic bone formation at lower concentrations compared to glycosylated BMP-2	
CHAPTER 5	102
Differential loading methods for BMP-2 within injectable calcium phosphate cement	
CHAPTER 6	124
The biological performance of injectable calcium phosphate PLGA cement in osteoporotic rats	
CHAPTER 7	146
Summary, address to the aims, closing remarks and future perspectives	
CHAPTER 8	156
Samenvatting, evaluatie van de doelstellingen, afsluitende opmerkingen en toekomstperspectieven	
CHAPTER 9	166
Acknowledgments (Dankwoord), Curriculum Vitae and List of publications	



CHAPTER **1**

Introduction and the objectives of this thesis

FCJ van de Watering, JJJP van den Beucken, RP Felix Lanao,
JGC Wolke, JA Jansen

Adapted from:

Book Chapter: Biodegradation of calcium phosphate cement composites In: N. Eliaz (Ed), Degradation of Implant Materials, 2012, DOI:10.1007/978-1-4614-3942-4_7

Introduction

Annually, more than 1 million patients are treated worldwide for skeletal complications in the fields of orthopedic surgery, plastic and reconstructive surgery, dental implantology, maxillofacial surgery and neurosurgery. These bone defects can be caused by congenital skeletal abnormalities, trauma, oncologic surgery and failures of physiologic osteosynthesis.

A good bone graft has four main characteristics: it is (1) bioactive, which leads to the ability to bond to bone tissue without the intervention of fibrous tissue, (2) osteoconductive, thus able to guide bone tissue growth along the surface and into pores, (3) osteoinductive, i.e. capable of inducing differentiation of pluripotent stem cells into bone-forming osteoprogenitor cells, and (4) it stimulates osteogenesis, i.e. formation of bone by osteoblastic cells within the graft.

The use of autologous bone grafts is the gold standard in treating bone defects. Different donor sites are available depending on the application. For example, free vascularized bone flaps can be harvested from the radial forearm, fibula, iliac crest and scapula, and for non-vascularized bone autografts donor bone can be obtained from the iliac crest, rib, distal radius and olecranon [1]. Despite the advantageous clinical efficacy of autologous bone, transplantation with autologous bone grafts has also several drawbacks: low availability of transplantable tissue, donor site morbidity, and rapid depletion of the osteogenic capacity of the graft [2, 3].

Besides autologous bone graft, other treatment modalities can be used, such as allografts (i.e. human cadaveric bone obtained via the bone bank). Allografts are associated with many complications, including risk of viral transmission, bacterial infections, malignancy, toxins and systemic disorders like rheumatoid arthritis and autoimmune diseases. and are therefore not frequently used [4, 5].

An alternative for autologous grafts and allografts are the synthetic biomaterials. Synthetic biomaterials can be used as a scaffold or carrier material in the field of tissue engineering. The aim of bone tissue engineering research is to develop a functional bone substitute to regenerate damaged or lost bone tissue. The general approach in tissue engineering is to develop a material composed of one or a combination of (1) a scaffold and/or carrier, (2) biological compounds (growth factors and/or bioactive molecules), and (3) cells.

In the last decade, different materials have been described, including bioactive glass, polymers and calcium phosphate (CaP) based ceramics or cements [6]. The silica-based bioactive glasses (BGs) are a group of synthetic biomaterials with the unique ability to bond to living bone by forming a biologically active bone-like apatite layer on their surface [7-10] that acts as a template for calcium phosphate precipitation and directs new bone formation [7, 10, 11]. Additionally, it has been reported that BG has stimulatory effects on the osteogenesis and neovascularisation by attracting osteoprogenitor cells and by stimulating the differentiation into matrix-producing osteoblasts [7-11] and by stimulating the secretion of angiogenic factors [12, 13], respectively. CaP-based materials are of major interest in the bone regenerative therapies because they show a similar

biological composition as natural bone mineral. In addition, they are non-toxic, biocompatible, and allow direct bone bonding without intervening soft tissue layers. CaP-based materials can be prepared in the form of granules, blocks or cements.

CaP ceramics can be classified according to the crystal phase, e.g. hydroxyapatite (HA), β -tricalcium phosphate (β -TCP), biphasic calcium phosphate (BCP), amorphous calcium phosphate (ACP), carbonated apatite (CA), and calcium deficient hydroxyapatite (CDHA). A list of abbreviations of CaP-crystals with chemical formula and Ca/P-ratio is given in Table 1 [14].

CaP ceramics have a compressive strength (300 to 900 MPa) and tensile strength (40 to 300 MPa) similar or higher than those of cortical bone. However, due to the lack of elasticity the material is very brittle and therefore not suitable for load-bearing applications. Other disadvantages of CaP ceramics are their low degradation rate [14] and relatively poor handling properties. CaP ceramics are available in a fixed form and, therefore, the material is difficult to shape into the dimensions of the bone defect. These negative properties of CaP ceramics might be improved by using CaP cements (CPC).

Calcium phosphate cements

CPC consist of a powder phase of calcium and phosphate salts, which after mixing with an aqueous solution will form an injectable paste at body temperature. The advantage of using CPC as a bone substitute material is that it has a similar chemical composition, the same calcium and phosphate ions ratio as the mineral phase of bone. In addition, the cement paste can be directly injected in bone defects, which leads to less invasive and a faster surgery (Figure 1) as compared to ceramic bone substitutes that have to be shaped to the defect dimensions during operations, which is more labor intensive [15-17]. For clinical application, a certain initial and final setting time of the CPC is required.



Figure 1 CPC injection in a femoral condyle defect in a rabbit. (A) femoral condyle defect, (B) injection of the CPC, (C) CPC after *in situ* setting.

The clinical meaning of the final setting time relates to the time necessary to set the cement sufficiently so it can be touched without damaging it. For clinical application, it means that after mixing, the cement must be applied before the

initial setting time, and that the wound needs to be closed after the final setting time.

Self-setting CPC was first described by Brown and Chow (1986) and consisted of only CaP compounds (i.e. tetracalcium phosphate monoxide (TTCP) and dicalcium phosphate dehydrate (DCPD)). Their study aimed at the development of slurries for remineralizing carious lesions. Studies on the reaction of TTCP + DCPD to hydroxyapatite (HA) resulted in the finding that some of the aqueous pastes harden in time. This inadvertent discovery resulted in a new type of self-hardening cements consisting only of CaP [15].

In general, it has been demonstrated that different CPC compositions are non-toxic, biocompatible and osteoconductive [15-17] in different animal models, for example in dogs [18, 19], goats [20, 21], and rabbits [22]. Multiple studies have reported that a temporal increase of newly formed bone can be seen in different CPC [16, 21, 23] indicating that CPC are promising candidates for bone regeneration. Several CPC formulations have been approved by the Federal Drug Administration for clinical use. Examples of these commercially available CPC are BoneSource™, Cementek® and Calcibon®. In Table 2, a list of commercially available CPC is given [14].

CPC biodegradability

The replacement of a biomaterial by living bone is preferred because this avoids potential complications later on, such as inflammation, stiffness, pain and bacterial seeding. To obtain replacement of bone, new bone formation and resorption of the material, e.g. biodegradation of the material, is required. The rate of material degradation and newly formed bone should optimally be in perfect balance to maintain mechanical stability (integrity of the ceramic scaffold) and allow a gradual takeover of mechanical strength by newly-formed bone tissue.

Biodegradation of CaP-based material can occur via two processes, namely (1) extracellular liquid dissolution, and (2) disintegration into small particles that can be intracellularly digested or transported to other adjacent tissues. The first process depends on the solubility product of the formed CaP biomaterial, while the second process is mainly dependent on the solubility product of the connecting agents of the powder particles after crystallization [24].

The biodegradation of the material is dependent on different factors, including the final product of the cement setting. For example, apatite is a more stable compound, and therefore the degradation rate is slower as compared to brushite [25]. Due to the slower degradation rate, the material has a relatively good mechanical stability, albeit insufficient for load-bearing applications. On the other hand, a less stable compound like brushite leads to a faster biodegradation. In addition, the CaP chemical composition itself can influence the material degradation. This is exemplified by an approach in which calcium sulphate (CS) was added to CPC, composed of TTCP and DCPA. Although biocompatible, CS is less suitable for bone substitution because of its rapid resorption.

Table 1 Abbreviations of CaP-compounds with corresponding chemical formula and Ca/P-ratio

Abbreviation	Name	Formula	Ca/P-ratio
ACP	Amorphous calcium phosphate	-	$1.25 < x < 1.55$
BCP	Biphasic calcium phosphate	$\text{Ca}_3(\text{PO}_4)_2 + \text{Ca}_{10}(\text{PO}_4)_6(\text{OH})_2$	$1.50 < x < 1.67$
CA	Carbonated apatite, dahlite	$\text{Ca}_5(\text{PO}_5, \text{CO}_3)_3$	1.67
CDHA	Calcium deficient hydroxyapatite	$\text{Ca}_{10-x}(\text{HPO}_4)_x(\text{PO}_4)_{6-x}(\text{OH})_{2-x}$	$1.50 < x < 1.67$
DCPA	Dicalcium phosphate anhydrous, Monetite	CaHPO_4	1.00
DCPD	Dicalcium phosphate dihydrate, Brushite	$\text{CaHPO}_4 \cdot 2\text{H}_2\text{O}$	1.00
HA	Hydroxyapatite	$\text{Ca}_{10}(\text{PO}_4)_6(\text{OH})_2$	1.67
MCPM	Monocalcium phosphate monohydrate	$\text{Ca}(\text{H}_2\text{PO}_4)_2 \cdot \text{H}_2\text{O}$	0.50
OCP	Octacalcium phosphate	$\text{Ca}_8\text{H}_2(\text{PO}_4)_6 \cdot 5\text{H}_2\text{O}$	1.33
pHA	Precipitated hydroxyapatite	$\text{Ca}_{10-x}(\text{HPO}_4)_x(\text{PO}_4)_{6-x}(\text{OH})_{2-x}$	$1.50 < x < 1.67$
α -TCP	α -Tricalcium phosphate	$\alpha\text{-Ca}_3(\text{PO}_4)_2$	1.50
β -TCP	β -Tricalcium phosphate	$\beta\text{-Ca}_3(\text{PO}_4)_2$	1.50
TTCP	Tetracalcium phosphate	$\text{CaO} \cdot \text{Ca}_3(\text{PO}_4)_2$	2.00

Interestingly, a mixture of CS, TTCP and DCPA leads to a good biocompatibility and enhanced degradability and bone ingrowth as compared to CPC consisting of only TTCP and DCPA [26]. In addition, the chemical composition of the CPCs plays also a role in the active resorption of the cement. For example, it has been reported that a cement produced by a mixture of sodium calcium phosphate, $\text{Na}_3\text{Ca}_6(\text{PO}_4)_5$, tetracalcium phosphate and β -tricalcium phosphate powder and malic acid or citric acid have a different relationship regarding the number of osteoclasts on the cement [27]. Since osteoclastic activity can be a marker for the evaluation of bioresorbability, it was suggested that cement mixed with malic acid is more promising for bone substitution in an active manner than cement mixed with citric acid. Also, the patient plays an important role in material degradation. Depending on the patient's age, sex, and general metabolic health condition, the speed of degradation can be different.

Table 2 Details of currently available commercially available calcium phosphate cements

Cement	Constituents	End product	Setting time	Compression strength (MPa)	Porosity
Biobon (α-BSM)[®]	ACP, DCPD	Poorly crystalline, HA, Ca/P=1.45	15-20 min (37°C)	12	50-60% Micro
Biopex[®]	75% α-TCP, 18% TTCP, 5% DCPD, 2% HA	HA	8 min	80	Micro
Bone sourceTM	TTCP, DCPD	HA, Ca/P=1.67	10-15 min (37°C)	36	Micro
Calcibon[®]	61% α-TCP, 26% DCPA, 10% CaCO ₃ , 3% pHA	Calcium deficient CA, Ca/P=1.53	2-4 min (37°C)	60-70	44% Micro
Cementek[®]	α-TCP, TTCP, Ca(OH) ₂	HA, Ca/P=1.64	40 min	20	50% Micro
ChronOS inject[®]	44% β-TCP, 21% MCPM, 31% β-TCP granules, 5% MgHPO ₄ *3H ₂ O	Brushite (DCPD)	12 min	3	Micro
MimixTM	α-TCP, TTCP, Citric acid	HA	(37°C)	22	Micro
Norian-SRS[®]	MCPM, α-TCP, CaCO ₃	Dahlite (CA), Ca/P=1.67	12 h	28-55	Very low

In addition, the implantation site influences scaffold biodegradation and bone formation in the vicinity of the scaffold. For example, ceramic material placed in a femoral or cranial defect will be exposed to different environments, including differences in biomechanical loading, surrounding tissue and blood/nutrient supply. Besides the environment, the origin of the bone tissue (long bone formation (femur) is endochondral, while cranial bone formation is intramembranous) may play a role in degradation and bone formation due to distinctive signaling properties [28]. Other factors involved in the biodegradability are porosity of the material, crystallinity (crystal size, crystal perfection and grain size), particle size of the CaP powder, and liquid/powder ratio [24, 29, 30]. These factors influence each

other, and are influenced by the chemical composition of the material. For example, CaP compounds that transform into relatively highly crystalline hydroxyapatite after hydration will be essentially non-resorbable *in vivo* [24].

CPC porosity

CPC contains an intrinsic high nano/sub-micron-sized porosity. Several parameters, including particle size of the powder phase [29] and liquid/powder ratio [30] can affect the creation of this type of porosity and, hence, material degradation, and consequently allow bone ingrowth. Nanoporosity is an important parameter to be controlled in CPC materials because it enables fluid flow within the material and can affect protein adsorption. In contrast to nano/sub-micron-sized porosity, macroporosity enables tissue ingrowth and is the key factor for CPC degradation and its substitution by new bone tissue.

Macroporosity

Macropores have been built into biomedical materials since the early 1970s [31, 32]. Resorbability of a material is an important clinical property; it is preferred that the CPC will degrade in a short period of time parallel to new bone tissue formation. Pores of a suitable diameter and an adequate interconnectivity are essential for bone tissue ingrowth and for enhancing CPC degradation. Debates about the adequate pore size for bone replacement materials are still ongoing. Researchers have suggested that a pore size larger than 100 μm is sufficient for tissue ingrowth [33, 34], whereas other investigations conclude that larger pores (up to 500 μm) have to be preferred [35]. Although highly porous materials will lead to a faster degradation, an adequate balance between degradation and structural integrity should be found. Figure 2 gives an overview of typical porous 3D structures.

Interconnectivity

Besides bone ingrowth in the cement pores, interconnectivity is a key factor for new tissue formation within the cement. When the pores form an interconnected network, cellular and vascular penetration will be favored, ensuring new tissue formation in all void areas of the implanted material. Furthermore, variations in interconnectivity will lead to modifications in the architecture and mechanical properties of the CPC. A suitable balance between pore size, pore volume, interconnectivity and structural integrity is a major issue in the development of CPC-based bone substitution materials.

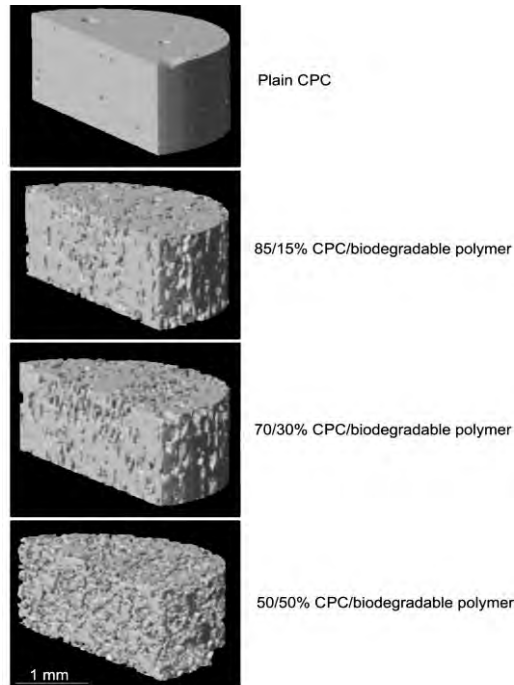


Figure 2 μ CT images of composite discs with different CPC/biodegradable polymer ratio after burning out the polymer component. A higher amount of biodegradable polymer leads to an increase in porosity of the scaffold material. Bar represents 1 mm.

Enhancement of macroporosity

In general, the degradation rate of plain CPC is limited (Figure 3). For a better bone regeneration, different methods have been used to induce macroporosity in CPCs, such as inclusion of water-soluble additives, foam-forming agents, fabrication of scaffolds by additive manufacturing technologies and biodegradable polymeric microspheres.

Water-soluble additives

The inclusion of water-soluble additives in CPCs is a common approach to induce macroporosity. Also known as the particle leaching technique, it is often used to create porosity in other bone substitute materials such as pre-set ceramics or polymeric scaffolds. Saccharides such as sucrose, pectin, chitosan or mannitol as well as the salts sodium chloride and sodium phosphate are water-soluble compounds to generate macroporosity in CPCs. For example, sucrose is a disaccharide derived from glucose and fructose. Sucrose crystals of specific sizes have been included in CPC, and macroporosity is generated after dissolution of the crystals during incubation of the samples in aqueous media [36]. In addition, A

more novel technique is the creation of microspheres from a saccharide. Pectin is a water-soluble polysaccharide that, in the form of microspheres, has been recently introduced in CPC to create round pores after degradation [37].

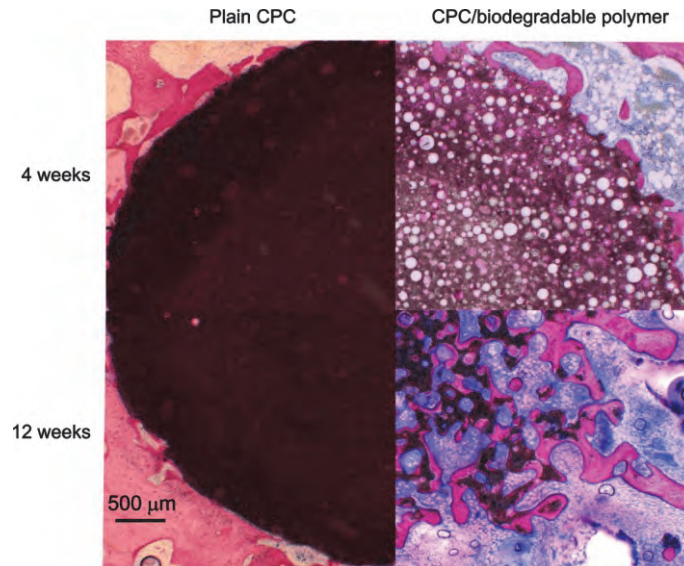


Figure 3 Histological sections of a femoral condyle of a rat injected with plain CPC or CPC with biodegradable polymer, after 4 and 12 weeks of implantation time. In the plain CPC implant, degradation and bone ingrowth is limited and restricted to the edges of the defect. In contrast, CPC with biodegradable polymer shows an increase in implant degradation and bone ingrowth from 4 weeks implantation onwards. Methylene blue and basic fuchsin staining. Bar represents 500 μm .

Foam-forming agents

A different approach to enhance porosity in CPC is to combine it with an agent that, by foaming, will generate gas bubbles that will lead to the generation of pores. Hydrogen peroxide bubbling [38], or the creation of CO₂ bubbles from sodium bicarbonate during the cement setting [39, 40], are examples of foam-forming methods to generate porosity.

Acetic and citric acids have been investigated as porogens by the gas-foaming technique. The final cement presents good injectable properties and higher porosity when combined with citric acid [41]. Furthermore, citric acid has also been used in combination with sodium bicarbonate as effervescent agents to generate porosity [42].

A similar technique is to mix the cement paste with a foam obtained previously from a foaming agent. A foam from the natural protein albumin has been used in this approach, generating macroporous scaffolds with promising *in vivo* results [43-45]. Following this procedure, no potentially toxic gas is liberated after

implantation of the cement, since the foam is generated before mixing it with the cement paste.

Additive manufacturing techniques

Rapid prototyping is an advanced manufacturing technique that allows the automatic construction of physical objects using additive manufacturing technology. Using this concept, CPC scaffolds with highly controlled internal pore architectures have been obtained [46, 47]. Stereolithography is another additive manufacturing process which has been applied for CaP scaffold fabrication with a controlled internal channel architecture [48]. However, a major drawback of these techniques is that the scaffolds have to be fabricated prior to implantation in the body, meaning that this approach is not suitable for injectable and/or minimally invasive procedures.

Surfactants

Sodium dodecyl sulphate (SDS) [49] has been applied within CPC because of its air-trapping properties. Similar to other surfactants, SDS presents a low surface tension. Air bubbles are incorporated during the mixing of the powder and the liquid component of the cement. These bubbles become covered by a sheath of SDS molecules, creating macroporosity after the CPC solidification. Alternatively, cetyltrimethyl ammonium is a surfactant that has been applied as CPC porosity inducer [50].

Biodegradable polymers

Approximately 30% of bone is composed of organic compounds, of which 90 to 95% is collagen. Consequently, natural polymers are being widely studied in relation to bone tissue engineering. Collagen presents a slow degradation rate, which makes it unsuitable as porosity inducer for CPCs. In contrast, gelatin is a natural enzymatically degradable polymer derived from collagen with a faster degradation rate. For these reasons, gelatin has been used in the form of microspheres to generate macroporosity in CPCs after its degradation [51-53].

Besides natural polymers, there is a wide range of synthetic polymers that can be used to induce macroporosity in CPCs. The synthetic polymers poly(epsilon-caprolactone) and poly(L-lactic acid) have been used as fibers to enhance resistance of CaP materials in a first stage and porosity after polymer degradation [54].

Poly(DL-lactic-co glycolic acid) (PLGA) is employed for the production of microspheres to be embedded in CPC material and generate porosity after polymer hydrolytic degradation [55-57]. In addition, the enzymatically degradable poly(trimethylene carbonate) (PTMC) has been processed also in the form of microspheres and introduced in CPCs, generating interconnected macroporosity and minimal inflammatory response [58, 59].

In Figure 4, an overview of gelatin, PTMC and PLGA inclusion and degradation in CPC is shown.

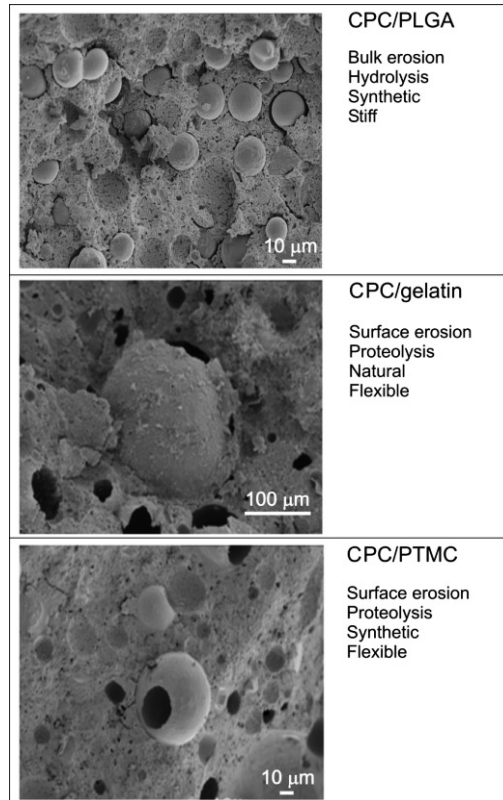


Figure 4 CPC/PLGA, CPC/gelatin and CPC/PTMC samples. The different characteristics of the polymers lead to differences in material degradation of the CPC.

Combinations

Finally, it has to be mentioned that, in several studies, more combinations of the previously mentioned methods have been investigated to generate porosity in CPCs. For example, CO₂ foaming has been used to induce porosity in combination with PLGA-microparticles embedded in CPC for the creation of secondary porosity at a later time point [60]. Furthermore, mannitol crystals have been used to generate early macroporosity in combination with slower resorbable chitosan fibers that will improve the mechanical properties of the cement at initial time points, but subsequently will degrade, enhancing the already generated macroporosity after mannitol dissolution [61, 62].

CPC as a (drug) delivery system

Besides the role as a bone substitute, CPC can be used as a carrier for local and controlled drug release. This makes the material very attractive because it enables (i) directed bone healing, and (ii) treatment of the potential disease underlying the bone defect. Examples of skeletal diseases to treat are bone tumors, osteoporosis or osteomyelitis [63].

Several aspects need to be considered regarding the incorporation of drugs to CPC. First of all, it needs to be verified that the setting reaction and hardening mechanisms and physico-chemical properties do not alter after the addition of drugs. Secondly, the drug release kinetics *in vitro* needs to be characterized, e.g. by *in vitro* release experiments with radioiodinated drugs of interest [64]. Subsequently, a release profile is obtained by measuring in time the remaining activity in a gamma counter. This needs to be followed by an assessment of the *in vivo* efficacy of the drug delivery carrier [64], after which the clinical use must be evaluated [63]. The efficacy needs to be analyzed because the activity of the drugs and/or bioactive molecule might be lost due to the chemical reactions during cement setting, and therefore the drug and/or bioactive molecule will have no clinical effect [65, 66]. The incorporation of the drugs or other bioactive molecules can be in the liquid phase [67] and/or powder phase [68] of the CPC.

Loading growth factors and/or bioactive molecules

As mentioned before, CPC degradation is slow and can be increased by the incorporation of macroporosity to CPC via polymer microparticle addition [39, 51, 57, 69, 70]. If the porosity of the material increases in time, then the release profile of the drugs will not only be dependent on the diffusion through the material. Increasing the porosity is therefore not only beneficial for the material degradation, but also for the release profile of incorporated drugs.

Another advantage of the inclusion of polymers is that these polymers can serve as a carrier system to obtain a more sustained release of drugs and/or bioactive molecules. For example, It is shown that a sustained release of recombinant human bone morphogenetic protein-2 (rhBMP-2) from PLGA-microparticles resulted in more and faster bone formation in rabbit calvarial defects as compared to immediate release of rhBMP-2 [71]. In addition, other CPC carrier systems based on different polymeric microparticles such as gelatin [72] or the natural occurring pectin have demonstrated to be beneficial for the retention of drugs [37].

The drugs and/or bioactive molecules can be either absorbed on the surface of the microparticle after microparticle fabrication, or entrapped in the microparticles during the microparticle fabrication. Different types of molecules can be loaded or entrapped in the microparticles, including antibiotics, anti-inflammatory drugs [73, 74], and growth factors [75-78]. In addition, these delivery systems can be used to deliver non-proteinaceous compounds (e.g. genes [79, 80]), and even cells [81].

Growth factor delivery

Bone healing is a complex physiological process that is initiated and controlled by growth factors, such as members of the transforming growth factor (TGF) superfamily, which includes TGF- β that plays a significant role in the repair of skin and bone [75], as well as Bone Morphogenetic Proteins (e.g. BMP-2), which play an important regulatory role in many steps of bone morphogenesis [76]. BMPs seem to play an important role in increasing the material degradation and bone forming capacity of CPC. For example, it has been reported that addition of BMP-2 to the PLGA-microparticles in CPC composites placed in a rat critical sized cranial defect model significantly increases the degradation and the bone forming capacity of the material as compared with plain CaP/PLGA cement composites, from 4-weeks implantation period onwards (Figure 5) [77]. Another study reported that injectable rhBMP-2/CPC stimulated bone formation and blood vessel ingrowth after two months in vertebroplasty, as compared to rhBMP-2 /polymethylmethacrylate (PMMA) bone substitute [82]. In addition, an effect of rhBMP-2 has been observed in an equine model, where surgically osteotomies and ostectomies of the accessory metatarsal bones were induced. The rhBMP-2/CPC increased early bone formation as compared to non-treated bone defects [83].

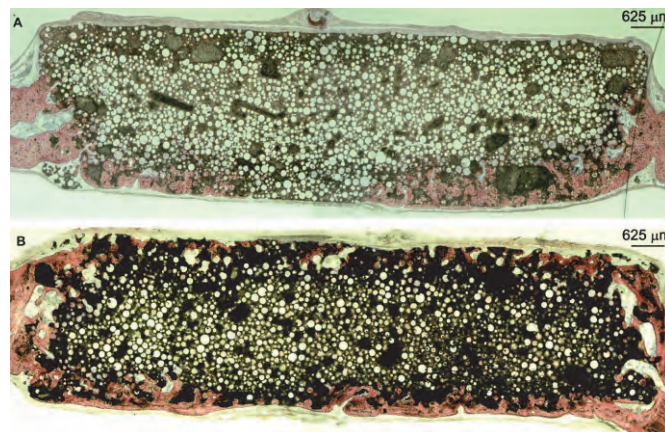


Figure 5 Histological sections of cranial defects, consisting of either (1) plain CPC, or (2) CPC loaded with BMP-2, after 12 weeks. CPC/PLGA shows limited ingrowth of bone after 12 weeks of implantation. In the CPC/PLGA loaded with BMP-2, more bone formation is observed. Methylene blue and basic fuchsin staining. Bar represents 625 μm .

Another example of a growth factor used to induce material degradation and bone formation is TGF- β . It has been demonstrated that addition of TGF- β to CPCs within the liquid component is released in a bioactive form and still capable of stimulating the differentiation of preosteoblastic cells *in vitro* [84] and results *in vivo* in an increased bone formation when implanted in 5-mm rat cranial defects [78]. However, depending on the loading of the TGF- β and the chemical

composition, different results may be obtained. For example, addition of TGF- β to gelatin microparticles in CPC composites significantly accelerated implant degradation, and only a tendency toward increased bone ingrowth 12 weeks postoperatively as compared to plain CaP/gelatin cement composites was observed [85].

Bone is a highly vascularized tissue, and therefore the formation of new blood vessels, angiogenesis, is essential for bone regeneration [86]. Thus, besides an important role for BMPs, angiogenesis stimulating factors seem to play an essential role in bone formation.

Vascular endothelial growth factor (VEGF) is a potent angiogenic growth factor, which is known to stimulate blood formation from several studies [87, 88]. The half-life time of VEGF is less than 1 hour following *in vivo* injection [89], and therefore a carrier system is required to have a controlled release of the growth factor. The method of delivery seems to influence the efficacy of VEGF. For example, when VEGF is directly injected *in vivo*, poorly perfused fragile capillaries without connection to the pre-existing circulation as well as agiomas are observed [90]. In contrast, sustained release of VEGF results in the formation of regularly organized vasculature [91]. The CPC/polymer microsphere carrier system is a promising candidate for sustained release VEGF, and has shown to promote vascularization within these bone substitute materials [92]. In addition, local sustained VEGF release from carrier biomaterials improved the healing of non-critical sized bone defects [93]; however, this is contradictory with another study which reported no difference in bone formation when VEGF was released locally from a carrier system [94]. The different VEGF release kinetics may be a result of differences in carrier system, VEGF concentration and animal model used. To mimic bone healing in a more natural fashion, a combination of different growth factors, such as angiogenic and osteogenic growth factors, may be beneficial. It is reported that dual delivery of VEGF and BMP-2 loaded on different scaffold materials can increase both capillary density and bone formation ectopically [95], whereas it leads to more bone formation orthotopically as compared to single delivery of BMP-2 [94]. The dual delivery of BMP-2 and fibroblast growth factor (FGF) by a CPC carrier has also been reported to more substantially induce new bone formation [96, 97].

Other products and/or molecules

Either from a biological point of view as well as considering cost effectiveness, research is focusing on the reduction of included growth factors or replacement of the growth factors by less expensive, alternative molecules. Previous studies on alternative molecules with angiogenic and osteogenic activity revealed some agents, which effectively increased bone formation, such as statins [98], isoflavone derivatives [99], copper ions [100], TAK-778 [101] and Icaritin [102]. Instead of delivering bioactive molecules, it is possible to deliver cells via CaP scaffolds [103]. In particular, the delivery of stem cells is promising because stem cells are

undifferentiated cells with the capacity to differentiate into one or more cell types, and have the ability of self-renewal [104]. In addition, the delivery of genetic material (e.g. DNA, RNA) can induce bone formation [79]. It has been reported that adenoviral vectors can be incorporated in synthetic CPC to provide locally effective and sustained release of genetic material [105]. The delivery of a plasmid encoding vascular endothelial growth factor(165) (pVEGF165) via collagen/CaP carrier resulted *in vivo* in an increase in bone volume [80]. Besides the delivery of plasmids encoding growth factors, the delivery of numerous signaling molecules involved in bone development and regeneration, such as the transcription factors Runt-related transcription factor 2 (Runx2) and Osterix, show promise for the regeneration of bone *in vivo* [106].

Performance of CPC in compromised conditions

As mentioned before, CPCs represent reliable candidates for the substitution of bone due to their similar chemical composition compared to the mineral phase of bone and their biocompatibility and osteoconductive properties. Several different formulations of CPC including biodegradable polymeric microparticles have been studied and demonstrated to be non-toxic, biocompatible and osteoconductive [15, 16, 107] in different animal models for example in rabbits [22], dogs [18, 19], and goats [21, 108]. However, the outcome of those studies is based on performance of CPCs in healthy individuals and therefore does not provide information on CPC performance in a compromised situation, such as in osteoporotic patients.

In osteoporotic conditions, the balance between bone formation (i.e. osteoblasts) and bone resorption (i.e. osteoclasts) is disturbed. This disturbance leads to a decrease in bone mass (i.e. osteopenia) and a decline in bone micro-architecture, which leads to an enhanced fragility of the skeleton and hence an increased risk of fractures [109]. The occurrence of osteoporosis is strongly related to hormonal changes since the lack of estrogen induce the increase of osteoclastogenesis and osteoclastic activity [110]. It is assumed that in the world population over 50 years of age, 1 in 3 women and 1 in 5 men will experience an osteoporotic fracture indicating the requirement for bone substitute materials in osteoporotic patients.

To study osteoporosis, different animal models have been used such as rodents, dogs, sheep and goats [111]. Osteoporosis can be introduced either via chemical stimulation, for example by the administration of prednisolone to rabbits [112] or via an ovariectomy in female animals or an orchidectomy in male animals [109, 111]. The removal of the ovaries or testis induces a decline in estrogen and androgen levels, respectively, which leads to reduced BMD and BMC. The most well-established osteoporosis animal model is the ovariectomized (OVX) rat. Following OVX, a rapid decrease in bone mass and strength occurs which mimics the bone changes following oophorectomy or menopause in humans [109]. In Figure 6 the bone architecture of healthy and OVX rats is depicted.

In view of the differences in bone morphology and metabolism between osteoporotic patients and healthy humans, the biological performance of CPC in osteoporotic patients may also be different. For example, it has been reported that calcium sulphate-based bone substitute materials are resorbed faster and possess an altered performance in a spine model in osteoporotic rats compared to healthy control animals. In addition, it has been reported that under osteoporotic conditions the cement-mediated bone augmentation is altered compared to healthy controls [113]. However, up to date no information on the performance of CPC (either supplemented with additives) is available.

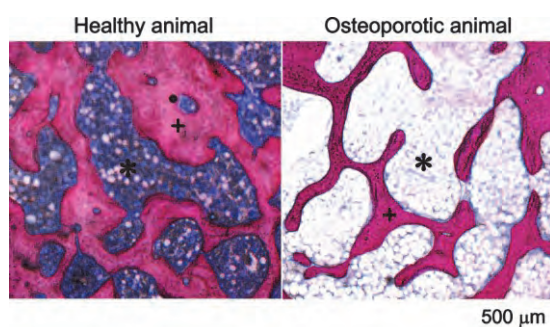


Figure 6 Histological sections of femoral condyle of healthy and osteoporotic rats. Bone (+) and trabecular spacing (*) are indicated. Bar represents 500 µm.

Objectives of this thesis

The general objective of the current thesis was to evaluate the potential improvement of different additives regarding the biological performance of CPC. To that end, the influence of porogen addition (i.e. PLGA-microparticles) on the biological performance of CPC was evaluated firstly, after which the effect on CPC performance of various incorporated biologically active additives (i.e. BG and BMP-2) was explored. Furthermore, the differences between the biological performance of CPC in healthy and osteoporotic conditions was evaluated.

The following research questions were addressed:

1. To what extent can addition of PLGA-microparticles improve the biological performance of CPC/PLGA (Chapter 2)?
2. Can the biological performance of CPC be improved by the addition of bioactive glass (Chapter 3)?
3. Does the solubility of BMP-2 influence the bioactivity, release profile of and osteoinductive properties of CPC scaffold material (Chapter 4)?
4. Does the BMP-2 loading method to CPC influence the release kinetics and osteoinductive potential of CPC (Chapter 5)?
5. What are the differences in biological performance of CPC between osteoporotic and healthy rats (Chapter 6)?

References

- [1] E.H.M. Hartman, P.H.M. Spauwen, J.A. Jansen, Donor-Site Complications in Vascularized Bone Flap Surgery, *J. Invest. Surg.* 15 (2002) 185-197.
- [2] E.W. Bodde, E. de Visser, J.E.J. Duysens, E.H. Hartman, Donor-Site Morbidity after Free Vascularized Autogenous Fibular Transfer: Subjective and Quantitative Analyses, *Plast. Reconstr. Surg.* 111 (2003) 2237-2242.
- [3] H.C. Pape, A. Evans, P. Kobbe, Autologous Bone Graft: Properties and Techniques, *J. Orthop. Trauma* 24 Suppl 1 (2010) S36-40.
- [4] S.M. Graham, A. Leonidou, N. Aslam-Pervez, A. Hamza, P. Panteliadis, M. Heliotis, A. Mantalaris, E. Tsiridis, Biological therapy of bone defects: the immunology of bone allo-transplantation, *Expert Opin Biol Ther.* 10 (2010) 885-901.
- [5] P. Vandevord, S. Nasser, P. Wooley, Immunological responses to bone soluble proteins in recipients of bone allografts, *J. Orthop. Res.* 23 (2005) 1059-1064.
- [6] P. Ruhé, J. Wolke, P. Spauwen, J. Jansen, Calcium phosphate ceramics for bone tissue engineering, in: J. Bronzino (Ed.) *Biomedical Engineering Handbook*, section Tissue Engineering, CRC Press, Connecticut, 2005.
- [7] V.V. Välimäki, H.T. Aro, Molecular basis for the action of bioactive glasses as bone graft. , *Scandinavian Journal of Surgery* 95 (2006) 95–102.
- [8] L.L. Hench, J.M. Polak, Third-generation biomedical materials, *Science* 295 (2002) 1014-1017.
- [9] I.D. Xynos, A.J. Edgar, L.D.K. Buttery, L.L. Hench, J.M. Polak, Ionic Products of Bioactive Glass Dissolution Increase Proliferation of Human Osteoblasts and Induce Insulin-like Growth Factor II mRNA Expression and Protein Synthesis, *Biochem. Biophys. Res. Commun.* 276 (2000) 461-465.
- [10] L.L. Hench, I.D. Xynos, J.M. Polak, Bioactive glasses for in situ tissue regeneration, *J. Biomater. Sci. Polym. Ed.* 15 (2004) 543-562.
- [11] J. Moura, L.N. Teixeira, C. Ravagnani, O. Peitl, E.D. Zanotto, M.M. Beloti, H. Panzeri, A.L. Rosa, P.T. de Oliveira, In vitro osteogenesis on a highly bioactive glass-ceramic (Biosilicate®), *J. Biomed. Mater. Res. A* 82A (2007) 545-557.
- [12] A. Gorustovich, J.A. Roether, A.R. Boccaccini, Effect of Bioactive Glasses on Angiogenesis: A Review of In Vitro and In Vivo Evidences *Tissue Engineering Part B* 16 (2010) 199-207.
- [13] A. Hoppe, N.S. Güldal, A.R. Boccaccini, A review of the biological response to ionic dissolution products from bioactive glasses and glass-ceramics, *Biomaterials* 32 (2011) 2757-2774.
- [14] W.J.E.M. Habraken, J.G.C. Wolke, J.A. Jansen, Ceramic composites as matrices and scaffolds for drug delivery in tissue engineering, *Adv Drug Deliv Rev.* 59 (2007) 234-248.
- [15] L. Chow, Next generation calcium phosphate-based biomaterials, *Dent. Mater. J.* 28 (2009) 1-10.
- [16] A. Ambard, L. Mueninghoff, Calcium Phosphate Cement: Review of Mechanical and Biological Properties, *J. Prosthodont.* 15 (2006) 321-328.
- [17] R. LeGeros, Properties of osteoconductive biomaterials: calcium phosphates., *Clinical Orthopaedics and Related Research* 395 (2002) 81-98.
- [18] H. Yuan, Y. Li, J. de Bruin, K. de Groot, X. Zhang, Tissue responses of calcium phosphate cement: a study in dogs, *Biomaterials* 21 (2000) 1283-1290.
- [19] V. Arisan, T. Ozdemir, A. Anil, J. Jansen, K. Ozer, Injectable calcium phosphate cement as a bone-graft material around peri-implant dehiscence defects: a dog study, *Int. J. Oral Maxillofac. Implants* 23 (2008) 1053-1062.
- [20] E. Ooms, J. Wolke, J. van der Waerden, J. Jansen, Trabecular bone response to injectable calcium phosphate (Ca-P) cement, *J. Biomed. Mater. Res.* 61 (2002) 9-18.
- [21] E.M. Ooms, J.G.C. Wolke, M.T. van de Heuvel, B. Jeschke, J.A. Jansen, Histological evaluation of the bone response to calcium phosphate cement implanted in cortical bone, *Biomaterials* 24 (2003) 989-1000.
- [22] S.C.S.X.B. Cavalcanti, C.L. Pereira, R. Mazzonetto, M. de Moraes, R.W.F. Moreira, Histological and histomorphometric analyses of calcium phosphate cement in rabbit calvaria, *Journal of Cranio-Maxillofacial Surgery* 36 (2008) 354-359.
- [23] M. Youji, I. Kunio, T. Masaaki, T. Taketomo, Y. Yuki, N. Masaru, K. Masayuki, A. Kenzo, Tissue response to fast-setting calcium phosphate cement in bone, *J. Biomat Mater Res* 37 (1997) 457-464.

CHAPTER 1

- [24] J. Lu, M. Descamps, J. Dejou, G. Koubi, P. Hardouin, J. Lemaitre, J. Proust, The biodegradation mechanism of calcium phosphate biomaterials in bone, *J Biomat Mater Res B* 63 (2002) 408-412.
- [25] E. Charrière, S. Terrazzone, C. Pittet, P. Mordasini, M. Dutoit, J. Lemaître, P. Zysset, Mechanical characterization of brushite and hydroxyapatite cements, *Biomaterials* 22 (2001) 2937-2945.
- [26] G. Hu, L. Xiao, H. Fu, D. Bi, H. Ma, P. Tong, Study on injectable and degradable cement of calcium sulphate and calcium phosphate for bone repair, *J Mater Sci Mater Med.* 21 (2010) 627-634.
- [27] Y. Doi, Y. Shimizu, Y. Moriwaki, M. Aga, H. Iwanaga, T. Shibutani, K. Yamamoto, Y. Iwayama, Development of a new calcium phosphate cement that contains sodium calcium phosphate, *Biomaterials* 22 (2001) 847-854.
- [28] U. Chung, H. Kawaguchi, T. Takato, K. Nakamura, Distinct osteogenic mechanisms of bones of distinct origins, *J. Orthop. Sci.* 9 (2004) 410-414.
- [29] M.P. Ginebra, F.C.M. Driessens, J.A. Planell, Effect of the particle size on the micro and nanostructural features of a calcium phosphate cement: a kinetic analysis, *Biomaterials* 25 (2004) 3453-3462.
- [30] M. Espanol, R.A. Perez, E.B. Montufar, C. Marichal, A. Sacco, M.P. Ginebra, Intrinsic porosity of calcium phosphate cements and its significance for drug delivery and tissue engineering applications, *Acta Biomater.* 5 (2009) 2752-2762.
- [31] S. Hulbert, S. Morrison, J. Klawitter, Tissue reaction to three ceramics of porous and non-porous structures, *J Biomed Mater Res* 6 (1972) 347-374.
- [32] P. Egli, W. Muller, R. Schenk, Porous hydroxyapatite and tricalcium phosphate cylinders with two different pore size ranges implanted in cancellous bone of rabbits. A comparative histomorphometric and histologic study of bony ingrowth and implant substitution, *Clin Orthop Relat Res* (1988) 127-138.
- [33] K. De Groot, Effect of porosity and physicochemical properties on the stability, resorption, and strength of calcium phosphate ceramics *Ann. N. Y. Acad. Sci.* 523 (1988) 227-233.
- [34] A. el-Ghannam, P. Ducheyne, I. Shapiro, Bioactive material template for *in vitro* synthesis of bone, *J Biomed Mater Res* 29 (1995) 359-370.
- [35] B.S. Chang, C.K. Lee, K.S. Hong, H.J. Youn, H.S. Ryu, S.S. Chung, K.W. Park, Osteoconduction at porous hydroxyapatite with various pore configurations, *Biomaterials* 21 (2000) 1291-1298.
- [36] S. Takagi, L.C. Chow, Formation of macropores in calcium phosphate cement implants, *J Mater Sci Mater Med.* 12 (2001) 135-139.
- [37] S. Girod Fullana, H. Ternet, M. Freche, J.L. Lacout, F. Rodriguez, Controlled release properties and final macroporosity of a pectin microspheres-calcium phosphate composite bone cement, *Acta Biomater.* 6 (2010) 2294-2300.
- [38] A. Almirall, G. Larrecq, J.A. Delgado, S. Martínez, J.A. Planell, M.P. Ginebra, Fabrication of low temperature macroporous hydroxyapatite scaffolds by foaming and hydrolysis of an α -TCP paste, *Biomaterials* 25 (2004) 3671-3680.
- [39] R. del Real, J. Wolke, M. Vallet-Regí, J. Jansen, A new method to produce macropores in calcium phosphate cements, *Biomaterials* 23 (2002) 3673-3680.
- [40] R. del Real, E. Ooms, J. Wolke, M. Vallet-Regí, J. Jansen, In vivo bone response to porous calcium phosphate cement, *J. Biomed. Mater. Res. A* 65A (2003) 30-36.
- [41] S. Hesaraki, D. Sharifi, Investigation of an effervescent additive as porogenic agent for bone cement macroporosity, *Biomed. Mater. Eng.* 17 (2007) 29-38.
- [42] H. Saeed, Z. Ali, M. Fatollah, The influence of the acidic component of the gas-foaming porogen used in preparing an injectable porous calcium phosphate cement on its properties: Acetic acid versus citric acid, *J Biomat Mater Res B* 86B (2008) 208-216.
- [43] N. Miño-Fariña, F. Muñoz-Guzón, M. López-Peña, M. Ginebra, S. del Valle-Fresno, D. Ayala, A. González-Cantalapiedra, Quantitative analysis of the resorption and osteoconduction of a macroporous calcium phosphate bone cement for the repair of a critical size defect in the femoral condyle, *Vet. J.* 179 (2009) 264-272.
- [44] S. del Valle, N. Miño, F. Muñoz, A. González, J. Planell, M.P. Ginebra, In vivo evaluation of an injectable Macroporous Calcium Phosphate Cement, *J Mater Sci Mater Med.* 18 (2007) 353-361.
- [45] M.-P. Ginebra, J.-A. Delgado, I. Harr, A. Almirall, S. Del Valle, J.A. Planell, Factors affecting the structure and properties of an injectable self-setting calcium phosphate foam, *J. Biomed. Mater. Res. A* 80A (2007) 351-361.

- [46] G. Dagang, X. Kewei, H. Yong, The *in situ* synthesis of biphasic calcium phosphate scaffolds with controllable compositions, structures, and adjustable properties, *J Biomat Mater Res A* 88A (2009) 43-52.
- [47] S. Xu, D. Li, C. Wang, Z. Wang, B. Lu, Cell proliferation in CPC scaffold with a central channel, *Biomed. Mater. Eng.* 17 (2007) 1-8.
- [48] X. Li, D. Li, B. Lu, L. Wang, Z. Wang, Fabrication and evaluation of calcium phosphate cement scaffold with controlled internal channel architecture and complex shape, *Proc Inst Mech Eng H* 221 (2007) 951-958.
- [49] S. Sarda, M. Nilsson, M. Balcells, E. Fernández, Influence of surfactant molecules as air-entraining agent for bone cement macroporosity, *J. Biomed. Mater. Res. A* 65A (2003) 215-221.
- [50] X. Wang, J. Ye, X. Li, H. Dong, Production of in-situ macropores in an injectable calcium phosphate cement by introduction of cetyltrimethyl ammonium bromide, *J Mater Sci Mater Med.* 19 (2008) 3221-3225.
- [51] W. Habraken, L. de Jonge, J. Wolke, L. Yubao, A. Mikos, J. Jansen, Introduction of gelatin microspheres into an injectable calcium phosphate cement, *J. Biomed. Mater. Res. A* 87A (2008) 643-655.
- [52] W.J.E.M. Habraken, J.G.C. Wolke, A.G. Mikos, J.A. Jansen, Porcine gelatin microsphere/calcium phosphate cement composites: An *in vitro* degradation study, *J. Biomed. Mater. Res. B* 91B (2009) 555-561.
- [53] D.P. Link, J. van den Dolder, J.J.J.P. van den Beucken, W. Habraken, A. Soede, O.C. Boerman, A.G. Mikos, J.A. Jansen, Evaluation of an orthotopically implanted calcium phosphate cement containing gelatin microparticles, *J. Biomed. Mater. Res. A* 90A (2009) 372-379.
- [54] Y. Zuo, F. Yang, J.G.C. Wolke, Y. Li, J.A. Jansen, Incorporation of biodegradable electrospun fibers into calcium phosphate cement for bone regeneration, *Acta Biomater.* 6 (2010) 1238-1247.
- [55] E. Bodde, C. Cammaert, J. Wolke, P. Spauwen, J. Jansen, Investigation as to the osteoinductivity of macroporous calcium phosphate cement in goats, *J Biomed Mater Res B* 83B (2007) 161-168.
- [56] W. Habraken, J. Wolke, A. Mikos, J. Jansen, Injectable PLGA microsphere/calcium phosphate cements: physical properties and degradation characteristics *J. Biomater. Sci. Polym. Ed.* 17 (2006) 1057-1074.
- [57] D. Link, D. J van den, J.v.d. Beucken, V. Cuijpers, J. Wolke, A. Mikos, J. Jansen, Evaluation of the biocompatibility of calcium phosphate cement/PLGA microparticle composites, *J Biomat Mater Res A* 87A (2008) 760-769.
- [58] W.J.E.M. Habraken, Z. Zhang, J.G.C. Wolke, D.W. Grijpma, A.G. Mikos, J. Feijen, J.A. Jansen, Introduction of enzymatically degradable poly(trimethylene carbonate) microspheres into an injectable calcium phosphate cement, *Biomaterials* 29 (2008) 2464-2476.
- [59] W.J.E.M. Habraken, H.B. Liao, Z. Zhang, J.G.C. Wolke, D.W. Grijpma, A.G. Mikos, J. Feijen, J.A. Jansen, *In vivo* degradation of calcium phosphate cement incorporated into biodegradable microspheres, *Acta Biomater.* 6 2200-2211.
- [60] P. Ruhé, E. Hedberg-Dirk, N.T. Padron, P. Spauwen, J. Jansen, A. Mikos, Porous Poly(DL-lactic-co-glycolic acid)/Calcium Phosphate Cement Composite for Reconstruction of Bone Defects, *Tissue Eng.* 12 (2006) 789-800.
- [61] H.H.K. Xu, M.D. Weir, C.G. Simon, Injectable and strong nano-apatite scaffolds for cell/growth factor delivery and bone regeneration, *Dent. Mater.* 24 (2008) 1212-1222.
- [62] H. Xu, L. Carey, C. Simon, Premixed macroporous calcium phosphate cement scaffold, *J Mater Sci Mater Med.* 18 (2007) 1345-1353.
- [63] M.P. Ginebra, T. Traykova, J.A. Planell, Calcium phosphate cements as bone drug delivery systems: A review, *J. Controlled Release* 113 (2006) 102-110.
- [64] P. Ruhé, O. Boerman, F. Russel, A. Mikos, P. Spauwen, J. Jansen, *In vivo* release of rhBMP-2 loaded porous calcium phosphate cement pretreated with albumin, *J Mater Sci Mater Med.* 17 (2006) 919-927.
- [65] J.K. Tessmar, A.M. Göpferich, Matrices and scaffolds for protein delivery in tissue engineering, *Adv Drug Deliv Rev.* 59 (2007) 274-291.
- [66] J.D. Kretlow, L. Klouda, A.G. Mikos, Injectable matrices and scaffolds for drug delivery in tissue engineering, *Adv Drug Deliv Rev.* 59 (2007) 263-273.

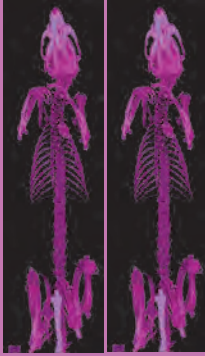
CHAPTER 1

- [67] M.H. Alkhraisat, C. Rueda, J. Cabrejos-Azama, J. Lucas-Aparicio, F.T. Mariño, J. Torres García-Denche, L.B. Jerez, U. Gbureck, E.L. Cabarcos, Loading and release of doxycycline hyclate from strontium-substituted calcium phosphate cement, *Acta Biomater.* 6 (2010) 1522-1528.
- [68] T. Masaaki, M. Youji, I. Kunio, N. Masaru, K. Masayuki, A. Kenzo, S. Kazuomi, Effects of added antibiotics on the basic properties of anti-washout-type fast-setting calcium phosphate cement, *J Biomat Mater Res* 39 (1998) 308-316.
- [69] H. Xu, J. Quinn, S. Takagi, L. Chow, F. Eichmiller, Strong and macroporous calcium phosphate cement: Effects of porosity and fiber reinforcement on mechanical properties, *J. Biomed. Mater. Res.* 57 (2001) 457-466.
- [70] P. Ruhé, E. Hedberg, N.T. Padron, P. Spauwen, J. Jansen, A. Mikos, Biocompatibility and degradation of poly(DL-lactic-co-glycolic acid)/calcium phosphate cement composites, *J. Biomed. Mater. Res. A* 74A (2005) 533-544.
- [71] B.H. Woo, B.F. Fink, R. Page, J.A. Schrier, Y.W. Jo, G. Jiang, M. DeLuca, H.C. Vasconez, P.P. DeLuca, Enhancement of Bone Growth by Sustained Delivery of Recombinant Human Bone Morphogenetic Protein-2 in a Polymeric Matrix, *Pharm. Res.* 18 (2001) 1747-1753.
- [72] W.J.E.M. Habraken, O.C. Boerman, J.G.C. Wolke, A.G. Mikos, J.A. Jansen, *In vitro* growth factor release from injectable calcium phosphate cements containing gelatin microspheres, *J Biomat Mater Res A* 91A (2009) 614-622.
- [73] O. Kisanuki, H. Yajima, T. Umeda, Y. Takakura, Experimental study of calcium phosphate cement impregnated with dideoxy-kanamycin B, *J. Orthop. Sci.* 12 (2007) 281-288.
- [74] K. Urabe, K. Naruse, H. Hattori, M. Hirano, K. Uchida, K. Onuma, H. Park, M. Itoman, In vitro comparison of elution characteristics of vancomycin from calcium phosphate cement and polymethylmethacrylate, *J. Orthop. Sci.* 14 (2009) 784-793.
- [75] M. Centrella, M.C. Horowitz, J.M. Wozney, T.L. McCarthy, Transforming Growth Factor- β Gene Family Members and Bone, *Endocr Rev.* 15 (1994) 27-39.
- [76] X. Cao, D. Chen, The BMP signaling and in vivo bone formation, *Gene* 357 (2005) 1-8.
- [77] E. Bodde, O. Boerman, F. Russel, A. Mikos, P. Spauwen, J. Jansen, The kinetic and biological activity of different loaded rhBMP-2 calcium phosphate cement implants in rats, *J. Biomed. Mater. Res. A* 87A (2008) 780-791.
- [78] E. Blom, J. Klein-Nulend, L. Yin, M. van Waas, E. Burger, Transforming growth factor- β 1 incorporated in calcium phosphate cement stimulates osteotransductivity in rat calvarial bone defects, *Clin. Oral Implants Res.* 12 (2001) 609-616.
- [79] J.E. Phillips, C.A. Gersbach, A.J. García, Virus-based gene therapy strategies for bone regeneration, *Biomaterials* 28 (2007) 211-229.
- [80] M. Keeney, J.J.J.P. van den Beucken, P.M. van der Kraan, J.A. Jansen, A. Pandit, The ability of a collagen/calcium phosphate scaffold to act as its own vector for gene delivery and to promote bone formation via transfection with VEGF165, *Biomaterials* 31 (2010) 2893-2902.
- [81] D.W. Michael, H.K.X. Hockin, G.S. Carl, Jr., Strong calcium phosphate cement-chitosan-mesh construct containing cell-encapsulating hydrogel beads for bone tissue engineering, *J Biomat Mater Res A* 77A (2006) 487-496.
- [82] B.M.D. Bai, Z. Yin, Q. Xu, M. Lew, Y. Chen, J. Ye, J. Wu, D. Chen, Y. Zeng, Histological Changes of an Injectable rhBMP-2/Calcium Phosphate Cement in Vertebroplasty of Rhesus Monkey, *Spine* 34 (2009) 1887-1892.
- [83] M. Perrier, Y. Lu, B. Nemke, H. Kobayashi, A. Peterson, M. Markel, Acceleration of Second and Fourth Metatarsal Fracture Healing with Recombinant Human Bone Morphogenetic Protein-2/Calcium Phosphate Cement in Horses, *Vet. Surg.* 37 (2008) 648-655.
- [84] E.J. Blom, J. Klein-Nulend, C.P.A.T. Klein, K. Kurashina, M.A.J.v. Waas, E.H. Burger, Transforming growth factor-beta1 incorporated during setting in calcium phosphate cement stimulates bone cell differentiation in vitro, *J. Biomed. Mater. Res.* 50 (2000) 67-74.
- [85] D.P. Link, J. van den Dolder, J.J. van den Beucken, J.G. Wolke, A.G. Mikos, J.A. Jansen, Bone response and mechanical strength of rabbit femoral defects filled with injectable CaP cements containing TGF- β 1 loaded gelatin microparticles, *Biomaterials* 29 (2008) 675-682.
- [86] H.P. Gerber, N. Ferrara, Angiogenesis and Bone Growth, *Trends Cardiovasc. Med.* 10 (2000) 223-228.

- [87] S. Soker, M. Machado, A. Atala, Systems for therapeutic angiogenesis in tissue engineering, *World J. Urol.* 18 (2000) 10-18.
- [88] M.H. Sheridan, L.D. Shea, M.C. Peters, D.J. Mooney, Bioabsorbable polymer scaffolds for tissue engineering capable of sustained growth factor delivery, *J. Controlled Release* 64 (2000) 91-102.
- [89] K.Y. Lee, M.C. Peters, D.J. Mooney, Comparison of vascular endothelial growth factor and basic fibroblast growth factor on angiogenesis in SCID mice, *J. Controlled Release* 87 (2003) 49-56.
- [90] C. Drake, C. Little, Exogenous vascular endothelial growth factor induces malformed and hyperfused vessels during embryonic neovascularization, *Proc Natl Acad Sci* 92 (1995) 7657-7661.
- [91] A.H. Zisch, M.P. Lutolf, J.A. Hubbell, Biopolymeric delivery matrices for angiogenic growth factors, *Cardiovasc Pathol* 12 (2006) 295-310.
- [92] Z. Patel, H. Ueda, M. Yamamoto, Y. Tabata, A. Mikos, *In Vitro* and *In Vivo* Release of Vascular Endothelial Growth Factor from Gelatin Microparticles and Biodegradable Composite Scaffolds, *Pharm. Res.* 25 (2008) 2370-2378.
- [93] K. Darnell, W. Zhuo, H. Kim, J.M. David, H.K. Paul, VEGF Scaffolds Enhance Angiogenesis and Bone Regeneration in Irradiated Osseous Defects, *J Bone Miner Res* 21 (2006) 735-744.
- [94] Z.S. Patel, S. Young, Y. Tabata, J.A. Jansen, M.E.K. Wong, A.G. Mikos, Dual delivery of an angiogenic and an osteogenic growth factor for bone regeneration in a critical size defect model, *Bone* 43 (2008) 931-940.
- [95] N. Kakudo, K. Kusumoto, Y.B. Wang, Y. Iguchi, Y. Ogawa, Immunolocalization of vascular endothelial growth factor on intramuscular ectopic osteoinduction by bone morphogenetic protein-2, *Life Sci.* 79 (2006) 1847-1855.
- [96] L. Wang, Y. Huang, K. Pan, X. Jiang, C. Liu, Osteogenic Responses to Different Concentrations/Ratios of BMP-2 and bFGF in Bone Formation, *Ann. Biomed. Eng.* 38 (2010) 77-87.
- [97] S. Alam, K. Ueki, K. Marukawa, T. Ohara, T. Hase, D. Takazakura, K. Nakagawa, Expression of bone morphogenetic protein 2 and fibroblast growth factor 2 during bone regeneration using different implant materials as an onlay bone graft in rabbit mandibles, *Oral Surg Oral Med Oral Pathol Oral Radiol Endod* 103 (2007) 16-26.
- [98] G. Mundy, R. Garrett, S. Harris, J. Chan, D. Chen, G. Rossini, B. Boyce, M. Zhao, G. Gutierrez, Stimulation of Bone Formation in Vitro and in Rodents by Statins, *Science* 286 (1999) 1946-1949.
- [99] K. Notoya, K. Yoshida, R. Tsukuda, S. Taketomi, Effect of ipriflavone on expression of markers characteristic of the osteoblast phenotype in rat bone marrow stromal cell culture, *J. Bone Miner. Res.* 9 (1994) 395-400.
- [100] J. Barralet, U. Gbureck, P. Habibovic, E. Vorndran, C. Gerard, C.J. Doillon, Angiogenesis in Calcium Phosphate Scaffolds by Inorganic Copper Ion Release, *Tissue Eng Part A* 15 (2009) 1601-1609.
- [101] K. Notoya, H. Nagai, T. Oda, M. Gotoh, T. Hoshino, H. Muranishi, S. Taketomi, T. Sohda, H. Makino, Enhancement of osteogenesis in vitro and in vivo by a novel osteoblast differentiation promoting compound, TAK-778., *Pharmacol Exp Ther* 290 (1999) 1054-1064.
- [102] J. Zhao, S. Ohba, Y. Komiyama, M. Shinkai, U.-i. Chung, T. Nagamune, Icarin: A Potential Osteoinductive Compound for Bone Tissue Engineering, *Tissue Eng Part A* 16 (2010) 233-243.
- [103] M.D. Weir, H.H.K. Xu, Human bone marrow stem cell-encapsulating calcium phosphate scaffolds for bone repair, *Acta Biomater.* 6 (2010) 4118-4126.
- [104] R.M. Shanti, W.-J. Li, L.J. Nesti, X. Wang, R.S. Tuan, Adult Mesenchymal Stem Cells: Biological Properties, Characteristics, and Applications in Maxillofacial Surgery, *J. Oral Maxillofac. Surg.* 65 (2007) 1640-1647.
- [105] R.E. Kirschner, J. Karmacharya, G. Ong, O. Hunenko, J.E. Losee, B. Martin, T.M. Crombleholme, Synthetic Hybrid Grafts for Craniofacial Reconstruction: Sustained Gene Delivery Using a Calcium Phosphate Bone Mineral Substitute, *Ann. Plast. Surg.* 46 (2001) 538-545.
- [106] H. Takeuchi, M. Nagayama, Y. Imaizumi, T. Tsukahara, J. Nakazawa, Y. Kusaka, K. Ohtomo, Immunohistochemical analysis of osteoconductivity of beta-tricalciumphosphate and carbonate apatite applied in femoral and parietal bone defects in rats, *Dent. Mater. J.* 28 (2009) 595-601.
- [107] R. LeGeros, Properties of osteoconductive biomaterials: calcium phosphates., *Clin. Orthop. Res.* 395 (2002) 81-98.
- [108] E. Ooms, J. Wolke, J. van der Waerden, J. Jansen, Trabecular bone response to injectable calcium phosphate (Ca-P) cement, *J Biomed Mater Res* 61 (2002) 9-18.

CHAPTER 1

- [109] W.S.S. Jee, W. Yao, Overview: animal models of osteopenia and osteoporosis, *J Musculoskel Neuron Interact* 1 (2001) 193-207.
- [110] U.H. Lerner, Bone Remodeling in Post-menopausal Osteoporosis, *J. Dent. Res.* 85 (2006) 584-595.
- [111] A. Turner, Animal models of osteoporosis-necessity and limitations, *European Cells and Materials* 1 (2001) 66-81.
- [112] B. Grardel, B. Sutter, B. Flautre, E. Viguiet, F. Lavaste, P. Hardouin, Effects of glucocorticoids on skeletal growth in rabbits evaluated by dual-photon absorptiometry, microscopic connectivity and vertebral compressive strength, *Osteoporosis International* 4 (1994) 204-210.
- [113] M.L. Wang, J. Massie, R.T. Allen, Y.-P. Lee, C.W. Kim, Altered bioreactivity and limited osteoconductivity of calcium sulfate-based bone cements in the osteoporotic rat spine, *The Spine Journal* 8 (2008) 340-350.



CHAPTER 2

Calcium phosphate/PLGA composite bone substitute materials: evaluation of temporal degradation and bone ingrowth in a rat critical-sized cranial defect

FCJ van de Watering, JJJP van den Beucken, XF Walboomers
and JA Jansen

Clinical Oral Implants Research, 23 (2012) 151-159.

Introduction

Calcium phosphate (CaP) cements represent a promising candidate material for bone substitution in dentistry, orthopedics, and reconstructive surgery, due to their biocompatibility and osteoconductive properties, as well as the potential to use minimally invasive surgery because of their injectability [1, 2]. However, an important disadvantage of CaP cements is the slow degradation rate of the material and control thereof [3].

CaP cements contain an intrinsic nanoporosity (pore size 10 nm - 100 nm), which is insufficient to substantially enhance material degradation for clinical benefit or tissue ingrowth [4, 5]. Microporosity (pore size 1 - 50 μm) or macroporosity (pore size > 50 μm) can be introduced inside CaP cement, by using different approaches, in order to enhance material degradation. The use of sodium bicarbonate to obtain CO₂-gas bubbles during cement setting has demonstrated to create macroporosity [6], however with poor control over pore distribution. In contrast, mixing water-soluble crystals [7, 8] or biodegradable polymer microparticles (e.g. gelatin [9] or poly(D,L-lactic-co-glycolic) acid (PLGA) [10-13]) as porogens homogeneously through the cement powder has demonstrated to be a feasible method to obtain a homogeneous microporosity after *in situ* crystal leaching or microparticle degradation, respectively.

PLGA is biocompatible, non-toxic and its degradation properties can be modified by changing different parameters such as molecular weight or the lactic to glycolic acid ratio [14]. The degradation of PLGA depends on hydrolysis, where polyglycolic acid degrades faster than polylactic acid. In the form of microparticles, PLGA can have a role as porogen in CaP/PLGA composites [11, 12, 15]. Moreover, PLGA-microparticles have been proposed as a carrier for the delivery of drugs and/or growth factors into bone defects to direct biological responses [16-20]. The molecular weight (MW) of PLGA is influencing the degradation of the microparticles and thus the obtained porosity for bone tissue ingrowth. It is demonstrated that relatively high molecular weight (MW ~40kDa) PLGA-microparticles lead to a slower material degradation *in vivo* compared to PLGA-microparticles with lower molecular weight (MW ~5 kDa) [21].

Although the biological data of composites containing PLGA-microparticles of a MW of 5kDa are encouraging [21], no data are available on the temporal progression of bone defect closure. In addition, it was hypothesized that a further acceleration of *in vivo* material degradation might be achievable by adding a higher amount of PLGA-microparticles. Consequently, the rationale for the current study was to evaluate the bone regenerative effect of CaP/5kDa PLGA-cement composite material in a temporal fashion (i.e. implantation for 4, 8 and 12 weeks) and with variation in PLGA-microparticle amount (i.e. 20 vs. 30 wt.%) in critically-sized cranial defects in rats.

Materials and Methods

Materials

CaP cement consisted of 85% alpha tri-calcium phosphate (α -TCP), 10% dicalcium phosphate anhydrous (DCPA) and 5% precipitated hydroxyapatite. The cement liquid applied was a sterilized 2 wt.% aqueous solution of Na_2HPO_4 . Poly(DL-lactic-co-glycolic acid) (PLGA) (Purasorb[®], Purac, Gorinchem, The Netherlands) with a lactic to glycolic acid ratio of 50:50 and a molecular weight (M_w) of 4.54 ± 0.02 kg/mol was used for microparticle preparation.

Preparation of PLGA-microparticles

To prepare PLGA-microparticles, a double-emulsion-solvent-extraction technique (water-in-oil-in-water) was used, as described before [13]. Microparticles were produced by adding 500 μl of distilled water to 1400 mg PLGA in 2 ml dichloromethane. The mixture was emulsified using a Turrax[®] emulsifier for 60 seconds at 6000 rpm. Then 6 ml 0.3% aqueous poly(vinyl alcohol) (PVA, Acros Organics, Geel, Belgium) solution was added and emulsified for another 60 sec at 6000 rpm to produce the second emulsion. The emulsion was transferred to a stirred beaker, after which 394 ml 0.3% PVA solution and 400 ml of 2% isopropyl alcohol solution was added slowly. After 1 hour of stirring, the microparticles were allowed to settle for 15 min and the solution was decanted. Then, the microparticles were washed and collected through centrifugation at 1500 rpm for 5 min, lyophilized and stored at -20°C until use. The size distribution of the microparticles was determined by image analysis (Leica Qwin[®], Leica Microsystems). The microparticles were imaged by scanning electron microscopy (SEM; JEOL6310 at 15kV).

Preparation of CaP/PLGA composites [21]

PLGA-microparticles were homogeneously mixed with the CaP cement powder at 20 or 30 wt.% resulting in two experimental composite formulations, i.e. C20% and C30%, respectively. In a 2-ml syringe (BD Plastipak[™], Becton Dickinson S.A., Madrid, Spain) with closed tip, 2 wt.% Na_2HPO_4 was added to the CaP/PLGA in a liquid/powder ratio of 0.35 and mixed for 20 seconds using a mixing apparatus (Silamat[®], Vivadent, Schaan, Liechtenstein). After mixing, the composite cements were immediately injected in Teflon molds (7.8 mm in diameter and 1.8 mm thick). After overnight setting at room temperature, the pre-set composites were removed from the molds and analyzed using SEM. The pre-set composites were sterilized by gamma radiation with 25 kGy (Isotron B.V., Ede, The Netherlands) and stored at -20°C until use.

Characterization of the pre-set CaP/PLGA composites

Porosity measurements

The microporosity (i.e. additional porosity after PLGA-microparticles degradation) and total porosity (i.e. intrinsic porosity + microporosity) were determined by measuring the weight of pre-set composite discs with and without PLGA-microparticles and similar composite discs that received a heat-treatment to burn out PLGA. To burn out the polymer CaP/PLGA composites ($n=9$) were placed in a furnace at 650°C for 2 h. Subsequently, microporosity and total porosity were calculated using the following equations [13]:

Equation 1

$$\varepsilon_{\text{tot}} = \left(1 - \frac{m_{\text{burnt}}}{V * \rho_{\text{HAP}}}\right) * 100\%$$

Equation 2

$$\varepsilon_{\text{micro}} = \left(1 - \frac{m_{\text{nanoporous}}}{m_{\text{nanoporous}}}\right) * 100\%$$

Legend

- ε_{tot} = Total porosity (%)
- $\varepsilon_{\text{micro}}$ = Microporosity (%)
- m_{burnt} = Average mass sample (after burning out polymer) (g)
- $m_{\text{nanoporous}}$ = Average mass intrinsic nanoporous sample (CaP cement disc without PLGA) (g)
- V = Volume sample (cm³)
- ρ_{HAP} = Density hydroxyapatite (g/cm³)

Microcomputed tomography

To visualize the pre-set composite materials, the materials were placed in a furnace at 650°C for 2 h to burn out the polymer. Subsequently, microcomputed tomography was used at a voltage of 100 kV and an intensity of 98 μ A with a resolution of 3.8 μ m (Skyscan-1072 X-ray microtomograph, TomoNT version 3N.5, Skyscan®, Belgium). PLGA-microparticles appear as pores in the CaP cement disc.

Surgical procedure

Forty-eight healthy young adult (8 weeks old) male Wistar rats, weighing 295 ± 29 g were used as experimental animals. National guidelines for the care and use of laboratory animals were observed. The research was reviewed and approved by the Experimental Animal Committee of the Radboud University (RUDEC 2008-108). Anesthesia was induced and maintained by Isoflurane inhalation (Rhodia Organique Fine Limited, Avonmouth, Bristol, UK) via intubation. To minimize post-operative discomfort, buprenorphine (Temgesic®; Reckitt Benckiser Health Care Limited, Schering-Plough, UK) was administered intraperitoneally (0.02 mg/kg) directly after the operation and subcutaneously for two days after surgery.

To insert the implants, the rats were immobilized on their abdomen and the skull was shaved and disinfected with chlorhexidine. A longitudinal incision was made from the nasal bone to the occipital protuberance. To minimize pain, Lidocaine HCL 1% (B. Braun, Melsungen, Germany) was dripped onto the periosteum before incision and exposure of the parietal bone. A critical sized bone defect was created by marking the defect outline with a dental trephine drill (outside diameter 8.0 mm, ACE dental implant system, Brockton MA, USA) after which a full thickness bone defect was created by removing cortical bone with an ultrasonic device (Piezosurgery, Mectron, Carasco, Italy) with caution for the underlying dura mater and sagittal sinus and using constant cooling with sterile saline. Due to the ultrasonic frequency, the device only cuts hard tissues in a highly precise and safe manner without damaging soft tissues. Pre-set implants were placed in the created defects, after which the wound was closed in two layers with resorbable Vicryl® 4-0 (Johnson&Johnson, St.Stevens-Woluwe, Belgium).

The animals were housed in pairs. In the initial postoperative period, the intake of water and food was monitored. Further, the animals were observed for signs of pain, infection and proper activity. At the end of the implantation time, the rats were sacrificed by CO₂ suffocation.

Implant retrieval and histological preparations

Implants were retrieved after a 4, 8 or 12 week implantation period. The implants with surrounding tissue were excised and fixed in phosphate-buffered formaldehyde solution (pH 7.4). Subsequently, the tissue blocks were dehydrated in increasing ethanol concentrations (70-100%) and embedded in methylmethacrylate. Perpendicularly in the middle of the implants, thin sections (10 µm) were prepared using a microtome with diamond blade (Leica Microsystems SP 1600, Nussloch, Germany) [22]. Three sections of each implant were stained with methylene blue and basic fuchsin and examined using light microscopy (Leica Microsystems AG, Wetzlar, Germany).

Histological and Histomorphometrical evaluation

All histological sections (three sections per implant) were quantitatively scored using computer-based image analysis techniques (The Leica® Qwin Pro-image analysis system, Wetzlar, Germany). From digitalized images (magnitude 5x), the amount of remaining cement and newly-formed bone were determined within two regions of interest, i.e.: (1) ROI 1, positioned within the original area as occupied by the implant, and (2) ROI 2, situated directly under ROI1 in order to measure bone bridging (Figure 1). Material degradation was related to the amount of remaining implant and was determined by measuring the area percentage implant material within ROI1. The amount of newly-formed bone was determined in µm² and allocated as bone ingrowth (newly-developed bone within ROI1) and total newly-formed bone (newly-developed bone within ROI1+ROI2). Bone bridging was

determined by measuring the length of the implant (μm) cross-section that was associated with bone overgrowth and expressed as percentage of the total length of the original implant (width of ROI1; Figure 1). To compare the amount of newly-formed bone with the native amount, the native amount of cranial bone (μm^2) within ROI1 of three non-operated control animals was determined and averaged.

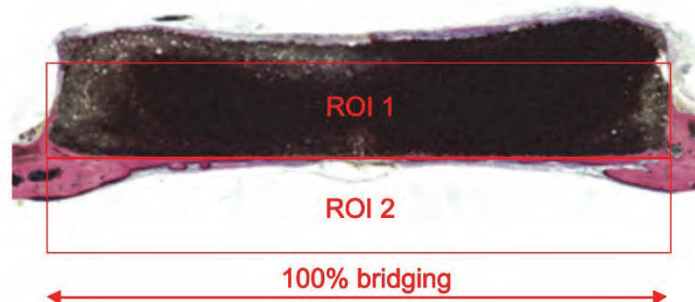


Figure 1 Schematic overview of histological and histomorphometrical evaluation. Two regions of interests (ROI) were created; ROI 1, positioned within the original area as occupied by the implant, and ROI 2, situated directly under ROI1. Within ROI 1, the amount of remaining implant was measured as a value of material degradation. The amount of newly-formed bone was determined in ROI 1 as bone ingrowth and ROI 1 + ROI 2 as amount of total newly-formed bone. Bone bridging was determined by measuring the length of the implant (μm) cross-section that was associated with bone overgrowth and expressed as percentage of the total length of the original implant (width of ROI1=100% bridging).

Statistical Analysis

Statistical analyses of implant degradation and bone formation measurements were performed using SPSS, version 16.0 (SPSS INC., Chicago, Illinois USA). The statistical comparisons were performed using a one-way analysis of variance (ANOVA) with a Tukey multiple comparison post-test. Differences were considered significant at p -values less than 0.05.

Results

Materials characterization

The preparation of PLGA-microparticles with the double-emulsion-solvent-extraction technique resulted in microparticles with an average size of $20.6 \pm 4 \mu\text{m}$. The size distribution is shown in Figure 2A. Morphological examination using SEM revealed that the microparticles had a spherical appearance with smooth surfaces (Figure 2B).

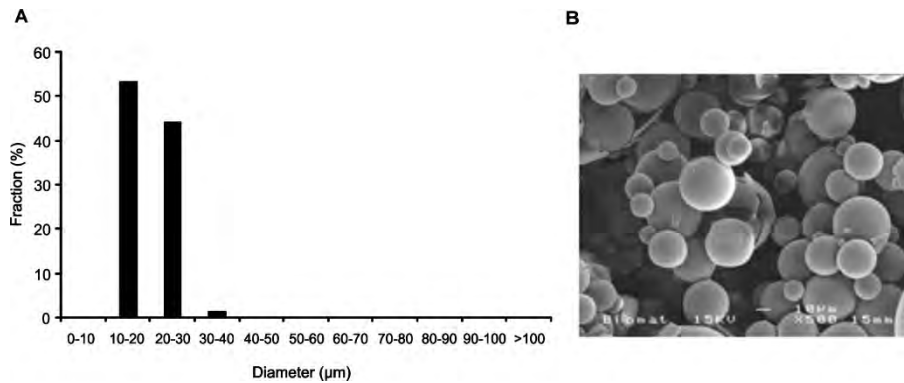


Figure 2 (A) The size distribution PLGA-microparticles prepared by the double-emulsion-solvent-extraction technique ($n=350$). The microparticles had an average size of $20.6 \pm 4 \mu\text{m}$ (B) SEM picture of PLGA-microparticles. Original magnification 500x , bar represents $10 \mu\text{m}$.

For the preparation of pre-set CaP/PLGA composites, the amount of PLGA (wt.%) was set at 20% (C20%) or 30% (C30%). The morphological form of C20% and C30% as visualized using microCT is presented in Figure 3A and B. Surface examination with SEM showed homogenous distribution of PLGA-microparticles within the implant material of both experimental groups. C30% showed an increased amount of particles at the surface as compared with C20% (Figure 3C and D).

The porosity measurements demonstrated porosity values of 27.5% (micro) and 64.5% (total) for C20% and 41.7% (micro) and 71.5% (total) and for C30% (Table 1).

General observation of the experimental animals

From the total of 48 animals available for surgery, 5 animals were sacrificed by CO_2 suffocation during the surgery as a consequence of extensive blood loss from the sagittal sinus. The remaining 43 animals recovered uneventfully from the surgical procedure and remained in good health. No signs of wound complications were observed post-operatively and macroscopic signs of inflammation or adverse tissue responses were absent during the course of the experiment. At the end of the experiment, a total of 43 implants were retrieved of which 38 were included for analyses. The exclusion of 2 implants from analysis was due to implant fracturing during histological processing, while 3 implants were excluded as they were found to be moved out of the cranial defect and were positioned above the bone wall of the cranial defect. An overview of the number of implants placed, retrieved, and used for evaluation is presented in Table 2.

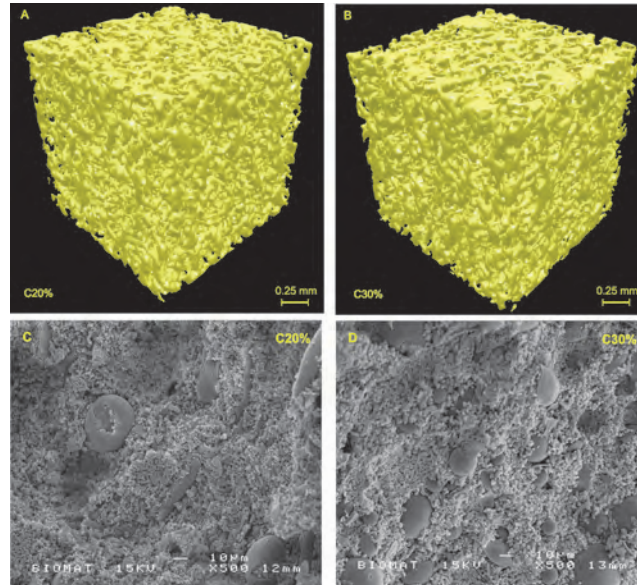


Figure 3 Microcomputed tomography images of (A) C20% and (B) C30%. μ CT reconstruction of segments (1 mm^3) of the two experimental composites show the volumetric appearance of both groups. PLGA-microparticles appear as pores in the CaP cement (bar represents 0.25 mm). SEM surface examinations of (C) C20% and (D) C30% revealed homogeneously distributed PLGA-microparticles in both groups and an apparently higher amount of particles in C30% (bar represents 10 μm).

Table 1 The porosity values obtained with the porosity measurements of the two experimental groups

	C20%	C30%
Intrinsic porosity	51.1 \pm 1.4	51.1 \pm 1.4
Microporosity	27.5 \pm 2.6	41.7 \pm 1.4
Total porosity	64.5 \pm 1.2	71.5 \pm 0.7

Table 2 Number of implants placed, retrieved and used for histomorphometrical analyses

Week	Implants placed			Implants retrieved			Implants used for analysis		
	4	8	12	4	8	12	4	8	12
C20%	7	7	7	7	7	7	7	7	6**
C30%	7	7	8	7	7	8	5**	7	6***

*Deviation from number of implants retrieved due to fracturing of implants during the histological processing or ** due to misplacement of the implant in cranial defect.

Descriptive light microscopy

Figure 4 presents an overview of histological sections of the different formulations (C20% and C30%) after implantation periods of 4, 8 and 12 weeks.

Upon visual inspection, the integrity of the implants was maintained throughout the entire implantation periods. The PLGA-microparticles were degraded and formed pores throughout the entire implant from 4 week implantation period onwards for C20% (Figure 5a and b) and C30% (Figure 5c and d). CaP degradation was generally limited, although CaP degradation at the implant periphery could be observed after 12 weeks of implantation, especially for the C30% formulation.

After a 4-week implantation period, the contact of the implant with the original defect edge was absent in all specimens and the existing gap was occupied with fibrous tissue. With increasing implantation period, new bone was formed between the original defect edges and the implants. At 12 weeks of implantation, direct bone contact was observed between the CaP cement and cranial bone for all specimens. Further, newly-formed bone was observed at the dura side of all implants of both groups already after 4 weeks implantation, which showed an increase with implantation period.

No bone formation was observed in the center of the implants in any of the sections. However, peripherally located PLGA-pores showed ingrowth of bone, fibrous tissue and bone marrow-like tissue which increased with implantation period. Bone ingrowth was most obvious in the C30% group after 12 weeks of implantation. None of the specimens revealed significant signs of inflammation.

Histomorphometrical evaluation

Implant degradation (Figure 6) was assessed using surface area measurement (%) of ROI1 that was occupied by implant material. Implant degradation was very limited without significant temporal progress for both C20% ($n>6$, from $95.1 \pm 1.3\%$ at week 4 to $94.8 \pm 2.1\%$ after 12 weeks, Table 3) and C30% ($n>5$, from $91.5 \pm 2.9\%$ at week 4 to $89.4 \pm 4.4\%$ after 12 weeks, Table 3). On the other hand, statistically significant differences in implant degradation were observed between C20% and C30% at each individual implantation period (week 4 $p=0.014$, week 8 $p=0.006$ and week 12 $p=0.026$, Table 4).

CHAPTER 2

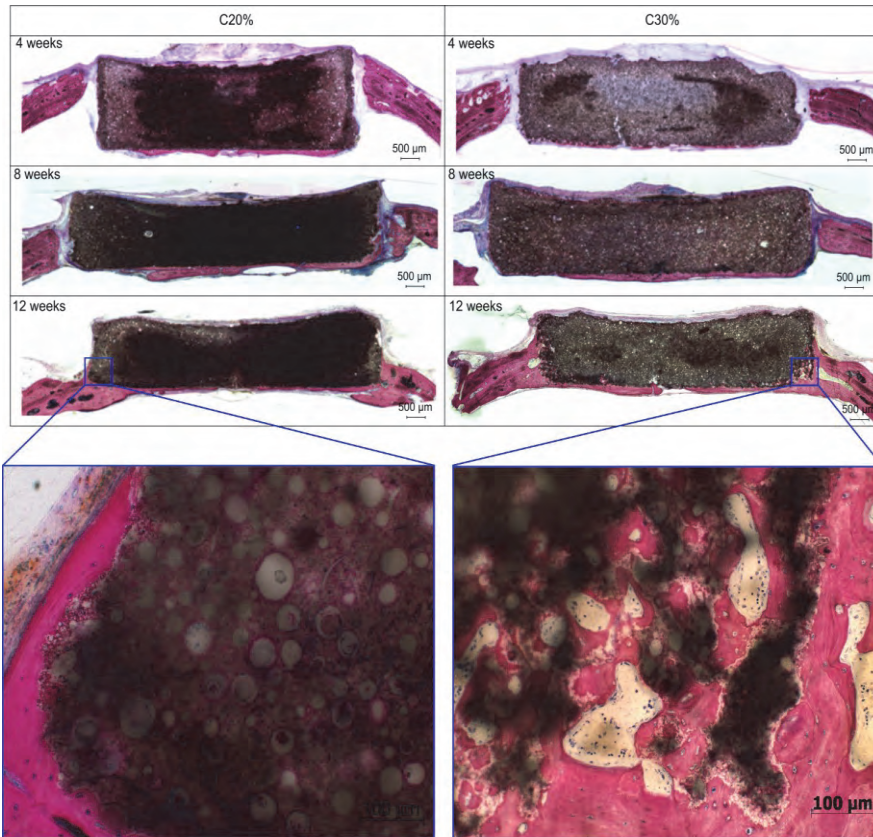


Figure 4 Representative histological sections of cranial defects of the two experimental groups, C20% and C30% after 4, 8 and 12 weeks. Bar represents 500 μm . Higher magnification of C20% show limited ingrowth of bone after 12 weeks of implantation; in the C30% ingrowth of bone after 12 weeks of implantation is observed. Methylene blue and basic fuchsin staining. Bar represents 100 μm .

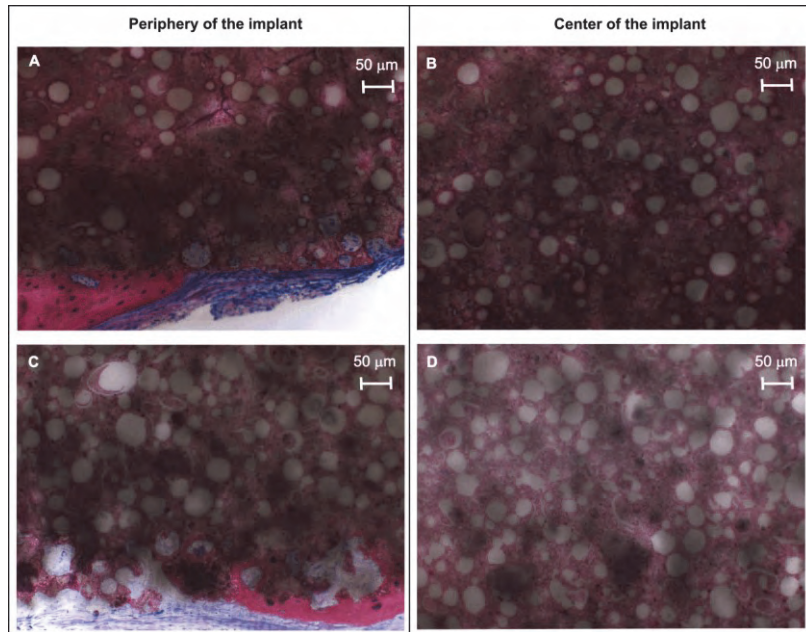


Figure 5 Magnified histological sections showing (A and C) degraded peripherally located and (B-D) centrally located PLGA-microparticles in C20% and C30%, respectively. Methylene blue and basic fuchsin staining. Bar represents 50 µm.

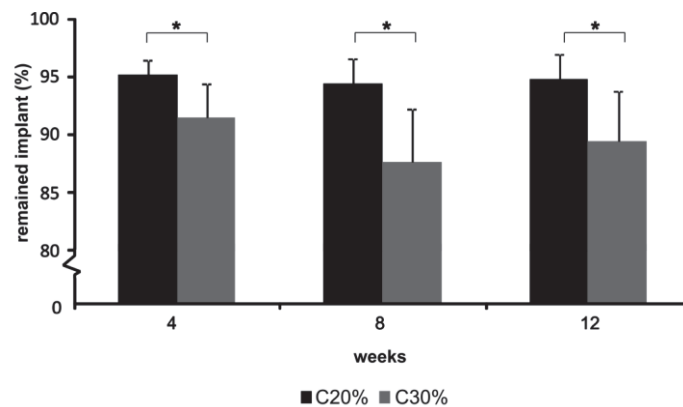


Figure 6 Results of histomorphometrical evaluation of C20% and C30% in critical size cranial defects. The amount of remaining implant after 4, 8 and 12 weeks of the two experimental groups ($n > 5$) are expressed as percentage of ROI1 (i.e. a standardized region of interest within the boundaries of the implant). Error bars represent means \pm standard deviation. * = $p < 0.05$.

Bone formation was determined by measurement of the area (μm^2) of bone within ROI1 and ROI2. Within the individual margins of both ROI1 and ROI2, bone formation showed a tendency to increase with implantation time, although no significant differences were observed between different time periods (for C20% ($n>6$) ROI1 ($p=0.122$) ranged from $56100.0 \pm 35320.1 \mu\text{m}^2$ to $160414.4 \pm 130655.6 \mu\text{m}^2$ after 12 weeks and ROI2 ($p=0.367$) from $242244.2 \pm 175432.4 \mu\text{m}^2$ to $525351.5 \pm 541371.6 \mu\text{m}^2$ after 12 weeks; for C30% ($n>5$) ROI1 ($p=0.100$) ranged from $135005.8 \pm 83266.4 \mu\text{m}^2$ to $457085.4 \pm 320027.1 \mu\text{m}^2$ after 12 weeks and ROI2 ($p=0.055$) from $239145.3 \pm 70833.7 \mu\text{m}^2$ to $460518.0 \pm 196864.0 \mu\text{m}^2$ after 12 weeks, Table 3) or between both groups at each individual implantation period (for ROI1 $p=0.102$, $p=0.627$, $p=0.108$ and for ROI 2 $p=0.971$, $p=374$, $p=0.805$ at week 4, 8 and 12 respectively, Figure 7a and b, Table 4).

On the other hand, total bone formation (i.e. bone formation within ROI1 + ROI2) demonstrated to significantly increase with implantation time for C30% (4wks vs. 12 wks $p=0.029$; 8wks vs. 12 wks $p=0.036$, $n>5$; total bone ranged from $374151.1 \pm 116841.1 \mu\text{m}^2$ to $917603.3 \pm 365808.3 \mu\text{m}^2$ after 12 weeks, Figure 7c, Table 3), whereas no significant differences were observed between both groups (week 4 $p=0.460$, week 8 $p=0.756$, week 12 $p=0.478$; Figure 7c, Table 4).

Bone bridging tended to increase with implantation time for both groups, without significant (intra- and inter-group) differences (for C20% intra-group $p=0.184$ and for C30% intra-group $p=0.087$, Table 3; for C20% vs C30% week 4 $p=0.345$, week 8 $p=0.382$ and week 12 $p=0.635$, Table 4; Figure 8). Bone bridging during the entire experiment ranged from $40.0 \pm 25.5\%$ to $65.0 \pm 20.0\%$ for C20% ($n>6$), and from $51.8 \pm 7.8\%$ to $70.5 \pm 16.2\%$ for C30% ($n>5$).

Relative to the average amount of calvarial bone present in healthy animals ($n=3$), the CaP/PLGA composite materials demonstrated to achieve bone formation after 12 weeks of implantation up to $19.5 \pm 14.7\%$ for the C20% ($n>6$) and $22.4 \pm 8.9\%$ for the C30% ($n>5$). A significant time-dependent increase in bone formation was observed only for C30% ($p=0.036$), whereas no significant differences were observed between both groups at individual time periods ($p>0.05$) (Figure 9).

CALCIUM PHOSPHATE/PLGA COMPOSITE BONE SUBSTITUTE MATERIALS

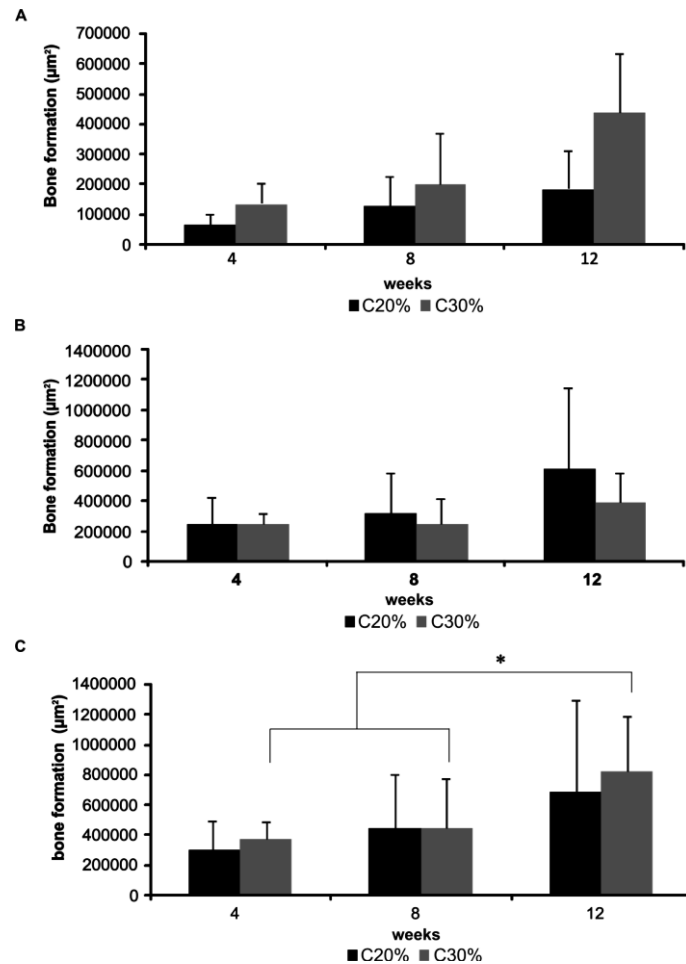


Figure 7 Bone regenerative capacity in C20% and C30% at 4, 8 and 12 week implantation period. (A) Bone formation is measured within the boundaries of the original implant (ROI1) and (B) directly underneath the implant (ROI2). Bone formation is similar at all time in both experimental groups. (C) A temporal increase of total bone formation (ROI1 + ROI2) was observed for C30% (4wks vs. 12 wks $p=0.029$; 8wks vs. 12 wks $p=0.036$). Error bars represent means \pm standard deviation. * = $p < 0.05$; $n > 5$.

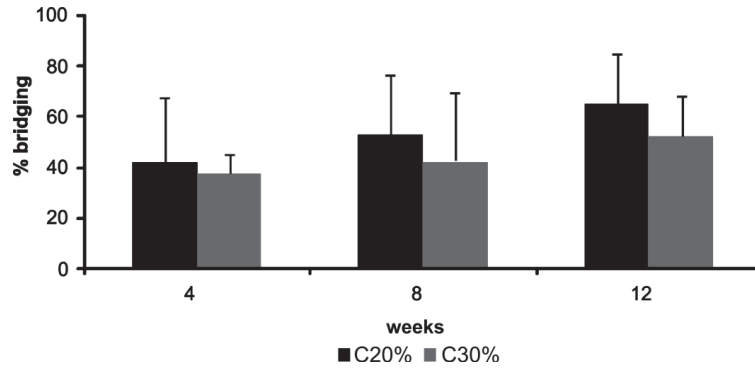


Figure 8 Bone bridging capacity in C20% and C30% at 4, 8 and 12 weeks implantation period. Bone bridging was determined by measuring the length of the implant (μm) cross-section that was accompanied with bone growth and expressed as percentage of the total length of the original implant. 12 weeks postoperatively none of the defects was completely closed. Error bars represent means \pm standard deviation ($n>5$).

C20%	Bridging %	C30%	Bridging %
Initial bone 	100 \pm 6.3	Initial bone 	100 \pm 6.3
Week 4 	7.3 \pm 4.8	Week 4 	9.1 \pm 2.9
Week 8 	12.0 \pm 8.7	Week 8 	10.6 \pm 8.0
Week 12 	19.5 \pm 14.7	Week 12 	22.4 \pm 8.9*

Figure 9 Overview of the temporal total bone formation for C20% and C30% compared to the initial amount of native bone. A temporal increase of total bone related to the native initial bone was observed for 12 weeks postoperatively in C30%. 12 weeks postoperatively none of the defects was completely closed. Methylene blue and basic fuchsin staining. Bar represents 500 μm . * = $p < 0.05$; $n>5$.

CALCIUM PHOSPHATE/PLGA COMPOSITE BONE SUBSTITUTE MATERIALS

Table 3 Overview of the histomorphometrical evaluation comparing in time the effect of the two experimental groups C20% and C30%

	Week 4	Week 8	Week 12	p-value (ANOVA) ^a
C20%				
Rem. Impl. (%)	95.1	94.7	94.8	0.919
BF ROI 1 (um ²)	56100.0	147688.5	160414.4	0.122
BF ROI 2 (um ²)	242244.2	345724.5	525351.5	0.367
TB (um ²)	298344.1	493413.0	685765.9	0.276
Bridging (%)	40.0	55.0	65.0	0.184
C30%				
Rem. Impl. (%)	91,521	87.6	89.4	0.302
BF ROI 1 (um ²)	135005.8	199148.7	457085.4	0.100
BF ROI 2 (um ²)	239145.3	234034.4	460518.0	0.055
TB (um ²)	374151.1	433183.1	917603,3	0.020
Bridging (%)	51.8	42.0	70,5	0.087

^a Grouping Variable; Time, Rem. Impl.; Remaining Implant, BF ROI 1; Bone formation in ROI 1, BF ROI 2; Bone formation in ROI 2, TB; Total bone formation (ROI 1 + ROI 2), Bridging; Bone Bridging.

Discussion

In this study, the influence of various amounts of PLGA-microparticles within pre-set CaP/PLGA cement discs on temporal degradation and bone ingrowth was evaluated in critical size cranial defects in rats. It was hypothesized that gradual cement degradation would occur after PLGA degradation and that a higher PLGA-content accelerates cement degradation as well as bone formation. The main findings show that discs containing 30 wt.% PLGA degraded significantly faster than 20 wt.% PLGA-equivalents, albeit that overall degradation was minimal for both types of cement discs. After twelve weeks of implantation, the total amount of newly-formed bone was ~20% of the native amount of calvarial bone in healthy animals for both experimental groups. Furthermore, bone formation and bone bridging demonstrated to be unaffected by amount of PLGA, although a significant temporal increase in total bone formation was observed only for cement discs containing 30 wt.% PLGA.

Table 4 Overview of the histomorphometrical evaluation comparing C20% and C30%

	C20%			C30%			p-value (ANOVA) ^a
	Average	SD	Median	Average	SD	Median	
Week 4							
Rem. Imp (%)	95.1	1.3	95.3	91.5	2.9	91.2	0.014
BF ROI 1 (um ²)	56100.0	35320.1	60441.7	135005.8	83266.4	86367.0	0.102
BF ROI 2 (um ²)	242244.2	175432.4	227753.3	239145.3	70833.7	212553.3	0.971
TB (um ²)	298344.1	195318.3	261322.0	374151.1	116841.1	392656.7	0.460
Bridging (%)	40.0	25.5	37.1	51.8	7.8	49.7	0.345
Week 8							
Rem. Imp. (%)	94.7	2.3	94.5	87.6	4.6	87.9	0.006
BF ROI 1 (um ²)	147688.5	99006.3	110244.6	199148.7	233756.7	104586.7	0.627
BF ROI 2 (um ²)	345724.5	262734.6	262916.7	234034.4	169231.5	255713.3	0.374
TB (um ²)	493413.0	354917.3	434582.0	433183.1	326254.5	489356.7	0.756
Bridging (%)	55.0	24.0	63.6	42.0	27.2	48.8	0.382
Week 12							
Rem. Imp. (%)	94.8	2.1	93.9	89.4	4.4	89.1	0.026
BF ROI 1 (um ²)	160414.4	130655.6	164968.6	457085.4	320027.1	315698.3	0.108
BF ROI 2 (um ²)	525351.5	541371.6	472108.3	460518.0	196864.0	457171.7	0.805
TB (um ²)	685765.9	625601.5	701414.7	917603.3	365808.3	808620.2	0.478
Bridging (%)	65.0	20.0	61.5	70.5	16.2	74.0	0.635

^a Grouping Variable; groups, Rem. Impl.; Remaining Implant, BF ROI 1; Bone formation in ROI 1, BF ROI 2; Bone formation in ROI 2, TB; Total bone formation (ROI 1 + ROI 2), Bridging; Bone Bridging.

In the present study, a full thickness critical-sized cranial defect was created by removing cortical bone with an ultrasonic device. The device only cuts hard tissue in a highly precise manner without damaging soft tissues due to the ultrasonic frequency. Therefore, the procedure creates a defect in a more safe manner with caution for the underlying dura mater and sagittal sinus compared to the trephine bur method. However, at 4 weeks of implantation, the bone/implant contact after creating the defect with an ultrasonic device was found to be less optimal compared to the trephine bur method as used by Bodde *et al.* (2008) [18]. Bone formation and material degradation is dependent on initial bone/implant contact and previous studies have demonstrated that the placement of pre-set CaP/PLGA cement discs results in complete fusion of the implant with the calvarial bone tissue without an intervening fibrous tissue layer [12, 21]. Consequently, initial bone/implant contact might be compromised when the cranial defect is prepared

using an ultrasonic device instead of a trephine bur. However, in line with the previous studies [12, 21], after 12 weeks of implantation, complete fusion of the calvarial bone and implant occurred in both groups indicating that the CaP/PLGA cement discs are bioactive and capable to close the gap between the calvarial bone and the implant without an intervening fibrous tissue. In addition, over time an increased amount of newly formed bone was observed at the dura side along the cement surface in both groups, which shows the bioactive characteristic of the cement.

In comparison with previous studies [12, 21], the present study showed large differences regarding the degradation of PLGA-containing CaP cement with equal and even higher amounts of PLGA. This difference in degradation and bone formation at 12 weeks postoperatively is remarkable, but likely related to the aforementioned change in defect preparation method, and further to issues involving PLGA-microparticle properties and/or the CaP cement composition. Due to a more standardized production procedure of PLGA-microparticles, the size distribution in the current study was minimized ($20.6 \pm 4 \mu\text{m}$) as compared to the other studies ($66 \pm 25 \mu\text{m}$ [12] or $21 \pm 18 \mu\text{m}$ [21]). In general, it is proposed that a pore size of at least 50 to 100 μm (microparticles size) is necessary for cell ingrowth [23], although in a previous study a microparticle size of $21 \pm 18 \mu\text{m}$ appeared to be sufficient to obtain cellular ingrowth throughout the implant [21]. In the current study, the peripherally located PLGA-pores showed ingrowth of bone tissue, whereas in the center of the implant no ingrowth was observed, albeit that the PLGA-microparticles were degraded already after a 4-week implantation period. It is likely that the standardized size of the PLGA-microparticles used in the current study may have influenced the porosity and especially the interconnectivity of the pores in the material. As standardization of the PLGA-preparation process is beneficial to obtain reproducibility, additional research has to be done to determine the most favorable size of the PLGA-microparticles in view of biological performance.

Further, it has to be emphasized that the composition of the cement in the current study (85% α -TCP, 10% CaHPO_4 and 5% precipitated hydroxyl-apatite [24]) differs from that in the earlier study of Bodde *et al.* (61% α -TCP, 26% CaHPO_4 , 10% CaCO_3 , and 3% precipitated hydroxyl-apatite) [21]. Both calcium phosphate cements harden as a calcium deficient hydroxyapatite (CDHA) due to the hydrolysis of the α -TCP [25]. α -TCP transforms after three days into an apatite-like structure that remains stable over time, whereas the monetite component (CaHPO_4) disappears between 2 and 8 weeks [4]. The difference between this novel bone cement formula and the previously used cement is mainly dependent on increased levels of α -TCP and precipitated hydroxyl-apatite as well as absence of CaCO_3 . In view of that, the different composition of the novel cement leads to a more stable cement from a ceramic point of view. However, *in vivo* experiments in which the effect of the difference in composition on degradation and biological responses are compared in a direct manner, have not been performed to date and are required to justify the assumption on cement stability.

As mentioned earlier, the experimental set-up, characteristics of the cement, size distribution of the PLGA-microparticles, (micro)porosity and the interconnectivity of the material all influence implant degradation and cellular ingrowth and therefore the bone forming capacity of the material. If one or all of these factors are slightly altered, the outcome of the study can differ from earlier findings. In addition, also the implant location may influence the degradation of the implant material. For example, material placed in femoral or cranial defects will be exposed to different environments, which includes the nature of biomechanical loading, surrounding tissue and blood/nutrient supply. Beside the environment, also the origin of the bones (i.e. long bone formation (femur) is endochondral while cranial bone formation is intramembranous), may play a role in the degradation and bone formation due to distinctive signaling properties [26]. Therefore, more research is necessary to elucidate the most favorable CaP/PLGA cement composition for different sites of application.

In conclusion, the present study demonstrated that a higher amount of PLGA-microparticles (30 vs. 20 wt.%) in CaP/PLGA cement composites has significant, though minimal effects on degradation. Bone formation showed not to be influenced by the amount of PLGA-microparticles within the composite, although a significant temporal increase in bone formation was observed only for composites containing 30 wt.% PLGA-microparticles. After 12 weeks of implantation, the total amount of newly-formed bone was ~20% compared to the amount of calvarial bone in healthy rats. Further optimization of CaP/PLGA cement is necessary to increase control over degradation and tissue ingrowth.

Acknowledgements

The authors gratefully acknowledge the support of the Smart Mix Program of the Netherlands Ministry of Economic Affairs and the Netherlands Ministry of Education, Culture and Science. The authors would like to thank Natasja van Dijk for her assistance with the histological preparations and Dr. Ir. Ewald Bronkhorst for his assistance with the statistical analysis. Scanning electron microscopy was performed at the Nijmegen Center for Molecular Life Sciences (NCMLS), the Netherlands.

References

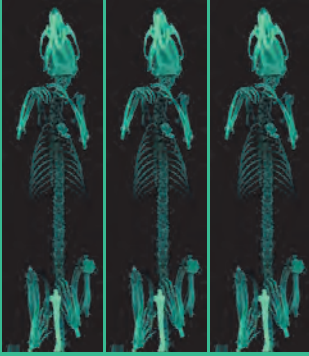
- [1] A. Ambard, L. Mueninghoff, Calcium Phosphate Cement: Review of Mechanical and Biological Properties, *Journal of Prosthodontics* 15 (2006) 321-328.
- [2] R. LeGeros, Properties of osteoconductive biomaterials: calcium phosphates., *Clinical Orthopaedics and Related Research* 395 (2002) 81-98.
- [3] J. Jansen, E. Ooms, N. Verdonchot, J. Wolke, Injectable calcium phosphate cement for bone repair and implant fixation, *Orthopedic Clinics of North America* 36 (2005) 89-95.
- [4] E. Ooms, J. Wolke, J. van der Waerden, J. Jansen, Trabecular bone response to injectable calcium phosphate (Ca-P) cement, *Journal of Biomedical Materials Research* 61 (2002) 9-18.

CALCIUM PHOSPHATE/PLGA COMPOSITE BONE SUBSTITUTE MATERIALS

- [5] E.M. Ooms, J.G.C. Wolke, M.T. van de Heuvel, B. Jeschke, J.A. Jansen, Histological evaluation of the bone response to calcium phosphate cement implanted in cortical bone, *Biomaterials* 24 (2003) 989-1000.
- [6] R. del Real, J. Wolke, M. Vallet-Regí, J. Jansen, A new method to produce macropores in calcium phosphate cements, *Biomaterials* 23 (2002) 3673-3680.
- [7] H.H.K. Xu, C.G. Simon, Fast setting calcium phosphate-chitosan scaffold: mechanical properties and biocompatibility, *Biomaterials* 26 (2005) 1337-1348.
- [8] H. Xu, J. Quinn, S. Takagi, L. Chow, F. Eichmiller, Strong and macroporous calcium phosphate cement: Effects of porosity and fiber reinforcement on mechanical properties, *Journal of Biomedical Materials Research* 57 (2001) 457-466.
- [9] W. Habraken, L. de Jonge, J. Wolke, L. Yubao, A. Mikos, J. Jansen, Introduction of gelatin microspheres into an injectable calcium phosphate cement, *Journal of Biomedical Materials Research Part A* 87A (2008) 643-655.
- [10] D.P. Link, J. van den Dolder, W.J.F.M. Jurgens, J.G.C. Wolke, J.A. Jansen, Mechanical evaluation of implanted calcium phosphate cement incorporated with PLGA microparticles, *Biomaterials* 27 (2006) 4941-4947.
- [11] P. Ruhé, E. Hedberg-Dirk, N.T. Padron, P. Spauwen, J. Jansen, A. Mikos, Porous Poly(DL-lactic-co-glycolic acid)/Calcium Phosphate Cement Composite for Reconstruction of Bone Defects, *Tissue Engineering* 12 (2006) 789-800.
- [12] P. Ruhé, E. Hedberg, N.T. Padron, P. Spauwen, J. Jansen, A. Mikos, Biocompatibility and degradation of poly(DL-lactic-co-glycolic acid)/calcium phosphate cement composites, *Journal of Biomedical Materials Research Part A* 74A (2005) 533-544.
- [13] W. Habraken, J. Wolke, A. Mikos, J. Jansen, Injectable PLGA microsphere/calcium phosphate cements: physical properties and degradation characteristics *Journal of Biomedical Science, Polymer Edition* 17 (2006) 1057-1074.
- [14] J. Anderson, M. Shive, Biodegradation and biocompatibility of PLA and PLGA microspheres, *Advanced Drug Delivery Reviews* 28 (1997) 5-24.
- [15] D. Link, J. van den Dolder, J. van den Beucken, V. Cuijpers, J. Wolke, A. Mikos, J. Jansen, Evaluation of the biocompatibility of calcium phosphate cement/PLGA microparticle composites, *Journal of Biomedical Materials Research Part A* 87A (2008) 760-769.
- [16] P. Ruhé, E. Hedberg, N.T. Padron, P. Spauwen, J. Jansen, A. Mikos, rhBMP-2 Release from Injectable Poly(DL-Lactic-co-glycolic Acid)/Calcium-Phosphate Cement Composites, *Journal of Bone and Joint Surgery* 85 (2003) 75-81.
- [17] P. Ruhé, O. Boerman, F. Russel, P. Spauwen, A. Mikos, J. Jansen, Controlled release of rhBMP-2 loaded poly(DL-lactic-co-glycolic acid)/calcium phosphate cement composites in vivo, *Journal of Controlled Release* 106 (2005) 162-171.
- [18] E. Bodde, O. Boerman, F. Russel, A. Mikos, P. Spauwen, J. Jansen, The kinetic and biological activity of different loaded rhBMP-2 calcium phosphate cement implants in rats, *Journal of Biomedical Materials Research Part A* 87A (2008) 780-791.
- [19] P. Ruhé, O. Boerman, F. Russel, A. Mikos, P. Spauwen, J. Jansen, *In vivo* release of rhBMP-2 loaded porous calcium phosphate cement pretreated with albumin, *Journal of Materials Science: Materials in Medicine* 17 (2006) 919-927.
- [20] B.H. Woo, B.F. Fink, R. Page, J.A. Schrier, Y.W. Jo, G. Jiang, M. DeLuca, H.C. Vasconez, P.P. DeLuca, Enhancement of Bone Growth by Sustained Delivery of Recombinant Human Bone Morphogenetic Protein-2 in a Polymeric Matrix, *Pharmaceutical Research* 18 (2001) 1747-1753.
- [21] E.W.H. Bodde, W.J.E.M. Habraken, A.G. Mikos, P.H.M. Spauwen, J.A. Jansen, Effect of Polymer Molecular Weight on the Bone Biological Activity of Biodegradable Polymer/Calcium Phosphate Cement Composites, *Tissue Engineering Part A* 15 (2009) 3183-3191.
- [22] H. van der Lubbe, C. Klein, K. de Groot, A simple method for preparing thin (10 microM) histological sections of undecalcified plastic embedded bone with implants, *Stain Technology* 63 (1988) 171-176.
- [23] M. Bohner, F. Baumgart, Theoretical model to determine the effects of geometrical factors on the resorption of calcium phosphate bone substitutes, *Biomaterials* 25 (2004) 3569-3582.
- [24] X. Wang, Y. Li, J. Jansen, S. Li, J. Wolke, Studies on Non-quenched Calcium Phosphate Cement: Influences of Quenching and Milling on setting Characteristic, *Key Engineering Materials* 330-332 (2007) 39-42.

CHAPTER 2

- [25] M.P. Ginebra, E. Fernandez, E.A.P. De Maeyer, R.M.H. Verbeeck, M.G. Boltong, J. Ginebra, F.C.M. Driessens, J.A. Planell, Setting Reaction and Hardening of an Apatitic Calcium Phosphate Cement, *Journal of Dental Research* 76 (1997) 905-912.
- [26] U. Chung, H. Kawaguchi, T. Takato, K. Nakamura, Distinct osteogenic mechanisms of bones of distinct origins, *Journal of Orthopaedic Science* 9 (2004) 410-414.



CHAPTER 3

Incorporation of bioactive glass in calcium phosphate cement Part II: Biological evaluation

ACM Renno[§], FCJ van de Watering[§], MC Crovace[§], ED Zanotto,
JG Wolke, JAJansen, JJJ van den Beucken

[§] These authors contributed equally to this study

Introduction

Apatite cements (such as calcium phosphate cement, CPC) represent a promising candidate material for bone substitution mainly due to their biocompatibility and osteoconductive properties [1-5]. An additional advantage of such a cement is the self-setting nature, which makes them injectable and allows the use of a minimally invasive surgical procedure during clinical use [2, 4, 5]. However, CPCs are characterized by a very slow degradation rate, which has to be considered as a disadvantage for several applications, like sinus elevation and the filling of extraction sockets [1, 5].

To enhance the biodegradability and tissue ingrowth of CPC, (micro)porosity can be introduced into the already intrinsically nanoporous cement [1, 5]. One promising strategy to create porosity into CPC is the introduction of biodegradable polymers, e.g. in the form of poly(D,L-lactic-co-glycolic) acid (PLGA) microparticles [6-9]. PLGA-microparticles degrade over time and hence create pores within the ceramic matrix that increase the surface-to-volume ratio of the CPC and allow tissue ingrowth [10, 11]. Many animal studies demonstrated that porosity created by degradation of PLGA-microparticles embedded within CPC increases cement degradation and accelerates the regeneration of a bone defect [9-12]. However, the osteoconductive properties of CPC/PLGA are not sufficient to achieve complete defect filling under critical conditions, like poorly vascularized sites and (elderly) patients with metabolic disorders [13]. Consequently, the enrichment of CPC/PLGA with osteopromotive or osteoinductive factors is necessary to improve their biological performance.

Bioactive glasses (BGs) are a group of synthetic silica-based bioactive materials with the unique ability to bond to living bone by forming a biologically active bone-like apatite layer on their surface [14-17] that acts as a template for calcium phosphate precipitation and directs new bone formation [14, 17, 18]. In addition, it has been reported that BGs attract and stimulate osteoprogenitor cells, which differentiate into matrix-producing osteoblasts and subsequently increase the rate of bone formation and bone ingrowth into BG-based granular material [19-22]. In view of this, the incorporation of BG into CPC seems a safe approach to improve the osteopromotive properties of CPC.

A recent *in vitro* study demonstrated that BG can successfully be introduced into CPC and CPC/PLGA composites, with a maximum of 30wt.% BG, without compromising the setting time and mechanical properties of CPC or CPC/PLGA composites [23]. These encouraging *in vitro* data on the introduction of BG into CPC composite material formed the basis for the current *in vivo* study, which aimed to evaluate the ectopic and orthotopic *in vivo* response to CPC/BG composites, with or without PLGA microparticles, in rats. Pre-set scaffolds in 4 different formulations (1: CPC; 2: CPC/BG; 3: CPC/PLGA; and 4: CPC/PLGA/BG) were implanted subcutaneously and in femoral condyle defects of rats. Histocompatibility (ectopic implants; histology) and bone responses (orthotopic implants; histology and histomorphometry) were evaluated after 2 and 6 weeks of implantation.

Materials and methods

Materials

Calcium phosphate cement (CPC) consisted of 85% alpha tri-calcium phosphate (α -TCP; CAM Bioceramics BV, Leiden, The Netherlands), 10% dicalcium phosphate anhydrous (DCPA; J.T. Baker Chemical Co., USA) and 5% precipitated hydroxyapatite (pHA; Merck, Darmstadt, Germany). 2% Na_2HPO_4 was used as liquid phase for the preparation of the cement. Acid-terminated poly(DL-lactic-co-glycolic acid) (PLGA; Purasorb[®], Purac, Gorinchem, The Netherlands) with a lactic to glycolic acid ratio of 50:50 and a molecular weight (M_w) of 17 kDa was used for microparticle preparation. Biosilicate[®] parent glass was used as type of bioglass (particle size: 2,5 μm) and was provided by Vitreous Materials Laboratory (LaMaV), Department of Materials Engineering, Federal University of São Carlos, Sao Carlos, Sao Paulo, Brasil [24].

Preparation of dense PLGA microparticles

Dense PLGA microparticles were prepared by a single emulsion technique, as described previously [3]. Briefly, 0.2 g of PLGA was dissolved in 2 mL of dichloromethane (DCM) (Merck, Darmstadt, Germany) in a 20 mL glass tube. Two mL of this solution was transferred into a stirred beaker containing 100 mL of 0.3% poly vinyl alcohol (PVA) (88% hydrolyzed, MW 22000, Acros, Geel, Belgium) solution. Subsequently, 50 mL of 2% isopropanol (IPN) (Merck) was added. The solution was stirred for 1 h. The microparticles were allowed to settle for 1 h and the clear solution was decanted. The suspension left was centrifuged and the clear solution on top was aspirated. Finally, the microparticles were washed and collected through centrifugation at 1500 rpm for 5 min, lyophilized and stored at -20 °C until use. The size distribution of the microparticles was determined by image analysis (Leica Qwin[®], Leica Microsystems, Wetzlar, Germany). The microparticles were imaged by scanning electron microscopy (SEM; JEOL6310 at 15kV).

Preparation of the pre-set composites

Four experimental groups were created: (1) CPC, (2) CPC/BG, (3) CPC/PLGA, and (4) CPC/PLGA/BG. Table 1 represents an overview of the composition of these materials.

For both subcutaneous and femoral implants, pre-set composites were made by adding different amounts of the base materials inside a 2 ml closed tip syringe (BD Plastipakt, Becton Dickinson S.A., Madrid, Spain; Table 1) and pre-mixing the powder mixture using a mixing apparatus (Silamat, Vivadent, Schaan, Liechtenstein). Subsequently, a Na_2HPO_4 solution (2 wt%) in a liquid/powder ratio of 0.35 was added into the syringe and the mixtures were mixed for another 20s. Directly after mixing, the composite cements were injected into Teflon molds (3 mm x 2.9 mm). After overnight setting at room temperature, the pre-set

composites were removed from the molds and analyzed using SEM. Before use, the pre-set composites were sterilized by γ -radiation with a minimum dose of 25 kGy (Isotron B.V., Ede, The Netherlands).

Table 1 Composition and porosity values of pre-set composite materials

Groups	CaP (wt. %)	BG (wt. %)	PLGA (wt. %)	Macro porosity	Total porosity
CPC	100	0	0	---	40.6 \pm 0.7
CPC/BG	70	30	0	---	41.6 \pm 0.8
CPC/PLGA	70	0	30	40.5 \pm 1.2	55.7 \pm 0.9
CPC/PLGA/BG	40	30	30	41.2 \pm 0.8	56.5 \pm 1.5

CPC, Calcium phosphate cement; BG, Bioactive glass; CPC/BG, BG incorporated into CPC; CPC/PLGA, dense PLGA-microparticles incorporated into CPC; CPC/PLGA/BG, dense PLGA-microparticles and BG incorporated into CPC; wt. %, weight percentage.

Characterization of pre-set composites

Porosity measurements

The microporosity (i.e. additional porosity after PLGA-microparticles degradation) and total porosity (i.e. intrinsic porosity/microporosity) were determined by measuring the weight of pre-set composite cylinders, with and without PLGA-microparticles. To burn out the PLGA-microparticles, composite scaffolds were placed in a furnace at 650°C for 2 h. Subsequently, microporosity and total porosity were calculated using the following equations [1]:

Equation 1

$$\varepsilon_{\text{tot}} = \left(1 - \frac{m_{\text{burnt}}}{V * \rho_{\text{HAP}}}\right) * 100\%$$

Equation 2

$$\varepsilon_{\text{micro}} = \left(1 - \frac{m_{\text{burnt}}}{m_{\text{nanoporous}}}\right) * 100\%$$

Legend

ε_{tot} = Total porosity (%)

$\varepsilon_{\text{micro}}$ = Microporosity (%)

m_{burnt} = Average mass sample (after burning out polymer) (g)

$m_{\text{nanoporous}}$ = Average mass intrinsic nanoporous sample (CaP cement disc without PLGA) (g)

V = Volume sample (cm³)

ρ_{HAP} = Density hydroxyapatite (g/cm³)

Surgical procedure

Twenty-four healthy young adult male Wistar rats (12 weeks old; weight 295 ± 29 g) were used as experimental animals. The animal experimental plan was reviewed and approved by the Experimental Animal Committee of the Radboud University (RU-DEC 2011-156) and national guidelines for the care and use of laboratory animals were observed.

Anesthesia was induced and maintained by Isoflurane inhalation (Rhodia Organique Fine Limited). To minimize post-operative discomfort, buprenorfine (Temgesic; Reckitt Benckiser Health Care Limited, Schering-Plough, Hoddesdon, UK) was administered intraperitoneally (0.02mg/kg) directly after the operation and subcutaneously for 2 days after surgery.

To insert implants into the femoral condyles, the animals were immobilized on their back and both hind limbs were shaved, washed and disinfected with povidone-iodine. After exposure of the distal femoral condyle, a 1.0 mm pilot hole was drilled. The hole was gradually widened with drills of increasing size until a final defect size of 3 mm in width and 3 mm in depth was reached. Low rotational drill speeds (max. 450 rpm) and constant physiologic saline irrigation were used. After preparation, the defects were thoroughly irrigated and packed with sterile cotton gaze to stop bleeding. Surgery was performed in both legs of the rats and one defect was created in each condyle. The pre-set implants were placed in the created defect, according to a randomization scheme ($n=6$ per experimental group, per time point). Thereafter, the wound was closed with resorbable Vicryl® 5-0 (Johnson&Johnson, St.Stevens-Woluwe, Belgium) after which the skin was closed by staples (Agraven®; InstruVet BV, Cuijk, The Netherlands).

In addition, half of the animals (12 rats) received 4 pre-set implants placed subcutaneously into the back of each rat. To insert the implants, rats were immobilized on their abdomen and the skin was shaved, washed and disinfected with iodine. Four paravertebral incisions were made (two on each site of the vertebral column) and subcutaneous pockets were created by blunt dissection. The implants were randomly placed for each group ($n=6$ per experimental group, per time point). Finally, the skin was closed using staples (Agraven®, InstruVet BV). The animals were housed in pairs and the intake of water and food was monitored in the initial postoperative period. Further, the animals were observed for signs of pain, infection and proper activity. After 2 and 6 weeks of implantation, rats were sacrificed by CO₂ suffocation.

Histological procedures

After harvesting the specimens (the subcutaneous implants and femoral condyles), the specimens were fixated in 4% formaldehyde for 2 days, followed by dehydration in a graded series of ethanol and embedding in methylmethacrylate (MMA). After polymerization of the specimens, histological analysis was done. Therefore, for both subcutaneous implants and femoral condyles, thin sections (10

μm) were prepared perpendicular to the medial-lateral drilling axis of the implants using a microtome with a diamond blade (Leica Microsystems SP 1600, Nussloch, Germany) [25]. At least, three sections of each specimen were stained with methylene blue and basic fuchsin.

Histological and histomorphometrical evaluation

A histological grading scale was used to evaluate the capsule thickness, tissue response of the capsule surrounding the subcutaneous implants and the tissue directly adjacent to the implant surface in four pre-determined fields using light microscopy as previously reported (Table 2) [26, 27]. At least three sections of each specimen were examined using light microscopy (Leica Microsystems AG, Wetzlar, Germany). Two experienced observers (AR and FW) performed the scoring in a blinded manner.

The femoral condyle defects were quantitatively scored using computer-based image analysis techniques (Leica® Qwin Pro-image analysis system, Wetzlar, Germany) by defining a 3 mm diameter circular area (i.e. the diameter of the created defects) superimposed on the bone defect area as the region of interest (ROI). From digital images (magnification 2,5X), the amount of CPC and bone tissue within this ROI were determined [9].

Statistical analysis

Statistical analyses of material degradation and bone formation were performed using SPSS, version 16.0 (SPSS Inc., Chicago, IL, USA). The statistical comparisons were performed using a one-way analysis of variance (ANOVA) with a Tukey multiple comparison post-test. Differences were considered significant at P-values < 0.05.

Results

Materials characterization

Morphological examination of BG granulate revealed that the BG particles had an irregular structure with an average particle size of around 2.5 μm (Figure 1A). The preparation of PLGA-microparticles via the single-emulsion solvent-extraction technique resulted in PLGA-microparticles with an average size of $40 \pm 4 \mu\text{m}$. Morphological examination using SEM revealed that the PLGA-microparticles had a spherical appearance with a smooth surface (Figure 1B). SEM evaluation of the CPC surface showed a nanoporous structure (Figure 1C). Surface examination of CPC/BG, CPC/PLGA and CPC/PLGA/BG with SEM showed homogenous distribution of BG granulate and/or PLGA-microparticles within CPC, respectively (Figure 1D-F).

Table 2 Modified Histological Grading Scale for Soft Tissues

Evaluation	Response	Score
Capsule thickness	1–4 cell layers	4
	5–9 cell layers	3
	10–30 cell layers	2
	>30 cell layers	1
	Not applicable	0
Tissue response of the capsule surrounding the implants	Fibrous, mature, not dense, resembling connective or fat tissue in the noninjured regions.	4
	Fibrous, but immature, showing fibroblasts and little collagen.	3
	Granulous and dense, containing both fibroblasts and many inflammatory cells.	2
	Consists of masses of inflammatory cells with little or no signs of connective tissue organization.	1
	Cannot be evaluated because of infection or factors not necessarily related to the material.	0
Tissue response directly adjacent to the implant surface (Interface)	Fibroblasts contact the implant surface without the presence of macrophages or foreign body giant cells.	4
	Scattered foci of macrophages and foreign body cells are present.	3
	One layer of macrophages and foreign body cells is present.	2
	Multiple layers of macrophages and foreign body cells are present.	1
	Cannot be evaluated because of infection or other factors not necessarily related to the material.	0

Porosity measurements demonstrated total porosity values (due to intrinsic nanoporosity) of $40.6 \pm 0.7\%$ and $41.6 \pm 0.8\%$ for CPC and CPC/BG, respectively. Composite cements containing PLGA microparticles showed values of $40.5 \pm 1.2\%$ (macroporosity) and $55.7 \pm 0.9\%$ (total porosity) for CPC/PLGA and $41.2 \pm 0.8\%$ (macroporosity) and $56.5 \pm 1.5\%$ (total porosity) for CPC/PLGA/BG (Table 1).

General observation of the experimental animals

From the 24 animals used in this study, two animals were lost due to an anesthesia-induced respiratory depression, of which one animal received 2 femoral condyle implants and the second animal received 2 femoral condyle implants and 4 subcutaneous implants. The remaining animals recovered uneventfully from the surgical procedure and remained in good health during the entire implantation period. No clinical sign of inflammation or adverse tissue response were observed during the implantation period. At the end of the experiment, 44 subcutaneous implants were retrieved, of which 43 were used for analysis (1 CPC/PLGA/BG implant was excluded from analysis due to implant fracturing during histological processing). Furthermore, a total of 44 femoral condyle implants were retrieved

and all of them were included for analyses. An overview of the number of implants placed, retrieved and used for analysis is presented in Tables 3.

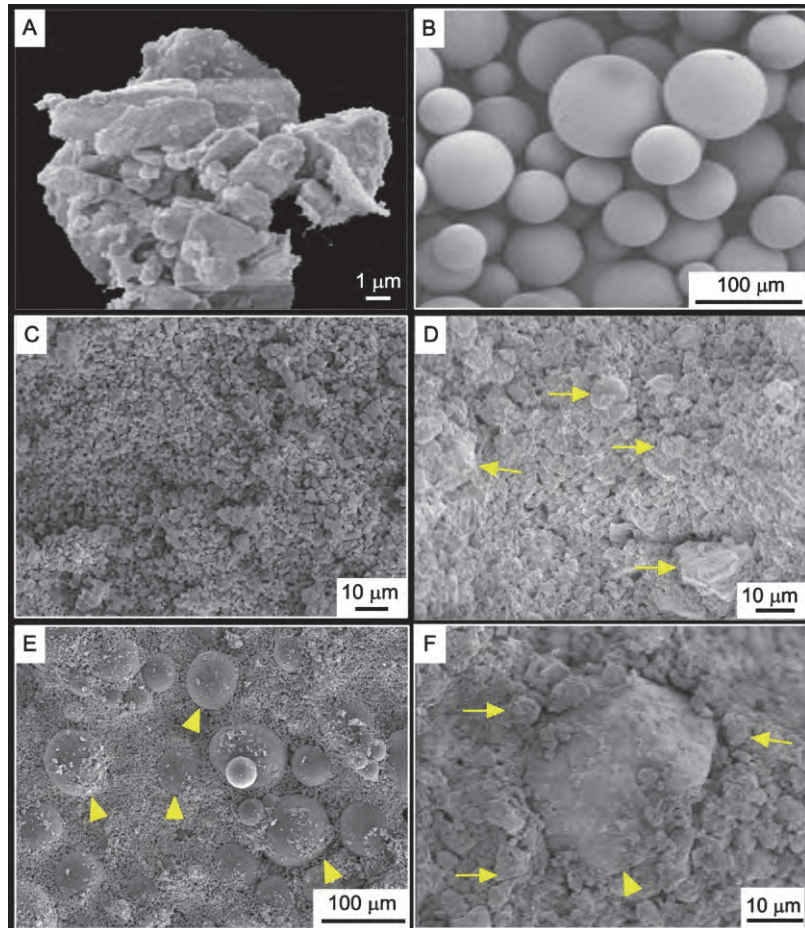


Figure 1 SEM micrographs of the (A) BG particles (B) dense PLGA-microparticles, (C) CPC, (D) CPC/BG, (E) CPC/PLGA and (F) CPC/PLGA/BG. BG (arrow) and PLGA-microparticles (arrowheads) are indicated in the SEM micrographs. Bar represents 1, 10 or 100 μm.

INCORPORATION OF BIOACTIVE GLASS IN CALCIUM PHOSPHATE CEMENT

Table 3 Number of implants placed, retrieved and used for histological analyses for the subcutaneous implants and femoral condyle defect implants

Week	Implants placed		Implants retrieved		Implants used for analysis	
	2	6	2	6	2	6
Subcutaneous implants						
CPC	6	6	5 ^a	6	5	6
CPC/BG	6	6	5 ^a	6	5	6
CPC/PLGA	6	6	5 ^a	6	5	6
CPC/PLGA/BG	6	6	5 ^a	6	5	5 ^b
Femoral Condyle implants						
CPC	6	6	5 ^a	6	5	6
CPC/BG	6	6	5 ^a	6	5	6
CPC/PLGA	6	6	6	5 ^a	6	5
CPC/PLGA/BG	6	6	6	5 ^a	6	5

CPC, Calcium phosphate cement; BG, Bioactive glass; CPC/BG, BG incorporated into CPC; CPC/PLGA, dense PLGA-microparticles incorporated into CPC; CPC/PLGA/BG, dense PLGA-microparticles and BG incorporated into CPC; wt. %, weight percentage; ^a Deviation from number of implants placed due to animal dead or ^b deviation from number of implants retrieved due to fracturing of implants during to the histological processing.

Descriptive histology of subcutaneous implants

Two weeks

Representative histological sections of all experimental groups 2 weeks after implantation are depicted in Figure 2. CPC and CPC/BG revealed no sign of material degradation and the implants were visual as a dense material (Figure 2A and C). CPC/PLGA showed PLGA-microparticle degradation, which was visualized by the formation of pores within the material (Figure 2E). CPC/PLGA/BG revealed clear degradation and changes in the morphological shape of the implants (Figure 2G). At a higher magnification, CPC, CPC/BG, CPC/PLGA/BG implants were found to be surrounded by a medium-thick granulous capsule of 10-30 cell layers containing moderate numbers of inflammatory cells and fibroblasts (Figure 2B, D and H). CPC/PLGA showed the presence of a granulous capsule consisting of more than 30 cell layers and large numbers of inflammatory cells were present within the capsule (Figure 2F). Directly adjacent to the surface of the CPC, CPC/BG, and CPC/PLGA/BG implants (interface), moderate numbers of multinucleated giant-cells were observed, while at the interface of CPC/PLGA, many multinucleated giant-cells were seen.

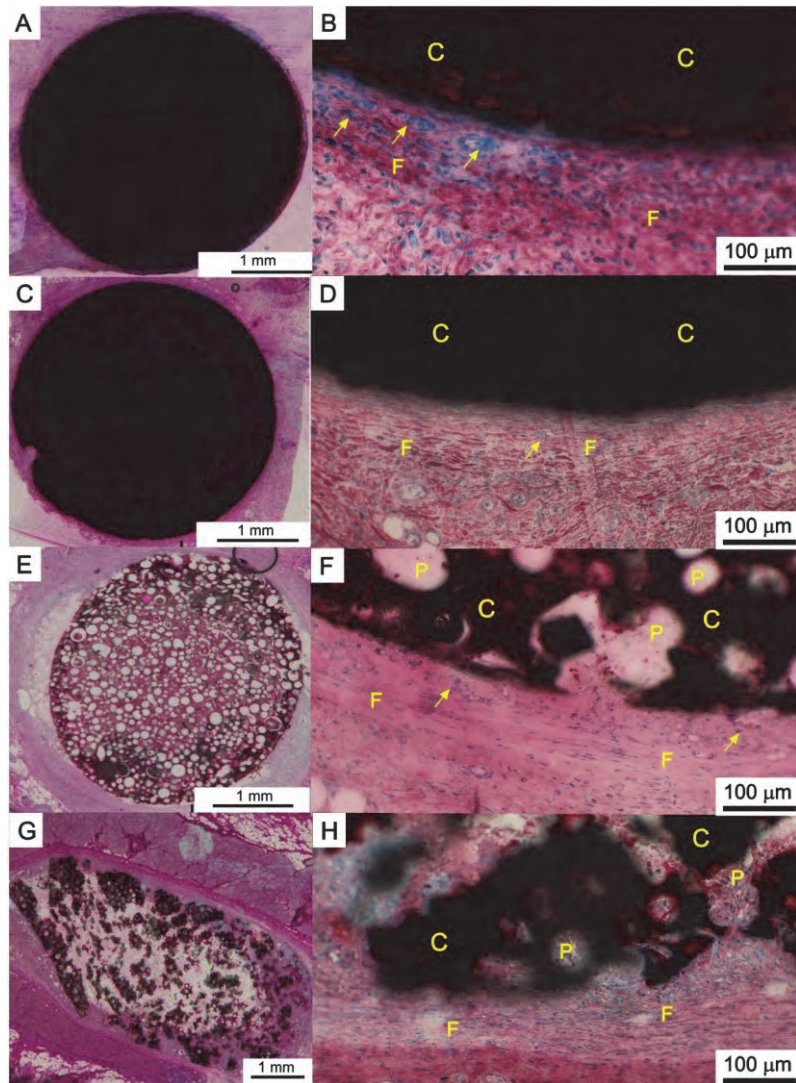


Figure 2 Representative histological sections of subcutaneous implants of the four experimental groups after two weeks of implantation; CPC (A-B), CPC/BG (C-D), CPC/PLGA (E-F) and CPC/PLGA/BG (G-H). Bar represents 1 mm. Composite material (C), Fibrous tissue (F), degraded PLGA-pores (P), and multi-nucleated giant cells (arrows) are indicated in the sections. Bar represents 100 μm. Methylene blue and basic fuchsin staining.

Six weeks

Representative histological sections of all experimental groups 6 weeks after implantation are depicted in Figure 3.

CPC and CPC/BG revealed no sign of material degradation and the implants were visual as dense material (Figure 3A and C). Implant degradation had continued for CPC/PLGA and CPC/PLGA/BG, showing most degradation in the periphery of CPC/PLGA (Figure 3E) with the larger extent of degradation for CPC/PLGA/BG (Figure 3G). Additionally, CPC/PLGA and CPC/PLGA/BG showed tissue ingrowth in the degrading areas of the implant.

At higher magnification, all experimental groups revealed a thinner capsule surrounding the implant compared to their 2-weeks implanted equivalents with a capsule thickness of 5-9 cell layers for CPC and 1-4 cell layers for the other formulations. The capsules surrounding CPC and CPC/BG consisted of fibroblasts (Figures 3B and 3D). CPC/PLGA and CPC/PLGA/BG implants were surrounded by a mature fibrous capsule which resembled connective tissue in the non-injured regions (Figures 3F and 3H). For CPC, CPC/BG and CPC/PLGA implants, still multi-nucleated giant-cells were present at the interface. For CPC/PLGA/BG, the fibrous capsule was in close contact with the implant surface without the presence of macrophages or multi-nucleated giant cells.

Quantitative histological evaluation of subcutaneous implants

Two weeks after implantation, statistical analysis of the quantitative histological data revealed a significantly thicker capsule for CPC/PLGA compared to all other formulations (Figure 4A; $p < 0.05$). In addition, a significantly more mature capsule and interface was observed for CPC/BG and CPC/PLGA/BG compared to CPC/PLGA (Figures 4B and 4C, respectively; $p < 0.05$). With increasing implantation time, the capsule thickness, capsule quality and interface quality significantly improved for all experimental groups ($p < 0.01$). At 6 weeks, a significantly thinner capsule surrounding CPC/PLGA/BG was observed compared to CPC and CPC/BG (Figure 4A; $p < 0.05$). Moreover, the quality of the capsule and interface was significantly more mature for CPC/BG/PLGA compared to CPC and CPC/BG (Figures 4B and 4C respectively; $p < 0.05$).

Descriptive histology of femoral condyle implants

Two weeks

An overview of representative histological sections of all experimental groups after a 2 week implantation period is depicted in Figure 5. Although the majority of the implants within the femoral condyle defect were placed correctly, implantation was occasionally imprecise as the bone defect crossed the growth plate or somewhat too much toward the edge of the femoral condyle.

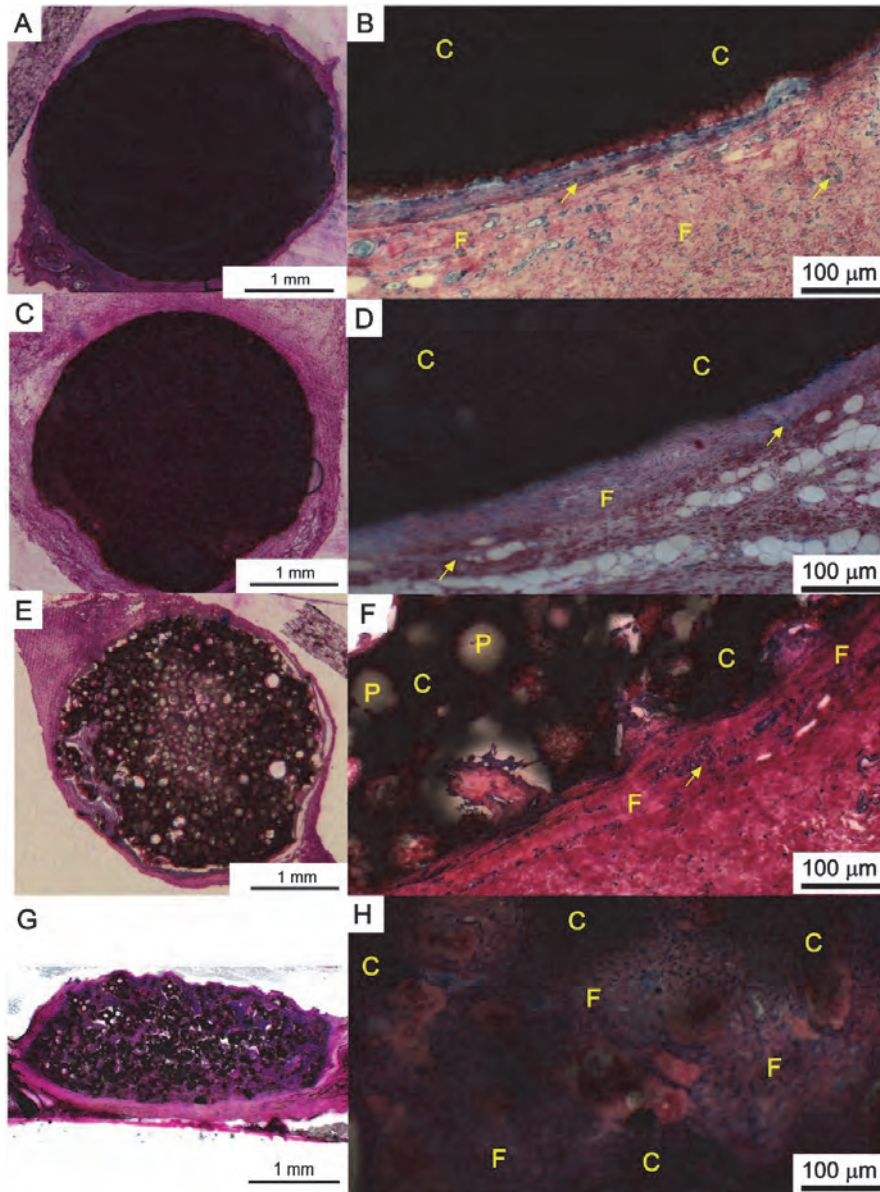


Figure 3 Representative histological sections of subcutaneous implants of the four experimental groups after six weeks of implantation; CPC (A-B), CPC/BG (C-D), CPC/PLGA (E-F) and CPC/PLGA/BG (G-H). Bar represents 1 mm. Composite material (C), Fibrous tissue (F), degraded PLGA-pores (P), and multi-nucleated giant cells (arrows) are indicated in the sections. Bar represents 100 μm. Methylene blue and basic fuchsin staining.

INCORPORATION OF BIOACTIVE GLASS IN CALCIUM PHOSPHATE CEMENT

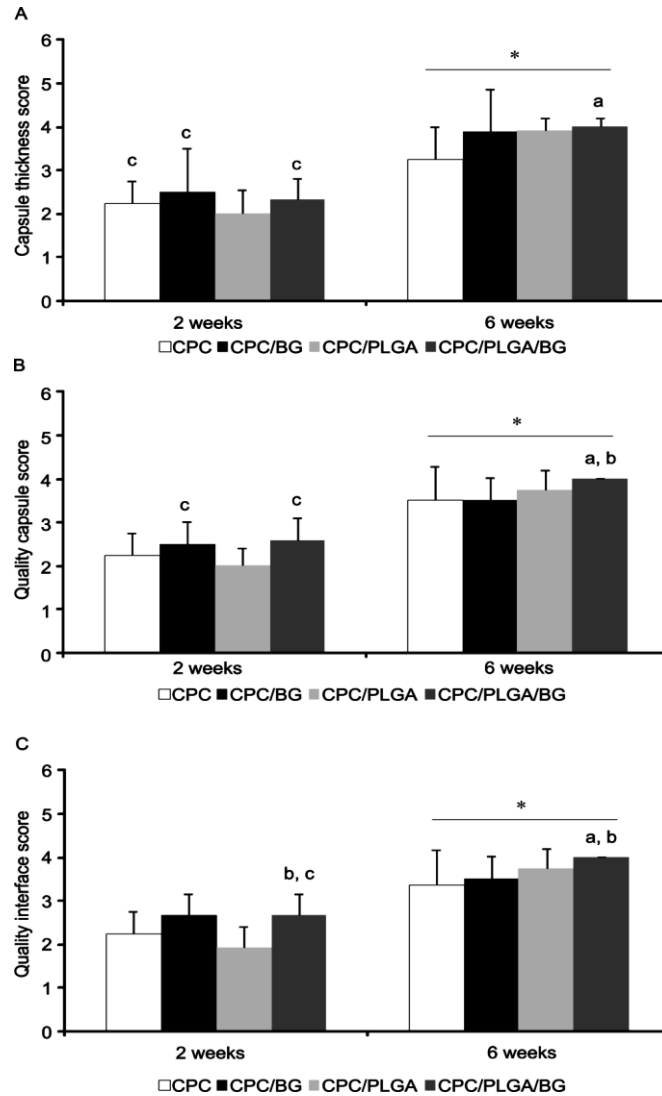


Figure 4 Histological evaluation of capsule thickness (A), the quality of the capsule (B) and the quality of the interface (C) of the different subcutaneous implants i.e. CPC, CPC/BG, CPC/PLGA and CPC/PLGA/BG after 2 and 6 weeks implantation using the histological grading scale. Error bars represent means \pm standard deviation. (a) $p < 0.05$ compared to CPC; (b) $p < 0.05$ compared to CPC/BG; (c) $p < 0.05$ compared to CPC/PLGA; (*) $p < 0.05$ compared to 2-weeks equivalent.

Both CPC and CPC/BG showed no signs of degradation, but rather a tight interaction with the surrounding bone (Figures 5A-D). For CPC/PLGA, the integrity of the implant was slightly affected peripherally, with soft tissue in the contact area between the edges of the bone defect and the implant. Limited newly formed bone was observed in the periphery of the implant (Figure 5E and F). For CPC/PLGA/BG, the integrity of the implant was completely affected. Degradation of the material allowed the ingrowth of soft tissue accompanied by some bone formation in the central defect region. The region between the implant and the edges of the original defect was either filled with soft tissue or a close contact between bone tissue and implant was observed throughout the degraded material (Figure 5G and 5H).

Six weeks

An overview of representative histological sections of all experimental groups after a 6 week implantation period is depicted in Figure 6.

A limited degradation at the peripheral area of the implants was noticed for CPC. In the contact area between the defect border and CPC, fibrous tissue was observed and, occasionally, bone remodeling was found (Figure 6A and B). For CPC/BG, very limited degradation of the material was seen in the peripheral region of the implant, with newly formed bone in the areas where CPC/BG had degraded (Figure 6C and D). For CPC/PLGA, material degradation had continued leaving lower amounts of material in the defect area compared to the 2 week implantation period. Moreover, in the created PLGA-pores located in the central region of the implants soft tissue and some bone ingrowth was observed. The peripherally located PLGA-pores were always filled with bone tissue (Figure 6E and F). The degradation of CPC/PLGA/BG had continued and the material was almost completely degraded after 6 weeks. In addition, throughout the defect area bone ingrowth was found (Figure 6G and H).

Histomorphometry of tissue response to femoral condyle implants

Scaffold degradation

Quantitative results on scaffold degradation are presented in Figure 7A. After 2 weeks of implantation, CPC/PLGA and CPC/PLGA/BG revealed significantly lower amounts of material within the ROI compared to CPC and CPC/BG ($p < 0.05$). With increasing implantation time, CPC/BG, CPC/PLGA and CPC/PLGA/BG showed significantly more scaffold degradation ($p < 0.05$), while no temporal differences were observed for CPC. At 6 weeks, the material amount for CPC/BG, CPC/PLGA and CPC/PLGA/BG were significantly lower compared to CPC ($p < 0.05$). In addition, the amount of material for CPC/PLGA/BG was significantly decreased compared to CPC/BG and CPC/PLGA. No differences were observed between CPC/BG and CPC/PLGA ($p = 0.75$); the amount of material in ROI ranged for CPC from $92 \pm 4\%$ to $96 \pm 4\%$ after 6 weeks; for CPC/BG from $78 \pm 9\%$ to $52 \pm 2\%$ after 6

weeks; for CPC/PLGA from $56 \pm 13\%$ to $47 \pm 2\%$ after 6 weeks; for CPC/PLGA/BG from $35 \pm 14\%$ to $10 \pm 3\%$ after 6 weeks).

Bone formation

Quantitative results on bone formation within the ROI are depicted in Figure 7B. After 2 weeks of implantation, no significant differences in bone formation were observed between the different scaffolds. With increasing implantation time, the amount of bone for CPC/BG, CPC/PLGA and CPC/PLGA/BG had significantly increased ($p < 0.05$). At 6 weeks, histomorphometrical analysis revealed significantly more bone formation for CPC/PLGA/BG compared to the other formulations ($p < 0.05$) as well as for CPC/BG and CPC/PLGA compared to CPC ($p < 0.05$; amount of bone formation ranged for CPC from $6 \pm 4\%$ to $13 \pm 4\%$ after 6 weeks; for CPC/BG from $11 \pm 4\%$ to $29 \pm 3\%$ after 6 weeks; for CPC/PLGA from $6 \pm 5\%$ to $32 \pm 7\%$ after 6 weeks; for CPC/PLGA/BG from $10 \pm 3\%$ to $42 \pm 10\%$ after 6 weeks).

Discussion

This study aimed to evaluate the effects on *in vivo* tissue response after incorporating BG into CPC (with or without PLGA-microparticles) using subcutaneous implantation and implantation into femoral condyle defects in rats after 2 and 6 weeks. It was hypothesized that addition of BG would not negatively affect the biocompatibility of CPC and CPC/PLGA and would have a positive effect on the formation of bone. The main findings of the subcutaneous implantation showed that BG incorporation had indeed a favorable effect on soft tissue responses in terms of capsule thickness, capsule quality and interface quality. In addition, the femoral condyle defect model revealed that incorporation of BG into CPC or CPC/PLGA significantly accelerated material degradation and enhanced bone formation.

Severe inflammatory response and tissue irritation caused by biomaterials can result in a delay of healing processes [28]. It is well known that the tissue response to an implanted biomaterial is determined by its chemical composition, which will dictate the intensity of the foreign body reaction and inflammatory process [28]. Several studies demonstrated that CPC, CPC/PLGA and BG alone are non-toxic and biocompatible [6, 9, 18, 27, 29-32]. In addition, Lee *et al.* (2010) observed enhanced soft tissue adaption after implantation of titanium implants coated with BG in combination with hydroxy-apaptite (HA). These findings are in line with the results of the current study, which demonstrated that CPC, either pure or combined with PLGA-microparticles and/or BG, does not evoke any severe inflammatory responses. Moreover, in the early post-implantation period, the incorporation of BG into CPC or CPC/PLGA enhanced the soft tissue reaction, evidenced by a thinner fibrous capsule with a better interface.

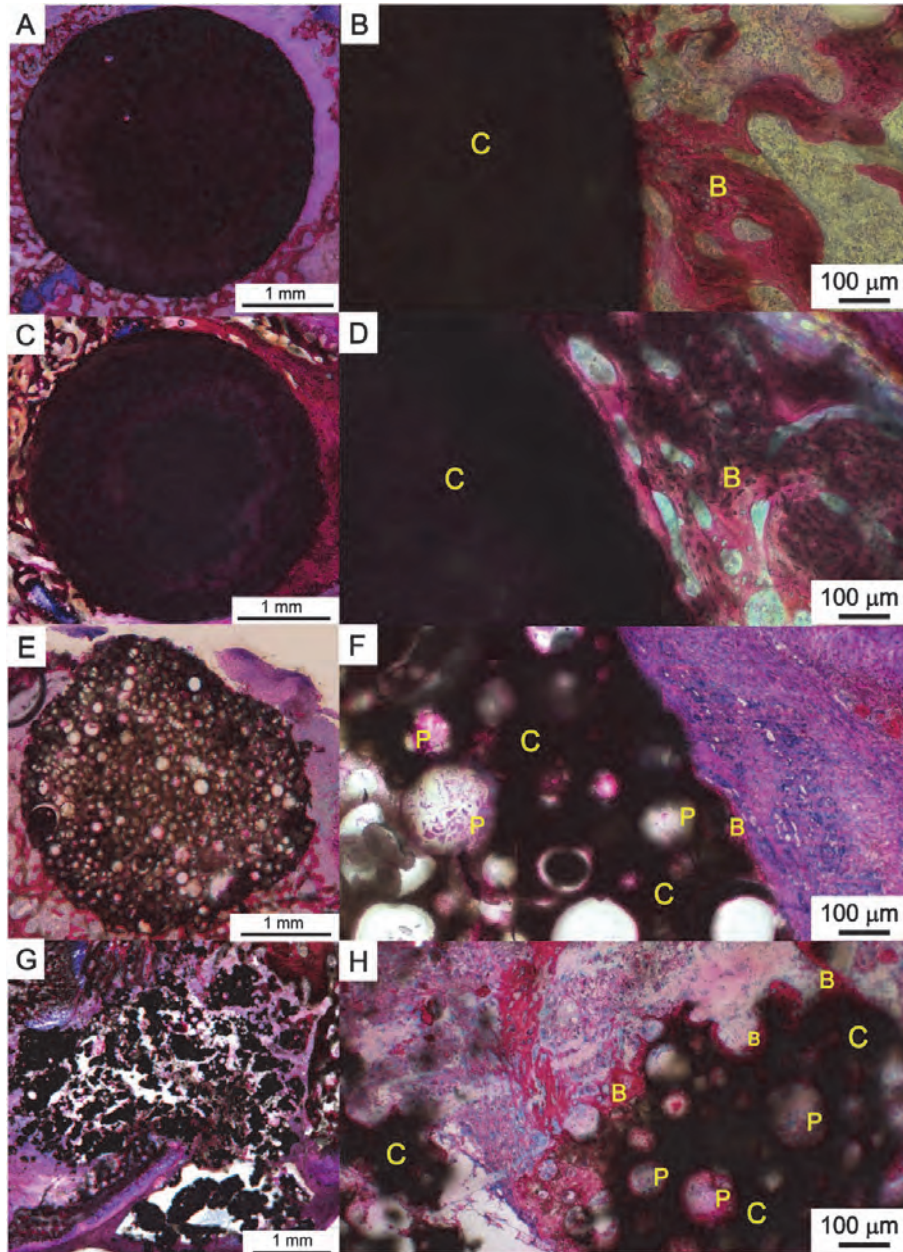


Figure 5 Representative histological sections of four experimental groups after two weeks of implantation in the femoral condyle defect; CPC (A-B), CPC/BG (C-D), CPC/PLGA (E-F) and CPC/PLGA/BG (G-H). Bar represents 1 mm. Composite material (C), Bone formation (B) and degraded PLGA-pores (P) are indicated in the sections. Bar represents 100 μm. Methylene blue and basic fuchsin staining.

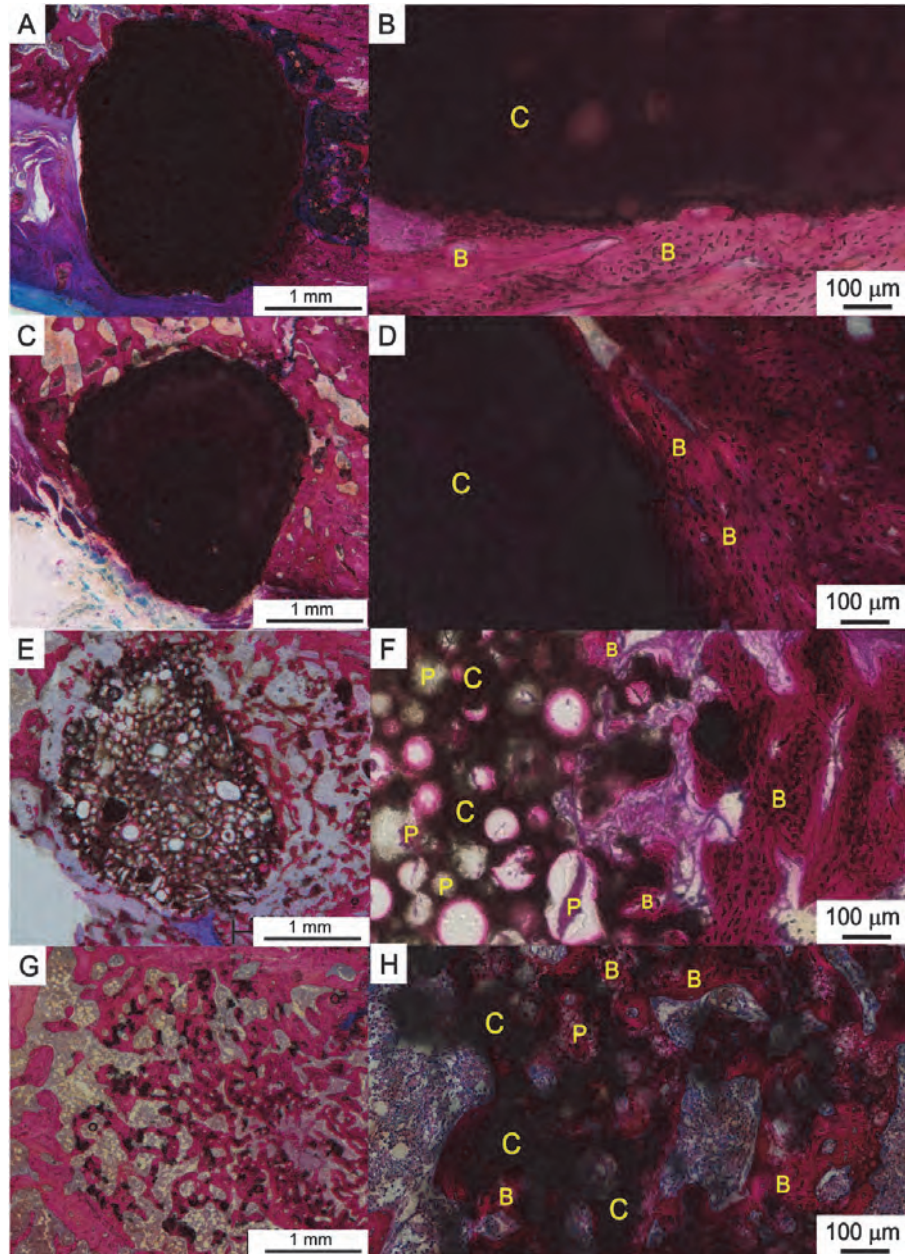


Figure 6 Representative histological sections of four experimental groups after six weeks of implantation in the femoral condyle defect; CPC (A-B), CPC/BG (C-D), CPC/PLGA (E-F) and CPC/PLGA/BG (G-H). Bar represents 1 mm. Composite material (C), Bone formation (B) and degraded PLGA-pores (P) are indicated in the sections. Bar represents 100 μm . Methylene blue and basic fuchsin staining.

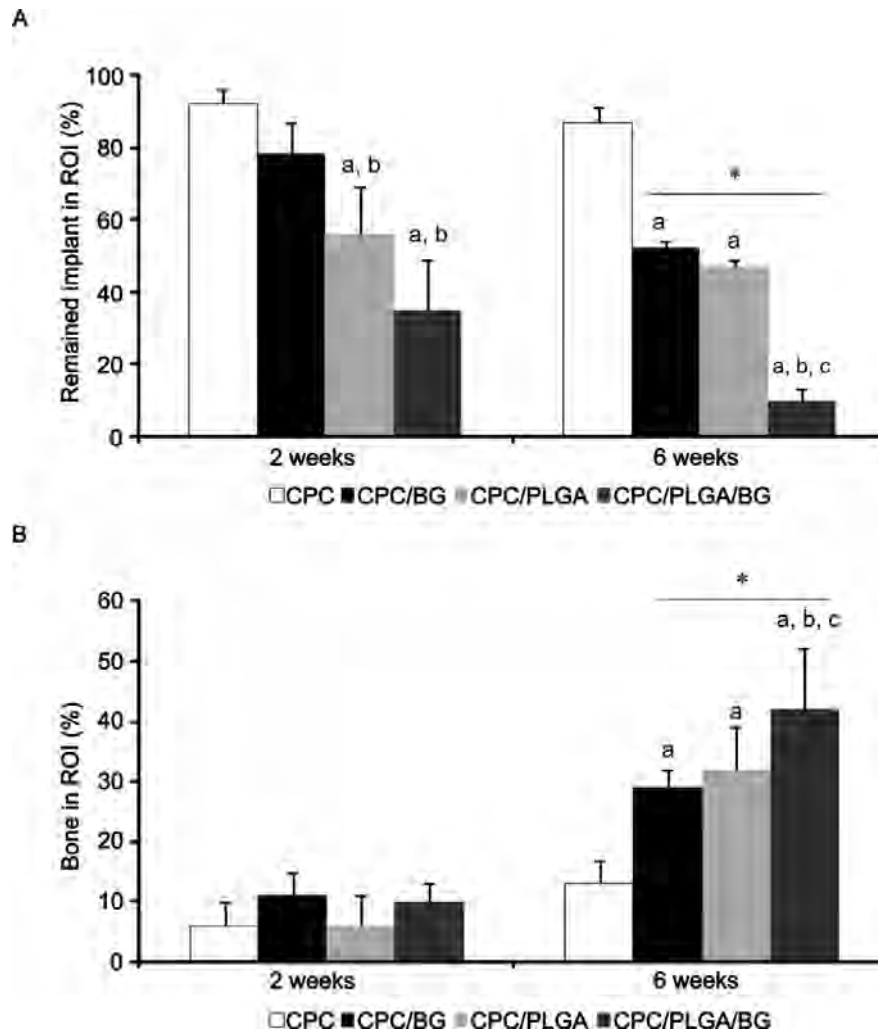


Figure 7 Results of histomorphometrical evaluation of the different formulations, i.e. CPC, CPC/BG, CPC/PLGA and CPC/PLGA/BG. (A) The amount of remained implant and (B) the amount of newly formed bone after 2 and 6 weeks are expressed as percentage of ROI (i.e. a standardized region of interest with similar dimensions as created defect). Error bars represent means \pm standard deviation. (a) $p < 0.05$ compared to CPC; (b) $p < 0.05$ compared to CPC/BG; (c) $p < 0.05$ compared to CPC/PLGA; (*) $p < 0.05$ compared to 2-weeks equivalent.

With increasing implantation time, the different CPC-formulations facilitated a relatively mild soft tissue reaction with a superiority for the CPC-formulation with BG incorporated into CPC/PLGA.

For the replacement of bone, resorption of the bone substitute material (e.g. biodegradation of the material) is required, since formation of new bone tissue and ingrowth thereof in the defect area needs the liberation of space [29, 33, 34]. The results of the current study indicate that the degradation rate of the material indeed substantially influences the formation of bone, as with increasing implant degradation higher amounts of newly-formed bone were observed. The inclusion of dense PLGA-microparticles within CPC has been previously demonstrated to result in improved CPC degradation and hence bone formation due to the release of lactic and glycolic acidic monomers, which produce an acidic environment that acts as a stimulus for CPC dissolution [3, 9]. The increased implant degradation observed for BG-supplemented CPC might be related to the increased BG dissolution immediately after contact with fluids [35, 36] resulting in lower amount of remaining implant material at an earlier time point compared to the slow degradable pure CPC. It is likely that the superior biological performance of BG combined with PLGA-microparticles supplemented CPC is determined by the positive effects of both BG and PLGA on the material degradation. Additionally, upon implantation, ionic dissolution products of BG have been shown to beneficially affect osteogenesis by attracting osteoprogenitor cells and by stimulating the differentiation into matrix-producing osteoblasts [14-18]. Furthermore, it has reported that BG has a stimulatory effect on neovascularisation by stimulating the secretion of angiogenic factors [35, 37], which together with the osteopromotive properties of BG might further influence bone formation when using BG-supplemented CPC, either pure or supplemented with PLGA. However, the current study addressed the effect of BG inclusion in CPC based on histological analysis rather than at cell level. Consequently, direct evidence of osteopromotion and angiogenesis by BG are not available from the current study. Nevertheless, the outcome of the current study confirmed our hypothesis that BG can improve the biological performance of CPC and CPC/PLGA after 6 weeks of implantation. Consequently, BG-supplemented CPC might be promising to improve the performance of CPC required for compromised conditions. However, in view of the differences in bone metabolism in healthy compared to compromised conditions (e.g. osteoporosis), the biological performance of BG-supplemented CPC might be different. As this study was limited to relatively short-term evaluation of the performance of preset BG-supplemented CPC under optimal conditions to provide full control over the complete filling of the defect, information on the long-term performance of the (injectable) material and under compromised conditions remains to be provided.

In conclusion, BG incorporation into CPC (or CPC/PLGA) improved the soft tissue response upon ectopic implantation compared to pure CPC (or CPC/PLGA). In addition, incorporating BG within CPC accelerated material degradation and increased bone formation in a femoral condyle defect in rats. Consequently, these

data highlight the potential of BG to be used as an additive to CPC to improve the biological performance for bone regeneration applications. Further long-term studies should be carried out to provide additional information concerning the late stages of material degradation and bone regeneration induced by the CPC/PLGA cements including BG. In addition, further research is required to evaluate the biological performance of BG supplemented CPC in compromised situations.

Acknowledgements

The authors gratefully acknowledge the support of the Smart Mix Program of the Netherlands Ministry of Economic Affairs and the Netherlands Ministry of Education, Culture and Science. The authors would like to thank Natasja van Dijk for assistance with the histological preparations. Scanning electron microscopy was performed at the Nijmegen Center for Molecular Life Sciences (NCMLS), the Netherlands

References

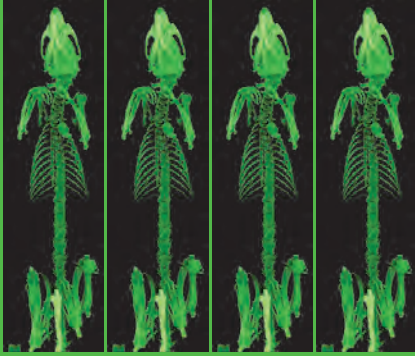
- [1] W. Habraken, J. Wolke, J. Jansen, Ceramic composites as matrices and scaffolds for drug delivery in tissue engineering. *Adv Drug Deliv Rev* 59 (2007) 234-48.
- [2] E. Bodde, W. Habraken, A. Mikos, P. Spauwen, J. Jansen, Effect of Polymer Molecular Weight on the Bone Biological Activity of Biodegradable Polymer/Calcium Phosphate Cement Composites. *Tissue Eng Part A* 15 (2009) 3183-91.
- [3] R. Félix Lanao, S. Leeuwenburgh, J. Wolke, J. Jansen, In vitro degradation rate of apatitic calcium phosphate cement with incorporated PLGA microspheres. *Acta Biomater* 7 (2011) 3459-68.
- [4] H. Liao, X. Walboomers, W. Habraken, Z. Zhang, Y. Li, D. Grijpma, Injectable calcium phosphate cement with PLGA, gelatin and PTMC microspheres in a rabbit femoral defect. *Acta Biomater* 7 (2011) 1752-9.
- [5] W. Habraken, J. Wolke, A. Mikos, J. Jansen, PLGA microsphere/calcium phosphate cement composites for tissue engineering: in vitro release and degradation characteristics. *J Biomater Sci Polym Ed* 19 (2008) 1171-88.
- [6] E. Bodde, C. Cammaert, J. Wolke, P. Spauwen, J. Jansen, Investigation as to the osteoinductivity of macroporous calcium phosphate cement in goats. *J Biomed Mater Res B* 83B (2007) 161-8.
- [7] P. Ruhé, O. Boerman, F. Russel, A. Mikos, P. Spauwen, J. Jansen, In vivo release of rhBMP-2 loaded porous calcium phosphate cement pretreated with albumin. *J Mater Sci Mater Med* 17 (2006) 919-27.
- [8] D. Link, J. van den Dolder, J. van den Beucken, V. Cuijpers, J. Wolke, A. Mikos, J. Jansen, Evaluation of the biocompatibility of calcium phosphate cement/PLGA microparticle composites. *J Biomed Mater Res A* 87A (2008) 760-9.
- [9] R. Félix Lanao, S. Leeuwenburgh, J. Wolke, J. Jansen, Bone response to fast-degrading, injectable calcium phosphate cements containing PLGA microparticles. *Biomaterials* 32 (2011) 8839-47.
- [10] W. Habraken, J. Wolke, A. Mikos, J. Jansen, Injectable PLGA microsphere/calcium phosphate cements: physical properties and degradation characteristics *J Biomater Sci Polym Ed* 17 (2006) 1057-74.
- [11] P. Ruhé, E. Hedberg, N. Padron, P. Spauwen, J. Jansen, A Mikos, rhBMP-2 Release from Injectable Poly(DL-Lactic-co-glycolic Acid)/Calcium-Phosphate Cement Composites. *J Bone Joint Surg Am* 85 (2003) 75-81.

INCORPORATION OF BIOACTIVE GLASS IN CALCIUM PHOSPHATE CEMENT

- [12] A. Plachokova, D. Link, J. van den Dolder, J. van den Beucken, J. Jansen, Bone regenerative properties of injectable PGLA–CaP composite with TGF- β 1 in a rat augmentation model. *J Tissue Eng Regen Med* 1 (2007) 457-64.
- [13] E. Bodde, O. Boerman, F. Russel, A. Mikos, P. Spauwen, J. Jansen, The kinetic and biological activity of different loaded rhBMP-2 calcium phosphate cement implants in rats. *J Biomed Mater Res A* 87A (2008) 780-91.
- [14] V. Välimäki, H. Aro, Molecular basis for the action of bioactive glasses as bone graft. *Scandinavian Journal of Surgery* 95 (2006) 95–102.
- [15] L. Hench, J. Polak, Third-generation biomedical materials. *Science* 295 (2002) 1014-7.
- [16] I. Xynos, A. Edgar, L. Buttery, L. Hench, J. Polak, Ionic Products of Bioactive Glass Dissolution Increase Proliferation of Human Osteoblasts and Induce Insulin-like Growth Factor II mRNA Expression and Protein Synthesis. *Biochem Biophys Res Commun* 276 (2000) 461-5.
- [17] L. Hench, I. Xynos, J. Polak, Bioactive glasses for in situ tissue regeneration. *J Biomater Sci Polym Ed* 15 (2004) 543-62.
- [18] J. Moura, L. Teixeira, C. Ravagnani, O. Peitl, E. Zanotto, M. Beloti, In vitro osteogenesis on a highly bioactive glass-ceramic (Biosilicate®). *J Biomed Mater Res A* 82A (2007) 545-57.
- [19] Z. Huan, S. Leeflang, J. Zhou, W. Zhai, J. Chang, J. Duszczak, In vitro degradation behavior and bioactivity of magnesium-Bioglass® composites for orthopedic applications. *J Biomed Mater Res B* 100B (2012) 437-46.
- [20] E. Schepers, P. Ducheyne, Bioactive glass particles of narrow size range for the treatment of oral bone defects: a 1–24 month experiment with several materials and particle sizes and size ranges. *J Oral Rehabil* 24 (1997)
- [21] H. Oonishi, L. Hench, J. Wilson, F. Sugihara, E. Tsuji, S. Kushitani, Comparative bone growth behavior in granules of bioceramic materials of various sizes. *J Biomed Mater Res* 44 (1999) 31-43.
- [22] R. Granito, A. Rennó, C. Ravagnani, P. Bossini, D. Mochiuti, V. Jorgetti, In vivo biological performance of a novel highly bioactive glass-ceramic (Biosilicate®): A biomechanical and histomorphometric study in rat tibial defects. *J Biomed Mater Res B* 97B (2011) 139-47.
- [23] A. Renno, M. Nedjadnik, F. van de Watering, M. Crovace, E. Zanotto, J. Wolke, J. Jansen, J. van den Beucken, Incorporation of bioactive glass in calcium phosphate cement. Part I: in vitro evaluation, manuscript in preparation
- [24] E. Zanotto, C. Ravagnani, O. Peitl, H. Panzeri, L. EH, Process and compositions for preparing particulate, bioactive or resorbable biosilicates for use in the treatment of oral ailments, WO2004/074199, Fundação Universidade Federal De São Carlos; Universidade De São Paulo, 20 Feb. 2004, Int. C. C03C10/00.
- [25] H. van der Lubbe, C. Klein, K. de Groot, A simple method for preparing thin (10 microM) histological sections of undecalcified plastic embedded bone with implants. *Stain Technol* 63 (1988) 171-6.
- [26] J. Jansen, W. Dhert, J. van der Waerden, A. von Recum, Semi-quantitative and qualitative histological analysis method for the evaluation of implant biocompatibility. *J Invest Surg* 7 (1994) 123-34.
- [27] D. Link, J. van den Dolder, J. van den Beucken, V. Cuijpers, J. Wolke, A. Mikos, J. Jansen Evaluation of the biocompatibility of calcium phosphate cement/PLGA microparticle composites. *J Biomed Mater Res A* 87A (2008) 760-9.
- [28] J. Anderson, A. McNally, Biocompatibility of implants: lymphocyte/macrophage interactions. *Seminars in Immunopathology* 33 (2011) 221-33.
- [29] F. van de Watering, J. van den Beucken, X. Walboomers, J. Jansen, Calcium phosphate/poly(d,l-lactic-co-glycolic acid) composite bone substitute materials: evaluation of temporal degradation and bone ingrowth in a rat critical-sized cranial defect. *Clin Oral Implants Res* 23 (2012) 151-9.

CHAPTER 3

- [30] R. Day, V. Maquet, A. Boccaccini, R. Jérôme, A. Forbes, In vitro and in vivo analysis of macroporous biodegradable poly(D,L-lactide-co-glycolide) scaffolds containing bioactive glass. *J Biomed Mater Res A* 75A (2005) 778-87.
- [31] G. Vargas, R. Mesones, O. Bretcanu, J. López, A. Boccaccini, A Gorustovich, Biocompatibility and bone mineralization potential of 45S5 Bioglass®-derived glass-ceramic scaffolds in chick embryos. *Acta Biomater* 5 (2009) 374-80.
- [32] M. Vogel, C. Voigt, C. Knabe, R. Radlanski, U. Gross, C. Müller-Mai, Development of multinuclear giant cells during the degradation of Bioglass® particles in rabbits. *J Biomed Mater Res A* 70A (2004) 370-9.
- [33] P. Ruhé, E. Hedberg, N. Padron, P. Spauwen, J. Jansen, A. Mikos, Biocompatibility and degradation of poly(DL-lactic-co-glycolic acid)/calcium phosphate cement composites. *J Biomed Mater Res A* 74A (2005) 533-44.
- [34] X. Qi, J. Ye, Y. Wang, Improved injectability and in vitro degradation of a calcium phosphate cement containing poly(lactide-co-glycolide) microspheres. *Acta Biomater* 4 (2008) 1837-45.
- [35] A. Hoppe, N. Gldal, A. Boccaccini, A review of the biological response to ionic dissolution products from bioactive glasses and glass-ceramics. *Biomaterials* 32 (2011) 2757-74.
- [36] M. Rahaman, D. Day, B. Sonny Bal, Q. Fu, S. Jung, L. Bonewald, Bioactive glass in tissue engineering. *Acta Biomater* 7 (2011) 2355-73.
- [37] A. Gorustovich, J. Roether, A. Boccaccini, Effect of Bioactive Glasses on Angiogenesis: A Review of In Vitro and In Vivo Evidences *Tissue Engineering Part B* 16 (2010) 199-207.



CHAPTER 4

Non-glycosylated BMP-2 can induce ectopic bone formation at lower concentrations compared to glycosylated BMP-2

FCJ van de Watering, JJJP van den Beucken, SP van der Woning,
A Briest, A Eek, H Qureshi, L Winnubst, OC Boerman and JA Jansen

Journal of Controlled Release, 159 (2012) 69-77.

Introduction

Bone tissue is one of the most frequently transplanted tissues in many fields, including dentistry and orthopedics [1]. Autologous bone grafts are still considered as the golden standard, albeit that several major drawbacks are related to the transplantation of autologous bone, such as postoperative morbidity, low availability and lack of functional shape of the transplantable tissue. Consequently, research is focusing on the development and evaluation of (synthetic) materials to replace autologous bone in grafting procedures.

Alternative (synthetic) materials for bone grafting are predominantly explored within calcium-based ceramics or cements [2, 3], bioactive glasses [4], polymer-based materials [5], and combinations thereof [6, 7]. Preferably, such synthetic bone substitute materials have osteogenic, osteoinductive, and osteoconductive properties meaning that similar to autologous bone grafts, bone substitute materials are capable of forming new bone tissue, inducing cells to differentiate into osteoblasts, acting as a three-dimensional structure onto which new tissue can grow, respectively. However, many bone substitute materials do not possess all of these characteristics. This makes that such materials are suitable for use in small, well-vascularized areas, but not for bone regenerative treatments in large, critical-sized defects or under compromised medical conditions. Consequently, strategies to enrich (synthetic) materials with biological factors (e.g. cytokines, chemokines, and growth factors) are necessary in order to improve their biological performance. Several members of the transforming growth factor- β family are renowned for their capacity to induce bone formation [8-10], of which the so-called bone morphogenetic proteins (BMPs) are frequently used in bone tissue engineering [8, 11]. BMPs, more specifically BMP-2, play a significant role in the regulation of many steps in bone morphogenesis due to their biological functions that include chemotaxis, differentiation, and mitosis of bone forming cells [11]. For the delivery of BMP-2 to a defect site, suitable carriers are necessary to provide effective availability of BMP-2 to induce differentiation of bone regenerative cells and contribute to bone defect healing [12]. It has been reported that addition of BMP-2 to natural and synthetic polymers [13-15], hydrogels [16], ceramics [17, 18] or composites materials [19, 20] as a carrier results in sustained release and bone formation. It is assumed that the scaffold material needs to be loaded with an "above threshold" amount of exogenous BMP to actuate bone regenerative cells to contribute to bone formation [12, 21, 22]. However, the absolute BMP-2 amounts required to stimulate bone formation vary among the different scaffold materials, emphasizing the lack of consensus on suitable loading amounts [12]. For example, the BMP-2 amounts used in calcium phosphate cement-based materials range from 2 [20] to 30 μg [23]. Either from a biological point of view as well as cost effectiveness, research is focusing on the reduction of the included growth factor. Native BMPs and recombinant equivalents produced in mammalian cells are post-translationally modified through N-linked glycosylation [24], which is a major factor affecting the solubility of BMP-2. Bacterially produced BMPs lack this glycosylation,

leading to a decrease in solubility. Hence, the use of the less soluble non-glycosylated BMP-2 might allow the application of lower BMP doses to induce bone formation [25].

In the present study, the bioactivity and osteoinductive properties of non-glycosylated BMP-2 (ngBMP-2) and glycosylated BMP-2 (gBMP-2) were comparatively evaluated. *In vitro* bioactivity assays, an *in vitro* release assay and an *in vivo* rat subcutaneous model using pre-set calcium phosphate cement (CPC) with adsorbed BMP-2, were used to assess the *in vitro* bioactivity, *in vitro* release profile and to evaluate the ectopic osteoinductive potential of a carrier loaded with ngBMP-2 compared to gBMP-2. It was hypothesized that ngBMP-2 was biologically active and capable of inducing differentiation and mineralization of osteoblast-like cells. In addition, it was hypothesized that due to the effects of glycosylation on solubility the retention of ngBMP-2 to CPC would be higher, resulting in the induction of bone at an ectopic site at lower concentrations compared to gBMP-2 loaded equivalents.

Materials and Methods

Materials

Calcium phosphate cement (CPC) consisted of 85% alpha tri-calcium phosphate (α -TCP; CAM Bioceramics BV, Leiden, The Netherlands), 10% dicalcium phosphate anhydrous (DCPA; J.T. Baker Chemical Co., USA) and 5% precipitated hydroxyapatite (pHA; Merck, Darmstadt, Germany). The CPC powders were ball-milled and had particle sizes of $9.7 \pm 2.0 \mu\text{m}$, $4.5 \pm 1.9 \mu\text{m}$, and $5.0 \pm 1.9 \mu\text{m}$ for α -TCP, pHA, and DCPA, respectively [26]. The cement liquid applied was a sterilized 2 wt.% aqueous solution of Na_2HPO_4 . Acid terminated poly(DL-lactic-co-glycolic acid) (PLGA; Purasorb®, Purac, Gorinchem, the Netherlands) with a lactic to glycolic acid ratio of 50:50 and a molecular weight (M_w) of $17 \pm 0.02 \text{ kg/mol}$ was used for microparticle preparation. Recombinant human ngBMP-2 was kindly provided by dr. P. Hortschansky (Hans Knoell Institute, Jena, Germany). Commercially available recombinant human glycosylated BMP-2 (gBMP-2; R&D Systems MN, USA) was used for comparison.

In vitro studies

Bioactivity assay with C2C12 cell line

The biological activity of both gBMP-2 and ngBMP-2 was tested by the induction of alkaline phosphatase (ALP) activity in C2C12 cells, as described before [27]. C2C12 cells were plated at a density of $2 \times 10^4 \text{ cells/cm}^2$ and grown for 24 h in Dulbecco's Modified Eagle Medium (DMEM; Gibco BRL Life Technologies B.V., Breda, The Netherlands) supplemented with 10 % fetal calf serum (FCS; Gibco). Subsequently, medium was replaced by DMEM containing 5% FCS either in the presence or absence of 1-1000 ng/ml ngBMP-2 or gBMP-2. After 72 hours ALP enzymatic activity

was quantified by measuring the formation of p-nitrophenol from p-nitrophenyl phosphate (PNPP, Sigma-Aldrich, St. Louis, MO, USA) as described previously [28]. ALP enzymatic activity was corrected for differences in cell number as determined by a Neutral Red assay [29].

Bioactivity assay with primary rat bone marrow-derived osteoblast-like cells

Two independent runs were performed, with for each run freshly isolated primary rat bone marrow-derived osteoblast-like cells (OBLCs) following the procedure described by Maniopoulos *et. al* (1988) [30]. All procedures were conducted in accordance with ISO-standards (9001:2008) and National Guidelines for care and use of laboratory animals after approval of the Experimental Animal Ethical Committee (RU-DEC 2008-199). In short, bone marrow was harvested from femora of male Wistar rats weighing between 120 g and 150 g. Femora were washed 3 times in α -minimal essential medium (α -MEM; Gibco) containing 0.5 mg/ml gentamycin (Gibco) and 3.0 μ g/ml Fungizone (Gibco). Epiphyses were cut off and diaphyses flushed out with 9 ml non-osteogenic medium (i.e. α -MEM supplemented with 10% FCS (Gibco) and 50 mg/ml gentamycin (Gibco)). The cells were divided into 2 groups; one group cultured in non-osteogenic medium and the other group in osteogenic medium (i.e. α -MEM supplemented with 10% FCS (Gibco), 50 μ g/ml ascorbic acid (Sigma), 10 mM Na β -glycerophosphate (Sigma), 10^{-8} M dexamethasone (Sigma) and 50 μ g/ml gentamycin (Gibco)). The cells were incubated in culture flasks at 37 °C in a humidified atmosphere of 95% normal air and 5% carbon dioxide. The medium was changed 3 times per week. After 7 days of primary culture, the cells were detached using trypsin/ethylenediaminetetraacetic acid (EDTA) (0.25% w/v trypsin/0.02% EDTA), concentrated via centrifugation, re-suspended in either non- or osteogenic medium, and seeded at a concentration of 1×10^4 cells/cm² in 24-well plates (medium volume: 1 ml). Cell culture was maintained using 4 different conditions: (1) non-osteogenic medium(-O); (2) ngBMP-2-supplemented non-osteogenic medium (500 ng/ml) (-OBMP); (3) osteogenic medium (+O); and (4) ngBMP-2 supplemented osteogenic medium (500 ng/ml) (+OBMP). The medium was changed 3 times a week. For respective groups, ngBMP-2 was added during the first week at medium refreshments at days 0, 1, 3 and 5.

Protein assay: To determine cell amounts, total protein measurements were performed using the bicinchoninic acid (BCA) assay (Sigma) on day 4, 8, 12 and 16 (n=3). The culture medium was removed and the cells were washed twice with PBS. After washing, one ml of MilliQ was added to each sample and the samples were stored at -80°C. Just before analysis, the samples were subjected to two freeze-thaw cycles. A standard curve was made using serial dilutions of bovine serum albumin in MilliQ (range: 0-40 μ g/ml). Then, 100 μ l of sample or standard was added to the wells of a 96-wells plate and 100 μ l of work solution (1% copper sulphate, 25% BCA in MilliQ and 24% sodium carbonate, sodium bicarbonate,

sodium tartrate in 0.2 N NaOH) was added to all the wells. The samples were incubated at 37 °C for 2 hours and left to cool down at room temperature. The 96-wells plate was read (Bio-Tek Instruments, Abcoude, the Netherlands) at 570 nm, and the protein concentrations were calculated from the obtained standard curve.

Alkaline Phosphatase Activity (ALP) assay: ALP was used as a marker for early osteoblast differentiation. For determination of ALP-activity, the same samples as for the protein assay were used. ALP-activity was determined by adding 80 µl of the samples and 20 µl of buffer solution (5mM magnesium chloride, 0.5M 2-amino-2methyl-1-propanol) to a 96-wells plate. A standard curve was prepared via serial dilutions of 4-nitrophenol (range: 0-25 nM), after which 100 µl was added to a 96-wells plate. 100 µl of substrate solution (5mM p-nitrophenylphosphate) was added to all wells and the plate was incubated for 1 hour at 37°C. The reaction was stopped by adding 100 µl of stop solution (0.3M sodium hydroxide) to all the wells. The plate was read at 405 nm, and ALP-activity values were normalized to the amount of cellular protein present in the samples.

Calcium assay: To assess the formation of mineralized matrix, culture plates were washed with PBS and one ml of 0.5 N acetic acid was added to the samples for overnight incubation during gentle agitation. A standard curve was made using serial dilutions of CaCl₂·2H₂O in acetic acid (range: 0-100 µg/ml). Then, 10 µl of the sample or standard was added to the wells of a 96-wells plate and 300 µl of work solution (5% o-cresolphthalein complexone, 5% 14.8 M ethanolamine, 2% hydroxyquinoline and 88% MilliQ) was added to all wells. Samples were incubated for 5 to 10 minutes at room temperature after which the plate was read at 570 nm.

Release experiment and in vivo studies

Preparation of PLGA-microparticles, pre-set CPC scaffolds and loading with BMP-2

PLGA-microparticles (~40 µm diameter) were prepared using a double-emulsion-solvent-extraction technique (water-in-oil-in-water), as described previously [31]. In brief, microparticles were produced by adding 500 µl of distilled water to 1400 mg PLGA in 2 ml dichloromethane. The mixture was emulsified using a Turrax® emulsifier for 60 seconds at 6000 rpm. Then, 6 ml 0.3% aqueous poly (vinyl alcohol) (PVA, Acros Organics, Geel, Belgium) solution was added and emulsified for another 60 sec at 6000 rpm to produce a second emulsion. The emulsion was transferred to a stirred beaker, after which 394 ml 0.3% PVA solution and 400 ml of 2% isopropyl alcohol solution was added slowly. After 1 hour of stirring, the microparticles were allowed to sediment for 15 min and the solution was decanted. Then, the microparticles were washed and collected through centrifugation at 1500 rpm for 5 min, lyophilized and stored at -20 °C until use. Pre-set CPC scaffolds were prepared by adding 300 mg PLGA microspheres to 700 mg CPC powder into a closed tip 2 mL plastic syringe (BD Plastipak™, Becton Dickinson S.A., Madrid, Spain), after which the content was stirred vigorously for 20 seconds to achieve

homogenous distribution of microparticles within the cement powder (Silamat® mixing apparatus, Vivadent, Schaan, Liechtenstein). Subsequently, 2 wt.% Na₂HPO₄ was added to the mixture in a liquid/powder ratio of 0.35 and mixed for 20 seconds using a mixing apparatus. After mixing, the cement was immediately injected in a Teflon mould to ensure a standardized shape of the scaffolds (Ø 7.8 mm, height 2.8 mm) and placed overnight at 37°C. To create an instantaneous open porous structure, the pre-set scaffolds were placed in a furnace at 650°C for 2 h to burn out the polymer. Finally, CPC scaffolds were sterilized by autoclavation and characterized using scanning electron microscopy (SEM; JEOL6310 at 15kV). The total porosity of the samples was calculated by the following equation [31]:

Equation 1

$$\epsilon_{\text{tot}} = \left(1 - \frac{m_{\text{burnt}}}{V * \rho_{\text{HAP}}}\right) * 100\%$$

Legend

ϵ_{tot}	= Total porosity (%)
m_{burnt}	= Average mass sample (after burning out polymer) (g)
V	= Volume sample (cm ³)
ρ_{HAP}	= Density hydroxyapatite (g/cm ³)

To measure the open interconnective porosity of the burned-out pre-set CPC scaffolds, mercury (Hg) porosimetry was performed using PoreMaster® GT mercury intrusion porosimeter (Quantachrome instruments, Odelzhausen, Germany). Burned-out pre-set CPC scaffolds were placed into the system and the intrusion of Hg was analyzed under low pressure conditions. Loading of the burned-out pre-set CPC scaffolds with BMP-2 was performed via adsorption. Therefore, a volume of 30 µl growth factor solution containing 1, 5 or 10 µg gBMP-2 or ngBMP-2 was applied to the surface of each side of the scaffold to obtain final amounts of 2, 10 or 20 µg BMP-2/scaffold. Thereafter, the scaffolds were frozen and lyophilized. To visualize the distribution of the added drugs within the burned-out pre-set CPC scaffolds, albumin from bovine serum (BSA) labeled with alexa fluor 488 (Invitrogen, Life Technologies Europe BV, Bleiswijk, The Netherlands) was used as model protein. The loading of labeled BSA (2, 10 or 20 µg BSA/scaffold) to the CPC was similar as described previously. Thereafter, the scaffolds were frozen and lyophilized. The BSA loaded CPC were overnight fixed in 4% formalin. Subsequently, the tissue blocks were embedded in methylmethacrylate. Perpendicularly through the implants, thin sections (10 µm) were prepared using a microtome with diamond blade (Leica Microsystems SP 1600, Nussloch, Germany) [32]. The sections were visualized using a reflectant fluorescence microscope with a Zeiss filter set 00, consisting of a 530–585 nm band-pass excitation filter (Carl Zeiss B.V., Sliedrecht, The Netherlands).

Release experiment

gBMP-2 and ngBMP-2 were labeled with ^{125}I , as described previously [33]. Briefly, in a 500 μl eppendorf tube coated with 100 μg iodogen, 10 μl of 0.5 M phosphate buffer saline (PBS) was added. Growth factor (25 μg) and 10-15 MBq ^{125}I (Perkin-Elmer, Boston, MA) was added and incubated at room temperature for 10 min, after which 100 μl of saturated tyrosine solution in PBS was added. The labeling efficiency of the reaction was 67.6% and 23% for gBMP-2 and ngBMP-2, respectively. To remove the non-bound ^{125}I , the reaction mixture was eluted using 0.1% BSA in PBS on a pre-rinsed disposable Sephadex G25M column (PD-10; Pharmacia, Uppsala, Sweden). The specific activity of the labeled protein was 18.7 $\mu\text{Ci}/\mu\text{g}$ for gBMP-2 and 9.1 $\mu\text{Ci}/\mu\text{g}$ for ngBMP-2. CPC scaffolds were loaded similarly as described above with either ^{125}I -gBMP-2 or ^{125}I -ngBMP-2 solutions using a hot/cold mixture of BMP-2, containing 1 μCi per scaffold (for gBMP 1 $\mu\text{Ci} \sim 0.053 \mu\text{g}$ BMP-2; for ngBMP 1 $\mu\text{Ci} \sim 0.110 \mu\text{g}$ BMP-2). A volume of 30 μl ^{125}I -gBMP-2 or ^{125}I -ngBMP-2 hot/cold solution containing 1, 5 or 10 μg BMP-2 was carefully loaded onto the surface of each side of the scaffold to obtain final amounts of 2, 10 or 20 μg BMP-2/scaffold. Thereafter, the scaffolds were frozen and lyophilized. CPC scaffolds loaded with ^{125}I -labeled BMP-2 (n=3) were placed in 10 ml glass vials for evaluation of *in vitro* BMP-2 release kinetics and incubated in 3 ml PBS at 37 °C on an orbital shaker at low rotational speed (60 rpm) for 28 days. At days 1, 4, 7, 14, 21 and 28, the samples were carefully transferred to new vials containing fresh PBS, after which gamma emission of the samples was measured in a shield well-type gamma counter (Wizard, Pharmacia-LKB, Uppsala, Sweden). Standards were measured simultaneously to correct for radioactive decay. The remaining activity in the scaffolds was expressed as percentage of the initial dose.

Surgical procedure

Twenty-four healthy young adult (8 weeks old) male Wistar rats were used as experimental animals. National guidelines for the care and use of laboratory animals were observed. The research was reviewed and approved by the Experimental Animal Committee of the Radboud University (RUDEC 2010-062). Anesthesia was induced and maintained by Isoflurane inhalation (Rhodia Organique Fine Limited, Avonmouth, Bristol, UK). To minimize post-operative discomfort, Rimadyl (Carprofen, Pfizer Animal Health, New York, USA) was administered intraperitoneally (5 mg/kg) before the surgery, directly after the surgery and subcutaneously for two days after surgery. Four CPC scaffolds were subcutaneously implanted into the back of each rat. To insert the scaffolds, rats were immobilized on their abdomen and the skin was shaved and disinfected with chlorhexidine. On both sides of the vertebral column, two small paravertebral incisions were made through the full thickness of the skin. Lateral to the incisions, a subcutaneous pocket was created using blunt dissection. Subsequently, one implant was inserted into each pocket. Finally, the skin was closed using staples (Agraven, Instruvet, Boxmeer, the Netherlands). In total, ninety-six implants were

placed according to a randomization scheme (n=8 for each group per implantation period). The animals were housed in pairs. In the initial postoperative period, the intake of water and food was monitored. Further, the animals were observed for signs of pain, infection and proper activity. At the end of the implantation time, the rats were sacrificed by CO₂-suffocation.

Implant retrieval and histological preparations

Implants were retrieved after a 4 or 12 week implantation period. After sacrifice, implants with surrounding tissue were excised and fixed in 4% formalin. Subsequently, the tissue blocks were dehydrated in increasing ethanol concentrations (70–100%) and embedded in methylmethacrylate. Perpendicularly through the implants, thin sections (10 µm) were prepared using a microtome with diamond blade (Leica Microsystems SP 1600, Nussloch, Germany) [32]. Three sections of each implant were stained with methylene blue and basic fuchsin and examined using light microscopy (Leica Microsystems AG, Wetzlar, Germany). From the control, 20 µg/cement ngBMP-2 and gBMP-2 12 weeks implantation groups, MMA samples were polished and gold sputter-coated prior to analysis with Scanning electron microscopy (JEOL 6330) using Back-Scattered Electron (BSE) mode for histomorphometrical analysis. Using BSE mode, it possible to distinguish bone from the implanted scaffold based on the respective densities of the two substances. In addition, two samples of the 20 µg/cement ngBMP-2 and gBMP-2 12 weeks implantation group were deplastified, decalcified (Sakura Finetek, Syntec Scientific, Dublin, Ireland) for 16 hours, dehydrated through a series of graded ethanol and embedded in paraffin. Using a microtome (Leica RM 2165, Leica Microsystems, Nussloch, Germany), 6 µm thick sections were prepared and stained with Goldner Trichrome.

Histological and histomorphometrical evaluation

Sections of MMA-embedded specimens (at least 3 sections per specimen) were quantitatively assessed using computer-based image analysis techniques (Leica® Qwin Pro-image analysis system, Wetzlar, Germany). From digital images (magnification: 5x), the total amount of newly-formed bone surrounding the CPC scaffold was determined and expressed in area measures (mm²). Sections of decalcified, paraffin-embedded specimens stained with Haematoxyline-eosine and Goldner trichrome (at least 3 sections per specimen) were qualitatively examined for tissue ingrowth.

Statistical analyses

Statistical analysis of the *in vitro* bioactivity assay measurements was performed using GraphPad InStat 3.05 software (GraphPad Software Inc., San Diego, CA) using one-way analysis of variance with a Tukey multiple comparison post test. Differences were considered significant at *p*-values less than 0.05. Statistical analysis

of the release experiment measurements was performed using SPSS, version 16.0 (SPSS INC., Chicago, Illinois USA). The statistical comparisons were performed using 2-tailed Student's t-test. Differences were considered significant at p -values less than 0.05. Statistical analysis of bone formation measurements was performed using SPSS, version 16.0 (SPSS INC., Chicago, Illinois USA). The statistical comparisons were performed using a one-way analysis of variance (ANOVA) with a Tukey multiple comparison post-test. Differences were considered significant at p -values less than 0.05.

Results

In vitro studies

Two independent runs of the bioactivity assay with C2C12 cells showed similar results. C2C12 cells cultured in the presence of the different types of BMP-2 demonstrated a dose-dependent ALP-activity. The threshold for the detection of ALP-activity was ~ 125 ng/ml for gBMP-2 and 250 ng/ml for ngBMP-2 with significant higher values ($p < 0.001$) for gBMP-2 at each concentration (Figure 1). Two independent runs of cell culture experiments with primary rat bone marrow derived OBLCs showed similar results. OBLCs cultured in all types of medium showed an increase in the cellular protein content between day 4 and 12 after cell seeding, with higher maximum values for -O and -OBMP. Thereafter, the protein content in all experimental groups decreased (Figure 2a). For all experimental groups, ALP-activity was observed from day 4 onwards, showing maximum values at day 8 (Figure 2b). In general, ngBMP-2 addition significantly increased ALP-activity in -O as well as +O in the first 8 days of culture. For mineralization (Figure 2c), a gradual increase in calcium amounts was observed from day 4 onward for +O and +OBMP. Significantly higher values ($p < 0.001$) were observed for +OBMP compared to +O at each individual time point. For -O and -OBMP, no increase in calcium amounts was observed.

CPC scaffolds, drug loading and release experiment

CPC scaffolds were characterized using SEM (Figure 3) and demonstrated different types of porosity: intrinsic microporosity (pore size ~ 10 nm - 100 nm) related to material setting and crystallization, and macroporosity (pore size: ~ 40 μ m) resulting after burning out PLGA-microparticles. The total porosity (consisting of the intrinsic porosity of material and additional porosity after PLGA-microparticle degradation) was determined by measuring the weight of pre-set composite discs (with and without PLGA-microparticles) and comparing it to a fictitious, solid hydroxyapatite disc with the same dimensions. The porosity measurements demonstrated a total porosity of 75.5 ± 1.3 %. The interconnective porosity as analyzed by Hg intrusion porosimetry revealed a porosity of 21.3 %. Drug loading was visualized using cross-sections of CPC-scaffolds loaded with different amounts of alexa fluor 488 labeled BSA (Figure 3). In all concentrations, the distribution of the protein is only observed

peripherally and not in the center of the implants. However, a dose-dependent effect is observed whereby with increasing BSA concentrations the protein infiltration is enlarged. The release and retention after 28 days of ^{125}I -gBMP-2 and ^{125}I -ngBMP-2 for the low (2 μg), middle (10 μg), and high (20 μg) dose implants are depicted in Figure 4 and Table 1. In general, all scaffolds retained their integrity during the entire experiment and showed an initial burst release within 1 day, followed by a sustained release till day 28 (Figure 4A). For gBMP-2, the burst release (Figure 4B) was 17.4 ± 7.8 , 14.3 ± 5.8 and 11.7 ± 1.0 % for low, middle and high dose loaded scaffolds, respectively. For ngBMP-2, the burst release was 16.1 ± 2.4 , 22.0 ± 0.7 and 16.0 ± 3.8 for low, middle and high dose loaded scaffolds, respectively. The overall sustained release (Figure 4B; % per day) from day 1-28 of ngBMP-2 compared to gBMP-2 was significantly lower ($p < 0.001$, overall sustained release of $0.63 \pm 0.07\%$ and $0.88 \pm 0.17\%$ for ngBMP-2 and gBMP-2, respectively). Separately, the sustained release from day 1 to day 28 was significantly lower for the low ngBMP-2 loaded scaffolds compared to gBMP-2 loaded scaffolds ($p < 0.05$, sustained release of 0.86 ± 0.15 and 0.56 ± 0.07 %/day for gBMP-2 and ngBMP-2, respectively). A similar tendency was observed for the middle and high ngBMP-2 loaded scaffolds compared to the high gBMP-2 loaded scaffolds (for the middle dosage $p = 0.146$, sustained release of 0.90 ± 0.26 and 0.63 ± 0.03 %/day for gBMP-2 and ngBMP-2, respectively; for the high $p = 0.130$, sustained release of 0.87 ± 0.161 and 0.69 ± 0.03 %/day for gBMP-2 and ngBMP-2, respectively). After 28 days, the total release (Figure 4B) for gBMP-2 was 40.6 ± 4.0 , 38.7 ± 3.4 and 35.1 ± 4.5 % for low, middle and high dose loaded scaffolds, respectively. For ngBMP-2, the total release was 31.4 ± 2.4 , 39.1 ± 0.5 and 34.6 ± 3.6 % for low, middle and high dose loaded scaffolds, respectively. These release results show significantly increased protein retention for ngBMP-2 in the low loaded groups compared to low gBMP-2 ($p < 0.05$), whereas no significant differences were observed for the middle and high loaded groups.

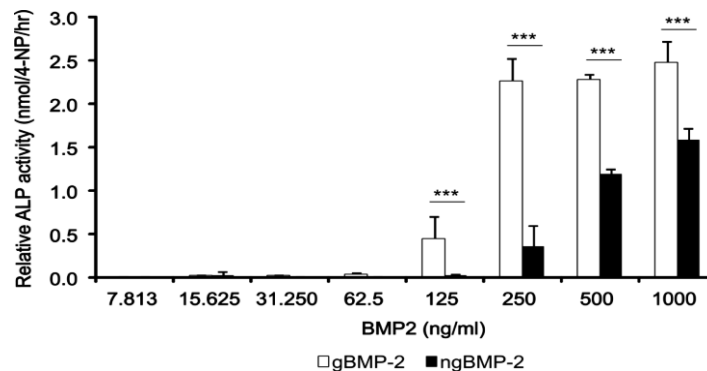


Figure 1 ALP activity of the C2C12 cells after 72 h stimulation with gBMP-2 or ngBMP-2. C2C12 cells demonstrate a dose-dependent ALP-activity. ALP-activity was significantly increased by gBMP-2, and ngBMP-2. Results are shown as means \pm SD of triplicate samples for one representative experiment out of two. (***) $p < 0.001$.

BIOACTIVITY AND OSTEOINDUCTIVE PROPERTIES OF ngBMP-2 vs gBMP-2

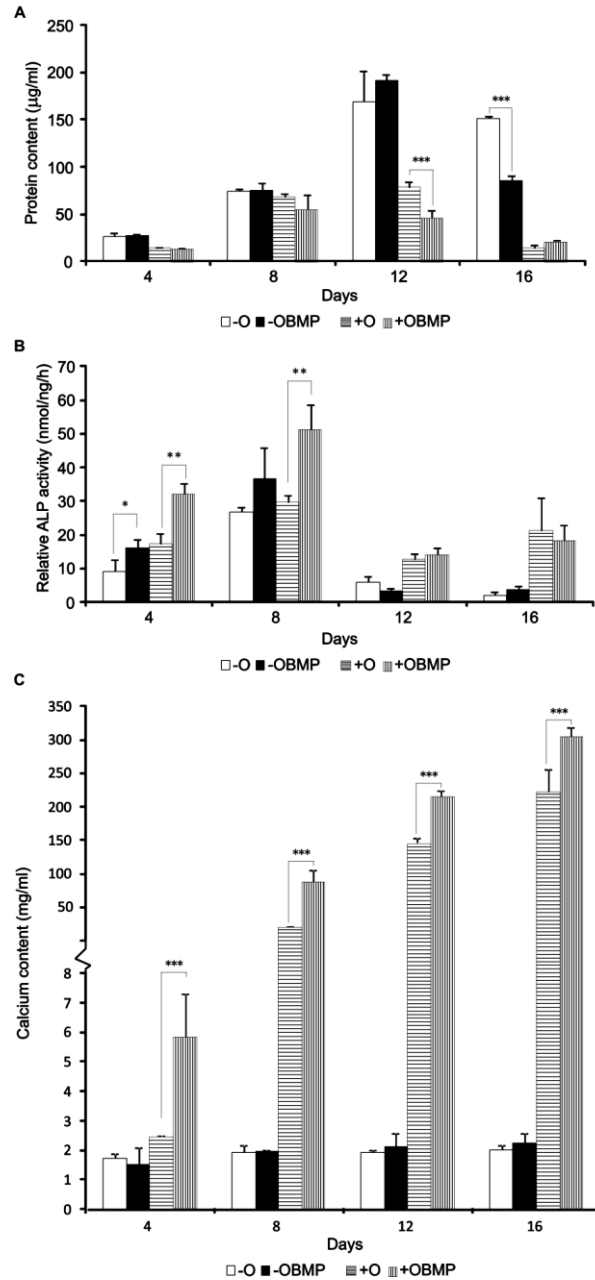


Figure 2 (A) Cellular protein content and (B) Alkaline phosphatase (ALP) activity of and (C) mineralization (calcium deposition) by rat osteoblast-like cells cultured in non-osteogenic (-O) or osteogenic (+O) medium in the presence or absence of ngBMP-2. Results are shown as mean \pm SD of triplicate samples for one representative experiment out of two. (***) $p < 0.001$.

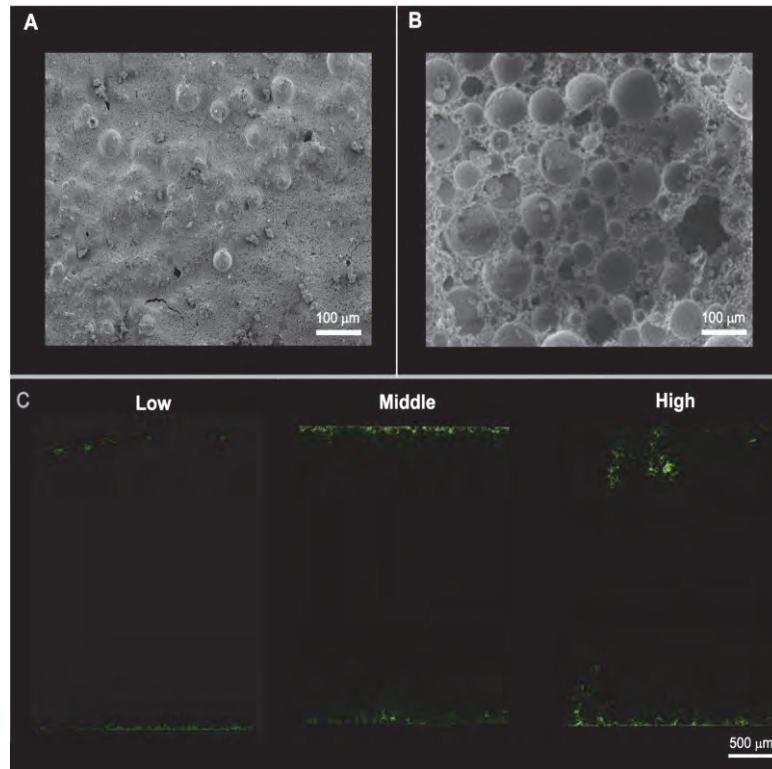


Figure 3 Characterization of porous CPC scaffolds. Microscopic SEM micrographs of composite material before (A) and after (B) burning out the PLGA-microparticles. Bar represents 100 μm. (C) The distribution of low, middle or high dose of the model protein alexa fluor 488 labeled BSA within porous CPC scaffolds. Bar represents 500 μm.

Table 1 The release in percentage of gBMP-2 and ngBMP-2 from porous CPC

	Burst release (%)	Cumulative sustained release (%)				
	D 1	D 4	D 7	D 14	D 21	D 28
gBMP-2						
L	17.4 ± 7.8	24.7 ± 1.3	29.4 ± 2.69	33.7 ± 3.8	36.5 ± 5.7	40.6 ± 4.0
M	14.3 ± 5.8	22.2 ± 1.8	25.7 ± 2.3	26.5 ± 9.2	35.5 ± 3.2	38.7 ± 3.4
H	11.7 ± 1.1	17.9 ± 2.5	23.7 ± 3.4	27.9 ± 3.5	31.3 ± 3.2	35.1 ± 4.5
ngBMP-2						
L	16.1 ± 2.4	20.1 ± 3.2	23.6 ± 4.1	28.2 ± 5.9	29.3 ± 3.7	31.4 ± 2.4*
M	22.0 ± 0.7	26.4 ± 0.5	31.5 ± 2.9 *	33.6 ± 0.3	36.5 ± 0.8	39.1 ± 0.5
H	16.0 ± 3.8	21.9 ± 3.5	25.2 ± 2.5	28.1 ± 5.4	31.2 ± 5.1	34.6 ± 3.6

Low (L), middle (M) and high (H): 2 μg, 10 μg or 20 μg loaded carrier with either gBMP-2 or ngBMP-2, *; $p < 0.05$ as compared between both groups at the specific time point.

BIOACTIVITY AND OSTEOINDUCTIVE PROPERTIES OF ngBMP-2 vs gBMP-2

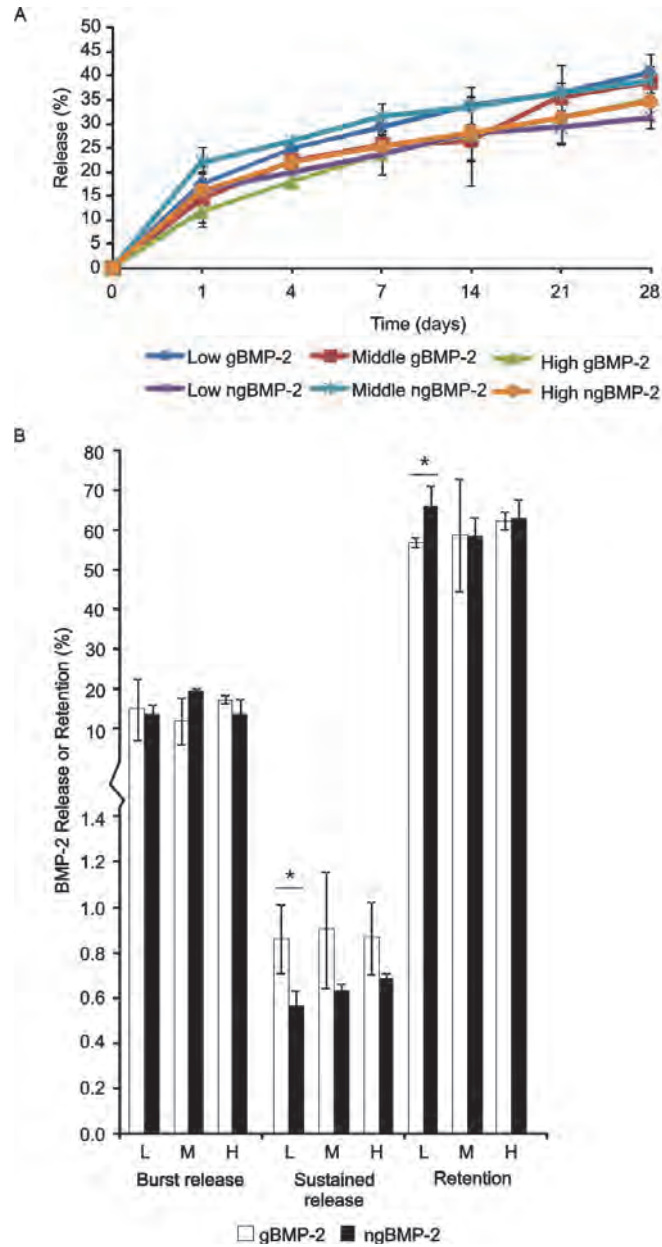


Figure 4 Longitudinal scintigraphic assessment of low (L), middle (M) and high (H) dose gBMP-2 and ngBMP-2 (A) released from loaded porous CPC scaffolds during 28 days and (B) the *in vitro* burst release (after 1 day), sustained release (the release per day from day 1-28) and the retention after 28 days. The release and retention is expressed as percentage of the ratio of initial loading amount. Error bars represents the mean \pm SD ($n=3$). (*) $p<0.05$.

Descriptive light microscopy

All specimens showed a fibrous capsule surrounding the scaffold after both 4 and 12 weeks of implantation, without the presence of inflammatory cells at the interface. Figure 5 presents an overview of histological sections of the specimens after each implantation period as well as higher magnifications of the newly-formed bone tissue at the interface between CPC scaffold and tissue. Bone formation was observed for all BMP-2 loaded implants after both 4 and 12 weeks of implantation, but was absent for unloaded controls. Bone formation and fibrous tissue were only observed peripherally and not in the center of the implants in any of the sections (Figure 5 and 6). Bone formation was most pronounced for high dose ngBMP-2 loaded scaffolds after 12 weeks of implantation.

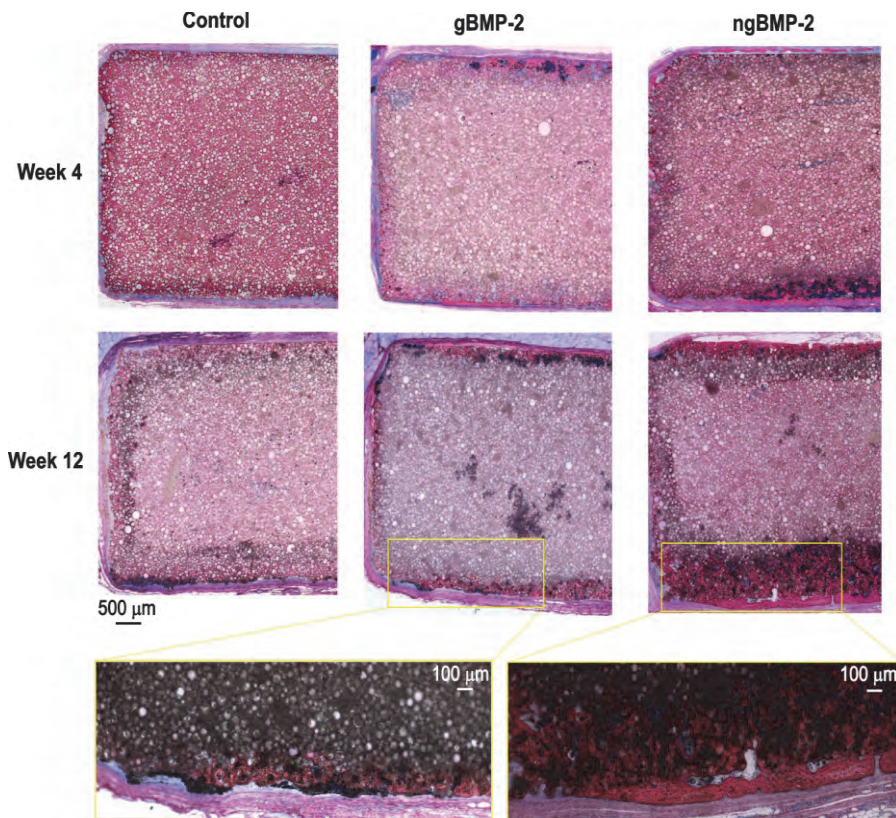


Figure 5 Histological sections of the low dose gBMP-2 and ngBMP-2 loaded porous CPC scaffolds after 4 and 12 weeks implantation. Bar represents 500 μm. Magnifications of the boxes show low dose gBMP-2 and ngBMP-2 loaded porous CPC scaffolds after 12 weeks of implantation. Bar represents 100 μm. Methylene blue and basic fuchsin staining.

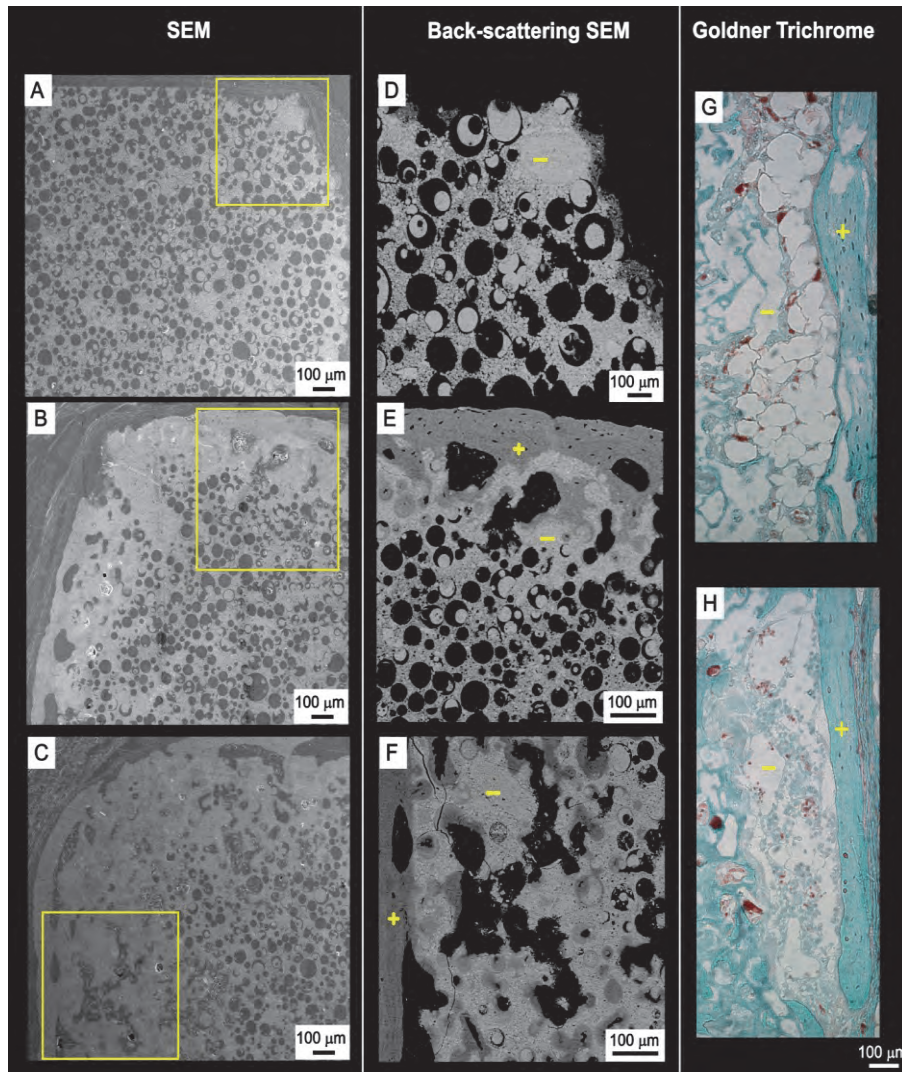


Figure 6 Cross-sections of Control (A, D) and high dose gBMP-2 (B, E, G) and ngBMP-2 (C, F, H) loaded porous CPC scaffolds after 12 weeks implantation observed with SEM, back scattering SEM and histological with Goldner trichrome staining, respectively. Bone (+) and CPC scaffold (-) are indicated in the back scattering SEM micrographs and Goldner trichrome stained sections.

Histomorphometrical evaluation

Quantitative results of ectopic bone formation are shown in Figure 7. After 4 weeks of implantation, a dose-dependent amount of bone formation was observed for both gBMP and ngBMP, whereas no bone formation was observed for controls. A significant higher amount of newly-formed bone ($p < 0.001$) was found for low dose ngBMP scaffolds compared to gBMP equivalents. The amount of newly-formed bone significantly increased in time (for gBMP-2 loaded scaffolds $p < 0.01$; for ngBMP-2 loaded scaffolds $p < 0.001$) for all types of scaffolds (except controls) with a maximum of $\sim 1 \text{ mm}^2$ after 4 weeks to a maximum of $\sim 7 \text{ mm}^2$ after 12 weeks. Similar to week 4 observations, significant higher amounts of newly-formed bone ($p < 0.001$) were found for low dose ngBMP scaffolds compared to gBMP equivalents after 12 weeks of implantation.

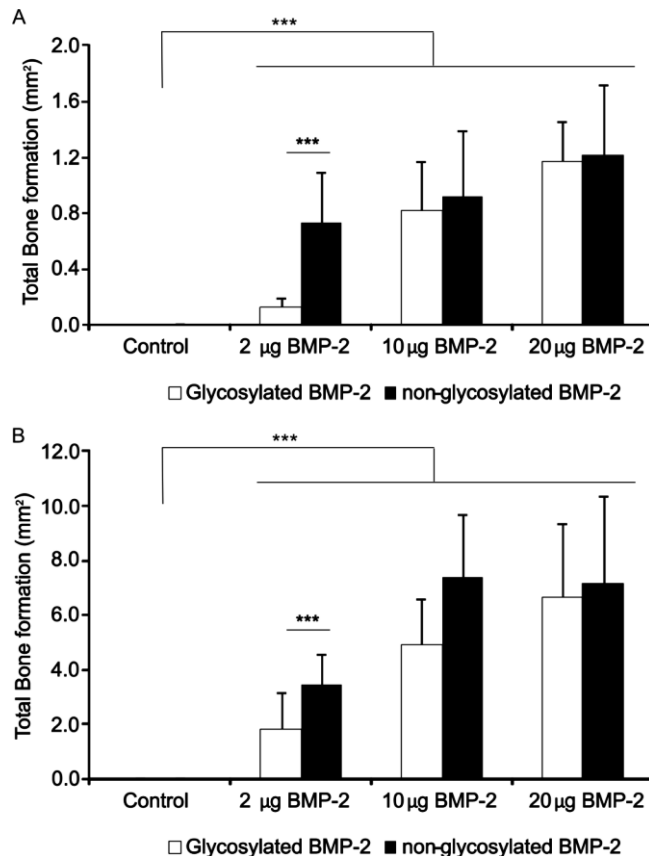


Figure 7 Osteoinductive capacity of gBMP-2 and ngBMP-2 loaded carriers at an ectopic location after 4 (A) and 12 (B) weeks implantation period. Bone formation is only observed in the BMP-2 loaded carriers. In addition, ngBMP-2 can significantly induce more bone at lower concentrations compared to gBMP-2 at both implantation periods. Error bars represent means \pm standard deviation. (***) = $p < 0.001$; $n > 7$.

Discussion

For clinical application, the availability of recombinant human BMP-2 at acceptable costs is mandatory. In view of that, large-scale BMP-2 production via a bacterial hosts might be a good alternative for mammalian cells for reasons of cost effectiveness [34]. However, bacterially produced BMP-2 lacks a glycosylation site and hence is structurally different to and less soluble than the native, post-translationally modified mammalian BMP-2. Consequently, this study comparatively evaluated the bioactivity of non-glycosylated (ng) and glycosylated (g) BMP-2 using *in vitro* bioactivity and release assays and an ectopic animal model, in which different amounts (2-20 ug) BMP-2 were loaded onto a porous calcium phosphate cement (CPC) carrier. It was hypothesized that less soluble ngBMP-2 was biologically active and would induce more bone ectopically compared to more soluble gBMP-2. *In vitro* bioactivity assays revealed that ngBMP-2 is less active than gBMP-2, however ngBMP-2 was still capable of inducing differentiation and mineralization of primary rat osteoblast-like cells. The overall sustained release from day 1-28 of ngBMP-2 was significantly lower as compared with gBMP-2. Separately, a significant decrease in sustained release for low ngBMP-2 loaded scaffolds as compared with gBMP-2 loaded scaffolds was observed leading to an increased amount of retained protein after 28 days. *In vivo* ectopic bone formation demonstrated that ngBMP-2 is capable of inducing significant more bone at low dosage (2 µg/CPC) from four weeks onward compared to gBMP-2.

The regenerative capacity of BMP-2 is dependent on its ability to stimulate the pre-osteoblastic cells to differentiate into bone forming cells leading to the formation of new bone. In the current study, a difference in levels of the activity of early osteoblastic differentiation marker ALP in C2C12 cells cultured in the presence of ngBMP-2 compared to gBMP-2 was observed. Nevertheless, ngBMP-2 demonstrated to be capable of inducing differentiation and mineralization of primary rat osteoblast-like cells. In contrast, several studies reported equal levels of ALP-activity for cells cultured in the presence of gBMP-2 or ngBMP-2 [35, 36] indicating a comparable *in vitro* potency of both types of BMP-2 as osteoinductive factor. Due to inconsistency in different reports on the efficacy of both types of BMP-2 in *in vitro* experiments, the precise effect of glycosylation on bioactivity remains unclear.

The release profiles of adsorbed ngBMP-2 and gBMP-2 showed an initial burst release (within 1 day) followed by a sustained release (from day 1-28) of in total approximately ~35% for the ngBMP-2 loaded scaffolds and ~38% for the gBMP-2 loaded scaffolds, which were similar to earlier reported ones, describing a release up to ~40% [37]. Despite similar release profiles of both BMPs, the sustained release per day for the low ngBMP-2 loaded scaffolds was significantly reduced and a tendency was observed in the middle and high ngBMP-2 loaded scaffolds compared to gBMP-2 loaded scaffolds. These results are in line with the data of the amounts of BMP-2 retained onto the implants after 28 days, showing significantly higher amounts for low ngBMP-2 compared to low gBMP-2, whereas for middle

and high loaded implants similar amounts were observed for ngBMP-2 and gBMP-2. Although after 28 days the BMP-2 retention is only significantly different for the low dosages, the overall sustained release of ngBMP-2 compared to gBMP-2 is significantly lower, indicating an effect of glycosylation on protein release. Interestingly, after a similar implantation period *in vivo*, low dosages of ngBMP-2 induced significantly more ectopic bone formation compared to low gBMP-2 dosages. As it is likely that the biological process of bone formation is related to the presence of BMP-2 at the implant and its solubility, the significantly increased amounts of ngBMP-2 retained onto the implants are suggested to be responsible for this observation. This higher retention of ngBMP-2 corroborates earlier findings [25] that indicated a decreased solubility of ngBMP-2 in fibrin matrices. Additionally, this indicates that the biological activity of BMP-2 is not directly depending on release but rather on availability and solubility, in either released or bound form, in a specific area.

The sustained release and thus bone formation is carrier dependent due to altered release rates of BMP-2 from the different carriers [12]. For example, the retention of gBMP-2 within an alginate mesh is significantly increased compared to a collagen sponge in the first week after which the difference diminishes [38]. Together with the finding of Brown *et al.* (2011), who reported a positive effect on bone formation after a BMP-2 burst release and a subsequent sustained release, it was suggested that a combination of relatively high initial release and a low sustained release thereafter may be beneficial for growth factor efficacy [39]. The release kinetics observed in the current study corroborate earlier findings and indicate a similar effect [37]. However, the BMP-2 activation in relation to the bioactivity of BMP-2 needs to be observed as a complex factor. It is assumed that BMP-2 not only acts in released form, but also when it is presented in an adsorbed form to the target cells [20, 40]. However, up to date the ability to discriminate the contribution of adsorbed and released forms of BMP-2 is not available.

The induction of ectopic bone tissue by BMP-2 adsorbed to pre-set CPC scaffolds showed to be both dose- and time-dependent with significantly higher bone formation induced by ngBMP-2 at low dosage compared to gBMP-2. The amount of ectopic bone formation was comparable to previous experiments with subcutaneous implantation of scaffolds containing adsorbed glycosylated (rh)BMP-2 [18, 41]. Bone tissue was predominantly formed in the periphery of the porous CPC scaffolds as well as at the material/tissue interface. This observation is likely related to the rapid and strong interaction between proteins (e.g. BMP-2) and the pre-set CPC scaffolds and the limitations micrometer-scale porosity brings along regarding cell penetration. In general, proteins rapidly adsorb to CaP-based materials due to electrostatic interactions [42], which even can become stronger upon conformational changes of adsorbed proteins. More particularly, Ruhé *et al.* studied the effect of albumin pre-treatment of pre-set, porous CPC scaffolds on BMP-2 release under different conditions [43] and demonstrated that albumin pre-treatment only had a marginal effect on the limited release of BMP-2, emphasizing the capacity of pre-set CPC scaffolds to retain adsorbed proteins. Penetration of

(bone) tissue into a porous relies on the size of the pores and their interconnectivity. In relation to CPC, Link *et al.* demonstrated that tissue ingrowth into pre-set CPC scaffolds containing PLGA microspheres occurred when pore size exceeded 50 μm and interconnectivity was obtained by incorporating sufficient porogen, in their case at least 20 wt% PLGA-microspheres [44]. The pre-set porous CPC scaffolds used in the present study were made using smaller PLGA microparticles (i.e. 40 μm) and a higher amount (i.e. 30 wt%). Based on the observations that bone formation and tissue ingrowth were limited to the periphery of the pre-set CPC scaffolds, as additionally shown using paraffin-embedded decalcified sections, the created porosity within these scaffolds apparently was insufficient for cell penetration.

In summary, the present study revealed that ngBMP-2 is less biologically active *in vitro* compared to gBMP-2, however still capable of inducing osteoblast-like cells to differentiate and mineralize. In addition, ngBMP-2 showed slower release from a CaP-based implant compared to gBMP-2. Despite lower biological activity and release *in vitro*, ngBMP-2 significantly increased ectopic bone formation at low dosages. This observation provides strong evidence that the efficacy of ngBMP-2 *in vivo* is enhanced compared to gBMP-2 and reflects its value for enrichment strategies for biomaterials, bone tissue engineering and bone regenerative treatments.

Acknowledgements

The authors gratefully acknowledge the support of the Smart Mix Program of the Netherlands Ministry of Economic Affairs and the Netherlands Ministry of Education, Culture and Science. The authors would like to thank Natasja van Dijk for assistance with the histological preparations, Cathelijne Frielink for help with ^{125}I -BMP-2 release experiments and Dr. Ir. Ewald Bronkhorst for assistance with statistical analyses. Scanning electron microscopy was performed at the Nijmegen Center for Molecular Life Sciences (NCMLS), the Netherlands.

References

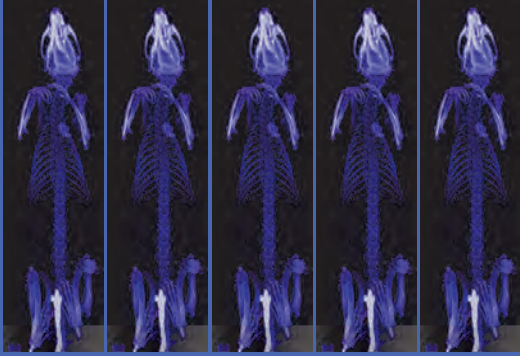
- [1] P.D. Delmas, M. Anderson, Launch of The Bone and Joint Decade 2000–2010, *Osteoporos. Int.* 11 (2000) 95-97.
- [2] L. C. Chow, Next generation calcium phosphate-based biomaterials, *Dent. Mater. J.* 28 (2009) 1-10.
- [3] M.P. Ginebra, M. Espanol, E.B. Montufar, R.A. Perez, G. Mestres, New processing approaches in calcium phosphate cements and their applications in regenerative medicine, *Acta Biomater.* 6 (2010) 2863-2873.
- [4] M.N. Rahaman, D.E. Day, B. Sonny Bal, Q. Fu, S.B. Jung, L.F. Bonewald, A.P. Tomsia, Bioactive glass in tissue engineering, *Acta Biomater.* 7 (2011) 2355-2373.
- [5] P.A. Gunatillake, R. Adhikari, Biodegradable synthetic polymers for tissue engineering, *Eur. cell. mater.* 5 (2003) 1-16.
- [6] C. Xu, P. Su, X. Chen, Y. Meng, W. Yu, A.P. Xiang, Y. Wang, Biocompatibility and osteogenesis of biomimetic Bioglass-Collagen-Phosphatidylserine composite scaffolds for bone tissue engineering, *Biomaterials* 32 (2011) 1051-1058.
- [7] P. Ruhé, E. Hedberg-Dirk, N.T. Padron, P. Spauwen, J. Jansen, A.

CHAPTER 4

- Mikos, Porous Poly(DL-lactic-co-glycolic acid)/Calcium Phosphate Cement Composite for Reconstruction of Bone Defects, *Tissue Eng.* 12 (2006) 789-800.
- [8] P.C. Bessa, M. Casal, R.L. Reis, Bone morphogenetic proteins in tissue engineering: the road from the laboratory to the clinic, part I (basic concepts), *J. Tissue. Eng. Regen. Med.* 2 (2008) 1-13.
- [9] P.C. Bessa, M. Casal, R.L. Reis, Bone morphogenetic proteins in tissue engineering: the road from laboratory to clinic, part II (BMP delivery), *J. Tissue. Eng. Regen. Med.* 2 (2008) 81-96.
- [10] J.A. Jansen, J.W.M. Vehof, P.Q. Ruhé, H. Kroeze-Deutman, Y. Kuboki, H. Takita, E.L. Hedberg, A.G. Mikos, Growth factor-loaded scaffolds for bone engineering, *J. Control. Release* 101 (2005) 127-136.
- [11] X. Cao, D. Chen, The BMP signaling and in vivo bone formation, *Gene* 357 (2005) 1-8.
- [12] H. Seeherman, J.M. Wozney, Delivery of bone morphogenetic proteins for orthopedic tissue regeneration, *Cytokine Growth Factor Rev.* 16 (2005) 329-345.
- [13] R.D. Welch, A.L. Jones, R.W. Bucholz, C.M. Reinert, J.S. Tjia, W.A. Pierce, J.M. Wozney, X.J. Li, Effect of Recombinant Human Bone Morphogenetic Protein-2 on Fracture Healing in a Goat Tibial Fracture Model, *J. Bone Miner. Res.* 13 (1998) 1483-1490.
- [14] K. Bessho, D.L. Carnes, R. Cavin, J.L. Ong, Experimental studies on bone induction using low-molecular-weight poly (DL-lactide-co-glycolide) as a carrier for recombinant human bone morphogenetic protein-2, *J. Biomed. Mater. Res.* 61 (2002) 61-65.
- [15] M. Isobe, Y. Yamazaki, M. Mori, K. Ishihara, N. Nakabayashi, T. Amagasa, The role of recombinant human bone morphogenetic protein-2 in PLGA capsules at an extraskeletal site of the rat, *J. Biomed. Mater. Res.* 45 (1999) 36-41.
- [16] L. Luca, A.-L. Rougemont, B.H. Walpoth, L. Boure, A. Tami, J.M. Anderson, O. Jordan, R. Gurny, Injectable rhBMP-2-loaded chitosan hydrogel composite: Osteoinduction at ectopic site and in segmental long bone defect, *J. Biomed. Mater. Res. A* 96A (2011) 66-74.
- [17] P.Q. Ruhé, H.C. Kroeze-Deutman, J.G.C. Wolke, P.H.M. Spauwen, J.A. Jansen, Bone inductive properties of rhBMP-2 loaded porous calcium phosphate cement implants in cranial defects in rabbits, *Biomaterials* 25 (2004) 2123-2132.
- [18] H.C. Kroeze-Deutman, P.Q. Ruhé, P.H.M. Spauwen, J.A. Jansen, Bone inductive properties of rhBMP-2 loaded porous calcium phosphate cement implants inserted at an ectopic site in rabbits, *Biomaterials* 26 (2005) 1131-1138.
- [19] L. Zhao, M. Tang, M.D. Weir, M.S. Detamore, H.H.K. Xu, Osteogenic Media and rhBMP-2-Induced Differentiation of Umbilical Cord Mesenchymal Stem Cells Encapsulated in Alginate Microbeads and Integrated in an Injectable Calcium Phosphate-Chitosan Fibrous Scaffold, *Tissue Eng. Part A* 17 (2011) 969-979.
- [20] E. Bodde, O. Boerman, F. Russel, A. Mikos, P. Spauwen, J. Jansen, The kinetic and biological activity of different loaded rhBMP-2 calcium phosphate cement implants in rats, *J. Biomed. Mater. Res. A* 87A (2008) 780-791.
- [21] J.W.M. Vehof, A.E. de Ruijter, P.H.M. Spauwen, J.A. Jansen, Influence of rhBMP-2 on Rat Bone Marrow Stromal Cells Cultured on Titanium Fiber Mesh, *Tissue Eng.* 7 (2001) 373-383.
- [22] J. van den Dolder, A.J.E. de Ruijter, P.H.M. Spauwen, J.A. Jansen, Observations on the effect of BMP-2 on rat bone marrow cells cultured on titanium substrates of different roughness, *Biomaterials* 24 (2003) 1853-1860.
- [23] R.E. Jung, F.E. Weber, D.S. Thoma, M. Ehrbar, D.L. Cochran, C.H.F. Hämmerle, Bone morphogenetic protein-2 enhances bone formation when delivered by a synthetic matrix containing hydroxyapatite/tricalciumphosphate, *Clin. Oral Implants Res.* 19 (2008) 188-195.
- [24] T.K. Sampath, J.E. Coughlin, R.M. Whetstone, D. Banach, C. Corbett, R.J. Ridge, E. Ozkaynak, H. Oppermann, D.C. Rueger, Bovine osteogenic protein is composed of dimers of OP-1 and BMP-2A, two members of the transforming growth factor-beta superfamily, *J. Biol. Chem.* 265 (1990) 13198-13205.
- [25] H. Schmoekel, J.C. Schense, F.E. Weber, K.W. Grätz, D. Gnägi, R. Müller, J.A. Hubbell, Bone healing in the rat and dog with nonglycosylated BMP-2 demonstrating low solubility in fibrin matrices, *J. Orthop. Res.* 22 (2004) 376-381.
- [26] K. Sariibrahimoglu, S.C.G. Leeuwenburgh, J.G.C. Wolke, L. Yubao, J.A. Jansen, Effect of calcium carbonate on hardening, physicochemical properties and in vitro degradation of injectable calcium phosphate cements *J. Biomed. Mater. Res. A* accepted for publication (2011).
- [27] T. Katagiri, A. Yamaguchi, T. Ikeda, S. Yoshiki, J.M. Wozney, V. Rosen, E.A. Wang, H. Tanaka, S. Omura, T. Suda, The non-osteogenic mouse pluripotent cell line, C3H10T1/2, is induced to differentiate

BIOACTIVITY AND OSTEOINDUCTIVE PROPERTIES OF ngBMP-2 vs gBMP-2

- into osteoblastic cells by recombinant human bone morphogenetic protein-2, *Biochem. Biophys. Res. Commun.* 172 (1990) 295-299.
- [28] E. Piek, L.S. Sleumer, E.P. van Someren, L. Heuver, J.R. de Haan, I. de Grijs, C. Gilissen, J.M. Hendriks, R.I. van Ravestein-van Os, S. Bauerschmidt, K.J. Dechering, E.J. van Zoelen, Osteo-transcriptomics of human mesenchymal stem cells: Accelerated gene expression and osteoblast differentiation induced by vitamin D reveals c-MYC as an enhancer of BMP2-induced osteogenesis, *Bone* 46 (2010) 613-627.
- [29] C.W.G.M. Lowik, M.J. Alblas, M. Vanderuit, S.E. Papapoulos, G. Vanderpluijm, Quantification of Adherent and Nonadherent Cells Cultured in 96-Well Plates Using the Supravital Stain Neutral Red, *Anal. Biochem.* 213 (1993) 426-433.
- [30] C. Maniopoulos, J. Sodek, A.H. Melcher, Bone formation in vitro by stromal cells obtained from bone marrow of young adult rats, *Cell Tissue Res.* 254 (1988) 317-330.
- [31] W. Habraken, J. Wolke, A. Mikos, J. Jansen, Injectable PLGA microsphere/calcium phosphate cements: physical properties and degradation characteristics *J. Biomater. Sci. Polym. Ed.* 17 (2006) 1057-1074.
- [32] H. van der Lubbe, C. Klein, K. de Groot, A simple method for preparing thin (10 microM) histological sections of undecalcified plastic embedded bone with implants, *Stain Technol.* 63 (1988) 171-176.
- [33] P.J. Fraker, J.C. Speck, Protein and cell membrane iodinations with a sparingly soluble chloroamide, 1,3,4,6-tetrachloro-3a,6a-diphenylglycoluril, *Biochem. Biophys. Res. Commun.* 80 (1978) 849-857.
- [34] S. Zerbs, A.M. Frank, F.R. Collart, Bacterial Systems for Production of Heterologous Proteins, *Methods Enzymol.* 463 (2009) 149-168.
- [35] S. Long, L. Truong, K. Bennett, A. Phillips, F. Wong-Staal, H. Ma, Expression, purification, and renaturation of bone morphogenetic protein-2 from *Escherichia coli*, *Protein Expr. Purif.* 46 (2006) 374-378.
- [36] K. Yano, M. Hoshino, Y. Ohta, T. Manaka, Y. Naka, Y. Imai, W. Sebald, K. Takaoka, Osteoinductive capacity and heat stability of recombinant human bone morphogenetic protein-2 produced by *Escherichia coli* and dimerized by biochemical processing, *J. Bone Miner. Metab.* 27 (2009) 355-363.
- [37] W.J.E.M. Habraken, O.C. Boerman, J.G.C. Wolke, A.G. Mikos, J.A. Jansen, *In vitro* growth factor release from injectable calcium phosphate cements containing gelatin microspheres, *J. Biomed. Mater. Res. A* 91A (2009) 614-622.
- [38] J.D. Boerckel, Y.M. Kolambkar, K.M. Dupont, B.A. Uhrig, E.A. Phelps, H.Y. Stevens, A.J. Garcia, R.E. Goldberg, Effects of protein dose and delivery system on BMP-mediated bone regeneration, *Biomaterials* 32 (2011) 5241-5251.
- [39] K.V. Brown, B. Li, T. Guda, D.S. Perrien, S.A. Guelcher, J.C. Wenke, Improving Bone Formation in a Rat Femur Segmental Defect by Controlling Bone Morphogenetic Protein-2 Release, *Tissue Eng. Part A* 17 (2011) 1735-1746.
- [40] H. Uludag, D. D'Augusta, J. Golden, J. Li, G. Timony, R. Riedel, J. Wozney, Implantation of recombinant human bone morphogenetic proteins with biomaterial carriers: A correlation between protein pharmacokinetics and osteoinduction in the rat ectopic model, *J. Biomed. Mater. Res. A* 50 (2000) 227-238.
- [41] J. Lee, C. Kim, K. Choi, U. Jung, J. Yun, S. Choi, K. Cho, The induction of bone formation in rat calvarial defects and subcutaneous tissues by recombinant human BMP-2, produced in *Escherichia coli*, *Biomaterials* 31 (2010) 3512-3519.
- [42] T.S. Tsapikouni, Y.F. Missirlis, Protein-material interactions: From micro-to-nano scale, *Mater. Sci. Eng. B* 152 (2008) 2-7. [43] P. Ruhé, O. Boerman, F. Russel, A. Mikos, P. Spauwen, J. Jansen, *In vivo* release of rhBMP-2 loaded porous calcium phosphate cement pretreated with albumin, *J. Mater. Sci. Mater. Med.* 17 (2006) 919-927.
- [44] D.P. Link, J. van den Dolder, J.J.J.P. van den Beucken, V.M. Cuijpers, J.G.C. Wolke, A.G. Mikos, J.A. Jansen, Evaluation of the biocompatibility of calcium phosphate cement/PLGA microparticle composites, *J. Biomed. Mater. Res. A* 87A (2008) 760-769.



CHAPTER 5

Differential loading methods for BMP-2 within injectable calcium phosphate cement

FCJ van de Watering, JDM Molkenboer-Kuenen, OC Boerman,
JJJP van den Beucken, and JA Jansen

J. Control. Release, DOI:[dx.doi.org/10.1016/j.jconrel.2012.07.007](https://doi.org/10.1016/j.jconrel.2012.07.007)

Introduction

Calcium phosphate (CaP) based materials are widely used as bone substitute materials in orthopedic, reconstructive and oral surgery due to their performance [1, 2]. CaP-based materials are available in various forms, for example as granules or blocks. More interestingly, injectable CaP-based pastes (e.g. of brushite or apatitic nature [3]) are also available and have the advantage of optimal bone defect filling through minimally invasive surgery. Injectable CaP-based cements have shown biocompatibility and osteoconductivity, although *in vivo* degradation and tissue ingrowth were difficult to control [1, 4, 5].

To enhance material degradation, different approaches have been explored to introduce porosity within CaP cement (CPC), including the use of sodium bicarbonate to obtain CO₂-gas bubbles during cement setting and mixing biodegradable polymer microparticles (e.g. gelatin [6] or poly(D,L-lactic-co-glycolic) acid (PLGA) [7-10]) as porogens homogeneously through the cement powder. Although porosity is instantaneous when using the CO₂-gas bubble method, the lack of control on pore size and distribution is disadvantageous [11]. In contrast, PLGA-microparticles create a delayed porosity, after the PLGA-microparticles are degraded by means of hydrolysis in a process called bulk erosion [10], with, importantly, homogeneously dispersed pores of desired size. In addition, Felix Lanao *et al.* (2011) reported that the hydrolysis of PLGA-microparticles can be controlled depending on the PLGA molecular weight, end-group chemistry, and/or morphology [12]. In view of this, CPC degradation and bone formation were shown to be highest when dense acid-terminated PLGA-microparticles were incorporated in CPC [13].

Further empowerment of CPC for biological performance can be achieved by incorporating biologically active compounds, including growth factors. Previously, it has been reported that biologically active additives can be absorbed on preset CPC. For example, CPC surface loading of the growth factor bone morphogenetic protein-2 (BMP-2) demonstrated to induce bone formation at ectopic locations in rats [14] and rabbits [15] and increased bone formation at orthotopic locations in rabbits [16]. However, the clinical application of CPC is in an injectable form, for which the loading of additives on the surface of preset CPC is not feasible. Consequently, a biologically active compound needs to be incorporated during the CPC setting (i.e. included into the powder or the liquid phase of CPC). In view of this, growth factor loading onto included porogens (e.g. PLGA-microparticles) represents an approach to introduce biologically active compounds for the injectable CPC. It has been reported that incorporation of BMP-2 adsorbed PLGA-microparticles into CPC results in a sustained *in vivo* release of the growth factor at both ectopic [17] and orthotopic locations [18] in rats, and an increased bone formation was observed compared to non-loaded scaffolds at orthotopic locations [18]. Another approach is to add biologically active compounds to the liquid phase of CPC. It has been reported that the inclusion of transforming growth factor (TGF)- β 1 to the liquid phase of CPC increased the formation of bone in rat calvarial bone

defects [19]. Since growth factor release and related biological effect are likely to be carrier dependent, the release kinetics and osteoinductive capacity of different loading approaches need to be evaluated.

In the present study, different loading methods for BMP-2 into CPC were evaluated in terms of *in vitro* and *in vivo* release and *in vivo* osteoinductive capacity. For injectable CPC, BMP-2 was either adsorbed onto dense PLGA-microparticles or added to the liquid phase of CPC. For comparison, BMP-2 was loaded onto the surface of pre-set, porous CPC. Radiolabeled BMP-2 was used to monitor release profiles *in vitro* as well as *in vivo* using a subcutaneous rat model, in which growth factor retention was analyzed via single-photon emission computed tomography (SPECT). BMP-2 loaded scaffolds without radiolabel were histologically analyzed for osteoinductive capacity of the different loading methods in a rat subcutaneous implantation model. It was hypothesized that in view of an injectable CPC, the addition of BMP-2 via incorporated PLGA-microparticles would result in an increased BMP-2 release and subsequent improved osteoinductive properties in CPC/PLGA compared to CPC/liquid due to a faster degradation of the PLGA-microparticles compared to that of the ceramic matrix of CPC.

Materials and Methods

Materials

Calcium phosphate cement (CPC) consisted of 85% alpha tri-calcium phosphate (α -TCP; CAM Bioceramics BV, Leiden, The Netherlands), 10% dicalcium phosphate anhydrous (DCPA; J.T. Baker Chemical Co., USA) and 5% precipitated hydroxyapatite (pHA; Merck, Darmstadt, Germany), and was sterilized using gamma irradiation (>25 kGy; Isotron BV, Ede, the Netherlands). The cement liquid applied was a sterilized 2 wt.% aqueous solution of Na_2HPO_4 . Acid terminated poly(DL-lactic-co-glycolic acid) (PLGA; Purasorb[®], Purac Biomaterials BV, Gorinchem, the Netherlands) with a lactic to glycolic acid ratio of 50:50 and a molecular weight (Mw) of 17 ± 0.02 kg/mol was used for microparticle preparation. Commercially available recombinant human BMP-2 (BMP-2; R&D Systems MN, USA) was used.

Analysis of the BMP-2 secondary structure

Circular dichroism (CD) spectra of BMP-2 (0.1 mg/ml) dissolved in 2 wt.% aqueous solution of Na_2HPO_4 or BMP-2 (0.1 mg/ml) dissolved in PBS were recorded in the range 195–260 nm at a scan rate of 2s per nm with a Jasco J-810 spectropolarimeter (Oklahoma City, OK) to visualize protein conformation. A quartz cell of 0.1 cm thickness was used. CD spectra values were expressed as mean residue ellipticities (in degrees cm^{-2} dmol^{-1}). The results were further subjected to a non-linear regression analysis to illustrate the secondary structure using the Gauss–Newton algorithm method.

Preparation of hollow and dense PLGA-microparticles

To prepare hollow PLGA-microparticles of around 50 μm in diameter, a double-emulsion-solvent-extraction technique (water-in-oil-in-water) was used, as described previously [10]. Microparticles were produced by adding 500 μl of distilled water to 1400 mg PLGA in 2 ml dichloromethane (DCM). The mixture was emulsified using a Turrax[®] emulsifier for 60 seconds at 6000 rpm. Then, 6 mL 0.3% aqueous poly(vinyl alcohol) (PVA, Acros Organics, Geel, Belgium) solution was added and emulsified for another 60 sec at 6000 rpm to produce the second emulsion. The emulsion was transferred to a stirred beaker, after which 394 mL 0.3% PVA solution and 400 mL of 2% isopropyl alcohol solution was added slowly. After 1 hour of stirring, the microparticles were allowed to settle for 15 min and the solution was decanted. Then, the microparticles were washed and collected through centrifugation at 1500 rpm for 5 min, lyophilized and stored at -20 °C until use. The size distribution of the microparticles was determined by image analysis (Leica Qwin[®], Leica Microsystems). The microparticles were imaged by scanning electron microscopy (SEM; JEOL6310 at 15kV).

To prepare dense PLGA-microparticles of around 50 μm in diameter, a single-emulsion technique was used, as described before [12]. Microparticles were produced by dissolving 0.4 g of PLGA in 4 mL DCM. The solution was transferred into a stirred beaker containing 150 mL of 0.3% PVA solution and 50 mL of 2% IPN solution. After 1 hour of stirring, the microparticles were allowed to settle for 1 hour min and the solution was decanted. Then, the microparticles were washed and collected through centrifugation at 1500 rpm for 1 min and lyophilized. Subsequently, the microparticles were sterilized by gamma irradiation (>25 kGy; Isotron BV, Ede, the Netherlands) and stored at -20 °C until use. The size distribution of the microparticles was determined by image analysis (Leica Qwin[®], Leica Microsystems). The microparticles were imaged by scanning electron microscopy (SEM; JEOL6310 at 15kV).

¹²⁵I-labeling of BMP-2

BMP-2 was labeled with ¹²⁵I, as described previously [20]. Briefly, in a 500 μl eppendorf tube coated with 100 μg iodogen, 10 μl of 0.5 M phosphate buffer saline (PBS) was added. Growth factor (75 μg) and 3 mCi ¹²⁵I (Perkin-Elmer, Boston, MA) was added and incubated at room temperature for 10 min. To remove the non-incorporated ¹²⁵I, the reaction mixture was loaded onto a pre-rinsed disposable Sephadex G-25 column (NAP5; GE healthcare Bio-Sciences AB, Uppsala, Sweden) that was eluted with PBS, 0.1% BSA. The labeling efficiency of the procedure was 55% and the specific activity of the labeled protein was 22.0 $\mu\text{Ci}/\mu\text{g}$.

Experimental groups

The following experimental groups were generated (for composition see Table 1):

1. CPC/control (pre-set dense CPC scaffold containing dense PLGA-microparticles)
2. CPC/porous (pre-set instant porous CPC scaffold; PLGA-microparticles burnt out)
3. CPC/PLGA (CPC/control scaffold with BMP-2 adsorbed onto dense PLGA-microparticles)
4. CPC/liquid (CPC/control scaffold with BMP-2 added to the liquid phase)
5. CPC/surface (CPC/porous scaffold with BMP-2 loaded on the surface)

Table 1 Overview of the different compositions

Group	CPC (wt.%)	PLGA (wt.%) Hollow or Dense	PLGA burnt out	BMP-2 added to
CPC/porous	70	30 (H)	yes	---
CPC/control	70	30 (D)	no	---
CPC/PLGA	70	30 (D)	no	PLGA- porogens
CPC/liquid	70	30 (D)	no	Liquid phase
CPC/surface	70	30 (H)	yes	Surface

Preparation of CPC/PLGA scaffolds

For the *in vitro* release experiment, the scaffolds were loaded with ^{125}I -BMP-2 solutions using a hot/cold mixture of BMP-2, containing 0.5 μCi per scaffold. For the *in vivo* release experiment, the scaffolds were loaded with ^{125}I -BMP-2 solutions using a hot/cold mixture of BMP-2, containing 15 μCi per scaffold. For the evaluation of the osteoinductive capacity of the different loading methods, BMP-2 without radiolabel was used.

The different experimental groups were generated as previously reported (for CPC/porous and CPC/surface see [14]; for CPC/control, CPC/PLGA and CPC/liquid see [12]; for composition see Table 1). In short, 0.69 g dense or 0.3 g hollow PLGA-microparticles was added to 0.7 g sterile CPC, after which sterile Na_2HPO_4 solution was added to the CPC/PLGA in a liquid/powder ratio of 0.40 and mixed for 20 seconds. After mixing, the cement was immediately injected into a Teflon mould to ensure a standardized shape of the scaffolds (\varnothing 7.8 mm, height 2.8 mm). For CPC/porous and CPC/surface, an instantaneous open porous structure was created by placing the pre-set scaffolds in a furnace at 650°C for 2 h to burn out the polymer.

For the adsorption of BMP-2 to the PLGA-particles, a volume of 240 μl 0.1% BSA/PBS solution containing 10 μg BMP-2 was added to the sterile dense PLGA-microparticles, after which the microparticles were frozen, lyophilized and used. To include BMP-2 in the liquid phase of CPC, a Na_2HPO_4 solution containing 10 μg BMP-2 was used. For surface-loaded BMP-2, a volume of 30 μl growth factor solution containing 5 μg BMP-2 was applied to the surface of each side of the instantaneous open porous scaffold to obtain 10 μg BMP-2/scaffold. Thereafter, the scaffolds were frozen and lyophilized.

Characterization of scaffold material

Porosity measurements

To determine total porosity of the scaffolds, CPC/control and CPC/porous ($n=6$) were placed in a furnace at 650°C for 2 h to burn out the polymer. Subsequently, the microporosity and total porosity were calculated using the following equations [10]:

Equation 1

$$\varepsilon_{\text{tot}} = \left(1 - \frac{m_{\text{burnt}}}{V * \rho_{\text{HAP}}}\right) * 100\%$$

Equation 2

$$\varepsilon_{\text{micro}} = \left(1 - \frac{m_{\text{burnt}}}{m_{\text{nanoporous}}}\right) * 100\%$$

Legend

ε_{tot} = Total porosity (%)

$\varepsilon_{\text{micro}}$ = Microporosity (%)

m_{burnt} = Average mass sample (after burning out polymer) (g)

$m_{\text{nanoporous}}$ = Average mass intrinsic nanoporous sample (CaP cement disc without PLGA) (g)

V = Volume sample (cm^3)

ρ_{HAP} = Density hydroxyapatite (g/cm^3)

Scanning Electron Microscopy (SEM)

CPC/control and CPC/porous scaffolds were sputter-coated with gold and examined and photographed using SEM (Jeol 6310, Nieuw-Vennep, The Netherlands) at an acceleration voltage of 10 kV.

Distribution of protein in the different formulations

To visualize the distribution of added protein when adsorbed or included in the different scaffolds, albumin from bovine serum (BSA) labeled with Alexa Fluor 488 (Invitrogen, Life Technologies Europe BV, Bleiswijk, The Netherlands) was used as a model protein. The loading of labeled BSA (10 μg BSA/scaffold) to the different CPCs was similar as described previously, resulting in group 3, 4 and 5. The scaffolds were frozen, lyophilized and fixed in 4% formalin overnight. Subsequently,

the tissue blocks were embedded in methylmethacrylate (MMA). Perpendicular to the scaffold diameter, thin sections (~10 µm) were prepared using a microtome with diamond blade (Leica Microsystems SP 1600, Nussloch, Germany) [21]. The MMA sections were visualized using a fluorescence microscope with a Zeiss filter set 00, consisting of a 530–585 nm band-pass excitation filter (Carl Zeiss B.V., Sliedrecht, The Netherlands).

In vitro release experiment

The different CPC scaffolds loaded with ¹²⁵I-BMP-2 (n=6; 0.5 µCi/scaffold) were placed in 10 ml glass vials for evaluation of the *in vitro* BMP-2 release kinetics and incubated in 3 ml PBS at 37 °C for 28 days. At days 1, 3, 7, 14, 21 and 28, the samples were carefully transferred to new vials containing fresh PBS, after which gamma emission of the scaffolds was measured in a shielded well-type gamma counter (Wizard, Pharmacia-LKB, Uppsala, Sweden). Standards were measured simultaneously to correct for radioactive decay. The remaining activity in the scaffolds was expressed as percentage of the initial dose.

In vivo experiment

Animals

Fifteen healthy young adult (8 weeks old) male Wistar rats were used as experimental animals, of which 9 animals were used for the *in vivo* release experiment (two implants per animal) and 6 animals were used to evaluate the osteoinductive capacity of the different CPC formulations (4 implants per animal). The research was reviewed and approved by the Experimental Animal Committee of the Radboud University (RUDEC 2011-186) and national guidelines for the care and use of laboratory animals were observed.

Surgical procedure

Anesthesia was induced and maintained by Isoflurane inhalation (Rhodia Organique Fine Limited, Avonmouth, Bristol, UK). To minimize post-operative discomfort, Rimadyl (Carprofen, Pfizer Animal Health, New York, USA) was administered subcutaneously (5 mg/kg) before the surgery. CPC scaffolds were subcutaneously implanted into the back of each rat. To insert the scaffolds, rats were immobilized on their abdomen and the skin was shaved and disinfected with chlorhexidine. On both sides of the vertebral column, two small paravertebral incisions were made through the full thickness of the skin. Lateral to the incisions, a subcutaneous pocket was created using blunt dissection. Subsequently, one implant was inserted into each pocket. Finally, the skin was closed using staples (Agraven, Instruvet, Boxmeer, the Netherlands). In total, for the *in vivo* release experiment eighteen implants (two implants per animal; n=6 for each experimental group) and for the osteoinductive capacity evaluation twenty-four implants (4 implants per animal;

$n=3$ for groups 1-2 and $n=6$ for groups 3-5) were placed according to a randomization scheme.

The animals were housed in pairs. In the initial postoperative period, the intake of water and food was monitored. Further, the animals were observed for signs of pain, infection and proper activity. At the end of the implantation time, the rats were sacrificed by CO₂-suffocation.

***In vivo* release experiment**

At days 0, 1, 3, 7, 14 and 21 after implantation of the CPC scaffolds, rats were scanned using a small-animal SPECT scanner (U-SPECT II, MILabs, The Netherlands). Anesthesia was induced and maintained by Isoflurane inhalation (Rhodia Organique Fine Limited, Avonmouth, Bristol, UK). On day 28, rats were sacrificed and scanned post mortem followed by a CT scan for anatomic reference. The animals were placed prone in the SPECT scanner and scanned for 40 min using a rat 1.0-mm-diameter-pinhole collimator tube. Scans were reconstructed with MILabs reconstruction software, which uses an ordered-subset expectation maximization algorithm, with a voxel size of 0.375 mm. The amount of radioactivity in a specified volume of interest around the implants was quantified and expressed as percentage of original dose per scaffold (PMOD software, version 3.15, PMOD Technologies Ltd.). To achieve accurate quantification, standards containing 0, 1, 3, 10 or 30 $\mu\text{Ci } ^{125}\text{I}$ were scanned at the same days.

Implant retrieval and histological preparations

The specimens without radiolabeled BMP-2 ($n=6$) were retrieved after a 4-week implantation period. After sacrifice, scaffolds with surrounding tissues were excised and fixed in 10% phosphate-buffered formaldehyde solution (pH 7.4). Subsequently, the tissue blocks were dehydrated in increasing ethanol concentrations (70 – 100%) and embedded in methylmethacrylate (MMA). Perpendicular to the diameter of the scaffolds, thin sections (10 μm) were prepared using a microtome with diamond blade (Leica Microsystems SP 1600, Nussloch, Germany) [21]. Three sections of each scaffold were stained with methylene blue and basic fuchsin and examined using light microscopy (Leica Microsystems AG, Wetzlar, Germany).

For CPC/PLGA, CPC/liquid and CPC/surface, two MMA samples were polished and gold sputter-coated prior to analysis with scanning electron microscopy (JEOL 6330) using Back-Scattered Electron (BSE) mode for histomorphometrical analysis.

Histological and histomorphometrical evaluation

Sections of MMA-embedded specimens (at least 3 sections per specimen) were quantitatively assessed using computer-based image analysis techniques (Leica® Qwin Pro-image analysis system, Wetzlar, Germany). The analysis technique is based on color recognition depending on staining intensity. From digital images

(magnification: 5x), the total amount of newly-formed bone surrounding the CPC scaffold was determined and expressed in area measures (mm^2).

Statistical analysis

Statistical analysis was performed using GraphPad InStat 3.05 software (GraphPad Software Inc., San Diego, CA) using one-way analysis of variance with a Tukey multiple comparison post test. Differences were considered significant at p -values less than 0.05.

Results

Analysis of the BMP-2 secondary structure

CD spectra of BMP-2 dissolved in PBS or 2% Na_2HPO_4 were comparatively analyzed, showing only limited differences in molar CD values at 200–235nm. Additionally, secondary structure analysis based on the obtained CD spectra revealed no significant differences in α -helix, β -sheet or random coil structure of BMP-2 dissolved in 2% Na_2HPO_4 compared to BMP-2 dissolved in PBS (Table 2).

Table 2 Secondary structure analysis of BMP-2 dissolved in 2% Na_2HPO_4 or PBS

	α -Helix	β -Sheet	Random coil (%)
BMP-2 dissolved in PBS	14	40	40
BMP-2 dissolved in 2% Na_2HPO_4	14	40	40

The analysis was conducted based on the CD spectrum using the Gauss–Newton algorithm method.

Characterization of scaffold material

The preparation of hollow PLGA-microparticles with a double-emulsion-solvent-extraction technique and dense PLGA-microparticles with a single-emulsion technique resulted in microparticles with a similar average size of $58.4 \pm 35.0 \mu\text{m}$ and $62.4 \pm 28.9 \mu\text{m}$ ($p > 0.05$), respectively.

Since the principle of CPC preparation was based on either combination of CPC with hollow PLGA-microparticles (CPC/porous and CPC/surface) or CPC with dense PLGA-microparticles (CPC/control, CPC/PLGA and CPC/liquid), surface examination of the scaffolds was carried out for only CPC/porous and CPC/control. Surface examination showed that for CPC/control, a homogenous distribution of PLGA-microparticles within the implant material was observed (Figure 1A). For CPC/porous, PLGA-microparticles were completely burnt out and an instant porous scaffold material was observed (Figure 1B). Porosity measurements of CPC/porous and CPC/control scaffolds demonstrated a microporosity of $42.5 \pm 3.0 \%$ and $59.9 \pm 2.9 \%$ and a total porosity of $72.3 \pm 1.4 \%$ and $80.7 \pm 1.4 \%$ for CPC/porous and CPC/control, respectively.

Protein distribution was visualized using Alexa Fluor 488-labeled BSA as a model protein (Figure 1C). The protein in CPC/surface was only observed peripherally and not in the center of the implants. In contrast, the protein in CPC/PLGA and CPC/liquid was distributed throughout the entire scaffold, showing localization of protein on the PLGA-microparticles for CPC/PLGA and a more dispersed pattern for CPC/liquid.

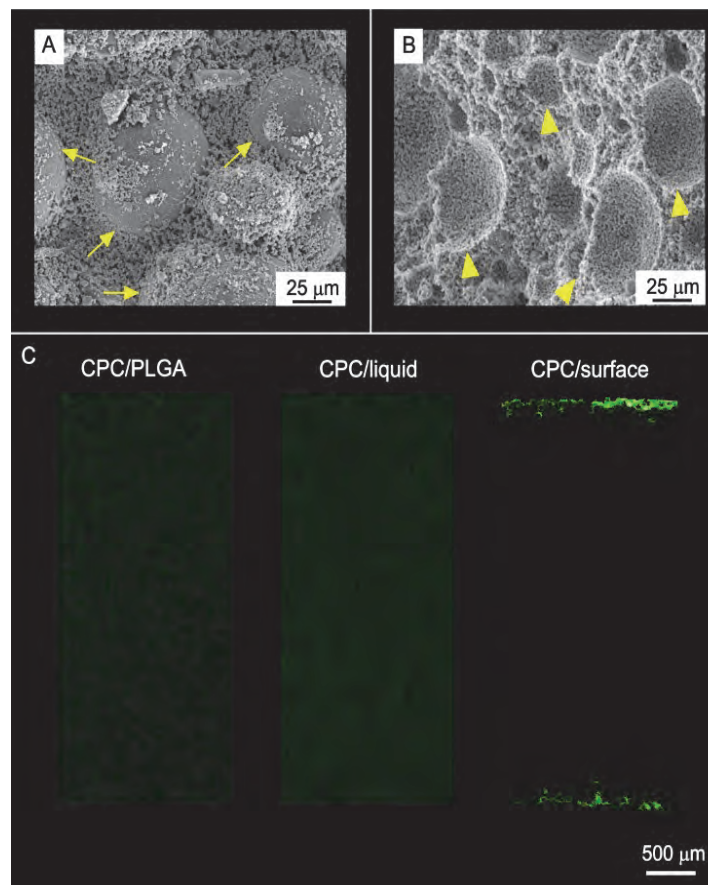


Figure 1 Characterization of scaffold material. Microscopic SEM images of scaffold material (A) CPC/control and (B) CPC/porous. Original magnification 75x, bar represents 25 μm. PLGA-microparticles (arrows) and created pores after burning out PLGA-microparticles (arrowheads) are indicated. (C) Protein distribution using alexa fluor 488 labeled BSA as a model protein. BSA was loaded on PLGA-microparticles and incorporated in CPC (CPC/PLGA), included in liquid phase of CPC (CPC/liquid) or absorbed onto the surface of instant porous preset CPC (CPC/surface), Bar represents 500 μm.

***In vitro* release**

The *in vitro* release for CPC/PLGA, CPC/liquid and CPC/surface, during 28 days is depicted in Figure 2. All scaffolds retained their integrity during the entire experiment. CPC/surface showed an initial burst release within 1 day (~40%), followed by a sustained release till day 28 (Figure 2A). Both CPC/PLGA and CPC/liquid showed a limited burst release within 1 day (~10%), followed by a sustained release from day 1 till day 28 with a similar pattern compared to CPC/surface (Figure 2A).

The cumulative BMP-2 release was significantly higher for CPC/surface compared to CPC/PLGA and CPC/liquid, reaching after 28 days a release of $70.0 \pm 2.2\%$, $45.7 \pm 1.7\%$ and $48.4 \pm 1.5\%$, respectively ($p < 0.0001$; Figure 2A). From day 3 onward, the cumulative BMP-2 release from CPC/liquid was significantly higher compared to CPC/PLGA ($p < 0.01$; Figure 2A).

The relative amounts of BMP-2 released during the different phases (i.e. burst release, sustained release, and retained BMP-2 after 28 days) are depicted in Figure 2B. For CPC/surface, the burst release was significantly higher compared to CPC/PLGA and CPC/liquid (Figure 2B; $p < 0.001$; for CPC/PLGA $10.5 \pm 2.3\%$ and for CPC/liquid $13.1 \pm 2.7\%$; for CPC/surface $40.4 \pm 4.6\%$). The release rate per day from day 1-28 (Figure 2B) of CPC/surface compared to CPC/PLGA and CPC/liquid was significantly lower ($p < 0.0001$, release rate of $0.53 \pm 0.02\%$, $0.52 \pm 0.02\%$ and $0.40 \pm 0.03\%$ per day for CPC/PLGA and CPC/liquid, CPC/surface, respectively). After 28 days, the retention for CPC/surface was significantly lower compared to CPC/PLGA and CPC/liquid ($p < 0.0001$, retention of $54.3 \pm 1.7\%$, $51.6 \pm 1.5\%$ and $30.0 \pm 2.2\%$ for CPC/PLGA, CPC/liquid and CPC/surface, respectively).

***In vivo* experiment**

General observation of the experimental animals

All 6 animals used for the evaluation of the osteoinductive capacity of the different formulations, recovered uneventfully from the surgical procedure and remained in good health. From the 9 animals used for the *in vivo* release experiment, one animal died after 21 days. Clinical examination indicated that the cause of death was an anaesthetic-induced respiratory depression during *in vivo* scanning. All remaining 8 animals recovered uneventfully from the surgical procedure and remained in good health. The total number of implants placed, retrieved and used for histomorphometrical evaluation is depicted in Table 3.

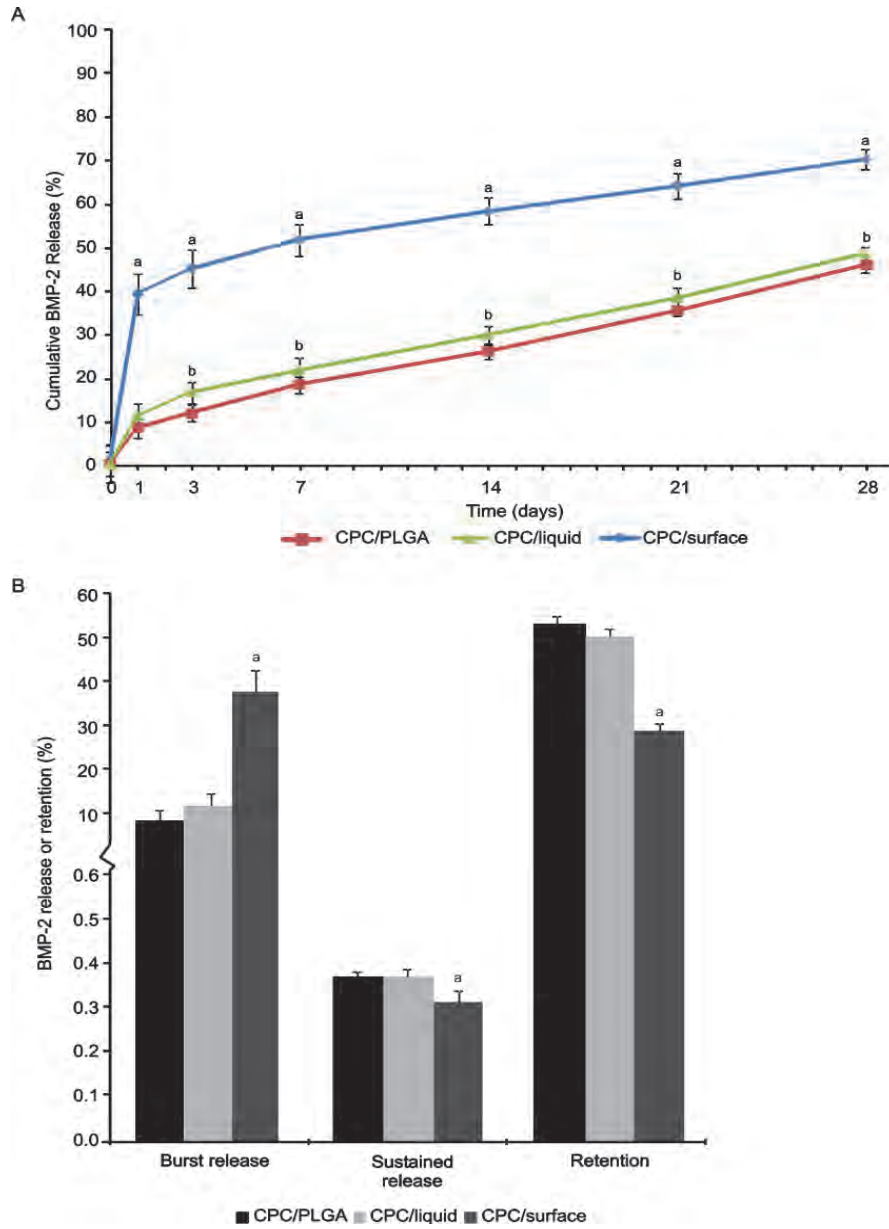


Figure 2 Longitudinal *in vitro* scintigraphic assessment (A) CPC/PLGA, CPC/liquid and CPC/surface during 28 days and (B) the *in vitro* burst release (after 1 day), sustained release (the release per day from day 1-28) and the retention after 28 days. The release and retention is expressed as percentage of the ratio of initial loading amount. Error bars represents the mean \pm SD ($n=6$). (a) $p<0.001$ compared to CPC/PLGA and CPC/liquid, (b) $p<0.01$ compared to CPC/PLGA.

DIFFERENTIAL LOADING METHODS FOR BMP-2 WITHIN INJECTABLE CPC

Table 3 Overview of implants placed, retrieved and used for histomorphometrical evaluation

	Implants placed	Implants retrieved	Implants used for analysis
CPC/porous	3	3	3
CPC/control	3	3	3
CPC/PLGA	6	6	5*
CPC/liquid	6	6	5*
CPC/surface	6	6	5*

*deviations from the number of implants retrieved due to fracturing of implants during histological processing.

***In vivo* release**

The *in vivo* release during 28 days from CPC/PLGA, CPC/liquid and CPC/surface, is depicted in Figure 3. CPC/surface showed an initial burst release within 1 day followed by a sustained release from day 1 till day 28 (Figure 4A). Both CPC/PLGA and CPC/liquid showed a limited burst release within 1 day (~10%), followed by a sustained release from day 1 till day 28 with a similar pattern compared to CPC/surface (Figure 4A). The cumulative BMP-2 release was significantly higher for CPC/surface compared to CPC/PLGA and CPC/liquid reaching up to $90.1 \pm 1.3\%$, 61.3 ± 4.7 and $65.2 \pm 1.9\%$ after 28 days, respectively ($p < 0.0001$; Figure 4A).

The relative amounts of BMP-2 released during the different phases (i.e. burst release, sustained release, and retained BMP-2 after 28 days) are depicted in Figure 4B. For CPC/surface, the burst release was significantly higher compared to CPC/PLGA and CPC/liquid (Figure 4B; $p < 0.001$; for CPC/PLGA $10.3 \pm 8.5\%$, for CPC/liquid 8.5 ± 3.0 and for CPC/surface $51.8 \pm 7.1\%$). The release rate per day from day 1-28 (Figure 4B; % per day) of CPC/surface compared to CPC/liquid was significantly lower ($p < 0.01$, release rate of $1.4 \pm 0.3\%$ and $2.1 \pm 0.1\%$ per day for CPC/surface and CPC/liquid, respectively). Between CPC/surface and CPC/PLGA ($p = 0.47$; for CPC/PLGA $1.8 \pm 0.4\%$) and between CPC/PLGA and CPC/liquid ($p = 0.14$) no differences were observed.

After 28 days, a significant lower protein retention for CPC/surface was observed compared to CPC/PLGA and CPC/liquid (Figure 4B; $p < 0.0001$; for CPC/PLGA $39.2 \pm 4.2\%$, for CPC/liquid $36.0 \pm 3.2\%$ and for CPC/surface $9.9 \pm 1.3\%$).

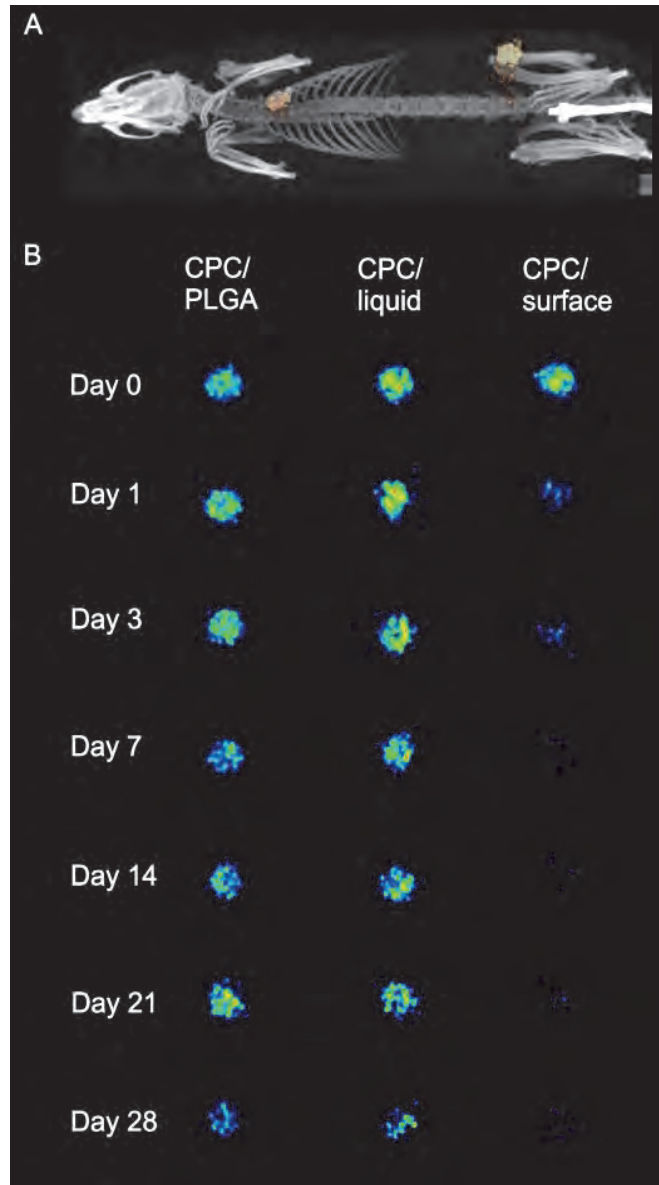


Figure 3 (A) Representative U-SPECT/CT-scan of rat implanted with CPC scaffolds. (B) Representative U-SPECT scans of CPC/PLGA, CPC/liquid or CPC/surface during 28 days.

DIFFERENTIAL LOADING METHODS FOR BMP-2 WITHIN INJECTABLE CPC

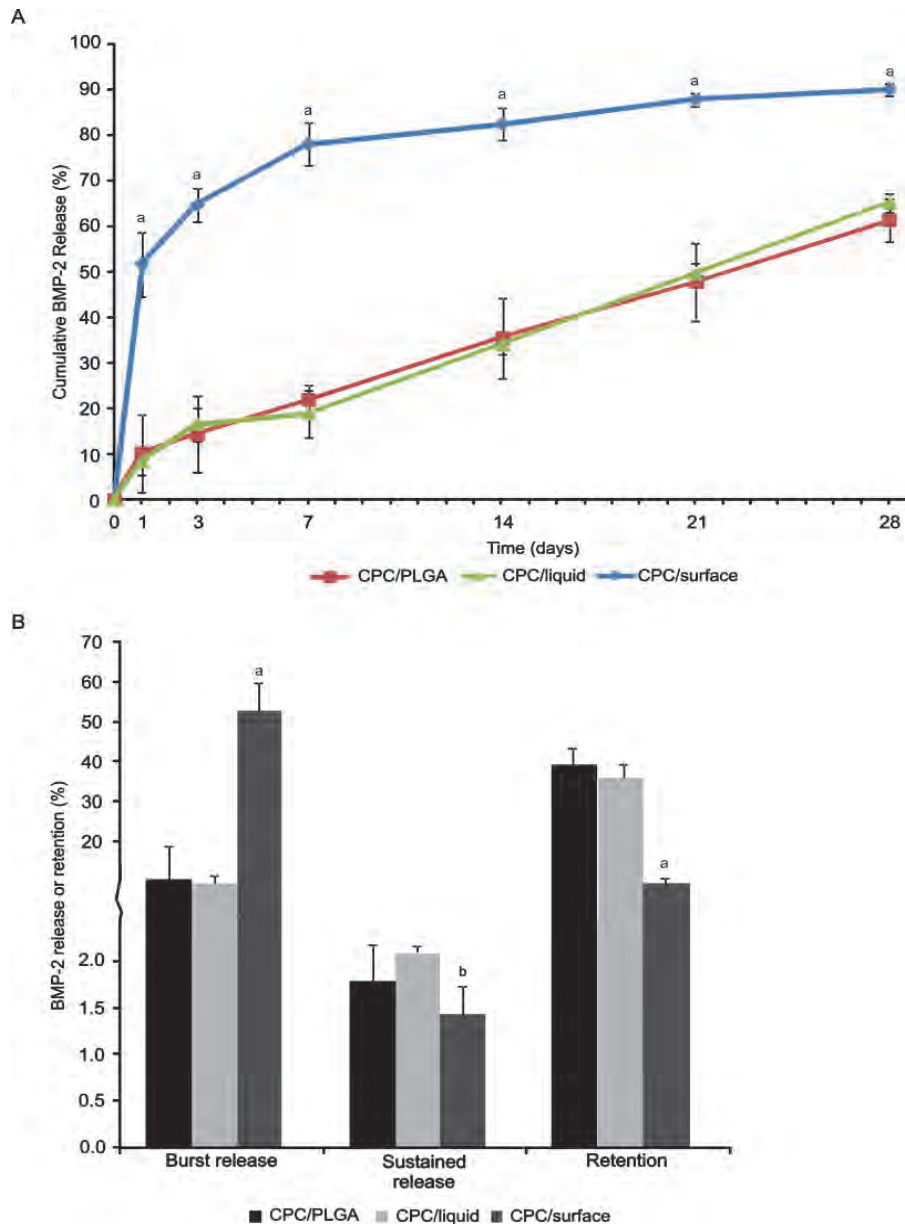


Figure 4 Longitudinal *in vivo* (A) release assessment analyzed via a small animal U-SPECT II scanner of CPC/PLGA, CPC/liquid and CPC/surface during 28 days and (B) the *in vitro* burst release (after 1 day), sustained release (the release per day from day 1-28) and the retention after 28 days. The release and retention is expressed as percentage of the ratio of initial loading amount. Error bars represents the mean \pm SD ($n=4$). (a) $p < 0.01$ compared to CPC/PLGA and CPC/liquid; (b) $p < 0.05$ compared to CPC/liquid.

Osteoinductive capacity of the different formulations

The structural integrity of the scaffolds was maintained in all experimental groups. A fibrous capsule surrounding CPC/control and CPC/porous, without the presence of inflammatory cells at the interface was observed (data not shown). Ingrowth of soft tissue was observed peripherally in CPC/control and throughout the implants in CPC/porous and no bone formation was observed in the vicinity of these scaffolds. A fibrous capsule surrounding CPC/PLGA, CPC/liquid and CPC/surface, without the presence of inflammatory cells at the interface was observed (data not shown). In 4 out of 5 CPC/surface, a limited amount of bone was formed at the periphery of the scaffold, while no bone formation was observed in the vicinity of CPC/PLGA and CPC/liquid scaffolds (Figure 5B). Back-scatter SEM micrographs confirmed the observed peripheral bone formation in CPC/surface (Figure 5C). Quantitative results of ectopic bone formation revealed a total amount of bone in the periphery of CPC/surface of $3.6 \pm 3.0 \text{ mm}^2$.

Discussion

To enhance the biological performance of CPC biologically active compounds, such as BMP-2, can be introduced. The clinical application of CPC in an injectable form requires an integrated loading of BMP-2 via either PLGA-microparticles or the liquid phase of the cement. In view of this, the current study comparatively evaluated the *in vitro* and *in vivo* release profiles as well as the osteoinductive potential of CPC scaffolds in a rat subcutaneous implantation model, in which BMP-2 was (i) loaded onto dense PLGA-microparticles (CPC/PLGA), (ii) added to the liquid phase of the cement (CPC/liquid), or (as a control) (iii) adsorbed onto the surface of preset scaffolds (CPC/surface). It was hypothesized that in view of an injectable CPC, the addition of BMP-2 via incorporated PLGA-microparticles would result in an accelerated BMP-2 release leading to improved osteoinductive properties for CPC/PLGA compared to CPC/liquid. The *in vitro* and *in vivo* release assays revealed that the BMP-2 burst release from CPC/surface was significantly increased compared to CPC/PLGA and CPC/liquid. The BMP-2 retention for CPC/surface was significantly lower after 28 days compared to CPC/PLGA and CPC/liquid, despite a significantly increased sustained release rate for CPC/PLGA and CPC/liquid. The ectopic rat model demonstrated that only CPC/surface is capable of inducing ectopic bone formation.

The release profiles of the different scaffold formulations revealed similar patterns consisting of a burst release followed by a sustained release. However, the cumulative release was significantly increased at all time points for surface-loaded BMP-2 compared to that for incorporated BMP-2 (via either PLGA-microparticles or the liquid phase of the CPC). This difference in cumulative release is mainly dependent on the large difference ($\sim 30\%$ *in vitro*, $\sim 40\%$ *in vivo*) in burst release observed for surface-loaded BMP-2 compared to that for incorporated BMP-2.

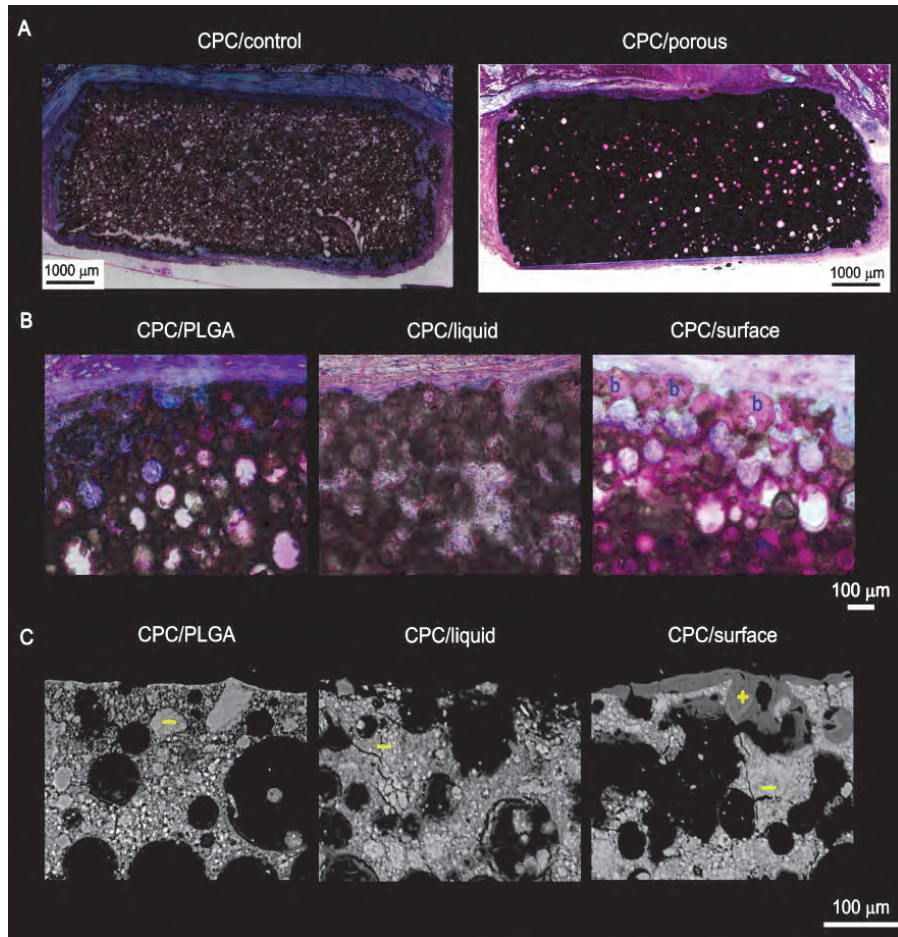


Figure 5 (A) Histological overview sections of CPC/control and CPC/porous. Bar represents 1000 μm. Histological sections are stained with methylene blue and basic fuchsin. (B) Magnification of histological sections of CPC/PLGA, CPC/liquid and CPC/surface. Bone (b) is indicated in the sections. Original magnification is 20x. Bar represents 100 μm. Histological sections are stained with methylene blue and basic fuchsin. (C) Cross-sections observed with back scattering SEM of CPC/PLGA, CPC/liquid and CPC/surface. For back scattering SEM micrographs bone appears dark gray (+) while the CPC scaffold is lighter (-).

The difference in burst release is likely to be related to the manufacturing process of the different scaffolds, which results in an evidently distinct protein distribution. Surface loaded BMP-2, was located peripherally and hence in direct contact with the surrounding environment in which BMP-2 could be released fast and freely. In contrast, incorporated BMP-2 was located throughout the CPC and hence any released BMP-2 had to diffuse out of the scaffold. In addition, the protein diffusion within CPC is dependent on the scaffold porosity, for which differences existed

regarding the temporal presence of porosity (i.e. directly for CPC/surface and after degradation of PLGA-microparticles for CPC/PLGA and CPC/liquid). Previous studies have demonstrated that the dense acid terminated PLGA-microparticles degrade *in vitro* between 2-6 weeks [12] and are completely degraded *in vivo* after 4 weeks (current manuscript) at ectopic locations. *In vitro* degradation of plain CPC (without PLGA microparticles) starts from week 1 [12, 22] and is limited, but can be substantially increased via the effect of acidic degradation products of PLGA. The fact that all 3 experimental groups still show a linear sustained release indicates that degradation (of the CPC) is governing release. However, a relationship between release and porosity is not univocally established. Remarkably, similar release kinetics were observed for CPC/PLGA and CPC/liquid, where it was expected that the rapid degradation of PLGA-microparticles would evoke a faster release of adsorbed BMP-2. In view of this, it appears that liberated BMP-2 molecules from the degraded PLGA-microparticles readily adsorb to the ceramic matrix of CPC, after which overall release kinetics show large similarity to scaffolds with BMP-2 loaded via the liquid phase of the cement [23, 24].

The *in vivo* release of BMP-2 in the current study was ~10-20% higher compared to the *in vitro* release of the different formulations. However, the observed *in vitro* and *in vivo* release kinetics of the different scaffolds followed a similar pattern. These findings corroborate earlier observations, in which despite similar release patterns (i.e. a burst release followed by a sustained release) differences regarding the amounts between the *in vitro* and *in vivo* release kinetics of BMP-2 from CPC were observed ranging from 50% [24] to 80% [25]. This difference is likely dependent on the availability of proteins within body fluid and the large buffering capacity of the body, which can be responsible for the difference in release amounts, re-adsorption of the protein and BMP-2 clearance from the vicinity of the scaffold [26]. Therefore, Ruhé *et al.* (2005) and Li *et al.* (2003) suggested to perform the *in vitro* release experiment in protein-rich buffer solution to simulate more the body fluid and therefore simulating more the *in vivo* release of the growth factor [24, 25]. However, for the extrapolation of *in vitro* data to the *in vivo* situation protein-rich buffer solution alone was not sufficient because the *in vitro* release profile of BMP-2 loaded CPC performed in a protein-rich-buffer still underestimated the *in vivo* release profile with ~20% [24]. Therefore, the predictive value of *in vitro* release patterns implicates an underestimation of the *in vivo* situation.

In the current study, the *in vivo* release of BMP-2 from the different CPC scaffolds was analyzed noninvasively with SPECT imaging. With SPECT the pharmacokinetic profile of ¹²⁵I-labelled proteins could be monitored quantitatively and the (localization of the) ¹²⁵I-labelled proteins could be visualized in the rats [27, 28]. However, tracking the released ¹²⁵I-BMP-2 molecules could not be visualized due to limitations in the sensitivity. Nevertheless, due to a fixed implant position, concentrated ¹²⁵I-BMP-2 molecules in the different scaffolds could be visualized and analyzed accurately and reliably.

Although it seems straightforward to assume that the biological activity of BMP-2 upon loading onto the surface of or into the scaffolds might be compromised,

earlier reports and side-experiments in the current study provide evidence to prove this assumption wrong. For example, in the current study as well as previously reported [14], the addition of surface-loaded BMP-2 increased the osteoinductive properties of CPC, indicating no effect on the bioactivity of BMP-2 upon surface loading. In addition, several reports showed that the different loading methods to incorporate BMP-2 into CPC used in the current study (i.e. adsorption of BMP-2 to PLGA-microparticles or addition of BMP-2 to the liquid phase of CPC) are capable to evoke either osteoinductive responses [17, 18] or enhance osteogenic responses [19]. Further indirect proof for retained biological activity of BMP-2 was obtained via secondary structure analysis of dissolved BMP-2, which revealed no conformational changes of the protein upon dissolution in the liquid phase of cement. Unfortunately, direct evidence for retained biological activity of BMP-2 upon loading into CPC via adsorption to PLGA-microparticles or addition to the liquid phase remains unavailable, since cell culture experiments with CPC scaffolds or releasate are impossible in view of the effects of calcium release from CPC [29, 30]. Taken together, the indirect evidence indicates that the lack of an osteoinductive effect of BMP-2 incorporated within CPC is mainly dependent on an insufficient amount of (burst) released BMP-2 rather than to an altered BMP-2 bioactivity.

Previous reports assumed that for clinical applications in a bone environment, a burst release is needed to result in an “above threshold” amount of exogenous BMP-2 to trigger bone regenerative cells to stimulate bone formation [31-33]. However, lack of consensus exists regarding appropriate amounts of BMP-2 [18, 34]. In view of that, the BMP-2 loading methods for injectable CPC used in this study appeared unable to induce bone formation ectopically. This observation is likely to be related to the release profile as mentioned earlier, but also to the spatial distribution of BMP-2 throughout the entire scaffold (in contrast to condensed availability at the periphery of the scaffold following surface-loading, which showed osteoinductive capacity). Still, BMP-2 loading for CPC via adsorption to PLGA-microparticles or addition to the liquid phase might be a feasible means to accomplish the stimulation of bone regeneration at orthotopic locations. Further, it has to be emphasized that addition of BMP-2 to the liquid phase of CPC is preferred above adsorption to PLGA-microparticles, since the manufacturing process is more straightforward and less labor-intensive.

In conclusion, the present study demonstrated that BMP-2 loading is feasible for injectable CPC via adsorption to PLGA-microparticles or addition to the liquid phase of CPC. These loading methods resulted in a similar release profile over the course of 28 days, despite distinct protein distribution patterns. Compared to CPC-scaffolds with surface-loaded BMP-2, these loading methods showed a similar release profile, except for a significantly decreased burst release. As such, the observed osteoinductive capacity for only CPC-scaffolds with surface-loaded BMP-2 is likely to be related to this difference in burst release. It remains unclear to what extent the differential BMP-2 loading methods for injectable CPC can affect the biological response in a bone environment.

Acknowledgements

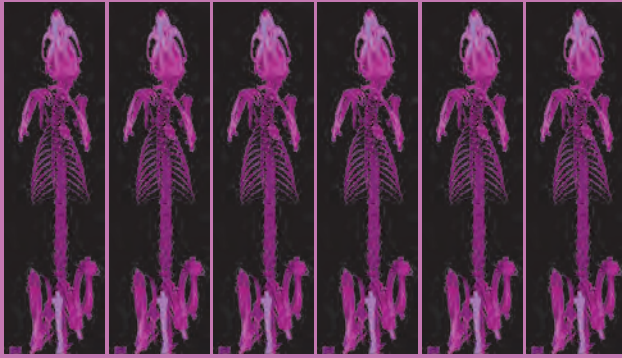
The authors gratefully acknowledge the support of the Smart Mix Program of the Netherlands Ministry of Economic Affairs and the Netherlands Ministry of Education, Culture and Science. The authors thank Natasja van Dijk for assistance with the histological preparations and Dennis Löwik and Britta Ramakers for their assistance with the CD analysis. Scanning electron microscopy was performed at the Nijmegen Center for Molecular Life Sciences (NCMLS), the Netherlands

References

- [1] L. C. Chow, Next generation calcium phosphate-based biomaterials, *Dent. Mater. J.* 28 (2009) 1-10.
- [2] LeGeros, Calcium Phosphate in Oral Biology and Medicine, Karger, Basel, 1991.
- [3] M.B. Bohner, Physical and chemical aspects of calcium phosphates used in spinal surgery, *Eur. Spine J.* 10 (2001) S114-S121.
- [4] R. LeGeros, Properties of osteoconductive biomaterials: calcium phosphates, *Clin. Orthop. Relat. R.* 395 (2002) 81-98.
- [5] J. Jansen, E. Ooms, N. Verdonchot, J. Wolke, Injectable calcium phosphate cement for bone repair and implant fixation, *Orthop. Clin. North Am.* 36 (2005) 89-95.
- [6] W. Habraken, L. de Jonge, J. Wolke, L. Yubao, A. Mikos, J. Jansen, Introduction of gelatin microspheres into an injectable calcium phosphate cement, *J. Biomed. Mater. Res. A* 87A (2008) 643-655.
- [7] D.P. Link, J. van den Dolder, W.J.F.M. Jurgens, J.G.C. Wolke, J.A. Jansen, Mechanical evaluation of implanted calcium phosphate cement incorporated with PLGA microparticles, *Biomaterials* 27 (2006) 4941-4947.
- [8] P. Ruhé, E. Hedberg-Dirk, N.T. Padron, P. Spauwen, J. Jansen, A. Mikos, Porous Poly(DL-lactic-co-glycolic acid)/Calcium Phosphate Cement Composite for Reconstruction of Bone Defects, *Tissue Eng.* 12 (2006) 789-800.
- [9] P. Ruhé, E. Hedberg, N.T. Padron, P. Spauwen, J. Jansen, A. Mikos, Biocompatibility and degradation of poly(DL-lactic-co-glycolic acid)/calcium phosphate cement composites, *J. Biomed. Mater. Res. A* 74A (2005) 533-544.
- [10] W. Habraken, J. Wolke, A. Mikos, J. Jansen, Injectable PLGA microsphere/calcium phosphate cements: physical properties and degradation characteristics *J. Biomater. Sci. Polym. Ed.* 17 (2006) 1057-1074.
- [11] R. del Real, J. Wolke, M. Vallet-Regí, J. Jansen, A new method to produce macropores in calcium phosphate cements, *Biomaterials* 23 (2002) 3673-3680.
- [12] R.P. Félix Lanao, S.C.G. Leeuwenburgh, J.G.C. Wolke, J.A. Jansen, In vitro degradation rate of apatitic calcium phosphate cement with incorporated PLGA microspheres, *Acta Biomater.* 7 (2011) 3459-3468.
- [13] R.P. Félix Lanao, S.C.G. Leeuwenburgh, J.G.C. Wolke, J.A. Jansen, Bone response to fast-degrading, injectable calcium phosphate cements containing PLGA microparticles, *Biomaterials* 32 (2011) 8839-8847.
- [14] F.C.J. van de Watering, J.J.J.P. van den Beucken, S.P. van der Woning, A. Briest, A. Eek, H. Qureshi, L. Winnubst, O.C. Boerman, J.A. Jansen, Non-glycosylated BMP-2 can induce ectopic bone formation at lower concentrations compared to glycosylated BMP-2, *J. Control. Release* (2012) 10.1016/j.jconrel.2011.1012.1041.
- [15] H.C. Kroese-Deutman, P.Q. Ruhé, P.H.M. Spauwen, J.A. Jansen, Bone inductive properties of rhBMP-2 loaded porous calcium phosphate cement implants inserted at an ectopic site in rabbits, *Biomaterials* 26 (2005) 1131-1138.
- [16] P.Q. Ruhé, H.C. Kroese-Deutman, J.G.C. Wolke, P.H.M. Spauwen, J.A. Jansen, Bone inductive properties of rhBMP-2 loaded porous calcium phosphate cement implants in cranial defects in rabbits, *Biomaterials* 25 (2004) 2123-2132.

DIFFERENTIAL LOADING METHODS FOR BMP-2 WITHIN INJECTABLE CPC

- [17] P. Ruhé, O. Boerman, F. Russel, P. Spauwen, A. Mikos, J. Jansen, Controlled release of rhBMP-2 loaded poly(dl-lactic-co-glycolic acid)/calcium phosphate cement composites in vivo, *J. Control. Release* 106 (2005) 162-171.
- [18] E. Bodde, O. Boerman, F. Russel, A. Mikos, P. Spauwen, J. Jansen, The kinetic and biological activity of different loaded rhBMP-2 calcium phosphate cement implants in rats, *J. Biomed. Mater. Res. A* 87A (2008) 780-791.
- [19] E.J. Blom, J. Klein-Nulend, E.H. Burger, M.A.J. Van Waas, L. Yin, Transforming growth factor- β 1 incorporated in calcium phosphate cement stimulates osteotransductivity in rat calvarial bone defects, *Clin. Oral. Implants. Res.* 12 (2001) 609-616.
- [20] P.J. Fraker, J.C. Speck, Protein and cell membrane iodinations with a sparingly soluble chloroamide, 1,3,4,6-tetrachloro-3a,6a-diphenylglycoluril, *Biochem. Biophys. Res. Commun.* 80 (1978) 849-857.
- [21] H. van der Lubbe, C. Klein, K. de Groot, A simple method for preparing thin (10 microM) histological sections of undecalcified plastic embedded bone with implants, *Stain Technol.* 63 (1988) 171-176.
- [22] R.J. Klijn, J.J. van den Beucken, R.P. Félix Lanao, G. Veldhuis, S.C. Leeuwenburgh, J.G. Wolke, G.J. Meijer, J.A. Jansen, Three different strategies to obtain porous calcium phosphate cements: comparison of performance in a rat skull bone augmentation model, *Tissue Engineer Part A.* 18 (2012) 1171-1182.
- [23] T.S. Tsapikouni, Y.F. Missirlis, Protein-material interactions: From micro-to-nano scale, *Mater. Sci. Eng. B* 152 (2008) 2-7.
- [24] P. Ruhé, O. Boerman, F. Russel, A. Mikos, P. Spauwen, J. Jansen, *In vivo* release of rhBMP-2 loaded porous calcium phosphate cement pretreated with albumin, *J. Mater. Sci. Mater. Med.* 17 (2006) 919-927.
- [25] R.H. Li, M.L. Bouxsein, C.A. Blake, D. D'Augusta, H. Kim, X.J. Li, J.M. Wozney, H.J. Seeherman, rhBMP-2 injected in a calcium phosphate paste (α -BSM) accelerates healing in the rabbit ulnar osteotomy model, *J. Orthop. Res.* 21 (2003) 997-1004.
- [26] P. Laffargue, P. Fialdes, P. Frayssinet, M. Rtaimate, H.F. Hildebrand, X. Marchandise, Adsorption and release of insulin-like growth factor-I on porous tricalcium phosphate implant, *J. Biomed. Mater. Res.* 49 (2000) 415-421.
- [27] D.H.R. Kempen, M.J. Yaszemski, A. Heijink, T.E. Hefferan, L.B. Creemers, J. Britson, A. Maran, K.L. Classic, W.J.A. Dhert, L. Lu, Non-invasive monitoring of BMP-2 retention and bone formation in composites for bone tissue engineering using SPECT/CT and scintillation probes, *J. Control. Release* 134 (2009) 169-176.
- [28] D.H.R. Kempen, L. Lu, K.L. Classic, T.E. Hefferan, L.B. Creemers, A. Maran, W.J.A. Dhert, M.J. Yaszemski, Non-invasive screening method for simultaneous evaluation of in vivo growth factor release profiles from multiple ectopic bone tissue engineering implants, *J. Control. Release* 130 (2008) 15-21.
- [29] D.P. Link, J. van den Dolder, J.G.C. Wolke, J.A. Jansen, The Cytocompatibility and Early Osteogenic Characteristics of an Injectable Calcium Phosphate Cement, *Tissue Eng.* 13 (2007) 493-500.
- [30] U. Hempel, A. Reinstorf, M. Poppe, U. Fischer, M. Gelinsky, W. Pompe, K.W. Wenzel, Proliferation and differentiation of osteoblasts on Biocement D modified with collagen type I and citric acid, *J. Biomed. Mater. Res. B* 71B (2004) 130-143.
- [31] H. Seeherman, J.M. Wozney, Delivery of bone morphogenetic proteins for orthopedic tissue regeneration, *Cytokine Growth Factor Rev.* 16 (2005) 329-345.
- [32] J.W.M. Vehof, A.E. de Ruijter, P.H.M. Spauwen, J.A. Jansen, Influence of rhBMP-2 on Rat Bone Marrow Stromal Cells Cultured on Titanium Fiber Mesh, *Tissue Eng.* 7 (2001) 373-383.
- [33] J. van den Dolder, A.J.E. de Ruijter, P.H.M. Spauwen, J.A. Jansen, Observations on the effect of BMP-2 on rat bone marrow cells cultured on titanium substrates of different roughness, *Biomaterials* 24 (2003) 1853-1860.
- [34] R.E. Jung, F.E. Weber, D.S. Thoma, M. Ehrbar, D.L. Cochran, C.H.F. Hämmerle, Bone morphogenetic protein-2 enhances bone formation when delivered by a synthetic matrix containing hydroxyapatite/tricalciumphosphate, *Clin. Oral. Implants. Res.* 19 (2008) 188-195.



CHAPTER 6

The biological performance of injectable calcium phosphate/PLGA cement in osteoporotic rats

FCJ van de Watering, P Laverman, M Gotthardt, VMJI Cuijpers,
OC Boerman, JJP van den Beucken, and JA Jansen

Introduction

Currently, over 75 million people in Europe, USA and Japan are affected with osteoporosis according to the International Osteoporosis Foundation (IOF) [1]. Osteoporosis is characterized by a decrease in bone mass (i.e. osteopenia) and a decline in bone micro-architecture, which leads to an enhanced fragility of the skeleton and hence an increased risk of fractures [2]. The decreased amount of bone mass and the loss of bone architecture is due to an excessive osteoclastic bone resorption and a reduced capacity of osteoblasts to replace the resorbed bone [3]. Together, the prevalence and increased risk of fractures make that in the world population over 50 years of age, 1 in 3 women and 1 in 5 men will experience an osteoporotic fracture [1].

In view of the differences in bone morphology and metabolism between osteoporotic patients and healthy humans, presumably the biological performance of bone implants in osteoporotic patients is different. For the evaluation of bone implant performance under such compromised conditions, several pre-clinical animal models are available [2, 4]. Osteoporosis can be introduced either via chemical stimulation, for example by the administration of prednisolone to rabbits [5] or via an ovariectomy in female animals or an orchidectomy in male animals [2, 4]. The removal of the ovaries or testis induces a decline in estrogen and androgen levels, respectively, which leads to a reduced bone mineral density and bone mineral content. The most well-established osteoporosis animal model is the ovariectomized (OVX) rat. Following ovariectomy, a rapid decrease in bone mass and strength occurs that mimics the bone changes following oophorectomy or menopause in humans [2]. In general, bone loss occurs first in trabecular bone, after which cortical bone is affected [2]. Furthermore, the degree of bone loss for the various trabecular bone sites occurs in different time lapses after OVX surgery. For example, bone loss becomes obvious already after 14 days in the proximal tibial metaphysis, whereas the femoral neck starts to show bone loss after approximately 30 days [2]. Consequently, studying bone implant performance in OVX rats requires proper selection of an adequate implant location, as in this animal model not all trabecular and cortical bone sites are affected to a similar extent.

Calcium phosphate cements (CPCs) represent reliable candidates for the substitution of bone due to their similar chemical composition compared to the mineral phase of bone and their biocompatibility and osteoconductive properties. From an application point of view, CPCs offer the advantage of using minimally invasive surgical techniques due to their injectability [6, 7]. The main disadvantage of CPC is its low degradation rate mainly due to the inadequate intrinsic porosity of the material (i.e. ~50% with pore sizes ~10 nm - 100 nm) [8, 9]. This porosity is insufficient for substantial material degradation and tissue ingrowth [7-11]. The degradation rate of CPC can be enhanced in a controllable manner by the homogeneous inclusion of biodegradable polymeric microparticles, such as gelatin [12] or poly(D,L-lactic-co-glycolic) acid (PLGA) [13-16], in the cement powder. After microparticle degradation, the ceramic matrix of CPC contains a homogeneously

dispersed porosity that accelerates the ingrowth of bone as observed in different animal models [8, 9, 17-19]. However, the outcome of these studies is only based on healthy subjects and consequently does not provide information on bone substitute material performance in a compromised situation, such as in osteoporotic patients.

In the present study, the performance of CPC containing PLGA microparticles (CPC/PLGA) was comparatively evaluated in healthy and osteoporotic rats (OVX). The biological performance of CPC/PLGA was studied in a rat femoral condyle defect over a time period of 4 and 12 weeks. It was hypothesized that the degradation of CPC would be increased due to a higher osteoclastic activity in osteoporotic animals and that the obtained space would be filled with newly formed bone at an earlier time point.

Materials and Methods

Materials

Calcium phosphate cement (CPC) consisted of 85% alpha tri-calcium phosphate (α -TCP; CAM Bioceramics BV, Leiden, The Netherlands), 10% dicalcium phosphate anhydrous (DCPA; J.T. Baker Chemical Co., USA) and 5% precipitated hydroxyapatite (pHA; Merck, Darmstadt, Germany). The cement liquid applied was a sterilized 2 wt.% aqueous solution of Na_2HPO_4 . Acid-terminated poly(DL-lactic-co-glycolic acid) (PLGA; Purasorb[®], Purac, Gorinchem, the Netherlands) with a lactic to glycolic acid ratio of 50:50 and a molecular weight (Mw) of 17 ± 0.02 kg/mol was used for microparticle preparation.

Preparation of PLGA-microparticles

To prepare hollow PLGA-microparticles, a double-emulsion-solvent-extraction technique (water-in-oil-in-water) was used, as described previously [16]. Microparticles were produced by adding 500 μl of distilled water to 1400 mg PLGA in 2 ml dichloromethane. The mixture was emulsified using a Turrax[®] emulsifier for 60 seconds at 6,000 rpm. Then, 6 ml 0.3% aqueous poly(vinyl alcohol) (PVA, Acros Organics, Geel, Belgium) solution was added and emulsified for another 60 sec at 6,000 rpm to produce the second emulsion. The emulsion was transferred to a stirred beaker, after which 394 ml 0.3% PVA solution and 400 ml of 2% isopropyl alcohol solution was added slowly. After 1 hour of stirring, the microparticles were allowed to settle for 15 min and the solution was decanted. Then, the microparticles were washed and collected through centrifugation at 1500 rpm for 5 min, lyophilized and stored at -20 °C until use. The size distribution of the microparticles was determined by image analysis (Leica Qwin[®], Leica Microsystems, Wetzlar, Germany).

Preparation of CPC/PLGA

CPC/PLGA was prepared by weighing 0.7 g of cement powder and 0.3 g of PLGA-microparticles in a 2 ml injection syringe (BS Plastipak, Becton Dickinson S.A., Madrid, Spain). This powder component was sterilized by gamma radiation with a minimum dose of 25 kGy (Isotron B.V., Ede, The Netherlands). A sterile aqueous solution of 2% Na₂HPO₄ was used as the liquid phase, with a liquid-to-powder ratio of 0.35 mL/g.

From preset CPC/PLGA disks, the microporosity and the total porosity was analyzed by placing the composite materials in a furnace at 650°C for 2 h to burn out the polymer. Subsequently, microporosity and total porosity were calculated using the following equations[16]:

Equation 1

$$\varepsilon_{\text{tot}} = \left(1 - \frac{m_{\text{burnt}}}{V * \rho_{\text{HAP}}}\right) * 100\%$$

Equation 2

$$\varepsilon_{\text{micro}} = \left(1 - \frac{m_{\text{burnt}}}{m_{\text{nanoporous}}}\right) * 100\%$$

Legend

- ε_{tot} = Total porosity (%)
- $\varepsilon_{\text{micro}}$ = Microporosity (%)
- m_{burnt} = Average mass sample (after burning out polymer) (g)
- $m_{\text{nanoporous}}$ = Average mass intrinsic nanoporous sample (CaP cement disc without PLGA) (g)
- V = Volume sample (cm³)
- ρ_{HAP} = Density hydroxyapatite (g/cm³)

Animals

Thirty-two healthy adult (16 weeks old) female Wistar rats were used as experimental animals, which underwent several procedures during the course of the experiment (Figure 1). Sixteen rats underwent an ovariectomy (OVX) and the other sixteen animals underwent a sham surgery (SHAM). From 4 OVX and 4 SHAM, *in vivo* computed tomography (CT) images were acquired at multiple time points to quantify the bone architecture (i.e. bone volume, trabecular thickness and trabecular spacing) in the femoral condyle: (i) before OVX or SHAM surgery, (ii) before creation of a condyle bone defect, and (iii) before sacrifice (at 4-week or 12 weeks). The studies were reviewed and approved by the Experimental Animal Committee of the Radboud University (RUDEC 2010-242) and carried out in accordance with national guidelines for the care and use of laboratory animals.

Surgical procedure to induce osteoporosis

The rats underwent acclimatization to laboratory conditions for 1 week after which a bilateral ovariectomy or sham surgery was performed. In short, anesthesia was

THE BIOLOGICAL PERFORMANCE OF CPC/PLGA CEMENT IN OSTEOPOROTIC RATS

induced and maintained by Isoflurane inhalation (Rhodia Organique Fine Limited). To minimize post-operative discomfort, Rimadyl (Carprofen, Pfizer Animal Health, New York, USA) was administered intraperitoneally (5 mg/kg) before the surgery. In addition, immediately and four hours after the surgery buprenorfine (Temgesic[®]; Reckitt Benckiser Health Care Limited, Schering-Plough, UK) was administered intraperitoneally (0.02 mg/kg). Sixteen animals underwent an ovariectomy (OVX) through two separate incisions in the lateral abdominal wall. The remaining 16 animals underwent a sham surgery (SHAM), in which the ovaria were exposed but not removed using an identical surgical approach as for the other animals. The 16 SHAM rats had free access to normal pellet food containing 1.17% calcium (Ca) and 0.91% phosphorus (P) and water, while the 16 OVX rats had free access to a low-calcium diet in which pellet food contained 0.01% Ca and 0.77% P. The rats were housed in pairs at a constant temperature of 23 °C and 60% humidity.

Surgical procedure to create femoral condyle bone defects

Six weeks after the OVX or SHAM surgery, one femoral condyle defect per animal was created (n=8 per experimental group, per time point). Anesthesia was induced and maintained by Isoflurane inhalation (Rhodia Organique Fine Limited). To minimize post-operative discomfort, Rimadyl (Pfizer Animal Health) was administered intraperitoneally (5 mg/kg) before the surgery. In addition, directly and 12 hours after the surgery buprenorfine (Reckitt Benckiser Health Care Limited) was administered intraperitoneally (0.02 mg/kg). First, the left hind limb of the rats were shaved, washed and disinfected with povidone-iodine, after which the rats were immobilized on their back. A longitudinal incision was made on the medial surface of the left femur. After exposure of the medial side of the distal femoral condyle, a bone defect (Ø 2.5 mm, depth 3 mm) was created perpendicular on the bone surface, using a dental drill (Elcomed 9927 SPS; W&H Dentalwerk Burmoos GmbH, Burmoos, Austria). A series of increasing bur diameters (1.5–2.0–2.3–2.5 mm) was used under constant saline cooling at a speed of 800 rpm. The drilled cavity was then washed with saline and dried using sterile cotton gaze. At the same time, 2% Na₂HPO₄ solution was added to the CPC/PLGA powder component in the syringe and mixed for 30 seconds using a dental amalgam mixer (Silamat[®]; Vivadent, Schaan, Liechtenstein). Subsequently, the material was injected into the cavity. After initial setting of the cement, the subcutaneous tissue layer was closed with resorbable Vicryl[®] 5-0 (Johnson&Johnson, St.Stevens-Woluwe, Belgium) after which the skin was closed by staples (Agraven[®]; InstruVet BV, Cuijk, The Netherlands).

After surgery, both experimental groups (SHAM and OVX) had free access to normal pellet food containing 1.17% calcium (Ca) and 0.91% phosphorus (P) and water. The animals were housed in pairs. In the initial postoperative period, the intake of water and food was monitored. In addition, the animals were observed for signs of pain, infection and proper activity.

Implant retrieval and histological processing

The treated left condyles (i.e. femoral condyles with a filled defect) and the untreated femoral condyles from the right leg of both experimental groups were retrieved after a 4- or 12-week implantation period. After sacrifice by CO₂-suffocation, the specimens were excised and fixed in phosphate-buffered formaldehyde solution (pH 7.4). Subsequently, the tissue blocks were dehydrated in increasing ethanol concentrations (70–100%).

From both OVX and SHAM animals, 7 out of 8 treated condyles and 3 untreated condyles of each implantation time were embedded in methylmethacrylate (MMA). After polymerization, thin sections (10 µm) were prepared in a cross-sectional direction perpendicular on the longitudinal direction of the implants using a microtome with diamond blade (Leica Microsystems SP 1600, Nussloch, Germany) [20]. Three sections of each specimen were stained with methylene blue and basic fuchsin and examined using light microscopy (Leica Microsystems AG, Wetzlar, Germany).

The remaining specimens (1 out of each experimental group) were decalcified in ethylenedinitrilotetraacetic acid (EDTA, Merck KGaA, Darmstadt, Germany) for 10 days, dehydrated through a series of graded ethanol and embedded in paraffin. Using a microtome (Leica RM 2165, Leica Microsystems, Nussloch, Germany), 6 µm thick sections were prepared and stained with hematoxylin-eosin (HE). In addition, tartrate-resistant acid phosphatase (TRAP) staining was applied to determine osteoclastic activity. To perform a TRAP staining, the sections were deparaffinized and preincubated in 0.2 M TRIS-HCl buffer (pH 9.0) for 2 h at 37 °C. After rinsing with distilled water, the sections were incubated in a solution consisting of hexazotized pararosaniline and MgCl₂ (pH 5.0) at 37 °C. Positive staining developed within 30 min, after which the sections were counterstained for 1 min with hemotoxylin, rinsed in water, dehydrated and mounted with DPX (BDH Laboratory supplies, Poole, England). Paraffin sections of rat skulls were included as positive controls.

Histological and histomorphometrical evaluation

The MMA histological sections ($n=3$) were assessed quantitatively using computer-based image analysis techniques (Leica® Qwin Pro-image analysis system, Wetzlar, Germany). From digitalized images of treated femoral condyles (magnification: 5x), a circular region of interest (ROI) was determined with a diameter equal to that of the final drill to create the defect (2.5 mm diameter circular area). Within this ROI, the amount of remained CPC, newly formed bone and trabecular spacing (i.e. the surface area between adjacent trabeculae) was determined.

In addition, from digitalized images of the untreated right femoral condyles (magnification: 5x), a circular region of interest (ROI) with a diameter equal to the created defects was positioned. Within this ROI, the percentage of bone formation and trabecular spacing was determined and compared to the amount of newly

formed bone and trabecular spacing observed within the created defect of the corresponding left femoral condyle.

Validation of the OVX rat model

In vivo computed tomography (CT) scanning

From 4 OVX and SHAM animals, *in vivo* CT images of both femoral condyles (i.e. left femur with defect 6 weeks and right femur without defect) were acquired with an animal CT scanner (Inveon, Siemens Preclinical Solutions, Knoxville, TN) at multiple time points (Figure 1) [21]. To acquire CT images, anesthesia was induced and maintained by isoflurane inhalation (Rhodia Organique Fine Limited, Avonmouth, Bristol, UK). The animals were placed in supine position in the scanner and images were acquired (spatial resolution 30 μm , 80 kV, 500 μA , exposure time 1000 ms). Projected files were then reconstructed using a cone beam algorithm. The bone architecture was analyzed using image analysis software (Inveon Research Workplace 3.0, Siemens Medical Solutions USA Inc, Knoxville, USA). From reconstructed CT scans, 3D models were built for visualization and morphometric analysis. For the morphometric analysis, a subregion of the femoral condyle was selected, which included the entire femoral condyle head from the top (without cortical bone layer) until 70 micro-tomographic slices down. By auto-interpolation of the layers, a volume of interest (VOI) was obtained. Within this VOI, the amount of trabecular bone and bone marrow were determined on basis of the density in Hounsfield units. Thereafter, bone morphometric parameters (bone volume, trabecular spacing and trabecular thickness) were calculated using the Inveon Research Workplace Bone Morphometry tool (Siemens Medical Solutions USA Inc).

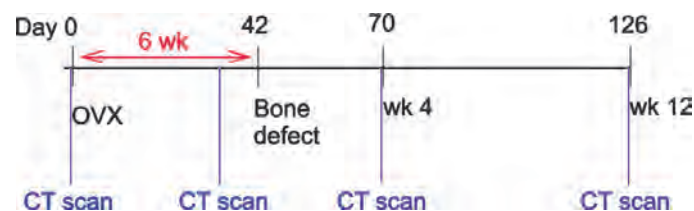


Figure 1 Schematic overview of experimental set-up. Six weeks after the ovariectomy (OVX), one femoral condyle bone defect per animal was created. Implants and non-treated femoral condyles were retrieved after a 4 or 12 week implantation period. To quantify the bone mineral density animals were scanned before inducing osteoporosis, before creating the bone defect and before each implantation time.

Histological and histomorphometrical evaluation

At both implantation periods, the MMA histological sections of untreated femoral condyles of both SHAM and OVX ($n=3$) were assessed quantitatively using computer-based image analysis techniques (Leica® Qwin Pro-image analysis system, Wetzlar, Germany). From digitalized images of the untreated right femoral condyles (magnification: 5x), a circular region of interest (ROI) with a diameter equal to the created defects was positioned. Within this ROI, the percentage of bone and trabecular spacing was determined. The amount of bone and trabecular spacing observed in OVX was compared to SHAM.

***Ex vivo* micro computed tomography (μ CT) scanning**

From one SHAM and OVX rat, the non-treated right femoral condyle was isolated to visualize the bone structure. For visualization, microcomputed tomography (μ CT) at a voltage of 100 kV and an intensity of 98 μ A and a resolution of 9.4 μ m was performed (Skyscan-1072 X-ray microtomograph, TomoNT version 3N.5, Skyscan®, Belgium).

Statistical analysis

Statistical analysis was performed using GraphPad InStat 3.05 software (GraphPad Software Inc., San Diego, CA) via one-way analyses of variance with a Tukey multiple comparison post test. Differences were considered significant at p -values less than 0.05.

Results

Characterization of PLGA-microparticles and CPC/PLGA composite

The preparation of PLGA-microparticles with the double-emulsion-solvent-extraction technique resulted in hollow microparticles with an average size of $35.7 \pm 19.8 \mu\text{m}$. The size distribution is shown in Figure 2A. Morphological examination using SEM revealed that the PLGA-microparticles had a spherical appearance with a smooth surface (Figure 2B).

For pre-set CPC/PLGA composite discs, examination by SEM showed homogeneous distribution of PLGA-microparticles throughout the entire ceramic matrix (Figure 2C). Porosity calculations demonstrated that microporosity (i.e. additional porosity after PLGA-microparticles degradation) and total porosity (consisting of intrinsic porosity and microporosity) demonstrated microporosity and total porosity values of $48.7 \pm 2.7\%$ and $75.5 \pm 1.3\%$, respectively.

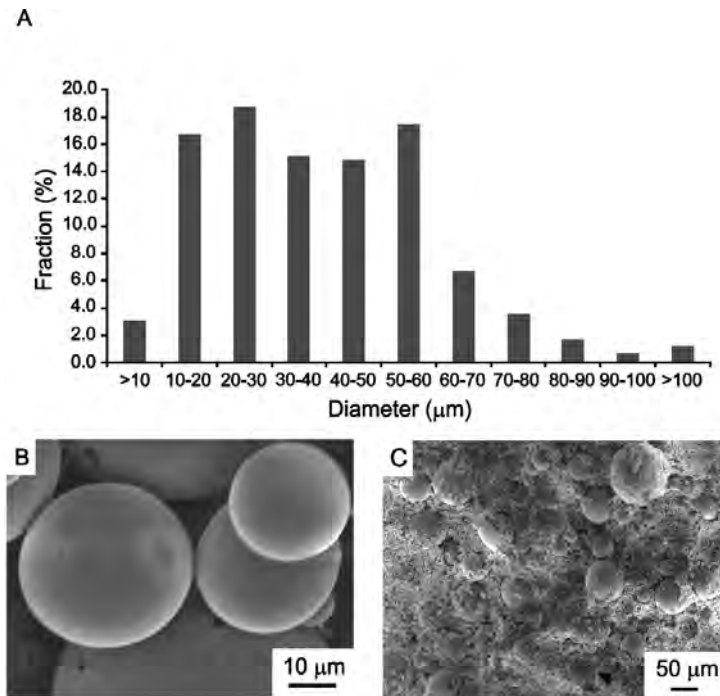


Figure 2 (A) The size distribution PLGA-microparticles prepared by the double-emulsion-solvent-extraction technique ($n=471$). The microparticles had an average size of $37.7 \pm 19.9 \mu\text{m}$ (B) SEM evaluation revealed spherical PLGA-microparticles with a smooth surface. Bar represents $10 \mu\text{m}$ (C) SEM picture of CPC with incorporated PLGA-microparticles. Bar represents $50 \mu\text{m}$.

General observation of the experimental animals

All 32 animals recovered uneventfully from the surgical procedure for OVX or SHAM and neither signs of wound complications nor signs of adverse tissue response were observed post-operatively. The creation of femoral bone defects resulted in loss of 1 SHAM animal due to an anesthesia-induced respiratory depression. The remaining 31 animals recovered uneventfully from the surgical procedure and remained in good health during the remaining experimental period, except for 1 OVX that suffered from inflammation at the defect location (i.e. swelling and pus formation). At the end of the experiment, a total of 31 implants were retrieved, of which 27 were included for analyses. The exclusion of 3 implants from analysis was due to specimen fracturing during histological processing and 1 implant was excluded due to an adverse tissue response that became apparent after microscopic evaluation. An overview of the number of implants placed, retrieved, and used for evaluation is presented in Table 1.

Validation of the osteoporotic rat model

Six weeks after OVX and SHAM surgery, the morphometric analyses of the *in vivo* CT scans of the femoral condyles revealed a significant decrease in bone volume (BV; $p < 0.001$) and trabecular thickness (TT; $p < 0.001$) and a significant increase in trabecular spacing (TS; $p < 0.05$) in OVX compared to SHAM (Table 2). In the period from defect creation till sacrifice at 4 or 12 weeks, a significantly decreased BV ($p < 0.001$) and TT ($p < 0.001$) and a significantly increased TS ($p < 0.046$) in OVX compared to SHAM were maintained in the femoral condyle (Table 2).

Representative 3D reconstructions obtained via *ex vivo* μ CT of the untreated femoral condyle of SHAM and OVX after periods of 4 and 12 weeks and histological sections of the untreated femoral condyle of SHAM and OVX after implantation periods of 12 are shown in Figure 3A and B, respectively. Histomorphometrical evaluation of untreated femoral condyles of SHAM and OVX showed a significant decrease in BV (at 4 weeks $p = 0.008$; at 12 weeks $p = 0.002$) and a significant increase in TS (at 4 weeks $p = 0.008$; at 12 weeks $p = 0.002$) in OVX compared to SHAM at both time points (Table 2).

Descriptive light microscopy of bone defects

Figure 4 presents an overview of the ROI in histological sections of the two experimental groups after implantation periods of 4 and 12 weeks. After 4 weeks, the structural integrity of the CPC was lost in both SHAM (Figure 4A) and OVX (Figure 4B), and newly-formed bone was observed throughout the degrading implant material. CPC degradation rate in OVX was increased compared to SHAM. For both SHAM and OVX, the newly-formed bone was trabecular-like, as characterized by the presence of an open porous structure (spacing) with bone marrow formation. The amount of newly-formed bone in OVX was lower compared to SHAM. In addition, the open porous structure in the newly-formed bone in OVX was enlarged compared to SHAM. TRAP staining revealed a similar osteoclastic activity for SHAM (Figure 5A and E) and OVX (Figure 5 B and F) within the ROI. After 12 weeks, CPC in both SHAM (Figure 4C) and OVX (Figure 4D) was almost completely degraded, showing less implant material in OVX. The formation of new bone had continued in SHAM and a complete interconnected bone network could be observed at the defect area. In contrast, the amount of newly-formed bone and trabecular spacing in OVX appeared similar to that observed at week 4. TRAP staining revealed absence of osteoclastic activity within the boundaries of the defect in both SHAM and OVX (Figure 5C and D).

THE BIOLOGICAL PERFORMANCE OF CPC/PLGA CEMENT IN OSTEOPOROTIC RATS

Table 1 Number of implants placed, retrieved and used for histomorphometrical analyses

Week	Implants placed		Implants retrieved		Implants used for analysis	
	4	12	4	12	4	12
SHAM	8	7	8	7	7 ^a	7 ^a
OVX	8	8	8	8	7 ^a	6 ^{a, b}

^a Deviation from number of implants retrieved due to fracturing of implants during to the histological processing or ^b due to adverse tissue response.

Table 2 The bone architecture of SHAM and OVX animals evaluated with *in vivo* CT scanning and histomorphometrical evaluation

		Before	6 wks after OVX		Week 4		Week 12		
			SHAM	OVX	SHAM	OVX	SHAM	OVX	
<i>In vivo</i> CT scanning	BV/TV	0.890 ± 0.010	0.920 ± 0.004	0.821 ± 0.014 a	0.913 ± 0.009	0.834 ± 0.019 a, b	0.921 ± 0.005	0.874 ± 0.019 b, c	
	Trabecular Spacing	0.016 ± 0.003	0.012 ± 0.002	0.026 ± 0.002 a	0.012 ± 0.001	0.024 ± 0.004 a, b	0.012 ± 0.001	0.016 ± 0.004 b, c	
	Trabecular Thickness	0.135 ± 0.015	0.156 ± 0.01	0.119 ± 0.005 a	0.146 ± 0.020	0.121 ± 0.004 a, b	0.139 ± 0.009	0.112 ± 0.011 b	
	HMM evaluation	Bone formation (%)	-	-	-	42.9 ± 3.2	32.0 ± 2.1 b	35.9 ± 2.6 c	19.9 ± 2.6 b, c
		Spacing (%)	-	-	-	57.1 ± 3.2	68.0 ± 2.1 b	64.1 ± 2.6 c	80.0 ± 2.6 b, c

BV/TV, Bone volume/total volume; OVX, Ovariectomy; HMM evaluation, Histomorphometrical evaluation; a; $p < 0.05$ compared to before; b, $p < 0.05$ compared to SHAM group; c, $p < 0.05$ compared to week 4.

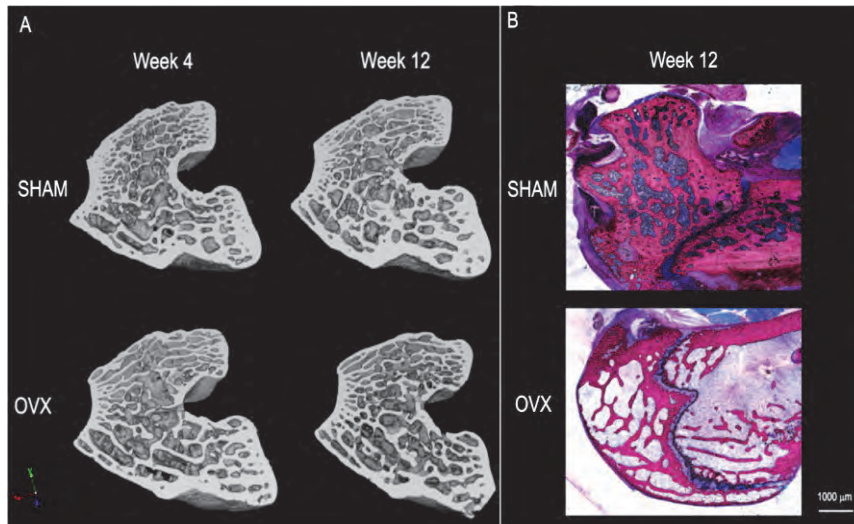


Figure 3 Representative (A) 3D-reconstructed images of ex vivo μ CT scanning after implantation periods of 4 and 12 weeks and (B) histological sections after 12 weeks implantation period of SHAM and OVX. Methylene blue and basic fuchsin staining. Bar represents 1000 μ m.

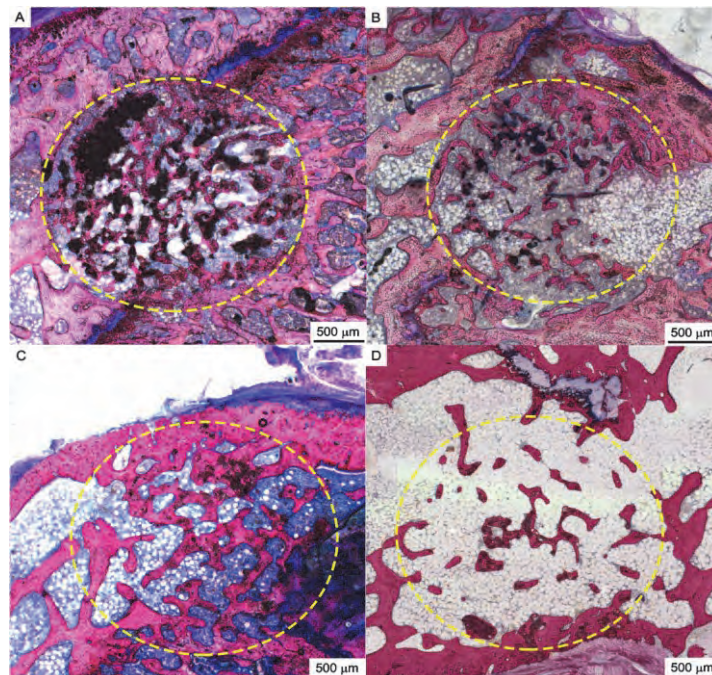


Figure 4 Representative histological sections of SHAM (A, C) and OVX (B, D) after 4 and 12 weeks, respectively. Bar represents 500 μ m. Methylene blue and basic fuchsin staining.

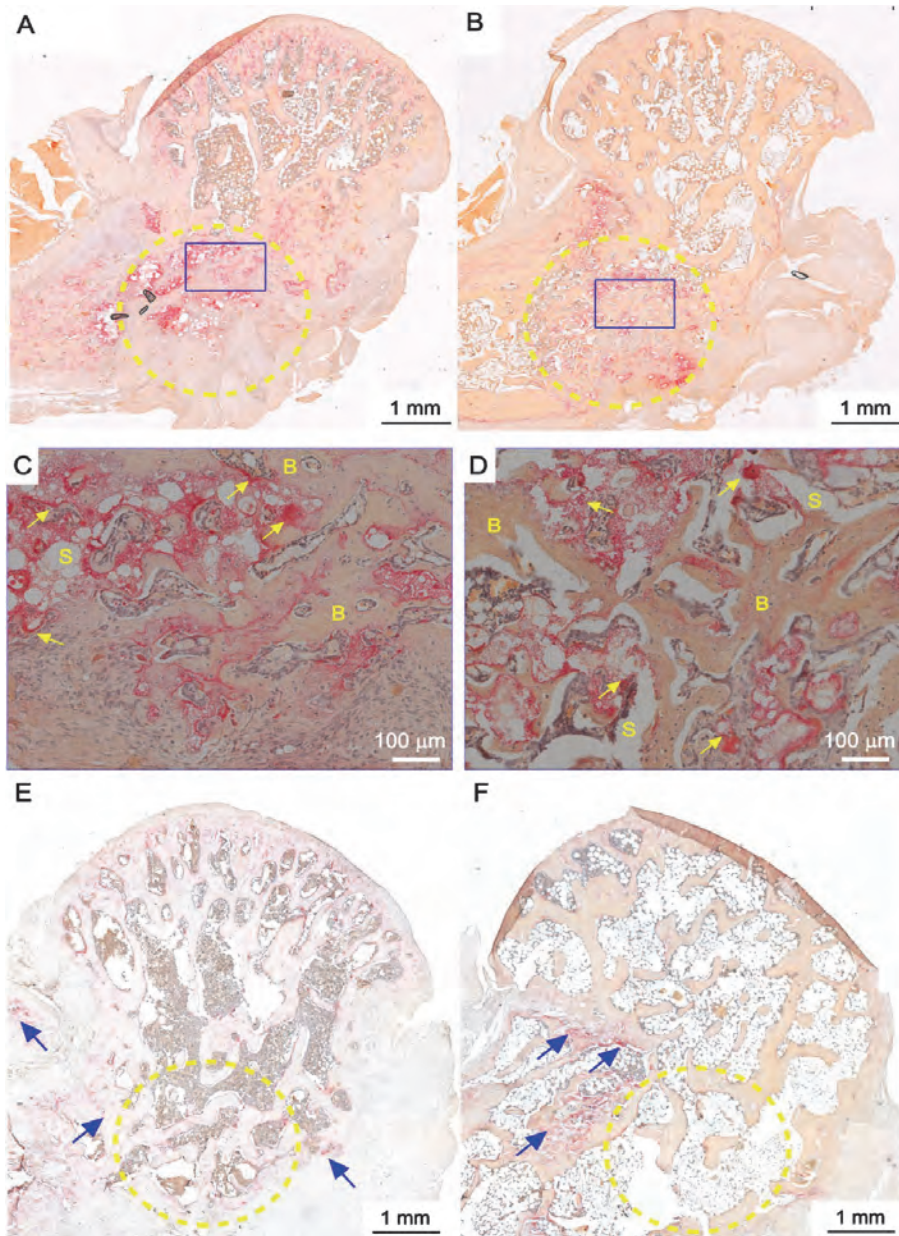


Figure 5 Representative histological sections of SHAM (A, E) and OVX (B, F) after 4 and 12 weeks, respectively. Bar represents 1 mm. Defect area is marked with yellow dashed line and osteoclast activity after 12 weeks (→) are indicated in the sections. Magnifications of blue boxes depicted in A and B are shown in C (SHAM) and D (OVX). Bone (B), trabecular spacing (S) and osteoclast activity after 12 weeks (→) are indicated in the sections. Bar represents 100 μm . Tartrate-resistant acid phosphatase (TRAP) staining.

Histomorphometrical evaluation

Comparative evaluation of CPC performance in SHAM and OVX

Quantitative results on the amount of remained CPC are presented in Figure 6A. For both SHAM and OVX, the amount of remained CPC was low, but without significant temporal progress (SHAM: from $7.2 \pm 2.7\%$ at week 4 to $7.2 \pm 9.5\%$ after week 12, $p=0.979$; OVX: from $1.9 \pm 2.2\%$ at week 4 to $0.4 \pm 0.4\%$ after week 12, $p=0.224$). Statistically significant differences in the amount of remained CPC between the SHAM and OVX ($p=0.016$) were observed after a 4 week implantation period.

Quantitative results on bone formation in the ROI are depicted in Figure 6B. Significantly more bone was formed in SHAM compared to OVX at both time points (SHAM: from $35.2 \pm 11.5\%$ at week 4 to $52.6 \pm 7.2\%$ after week 12 ; OVX: from $18.6 \pm 5.7\%$ at week 4 to $23.3 \pm 7.6\%$ after week 12; for week 4 $p=0.026$ and for week 12 $p=0.016$). For SHAM, a significant temporal increase in bone formation was observed between 4 and 12 weeks of implantation ($p=0.027$), but not for OVX ($p=0.329$).

Quantitative results of the amount of trabecular spacing are shown in Figure 6C. Significantly more spacing was observed in OVX compared to SHAM at both time points (SHAM: from $57.6 \pm 10.0\%$ at week 4 to $79.4 \pm 7.8\%$ after week 12 ; OVX: from $40.1 \pm 13.4\%$ at week 4 to $76.3 \pm 7.5\%$ after week 12; for week 4 $p=0.008$ and for week 12 $p=0.016$). No significant temporal progress in spacing was observed between implantation periods of 4 and 12 weeks (for SHAM $p=0.066$; for OVX $p=0.569$).

Comparative evaluation of bone amounts and trabecular spacing in the defect and contralateral femoral condyle

Since physiologically maximal bone amounts differ between OVX and SHAM animals (see Table 1), a comparative evaluation of bone amount and trabecular spacing was carried out between newly-formed bone in the defect area (left femoral condyles) and bone in the untreated fictitious area in the contralateral femoral condyle.

Quantitative results on bone amounts are represented in Figure 7A. At week 4, the amount of newly-formed bone in SHAM was comparable to untreated SHAM ($p=0.29$), whereas the amount of newly-formed bone in OVX was significantly decreased compared to untreated OVX ($p=0.01$). After 12 weeks, the amount of newly-formed bone in SHAM was significantly increased compared to untreated SHAM ($p=0.01$), whereas OVX showed similar bone amounts compared to untreated OVX ($p=0.83$).

Quantitative results on trabecular spacing are represented in Figure 7B. At week 4, the amount of trabecular spacing in SHAM was similar to that in untreated SHAM ($p=0.98$), whereas OVX showed significantly more trabecular spacing compared

THE BIOLOGICAL PERFORMANCE OF CPC/PLGA CEMENT IN OSTEOPOROTIC RATS

untreated OVX ($p=0.003$). After 12 weeks, trabecular spacing in SHAM and OVX was similar to untreated SHAM and OVX, respectively (SHAM $p=0.053$; OVX $p=0.46$).

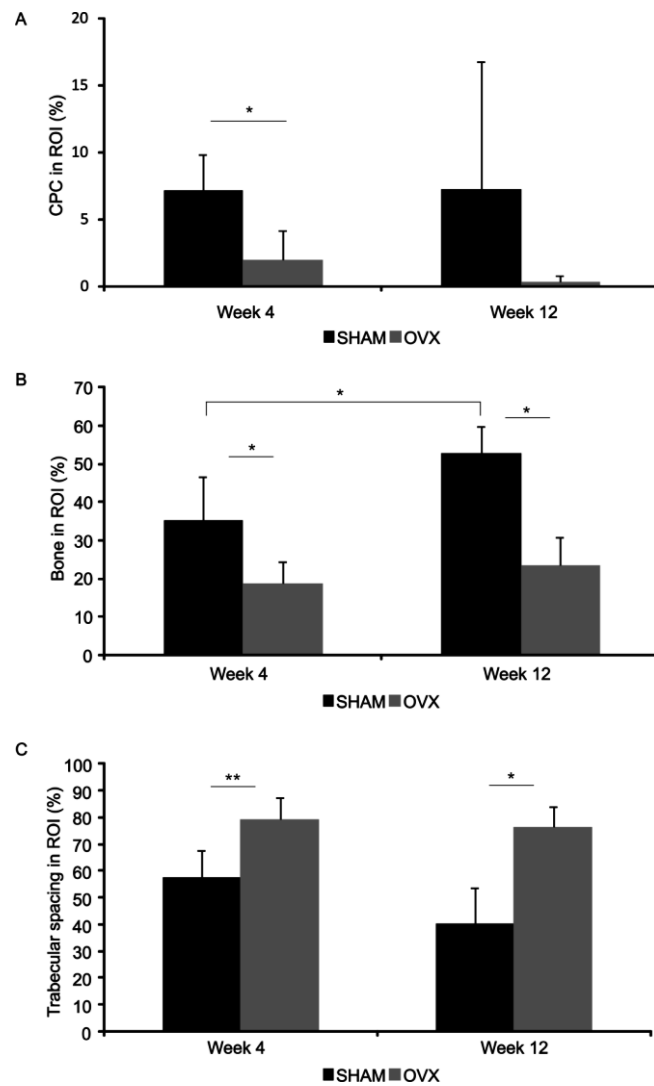


Figure 6 Results of histomorphometrical evaluation of SHAM and OVX in femoral condyle defects. The amount of (A) CPC, (B) bone formation and (C) trabecular spacing after 4 and 12 weeks of the two experimental groups are expressed as percentage of ROI (i.e. a standardized region of interest within the boundaries of the implant). Error bars represent means \pm standard deviation. (*) $p < 0.05$; (**) $p < 0.01$; $n \geq 6$.

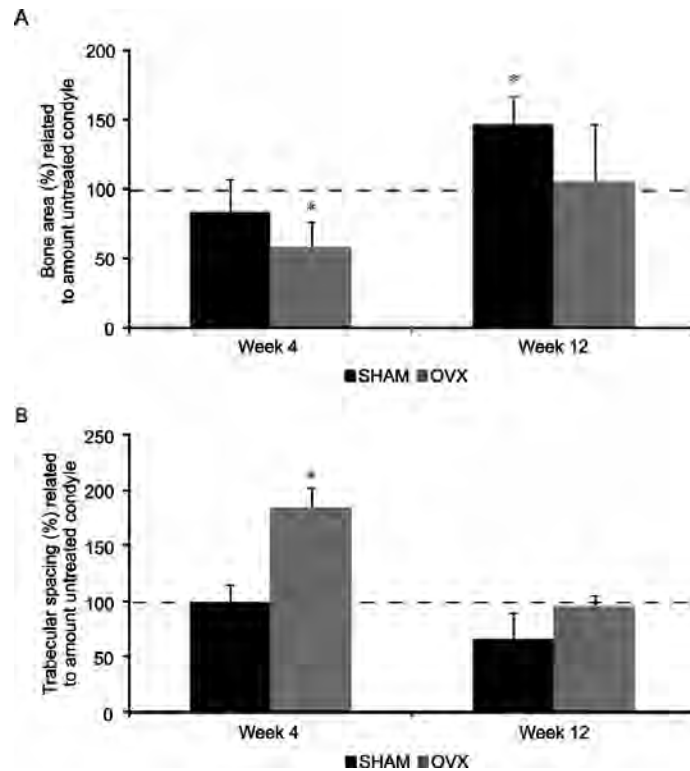


Figure 7 Results of histomorphometrical evaluation of bone amounts (A) and trabecular spacing (B) in the defect area (left femoral condyles) of SHAM and OVX. The amount of newly formed bone and trabecular spacing present in the defect area of SHAM and OVX was related to the amount of bone and trabecular spacing present in untreated fictitious area (with the same dimensions as the defect) of the right femoral condyle of SHAM and OVX. The amount of bone and trabecular spacing in the untreated right femoral condyles was set at 100% and indicated with dashed line. Error bars represent means \pm standard deviation. (*) $p < 0.05$; $n > 3$.

Discussion

In the present study, the degradation and bone forming capacity of injectable CPC/PLGA was comparatively evaluated in healthy (SHAM) and osteoporotic (OVX) rats using a rat femoral condyle defect after implantation periods of 4 and 12 weeks. It was hypothesized that OVX would accelerate CPC degradation due to a higher osteoclastic activity present in osteoporotic animals. Additionally, this accelerated CPC degradation was hypothesized to allow more new bone formation in the created space. The results revealed a significantly increased material degradation and decreased bone formation at both implantation periods in OVX compared to SHAM. In addition, the amount of bone formed in the femoral

condyle defects in OVX was significantly decreased compared to the amount of bone present in untreated OVX condyles at 4 weeks, although this effect was diminished after 12 weeks. In contrast, the amount of newly formed bone in the femoral condyle defect in SHAM was similar at 4 weeks and significantly increased after 12 weeks of implantation compared to the original amount of bone present in untreated SHAM condyles.

The ovariectomized rat is generally accepted as a suitable preclinical animal model for human postmenopausal osteoporosis [2, 4, 22]. However, according to the definition of the WHO, the observed bone changes in ovariectomized rats are denoted as osteopenia rather than osteoporosis (i.e. bone mass reduced but no increased risk in fractures) [1]. Nonetheless, in line with previous reports [2, 4, 22, 23], the present study demonstrated that over the course of the experiment OVX rats exhibited most of the characteristics as observed in human postmenopausal osteoporosis, including a significant decrease in trabecular bone mass and thickness and an increase in trabecular spacing, compared to healthy individuals as analyzed with histomorphometrical analysis and *in vivo* CT scanning indicating the presence of osteoporosis.

To obtain replacement of bone, new bone formation and resorption of the bone substitute material, e.g. biodegradation of the material, is required. The degradation rate and the formation of bone should be in balance to maintain mechanical stability and to allow a gradual takeover of mechanical strength by newly-formed bone tissue. In the current study, the material degradation was significantly increased in OVX compared to SHAM, but no increased amount of newly-formed bone in OVX was observed. This is in line with Wang *et al.* (2008), who reported an accelerated resorption and altered osteoconductive responses for calcium sulphate-based bone substitute materials in an osteoporotic spine model in OVX rats compared to healthy control animals [24]. The biodegradation of calcium phosphate-based bone substitute materials can occur in an active manner, where osteoclastic activity is necessary for the bioresorbability [25-28]. Although an increased osteoclastogenesis and osteoclastic activity can be observed in human postmenopausal osteoporosis caused by the lack of estrogen [3], the current study failed to show an apparent difference in osteoclastic activity within the boundaries of the defect between SHAM and OVX after 4 weeks implantation period. Furthermore, after a 12-week implantation period, osteoclastic activity appeared absent within the boundaries of the defect in OVX and SHAM. This indicates that the lack of bone formation in OVX after 4 weeks is mainly due to a reduced capacity of the osteoblasts to replace the material with bone rather than to excessive osteoclastic activity. In view of this, additional empowerment via the inclusion of drugs and/or growth factors, such as bone morphogenetic proteins (BMPs), into CPC for the use in osteoporotic conditions might be promising, since BMP-2 has been reported to increase the osteoinductive properties of the materials in healthy animals [29, 30] as well as stimulating the healing of osteoporotic rat fractures after BMP-7 injection [31]. Also, the use of antiresorptive agents (i.e. bisphosphonates) to inhibit osteoclastic activity might not be recommended in OVX

receiving CPC, since reduced osteoclastic activity might slow down the CPC degradation process and thus the creation of available space for the formation of bone. In addition to a potential negative effect on the CPC degradation, bisphosphonate treatment was shown before not to influence the healing of an OVX closed midshaft femoral fracture [31].

Furthermore, it needs to be emphasized that besides material properties of the bone substitute material also the implantation site is known to influence the bone forming capacity of a material: for example similar CPC as used in the current study placed in a cranial defect in healthy rats resulted in less CPC degradation and bone formation compared to the current study [32]. The straightforward explanation for this phenomenon is that at different locations materials will be exposed to different environments, which includes the nature of biomechanical loading, surrounding tissue and blood/nutrient supply. Besides environment, also the origin of the bones (i.e. long bone formation is endochondral while cranial bone formation is intramembranous), may play a role in the degradation and bone formation due to distinctive signaling properties [33]. Therefore, the most favorable CPC for use in osteoporotic patients is, similar to its application in healthy individuals, dependent on the local bone condition and the specific host response.

In conclusion, accelerated degradation of CPC/PLGA was observed in osteoporotic animals, but less bone formation was induced compared to healthy animals at 4 and 12 weeks after implantation. In addition, the amount of newly-formed bone under osteoporotic conditions after 4 weeks was less in the femoral condyle defect compared to that present at a non-defect, osteoporotic control femoral condyle, but equal after 12 weeks. On the other hand, in healthy conditions, the amount of newly-formed bone in the femoral condyle defect was equal to that present at a non-defect control femoral condyle at 4 weeks, while higher after 12 weeks. This indicates that bone regeneration at a defect site is slower, but can reach native amounts after longer time periods. Consequently, bone regenerative treatments in osteoporotic conditions seem to require additional empowerment of bone substitute materials to achieve equal bone amounts.

Acknowledgements

The authors gratefully acknowledge the support of the Smart Mix Program of the Netherlands Ministry of Economic Affairs and the Netherlands Ministry of Education, Culture and Science. The authors would like to thank Natasja van Dijk for assistance with the histological preparations. Scanning electron microscopy was performed at the Nijmegen Center for Molecular Life Sciences (NCMLS), the Netherlands

References

[1] International Osteoporosis Foundation, <http://www.iofbonehealth.org/>, L. Misteli (Ed.), November 2011.

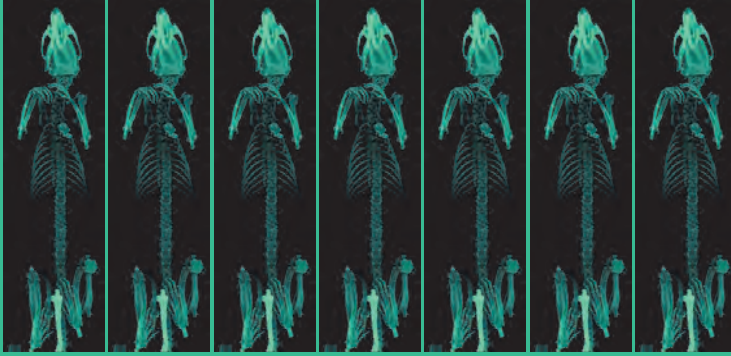
THE BIOLOGICAL PERFORMANCE OF CPC/PLGA CEMENT IN OSTEOPOROTIC RATS

- [2] W.S.S. Jee, W. Yao, Overview: animal models of osteopenia and osteoporosis, *J Musculoskel Neuron Interact* 1 (2001) 193-207.
- [3] U.H. Lerner, Bone Remodeling in Post-menopausal Osteoporosis, *J. Dent. Res.* 85 (2006) 584-595.
- [4] A. Turner, Animal models of osteoporosis-necessity and limitations, *Eur. Cells. Mater.* 1 (2001) 66-81.
- [5] B. Gardel, B. Sutter, B. Flautre, E. Viguier, F. Lavaste, P. Hardouin, Effects of glucocorticoids on skeletal growth in rabbits evaluated by dual-photon absorptiometry, microscopic connectivity and vertebral compressive strength, *Osteoporos. Int.* 4 (1994) 204-210.
- [6] A. Ambard, L. Mueninghoff, Calcium Phosphate Cement: Review of Mechanical and Biological Properties, *J. Prosthodont.* 15 (2006) 321-328.
- [7] R. LeGeros, Properties of osteoconductive biomaterials: calcium phosphates, *Clin. Orthop. Relat. R.* 395 (2002) 81-98.
- [8] E. Ooms, J. Wolke, J. van der Waerden, J. Jansen, Trabecular bone response to injectable calcium phosphate (Ca-P) cement, *J. Biomed. Mater. Res.* 61 (2002) 9-18.
- [9] E.M. Ooms, J.G.C. Wolke, M.T. van de Heuvel, B. Jeschke, J.A. Jansen, Histological evaluation of the bone response to calcium phosphate cement implanted in cortical bone, *Biomaterials* 24 (2003) 989-1000.
- [10] L. C. Chow, Next generation calcium phosphate-based biomaterials, *Dent. Mater. J.* 28 (2009) 1-10.
- [11] J. Jansen, E. Ooms, N. Verdonshot, J. Wolke, Injectable calcium phosphate cement for bone repair and implant fixation, *Orthop. Clin. North Am.* 36 (2005) 89-95.
- [12] W. Habraken, L. de Jonge, J. Wolke, L. Yubao, A. Mikos, J. Jansen, Introduction of gelatin microspheres into an injectable calcium phosphate cement, *J. Biomed. Mater. Res. A* 77A (2008) 643-655.
- [13] D.P. Link, J. van den Dolder, W.J.F.M. Jurgens, J.G.C. Wolke, J.A. Jansen, Mechanical evaluation of implanted calcium phosphate cement incorporated with PLGA microparticles, *Biomaterials* 27 (2006) 4941-4947.
- [14] P. Ruhé, E. Hedberg-Dirk, N.T. Padron, P. Spauwen, J. Jansen, A. Mikos, Porous Poly(DL-lactic-co-glycolic acid)/Calcium Phosphate Cement Composite for Reconstruction of Bone Defects, *Tissue Eng.* 12 (2006) 789-800.
- [15] P. Ruhé, E. Hedberg, N.T. Padron, P. Spauwen, J. Jansen, A. Mikos, Biocompatibility and degradation of poly(DL-lactic-co-glycolic acid)/calcium phosphate cement composites, *J. Biomed. Mater. Res. A* 74A (2005) 533-544.
- [16] W. Habraken, J. Wolke, A. Mikos, J. Jansen, Injectable PLGA microsphere/calcium phosphate cements: physical properties and degradation characteristics *J. Biomater. Sci. Polym. Ed.* 17 (2006) 1057-1074.
- [17] S.C.S.X.B. Cavalcanti, C.L. Pereira, R. Mazzone, M. de Moraes, R.W.F. Moreira, Histological and histomorphometric analyses of calcium phosphate cement in rabbit calvaria, *J. Cranio. Maxill. Surg.* 36 (2008) 354-359.
- [18] H. Yuan, Y. Li, J. de Bruin, K. de Groot, X. Zhang, Tissue responses of calcium phosphate cement: a study in dogs, *Biomaterials* 21 (2000) 1283-1290.
- [19] V. Arisan, T. Ozdemir, A. Anil, J. Jansen, K. Ozer, Injectable calcium phosphate cement as a bone-graft material around peri-implant dehiscence defects: a dog study, *Int. J. Oral Maxillofac. Implants* 23 (2008) 1053-1062.
- [20] H. van der Lubbe, C. Klein, K. de Groot, A simple method for preparing thin (10 microM) histological sections of undecalcified plastic embedded bone with implants, *Stain Technol.* 63 (1988) 171-176.
- [21] E.P. Visser, J.A. Disselhorst, M. Brom, P. Laverman, M. Gotthardt, W.J.G. Oyen, O.C. Boerman, Spatial Resolution and Sensitivity of the Inveon Small-Animal PET Scanner, *J. Nucl. Med.* 50 (2009) 139-147.
- [22] P.P. Lelovas, T.T. Xanthos, S.E. Thoma, G.P. Lyritys, I.A. Dontas, The Laboratory Rat as an Animal Model for Osteoporosis Research, *Comparative. Med.* 58 (2008) 424-430.
- [23] K. Dike N, The ovariectomized rat model of postmenopausal bone loss, *Bone Miner.* 15 (1991) 175-191.
- [24] M.L. Wang, J. Massie, R.T. Allen, Y.-P. Lee, C.W. Kim, Altered bioreactivity and limited osteoconductivity of calcium sulfate-based bone cements in the osteoporotic rat spine, *Spine J.* 8 (2008) 340-350.

CHAPTER 6

- [25] M.F. Baslé, D. Chappard, F. Grizon, R. Filmon, J. Delecrin, G. Daculsi, A. Rebel, Osteoclastic resorption of Ca-P biomaterials implanted in rabbit bone, *Calcif. Tissue Int.* 53 (1993) 348-356.
- [26] J.D. de Bruijn, Y.P. Bovell, J.E. Davies, C.A. van Blitterswijk, Osteoclastic resorption of calcium phosphates is potentiated in postosteogenic culture conditions, *J. Biomed. Mater. Res.* 28 (1994) 105-112.
- [27] S. Yamada, D. Heymann, J.M. Bouler, G. Daculsi, Osteoclastic resorption of calcium phosphate ceramics with different hydroxyapatite/ β -tricalcium phosphate ratios, *Biomaterials* 18 (1997) 1037-1041.
- [28] F. Monchau, A. Lefèvre, M. Descamps, A. Belquin-myrdycz, P. Laffargue, H.F. Hildebrand, In vitro studies of human and rat osteoclast activity on hydroxyapatite, β -tricalcium phosphate, calcium carbonate, *Biomol. Eng.* 19 (2002) 143-152.
- [29] E. Bodde, O. Boerman, F. Russel, A. Mikos, P. Spauwen, J. Jansen, The kinetic and biological activity of different loaded rhBMP-2 calcium phosphate cement implants in rats, *J. Biomed. Mater. Res. A* 87A (2008) 780-791.
- [30] Z.S. Patel, S. Young, Y. Tabata, J.A. Jansen, M.E.K. Wong, A.G. Mikos, Dual delivery of an angiogenic and an osteogenic growth factor for bone regeneration in a critical size defect model, *Bone* 43 (2008) 931-940.
- [31] T.J. Blokhuis, P. Buma, N. Verdonschot, M. Gotthardt, T. Hendriks, BMP-7 stimulates early diaphyseal fracture healing in estrogen deficient rats, *J. Orthop. Res.* DOI: 10.1002/jor.22013 (2011).
- [32] F.C.J. van de Watering, J.J.J.P. van den Beucken, X.F. Walboomers, J.A. Jansen, Calcium phosphate/poly(d,l-lactic-co-glycolic acid) composite bone substitute materials: evaluation of temporal degradation and bone ingrowth in a rat critical-sized cranial defect, *Clin. Oral. Implants. Res.* 23 (2012) 151-159.
- [33] U. Chung, H. Kawaguchi, T. Takato, K. Nakamura, Distinct osteogenic mechanisms of bones of distinct origins, *J. Orthop. Sci.* 9 (2004) 410-414.

THE BIOLOGICAL PERFORMANCE OF CPC/PLGA CEMENT IN OSTEOPOROTIC RATS



CHAPTER 7

Summary, address to the
aims, closing remarks
and future perspectives

Summary and address to the aims

Calcium phosphate-based, apatitic cements (CPC) represent a high-potential candidate material for application as a bone substitute material to fill up bone defects in the field of dental, orthopaedic and reconstructive surgery, because of their biocompatible, osteoconductive and injectable properties. A disadvantage of CPC, however, is the poor biodegradation, which impedes replacement by bone tissue and hence full regeneration of the defect. The biodegradation of CPC depends on different factors, including cement properties (e.g. chemical composition, setting reaction, porosity, crystallinity and particle size of the calcium phosphate compounds) and the patient (e.g. medical condition and implantation site). The biodegradation of the CPC and thus the ingrowth of bone has been shown to be improved by altering the porosity. The porosity can be increased via different approaches, for example the use of sodium bicarbonate to obtain CO₂-gas bubbles during CPC setting, mixing water-soluble crystals or biodegradable polymer microparticles (e.g. gelatin or poly(D,L-lactic-co-glycolic acid) (PLGA) as porogens homogeneously through the ceramic powder. To further empower the biological performance of CPC biologically active compounds can be introduced. However, many variables such as type of additive, additive dosage, release and retention need to be investigated to generate an effective injectable CPC for the reconstruction of different types of bone defects in a variety of patients.

In view of the above mentioned, the research described in this thesis focused on addressing the efficacy of CPC in healthy conditions, exploring the effect of various incorporated additives on CPC performance, and evaluating differences between CPC performance in healthy and osteoporotic conditions.

1. To what extent can addition of PLGA-microparticles improve the biological performance of CPC/PLGA?

Chapter two of this thesis provided temporal information on the biological performance of CPC containing different amounts of PLGA-microparticles in terms of material degradation and bone formation. Preset CPC supplemented with 20 or 30 wt.% PLGA-microparticles were implanted in a rat critical-sized cranial defect model. In forty-eight rats, a critical-sized cranial defect was created and C20% and C30% were implanted for 4, 8 and 12 weeks (n=8). Histological analysis of the retrieved specimens revealed that implant degradation for C30% was significantly faster compared to C20%, albeit that overall degradation was limited for both types of implants. Although bone formation was limited for both experimental groups, C30% showed a significant temporal increase of total bone formation. The percentage of defect bridging was comparable for C20% and C30% at all implantation periods. Based on the results of **Chapter 2**, the amount of PLGA-microparticles in CPC demonstrated to increase material degradation, while bone formation was found not to be influenced. The biological performance of CPC

supplemented with PLGA-microparticles is insufficient to fully regenerate a critical sized defect and therefore requires additional empowerment with biological active compounds.

2. Can the biological performance of CPC be improved by the addition of bioactive glass?

CPC supplemented with PLGA-microparticles represents a promising candidate material for bone substitution mainly due to their biocompatibility and osteoconductive properties however, the biological performance of CPC supplemented with PLGA-microparticles under healthy conditions is insufficient to fully regenerate critical sized bone defects (**Chapter 2**). Therefore, the enrichment of CPC/PLGA with biological active compounds is necessary in order to stimulate bone healing under critical conditions, including large bone defects, poorly vascularized sites, and (elderly) patients with metabolic disorders. In view of this, the incorporation of Bioactive glasses (BGs) into CPC seems a promising approach to improve the biological performance of CPC since BGs are known for their unique ability to bond to living bone which acts as a template for calcium phosphate precipitation and directs new bone formation. In addition, it has been reported that BGs attract and stimulate osteoprogenitor cells, which differentiate into matrix-producing osteoblasts and subsequently increase the rate of bone formation and bone ingrowth into BG-based granular material. Previous, it was demonstrated that BG could successfully be introduced into CPC, either pure or supplemented with PLGA-microparticles. Although *in vitro* data on the introduction of BG to CPC composite material were encouraging, the biocompatibility and *in vivo* bone response to these formulations remained unknown. Therefore, **Chapter 3** aimed to evaluate the *in vivo* response of BG supplemented CPC, either pure or supplemented with PLGA-microparticles, via both ectopic and orthotopic implantation models in rats. Pre-set scaffolds in 4 different formulations (1: CPC; 2: CPC/BG; 3: CPC/PLGA; and 4: CPC/PLGA/BG) were implanted subcutaneously and in femoral condyle defects of rats for 2 and 6 weeks. The results of **Chapter 3** revealed that BG incorporation improved the histocompatibility upon ectopic implantation compared to pure CPC, as demonstrated by an improved capsule and interface quality surrounding the implants. Additionally, incorporating BG within CPC accelerated material degradation and increased bone formation in a femoral condyle defect in rats. Consequently, these results highlight the potential of BG to be used as an additive to CPC to improve the biological performance for bone regeneration applications. Nevertheless, the current favorable data have to be confirmed in long-term *in vivo* studies, which also have to be performed under compromised wound healing conditions.

CHAPTER 7

3. Does the solubility of BMP-2 influence the bioactivity, release profile of and osteoinductive properties of CPC scaffold material?

BMP's play a significant role in the regulation of many steps in bone morphogenesis due to their biological functions that include chemotaxis, differentiation, and mitosis of bone forming cells. Similar to native BMP's, recombinant equivalents produced in mammalian cells are post-translationally modified through N-linked glycosylation. In contrast, bacterially produced BMP's lack this glycosylation leading to a decrease in solubility. This reduced solubility affects the release kinetics from bone substitute materials and hence might allow the application of lower BMP doses to induce bone formation. This seems promising for reducing the amount of included growth factor in bone substitute materials. Consequently, in **Chapter 4**, it was hypothesized that ngBMP-2 induces more profound ectopic bone formation at lower dosages compared to gBMP-2. To that end, gBMP-2 and ngBMP-2 were firstly *in vitro* comparatively evaluated for biological activity and release from pre-set CPC scaffolds. Thereafter, an ectopic implantation model in rats was used, in which gBMP-2 and ngBMP2 were loaded at various dosages (2-20 ug/implant) on the pre-set CPC scaffolds and implanted for 4 and 12 weeks. The results revealed that both the *in vitro* biological activity of and the *in vitro* release of ngBMP-2 are lower compared to gBMP2. Upon ectopic implantation, however, ngBMP-2 loaded implants induced more bone formation at lower concentrations from 4-weeks onward compared to gBMP-2 equivalents. The results of **Chapter 4** revealed that the solubility of BMP-2 protein influences the bioactivity and release profile of the growth factor, resulting in improved osteoinductive properties of scaffold loaded with ngBMP-2. Together, this indicates the value of ngBMP-2 as a more powerful alternative for mammalian produced recombinant BMP-2 for bone regenerative therapies.

4. Does the BMP-2 loading method to CPC influence the release kinetics and osteoinductive potential of CPC?

Clinical application of CPC (with incorporated PLGA-microparticles) in an injectable form implicates that loading methods for growth factors are limited. In view of this, **Chapter 5** addressed differential loading methods for BMP-2 and the effects on *in vitro* and *in vivo* release kinetics via an *in vitro* release experiment and *in vivo* using microSPECT imaging with ¹²⁵I-labeled BMP-2 as well as the osteoinductive capacity of differentially loaded scaffolds using a subcutaneous rat model. The differential loading methods comprised BMP-2 adsorption to PLGA-microparticles (CPC/PLGA), BMP-2 addition to the liquid phase of CPC (CPC/liquid), and BMP-2 adsorption to the surface of preset, porous CPC (CPC/surface) as a control. Additional controls consisted of porous CPC scaffolds (CPC/porous) and CPC/PLGA (CPC/control) without BMP-2 loading. The results of **Chapter 5** revealed that BMP-2 loading is feasible via adsorption to PLGA-microparticles and addition to the liquid phase of CPC, for which similar release profile were observed over the course of 28 days,

despite distinct protein distribution patterns. Compared to CPC/surface, CPC/PLGA and CPC/liquid showed a significantly lower burst release, followed by a similar sustained release profile. As such, the observed osteoinductive capacity for only CPC-scaffolds with surface-loaded BMP-2 is likely to be related to this difference in burst release. It remains unclear to what extent the differential BMP-2 loading methods for injectable CPC can affect the biological response in a bone environment.

5. What are the differences in biological performance of CPC between osteoporotic and healthy rats?

In the previous chapters of this thesis, the performance of CPC (with or without additives) was evaluated in healthy animals. As such, the outcome of these studies provided no information on the performance of CPC under compromised conditions, such as in osteoporotic patients. Consequently, **Chapter 6** comparatively evaluated the performance of injectable CPC/PLGA in healthy (SHAM) and osteoporotic rats (OVX) using a rat femoral condyle defect with implantation periods of 4 and 12 weeks. It was hypothesized that in OVX rats, the degradation of CPC/PLGA would be increased due to a higher osteoclastic activity present in osteoporotic animals and that the obtained space would be rapidly filled with newly formed bone. The results of **Chapter 6** revealed that despite an accelerated degradation of CPC/PLGA in osteoporotic animals, bone formation was slower compared to healthy animals after implantation periods of 4 and 12 weeks. In addition, after 4 weeks, the amount of newly-formed bone under osteoporotic conditions was less in the femoral condyle defect compared to that present at a non-defect, osteoporotic control femoral condyle, but equal after 12 weeks. On the other hand, under healthy conditions, the amount of newly-formed bone in the femoral condyle defect was equal to that present at a non-defect control femoral condyle at 4 weeks, while higher after 12 weeks. The results of **Chapter 6** indicate that bone regeneration at a defect site under osteoporotic conditions is slower, but can re-establish native amounts after longer time periods. Consequently, bone regenerative treatments in osteoporotic conditions seem to require additional empowerment of bone substitute materials to achieve equal bone amounts.

Closing remarks and future perspectives

In our search to optimize the biological performance of apatitic CPC, we supplemented CPC with PLGA-microparticles to create a porous scaffold to enhance material degradation and tissue ingrowth. To predict the degradation of the PLGA-supplemented CPC and hence the bone forming capacity, we considered the total porosity of the scaffolds (contributed to the intrinsic porosity of CPC and added PLGA-microparticles) to be an important parameter. Although the amount and size (distribution) of PLGA-microparticles varied among the different chapters of this thesis from 20 to 30 wt.% and from 20 to 60 μm , the total porosity of all

scaffolds was similar at around 70%. This indicates that the variations made regarding amount and size (distribution) of PLGA-microparticles evoked only limited variations in ultimate porosity of the CPC. *In vivo* experiments, in which the effect of different amounts of PLGA-microparticles on degradation and biological responses were compared in a direct manner have been performed (Chapter 2). However, no direct evidence of the influence of size on biological performance of CPC is available to date and requires further investigation. Despite similar porosity values, the extent of CPC degradation and subsequent bone forming capacity varied among the different chapters of this thesis. This difference is likely to be dependent on the experimental set-up (i.e. implant location). In addition, our results indicate that the interconnectivity of the material is also of importance. The most beneficial interconnective porosity is not yet known, although we showed in Chapter 4 that an interconnective porosity of ~20% is insufficient and further investigation is required. For clinical applications, reproducibility and standardization of the material is important. Many of these factors, such as the type and amount of the PLGA-microparticles and the components of the CPC, can be controlled. However, still a lot of work has to be done on the standardization of PLGA-microparticle size and insight into the relation between their size and amount to obtain effective interconnectivity within the CPC. To obtain reproducible interconnective porosity, combining different standardized sizes (with only limited size ranges) of PLGA-microparticles might be an option as previously described [1]. Therefore, future research has to focus on the relation between PLGA-microparticle size, amount, and interconnectivity, and the performance of these CPCs *in vivo*. Additionally, this relation has to be investigated at different *in vivo* locations and bone defect sizes under healthy as well as compromised conditions. Parallel research on CPC degradation revealed that the morphology of PLGA-microparticles (i.e. hollow or dense) has a stronger effect on degradation than both molecular weight and terminal end-group modification [2]. Therefore, in chronologically later performed research of this thesis, we supplemented CPC with these dense PLGA-microparticles. The objectives of these chapters was based on the evaluation of the biological performance of CPC/dense PLGA-microparticles supplemented with either osteopromotive BG particles or the osteoinductive growth factor BMP-2. Therefore, aside from the proof-of-principle that has recently been obtained in a rabbit femoral condyle [3], a biological evaluation of CPC incorporating dense PLGA-microparticles for different PLGA-microsphere particle sizes, amounts, implant sites, and medical conditions needs to be performed. After the realization that the biological performance of CPC was still unsatisfactory following optimization approaches based on combinations of the ceramic cement matrix and hollow PLGA-microparticles, our research focused on the empowerment of CPC by incorporating additives with a certain biological capacity. Candidate additives used for this purpose were BG and BMP-2. The loading method of additives varied as BG was mixed throughout the ceramic matrix, whereas BMP-2 was either adsorbed to PLGA-microparticles or added to the liquid phase of CPC. We demonstrated that incorporation of BG indeed improved the biological

SUMMARY, CLOSING REMARKS AND FUTURE PERSPECTIVES

performance at 6 weeks of implantation. Further long-term studies are necessary to provide additional information concerning the late stages of the bone matrix synthesis and degradation induced by the CPC/PLGA cements including BG. Additionally, we demonstrated that it is feasible to include BMP-2 within CPC via both methods, although growth factor release and related osteoinductive properties of the CPC were insufficient to induce ectopic bone formation subcutaneously in rats. It is likely that the lack of an osteoinductive effect was dependent on the limited BMP-2 burst release. This illustrates that the release kinetics of growth factors are complex and may be influenced by many variables as previously reported [4]. It remains unclear to what extent the differential BMP-2 loading methods for injectable CPC can affect the biological response in a bone environment. Taken together, the incorporation of the additives BG and BMP-2 to improve the biological performance of CPC showed promising results and could be used as a lead toward product development.

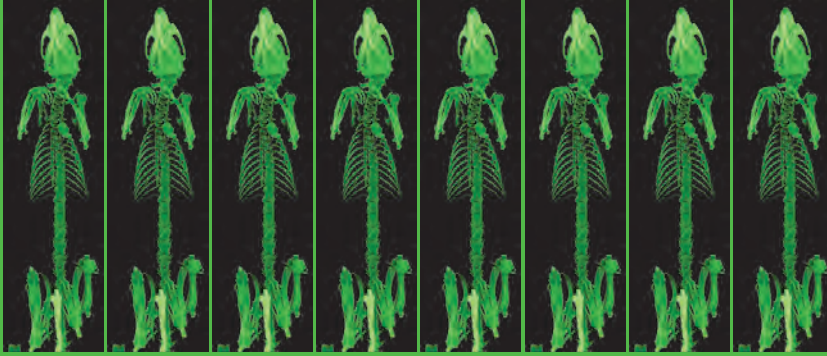
The majority of the patients requiring regeneration of (large) bone defects with bone substitute materials have a sub-optimal medical condition and thus bone metabolism, of which osteoporotic patients represent a somewhat worst-case scenario. Consequently, the need for an efficient CPC to treat bone defects in this group of patients is high. The differences in bone morphology and metabolism between compromised patients and healthy humans points to a different biological performance of CPC. As such, this thesis reported for the first time the biological performance of CPC with included PLGA-microparticles in osteoporotic conditions and revealed that bone regenerative treatments in osteoporotic conditions require additional empowerment of CPC. The investigated additives in this thesis might improve the biological performance in compromised conditions. Therefore, research has to focus on the potential of additives to improve the biological performance of CPC in osteoporotic conditions.

From a biological and cost-effective point of view (i.e. potential risks of side-effects, labor intensiveness and cost price) the use of biological active compounds has limitations. It is necessary to find a compromise between the cost price of empowered CPC and its biological efficacy under specific conditions. Preferably, clinicians should have the possibility to select the most appropriate CPC for each specific clinical application. To reach such an approach, the challenge is to identify the accurate combination of (i) standardized ceramic cement matrix, (ii) specific type of porogens, and (iii) additives, depending on patient-specific conditions (e.g. defect size, location, age, and medical condition). A final prerequisite is that such a customized injectable CPC becomes available in a simple, straightforward and controllable application system that allows gentle application of the CPC with optimal handling properties (i.e. viscosity, setting).

References

- [1] M.A. Lopez-Heredia, K. Sariibrahimoglu, W. Yang, M. Bohner, D. Yamashita, A. Kunstar, A.A. van Apeldoorn, E.M. Bronkhorst, R.P. Félix Lanao, S.C.G. Leeuwenburgh, K. Itatani, F. Yang, P. Salmon, J.G.C. Wolke, J.A. Jansen, Influence of the pore generator on the evolution of the mechanical properties and the porosity and interconnectivity of a calcium phosphate cement, *Acta Biomater.* in press (2011).
- [2] R.P. Félix Lanao, S.C.G. Leeuwenburgh, J.G.C. Wolke, J.A. Jansen, In vitro degradation rate of apatitic calcium phosphate cement with incorporated PLGA microspheres, *Acta Biomater.* 7 (2011) 3459-3468.
- [3] R.P. Félix Lanao, S.C.G. Leeuwenburgh, J.G.C. Wolke, J.A. Jansen, Bone response to fast-degrading, injectable calcium phosphate cements containing PLGA microparticles, *Biomaterials* 32 (2011) 8839-8847.
- [4] C. Combes, C. Rey, Adsorption of proteins and calcium phosphate materials bioactivity, *Biomaterials* 23 (2002) 2817-2823.

SUMMARY, CLOSING REMARKS AND FUTURE PERSPECTIVES



CHAPTER 8

Samenvatting, evaluatie
van de doelstellingen,
slotopmerkingen en
toekomstperspectieven

Samenvatting en evaluatie van de doelstellingen

Calcium fosfaat cement (CPC) is een kansrijk materiaal voor de behandeling van botdefecten op het gebied van tandheelkundige, orthopedische en reconstructieve chirurgie. CPC is veel belovend omdat het veel lijkt op de minerale fase van bot. Het bestaat uit een poeder en een vloeibare fase. Na het mengen van deze twee fases vormt zich een pasta die gemakkelijk in te spuiten is in een botdefect. Naast deze goede injecteerbare eigenschappen van CPC is het materiaal biocompatibel (een negatieve lichaamsreactie blijft uit) en osteoconductief (het materiaal fungeert als een matrix waarover bestaand bot wordt voorgeleid). Nadat het CPC geïnjecteerd is in een botdefect geeft het eerste plaats stabilisatie aan het defect, waarna lichaamseigen botweefsel het botdefect kan herstellen. Echter een nadeel van CPC is de lage degradatiesnelheid (afbraak) van het materiaal. Het degraderen van CPC is noodzakelijk omdat uiteindelijk het botdefect volledig hersteld (dus gevuld) moet worden met nieuw gevormd botweefsel. De degradatie van CPC hangt af van verschillende factoren, zoals de cement eigenschappen (o.a. chemische samenstelling, porositeit, kristalliniteit en de deeltjesgrootte van de calciumfosfaatverbindingen) en de patiënt (bijvoorbeeld een mogelijk aanwezige medische aandoening en de locatie van implantatie). Het is aangetoond dat de degradatie van CPC en daarmee de ingroei van bot sterk verbeterd kan worden door verhoging van de porositeit van het materiaal. Het inmengen van biologisch afbreekbare polymeer micropartikels (zoals gelatine of poly (melkzuur-coglycol)zuur; PLGA) door het CPC poeder leidt tot verhoogde porositeit in het materiaal doordat het PLGA micropartikel degradatieproces eerder optreedt dan de degradatie van het CPC. De biologische werking van CPC kan verder verbeterd worden door toevoeging van biologisch actieve moleculen (zoals groeifactoren) die de botvorming kunnen stimuleren. Factoren die de botvorming induceren worden ook wel osteoinductieve factoren genoemd. Vele variabelen zijn echter onbekend, zoals het type additief, de dosis en de methode waarop de additieven toegevoegd kunnen worden aan het injecteerbare CPC. Al deze variabelen moeten onderzocht worden om een goede botvervanger te ontwikkelen die gebruikt kan worden voor de regeneratie van verschillende type botdefecten.

Het onderzoek in dit proefschrift heeft betrekking op het bestuderen van de doeltreffendheid van CPC in gezonde omstandigheden, het effect van diverse toegevoegde additieven op de CPC prestatie, en het beoordelen van de verschillen tussen de CPC prestaties onder gezonde en osteoporotische omstandigheden.

1. In welke mate kan de biologische werking van CPC/PLGA verbeterd worden door toevoeging van PLGA micropartikels?

Hoofdstuk twee van dit proefschrift verstrekt temporele informatie over de biologische werking (o.a. materiaal degradatie en botvorming) van CPC waaraan verschillende hoeveelheden PLGA micropartikels zijn toegevoegd. In achtenveertig

ratten werd een kritische-grootte craniaal defect gemaakt waarin uitgeharde CPC disks aangevuld met 20 of 30 gewichtsprocent PLGA micropartikels (respectievelijk C20% en C30%) werden geïmplantéerd voor 4, 8 en 12 weken ($n=8$). Histologische analysemethoden toonden aan dat C30% aanzienlijk sneller degradeert dan C20%, maar dat de totale degradatie beperkt is in zowel C20% als C30%. Het percentage nieuw gevormd bot dat het botdefect overbrugde was vergelijkbaar voor C20% en C30% op alle implantatie periodes. Hoewel de botvorming beperkt was voor beide experimentele groepen, vertoonden C30% een significante temporele stijging van de totale botvorming. De resultaten van **hoofdstuk 2** tonen aan dat de materiaaldegradatie verbetert wanneer een grotere hoeveelheid PLGA micropartikels aan CPC wordt toegevoegd, terwijl de botvorming niet wordt beïnvloed. De biologische werking van CPC aangevuld met PLGA micropartikels is onvoldoende om kritische-grootte defecten volledig te regenereren. Hierdoor zijn extra toevoegingen van biologisch actieve factoren vereist om de botregeneratie te kunnen stimuleren.

2. Kan de biologische werking van CPC worden verbeterd door toevoeging van bioactief glas?

De biologische werking van CPC, aangevuld met PLGA micropartikels, is onder gezonde omstandigheden niet toereikend om kritische-grootte botdefecten volledig te regenereren (**hoofdstuk 2**). Verrijking van CPC/PLGA met biologisch actieve factoren is hierdoor noodzakelijk om botgenezing te stimuleren onder kritische omstandigheden, zoals grote botdefecten, slecht gevasculariseerde locaties en (oudere) patiënten met metabole stoornissen. De integratie van bioactief glas (BG) in CPC lijkt een veelbelovende aanpak om de biologische prestatie van CPC te verbeteren. BG's staan bekend om hun unieke vermogen te binden aan levend bot, waardoor er een sjabloon gevormd wordt voor calciumfosfaatprecipitatie die de vorming van nieuw bot stuurt. Daarnaast is bekend dat BG osteoprogenitorcellen aantrekt en stimuleert te differentiëren tot matrix-producerende osteoblasten (botvormende cellen). Hierdoor wordt de botvorming versneld en treedt ingroei van bot in BG gebaseerd materiaal op. Eerdere studies van de afdeling Biomaterialen toonden aan dat BG succesvol kan worden geïntroduceerd in CPC of CPC aangevuld met PLGA micropartikels. Ondanks dat de *in vitro* gegevens over de incorporatie van BG in CPC bemoedigend waren, was het onbekend hoe de *in vivo* respons (o.a. de biocompatibiliteit en botvormingseigenschappen) van dit materiaal was. Daarom werd in **hoofdstuk 3** de *in vivo* respons op toevoeging van BG aan CPC (puur of aangevuld met PLGA micropartikels) geëvalueerd. Uitgeharde CPC disks in vier verschillende formuleringen (1: CPC, 2: CPC/BG, 3: CPC/PLGA, en 4: CPC/PLGA/BG) werden subcutaan en in gecreëerde botdefecten in de laterale condyle van de femur (bovenbeen) van ratten geïmplantéerd voor 2 en 6 weken. Uit de resultaten bleek dat BG de histocompatibiliteit verbeterd in subcutaan geplaatste implantaten, vergeleken met puur CPC. Bovendien was in orthotopisch geplaatst CPC met

toegevoegd BG, de materiaaldegradatie en botvorming verhoogt. De resultaten van **hoofdstuk 3** suggereren dat BG kan worden gebruikt als een additief om de biologische prestaties van CPC te verbeteren, waardoor een betere botregeneratie kan worden verkregen. De huidige, gunstige resultaten moeten bevestigd worden op de langere termijn. Daarnaast moeten deze studies worden uitgevoerd in slecht genezende defecten (zoals in osteoporotische patiënten).

3. Heeft de oplosbaarheid van 'bone morphogenetic protein-2' (BMP-2) invloed op de bioactiviteit, het afgifteprofiel van en de osteoinductieve eigenschappen van CPC?

BMP's spelen een belangrijke rol in de regulatie van de botmorfogenese (o.a. het stimuleren van de differentiatie en mitose van osteoblasten). Lichaameigen BMP's en recombinant equivalenten geproduceerd in zoogdiercellen zijn post-translationeel gemodificeerd door N-gekoppelde glycosylering (gBMP-2). Bacterieel geproduceerde BMPs worden niet geglycolyseerd (ngBMP-2), wat leidt tot een verminderde oplosbaarheid. Dit heeft invloed op de afgifte van ngBMP-2 en daarmee bestaat de mogelijkheid om lagere BMP doses te gebruiken om botvorming te induceren. Het verlagen van de hoeveelheid toegevoegd groeifactor in botvervangende materialen is uit biologische en kosteneffectief oogpunt (d.w.z. potentiële risico's van bijwerkingen, arbeidsintensiviteit en de kostprijs) van groot belang. In **hoofdstuk 4** werd verondersteld dat ngBMP-2 meer ectopische botvorming bij lagere doseringen kan induceren dan gBMP-2. Om dit te evalueren werd eerst *in vitro* de biologische activiteit en afgiftepatroon bestudeerd van gBMP-2 en ngBMP-2 geladen dragermateriaal. Daarna werd een ectopisch implantatie model in ratten gebruikt, waarin gBMP-2 en ngBMP2 werden geladen in verschillende doseringen (2-20 µg/implantaat) op dragermateriaal en subcutaan geïmplanteerd voor 4 en 12 weken. De resultaten toonden aan dat zowel de *in vitro* biologische activiteit als de *in vitro* afgifte van ngBMP-2 lager was dan van gBMP2. Echter, vanaf 4 weken na ectopische implantatie van ngBMP-2 geladen implantaten vormt zich meer bot bij lagere concentraties dan in gBMP-2-equivalenten. Uit de resultaten van **hoofdstuk 4** blijkt dat de biologische activiteit en het afgifteprofiel van BMP-2 wordt beïnvloedt door de oplosbaarheid van het eiwit. Dit resulteerde in verbeterde osteoinductieve eigenschappen van botvervangend materiaal geladen met ngBMP-2. Tezamen suggereert dit dat ngBMP-2 een krachtig alternatief is voor in zoogdieren geproduceerd recombinant BMP-2 voor bot regeneratieve therapieën.

4. Heeft de wijze waarop BMP-2 toegevoegd wordt aan het CPC invloed op het BMP-2 afgifteprofiel en de osteoinductieve eigenschappen van CPC?

De klinische toepassing van CPC (met ingebouwde PLGA micropartikels) is in een injecteerbare vorm. Dit impliceert dat de methodes om groeifactoren toe te voegen aan CPC beperkt zijn. Het onderzoek in **hoofdstuk 5** richtte zich op het bestuderen van verschillende ladingsmethoden voor BMP-2 en de gevolgen van deze methode op de *in vitro* en *in vivo* BMP-2 afgifte. Via een *in vitro* BMP-2 afgifte experiment en *in vivo* m.b.v. microSPECT (een 3-dimensionale diagnostische beeldvormingstechniek waarbij gebruik wordt gemaakt van radioactief gelabelde stoffen, in dit geval radioactief gelabeld BMP-2) werd het afgiftepatroon van verschillende BMP-2 geladen CPC geanalyseerd. Vervolgens werd de osteoinductieve capaciteit van de verschillende implantaten geanalyseerd m.b.v. een subcutaan implantatie rat model. De verschillende ladingsmethoden bestonden uit BMP-2 adsorptie aan PLGA micropartikels waarna toegevoegd aan CPC (CPC/PLGA), en BMP-2 toegevoegd aan de vloeibare fase van CPC/PLGA (CPC/vloeistof). Uitgeharde poreuze CPC waaraan BMP-2 is toegevoegd d.m.v. adsorptie aan het oppervlak (CPC/oppervlak) diende als controle. Extra controles bestonden uit uitgeharde poreuze CPC implantaten (CPC/poreus) en CPC/PLGA (CPC/controle) zonder BMP-2. Uit de resultaten van **hoofdstuk 5** bleek dat BMP-2 lading mogelijk was via adsorptie aan PLGA micropartikels en via de vloeibare fase van CPC, waarbij hetzelfde afgifteprofiel waargenomen werd gedurende 28 dagen, ondanks een duidelijk verschil in de eiwitspreiding van het geladen BMP-2 in de twee groepen. De BMP-2 afgifte na 1 dag (de initiële afgifte) was voor zowel CPC/PLGA als CPC/vloeistof lager dan voor CPC/oppervlak, terwijl het afgifte patroon van dag 2-28 vergelijkbaar was tussen alle groepen. Hierdoor is het mogelijk dat het alleen in CPC/oppervlak geobserveerd osteoinductief vermogen ontstaan is door een verschil in de initiële afgifte. Het blijft echter onduidelijk of de verschillende BMP-2 ladingsmethoden voor een injecteerbaar CPC een effect hebben op de biologische prestatie in een botomgeving.

5. Wat zijn de verschillen in de biologische prestatie van CPC tussen osteoporose en gezonde ratten?

In de vorige hoofdstukken van dit proefschrift werd de biologische prestatie van de CPC (met of zonder additieven) onderzocht bij gezonde dieren. Als zodanig leveren de resultaten van deze studies geen informatie op over de biologische prestatie van de CPC onder kritische omstandigheden, zoals bij osteoporose patiënten. Hierdoor is in **hoofdstuk 6** de biologische prestatie van injecteerbaar CPC/PLGA in osteoporotische ratten (ovx) onderzocht en vergeleken met de prestatie in gezonde (sham) ratten. In de verschillende type ratten werd CPC/PLGA geïnjecteerd in botdefecten gecreëerd in de laterale condyle van de femur van ratten. De implantatie periodes waren 4 en 12 weken. De hypothese van de studie

was dat door een hogere activiteit van de osteoclasten (botafbrekende cellen) aanwezig in osteoporotische dieren, de degradatie van CPC/PLGA in ovx ratten versneld zal zijn en hierdoor de ontstane ruimte versneld zou worden opgevuld met nieuw bot. Uit de resultaten bleek dat op beide implantatieperiodes de botvorming trager was in vergelijking met gezonde dieren, ondanks een versnelde afbraak van CPC/PLGA in osteoporotische dieren. Bovendien was na vier weken de hoeveelheid gevormd bot onder osteoporotische omstandigheden in het gecreëerde botdefect minder dan in een intacte osteoporotische knie, maar was dit na 12 weken gelijk. Anderzijds, onder gezonde omstandigheden is de hoeveelheid nieuw gevormd bot na vier weken in het gecreëerde botdefect gelijk aan de hoeveelheid in een intacte gezonde knie en hoger na 12 weken. De resultaten van **hoofdstuk 6** geven aan dat de regeneratie van bot in een botdefect onder osteoporotische condities trager is, maar dat na verloop van tijd botregeneratie plaatsvindt tot de oorspronkelijke aanwezige hoeveelheid bot. Dit suggereert dat onder osteoporotische omstandigheden extra toevoegingen, of aanpassingen aan het botvervangend materiaal nodig zijn om tot een goede botregeneratieve behandeling te komen.

Slotopmerkingen en toekomstperspectieven

In onze zoektocht om de biologische werking van CPC te optimaliseren, hebben we aan het CPC PLGA micropartikels toegevoegd om een verhoogd poreus materiaal te creëren dat de materiaaldegradatie, en dus de ingroei van (bot)weefsel, verbetert. Om de degradatie van het CPC/PLGA te voorspellen en daarmee het vermogen om bot te regenereren, beschouwden we de totale porositeit van het materiaal als belangrijke parameter. De totale porositeit bestaat uit de intrinsieke porositeit van CPC en de toegevoegde porositeit na PLGA micropartikel degradatie. Hoewel de hoeveelheid (van 20 tot 30 gewichtsprocent) en de grootte van de PLGA micropartikels (van 20 tot 60 μm) varieerden tussen de verschillende hoofdstukken van dit proefschrift, was de totale porositeit vergelijkbaar, ongeveer 70%. Dit betekent dat de aangebrachte wijzigingen ten aanzien van de hoeveelheid en de grootte van PLGA micropartikels slechts beperkte verschillen in uiteindelijke porositeit van het CPC opleverden. Ondanks de *in vivo* experimenten met verschillende hoeveelheden PLGA toegevoegd aan CPC (**hoofdstuk 2**) is er tot op heden geen direct bewijs dat de grootte van de PLGA micropartikels invloed heeft op biologische werking van CPC. Derhalve vereist dit verder onderzoek. Ondanks soortgelijke porositeitswaarden varieert de mate van CPC degradatie en de daarop volgende botvormende capaciteit in de studies die beschreven staan in dit proefschrift. Dit verschil is waarschijnlijk veroorzaakt door verschillen in de proefopzet (bijvoorbeeld een verschil in implantaat locatie). Daarnaast blijkt uit de resultaten van dit proefschrift dat het netwerk van de poriën (de interconnectiviteit) in het materiaal ook van belang is. De meest gunstige interconnectiviteit is nog niet bekend, al komt uit de resultaten van **hoofdstuk 4** naar voren dat een interconnectiviteit van ongeveer 20% niet voldoende is.

Voor klinische toepassingen is reproduceerbaarheid en standaardisering van het materiaal van cruciaal belang. Veel factoren zoals de aard en hoeveelheid van de PLGA micropartikels en de verschillende componenten van het CPC poeder kunnen worden gereguleerd. Echter, meer onderzoek is vereist om het productieproces van PLGA micropartikels te standaardiseren, zodat de grootte van de partikels reproduceerbaar is. Om een reproduceerbare interconnectiviteit te verkrijgen, kunnen verschillende gestandaardiseerde PLGA micropartikels gecombineerd worden, zoals eerder beschreven [1]. Hierdoor moet toekomstig onderzoek zich richten op de relatie tussen de grootte en hoeveelheid van de PLGA micropartikels enerzijds, en de ontstane interconnectiviteit en biologische prestatie van het CPC *in vivo* anderzijds. Bovendien is het noodzakelijk om dit te onderzoeken op verschillende plaatsen *in vivo*, met verschillende afmetingen van botdefecten en onder gezonde en zieke omstandigheden.

Uit parallel onderzoek van de afdeling Biomaterialen van het UMC St. Radboud bleek dat de morfologie van de PLGA micropartikels (hol of massief) een sterker effect heeft op de materiaaldegradatie dan het moleculegewicht en de chemische eindgroep modificatie van de partikels [2]. Daarom zijn de experimenten in dit proefschrift die na deze constatering zijn gestart, uitgevoerd met deze massieve PLGA micropartikels. De doelstellingen van deze studies zijn gebaseerd op de evaluatie van de biologische werking van CPC met massieve PLGA micropartikels, aangevuld met ofwel de osteopromotieve factor BG (**hoofdstuk 3**) ofwel de osteoinductieve groeifactor BMP-2 (**hoofdstuk 5**). Recentelijk is een 'proof-of-principle' verkregen met CPC, waaraan massieve PLGA micropartikels zijn toegevoegd [3]. Echter is het noodzakelijk om de biologische prestatie van dit materiaal te bestuderen, waarbij CPC met (verschillende groottes en hoeveelheden) massieve PLGA micropartikels op verschillende locaties en onder verschillende medische condities wordt geïmplant.

Ondanks optimalisatiemethodes waarbij verschillende combinaties van CPC en holle PLGA micropartikels werden gebruikt, bleek de biologische prestatie van dit CPC ontoereikend om kritische-grootte defecten te regenereren (**hoofdstuk 2**). Hierdoor richtte het onderzoek in dit proefschrift zich tevens op het versterken van CPC door het toevoegen van additieven met een biologische activiteit t.a.v. botvorming. Mogelijke kandidaten waren BG (**hoofdstuk 3**) en BMP-2 (**hoofdstuk 4 en 5**). De methode waarop de additieven werden toegevoegd varieerde, waarbij BG werd gemengd in de keramische matrix (CPC poeder), terwijl BMP-2 ofwel geadsorbeerd werd aan de PLGA micropartikels, of wel werd toegevoegd aan de vloeibare fase van CPC. In dit proefschrift is aangetoond dat de biologische prestaties na 6 weken inderdaad verbeterden wanneer BG werd toegevoegd aan CPC of CPC/PLGA. Vervolgstudies met deze materialen zijn noodzakelijk om meer informatie te krijgen over de botformatie en afbraak op de langere termijn. Daarnaast is in dit proefschrift aangetoond dat BMP-2 toe te voegen is aan injecteerbaar CPC d.m.v. adsorptie aan de PLGA micropartikels of via toevoeging van BMP-2 aan de vloeibare fase van het injecteerbaar CPC. Echter zijn de osteoinductieve eigenschappen van beide materialen ontoereikend om op

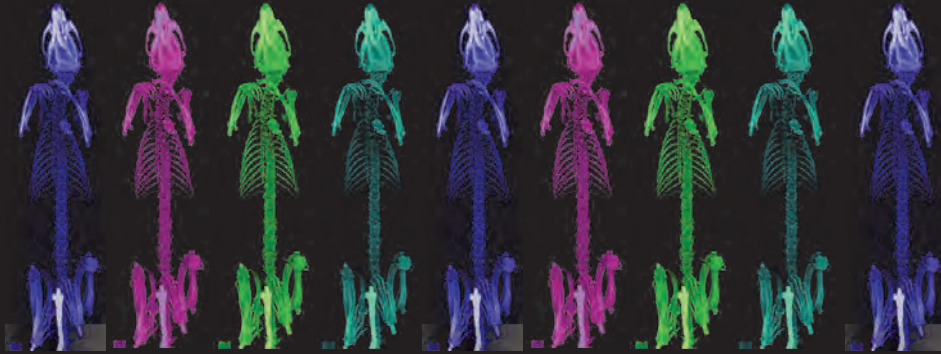
ectopische locaties in ratten botformatie te stimuleren. Het ontbreken van een osteoinductief effect in deze materialen komt waarschijnlijk door de beperkte initiële BMP-2 afgifte. Dit illustreert hoe complex de afgiftekinetiek van groeifactoren is. De afgiftekinetiek van groeifactoren wordt waarschijnlijk sterk beïnvloed door vele variabelen zoals eerder beschreven [4]. Tot op heden blijft het onduidelijk in hoeverre de BMP-2 ladingsmethode invloed heeft op de biologische prestatie van CPC in een botomgeving. Ondanks de onduidelijkheden ten aanzien van het effect van BG op de langere termijn en het effect van BMP-2 ladingmethodes in een botomgeving, is de integratie van de additieven BG en BMP-2 in CPC veelbelovend. Daarom kan mogelijk zowel BG als BMP-2 gebruikt worden als belangrijke component in de ontwikkeling van goed botsubstitutie materiaal.

De meerderheid van de patiënten die regeneratie van (grote) botdefecten met botvervangend materiaal nodig hebben, hebben een suboptimale medische toestand en dus een suboptimaal botmetabolisme. Osteoporose patiënten vertegenwoordigen een groep patiënten met een zogenaamd 'worst-case' scenario, waarbij het botmetabolisme zodanig slecht is dat er een duidelijk effect zichtbaar is ten aanzien van de botkwaliteit. Hierdoor is het noodzakelijk om een efficiënt CPC te ontwikkelen die de botdefecten in deze groep patiënten goed kan herstellen. De verschillen in botmorfologie en metabolisme tussen zieke en gezonde individuen duidt op een verschillende biologische prestatie van CPC. In dit proefschrift is voor het eerst de biologische prestatie van CPC/PLGA onder osteoporotische omstandigheden gerapporteerd (**hoofdstuk 6**). Hieruit bleek dat om een goede botregeneratie onder osteoporotische omstandigheden te verkrijgen extra toevoegingen aan het bestaande CPC/PLGA noodzakelijk zijn. De onderzochte additieven, BG en BMP-2, in dit proefschrift zijn goede kandidaten om de biologische prestatie van CPC/PLGA onder osteoporotische omstandigheden te verbeteren. Hierdoor is het noodzakelijk dat vervolgonderzoek zich richt op mogelijkheid van deze en eventueel andere additieven om de biologische prestatie van CPC in osteoporotische patiënten te verbeteren.

Vanuit een biologisch en kosteneffectief oogpunt (d.w.z. potentiële risico's van bijwerkingen, arbeidsintensiviteit en de kostprijs) zou het gebruik van biologisch actieve moleculen beperkt moeten worden. Het is noodzakelijk een compromis te vinden tussen de kostprijs van CPC en de biologische activiteit van het materiaal. Bij voorkeur moeten artsen de mogelijkheid hebben om de meest geschikte CPC te selecteren voor elke specifieke klinische toepassing. Voor het bereiken van een dergelijke aanpak is de uitdaging om de juiste combinatie van (i) gestandaardiseerde keramische cement matrix, (ii) de specifieke aard van toegevoegde poriën, en (iii) additieven te identificeren, afhankelijk van de patiëntspecifieke omstandigheden (zoals defectgrootte, locatie, leeftijd en medische conditie). Een laatste voorwaarde is dat het opmaat gemaakt injecteerbare CPC beschikbaar is in een eenvoudig, duidelijk en controleerbaar applicatiesysteem dat de toepassing van CPC met optimale verwerkingseigenschappen (o.a. goede viscositeit en uitharding van het materiaal) mogelijk maakt.

References

- [1] M.A. Lopez-Heredia, K. Sariibrahimoglu, W. Yang, M. Bohner, D. Yamashita, A. Kunstar, A.A. van Apeldoorn, E.M. Bronkhorst, R.P. Félix Lanao, S.C.G. Leeuwenburgh, K. Itatani, F. Yang, P. Salmon, J.G.C. Wolke, J.A. Jansen, Influence of the pore generator on the evolution of the mechanical properties and the porosity and interconnectivity of a calcium phosphate cement, *Acta Biomater.* in press (2011).
- [2] R.P. Félix Lanao, S.C.G. Leeuwenburgh, J.G.C. Wolke, J.A. Jansen, In vitro degradation rate of apatitic calcium phosphate cement with incorporated PLGA microspheres, *Acta Biomater.* 7 (2011) 3459-3468.
- [3] R.P. Félix Lanao, S.C.G. Leeuwenburgh, J.G.C. Wolke, J.A. Jansen, Bone response to fast-degrading, injectable calcium phosphate cements containing PLGA microparticles, *Biomaterials* 32 (2011) 8839-8847.
- [4] C. Combes, C. Rey, Adsorption of proteins and calcium phosphate materials bioactivity, *Biomaterials* 23 (2002) 2817-2823.



CHAPTER 9

Acknowledgements
(Dankwoord),
Curriculum Vitae and
list of publications

Acknowledgments (Dankwoord)

Dit is hem dan, mijn boekje. Na 4 jaar van onderzoek en vervolgens opschrijven is het af. Wat ben ik hier blij mee! Het waren jaren van hard werken, soms iets minder hard, soms frustraties maar vooral van veel plezier. Dit is mede mogelijk gemaakt door de velen collega's, co-auteurs, familie en vrienden. Ieder die op wat voor wijze mij hebben geholpen met mijn boekje ben ik zeer dankbaar. Enkele van hen wil ik persoonlijk bedanken.

Prof. dr. Jansen, Beste John, bedankt dat ik op jouw afdeling mijn promotie onderzoek kon uitvoeren. De wijze waarop jij je afdeling strak organiseert heb ik als zeer prettig ervaren. Tevens is jouw kennis en ervaring in de wetenschap een grote bron van inspiratie geweest.

Dr. van den Beucken, Beste Jeroen, tijdens mijn 4 jaar heb ik erg veel van je geleerd en onze samenwerking heeft uiteindelijk mooie dingen opgeleverd en wel binnen 4 jaar. Bedankt hiervoor! Tevens zal ik jouw oorverdovende lach niet snel vergeten.

My sweet paranimf Mati, you and me together is equal to fun! I am very pleased that you are more than just a colleague, you are a true friend. Thank you for listening to me, for all the fun and for the 'just one more beer' evenings. My other sweet paranimf Rosa, from the first day I started at the department you were my neighbor, my adviser, my help and my friend. Thank you for answering all of my scientific questions, for giving me advise and for all the nonsense we did together. And girls, never forget that blond girls rule the world!

To all my (former) colleagues and students of the department of Biomaterials thank you, Gracias, Grazie, 谢谢, Благодарам, Teşekkürler, Obrigado, շնորհակալություն, مرسي, Danke, for all your help and advice, IT WAS GREAT, BEDANKT! My time at the Biomaterials department was great due to all of you! I had fun at the lab but also during all of our drinks, (PhD defense) parties, Sinterklaas games, and at the lunch or coffee breaks due to our nice, funny and 'gezellige' conversations! Speciale dank voor de analisten, de superhero's, van de afdeling, Natasja, Martijn, Monique en Vincent, en onze lieve secretaresses Kim en Vera zonder jullie hulp en advies is een PhD student stuurloos!

Iedereen van het CDL bedankt! Met speciale dank aan Daphne en Debby van de SPF en Bianca, Kitty en Henk van de Prime!

Prof. Boerman, Beste Otto, tijdens mijn laatste jaar was ik vaker bij jullie te vinden dan op mijn eigen afdeling, dank voor deze mogelijkheid! Iedereen van jouw afdeling wil ik graag bedanken voor hun inzet tijdens mijn studies maar speciale dank gaat uit naar Janneke Molkenboer-Kuenen en Peter Laverman. Ik ben enorm blij dat ik bij en met jullie mijn academische carrière kan voortzetten.

ACKNOWLEDGMENTS, CV AND LIST OF PUBLICATIONS

Buiten alle mensen van het lab wil ik graag andere mensen in mijn omgeving bedanken, die op wat voor wijze mijn leven tijdens het promoveren makkelijker en vooral leuker hebben gemaakt: al mijn oud (HLO)studiegenoten, Pien (voor al je gezelligheid!), Dorien (het voelt alsof we elkaar al jaren kennen!), mijn lieve burens, Corrie & Lise (voor de leuke tijd bij Biomaterialen en ver daarbuiten), Manu, Rania & Ruggero (as you all became more than just colleagues) en Noemietje & Guille (never forget what I told you on your wedding day. It's the absolute truth!)

Alle (oud) dames van QZ D4, bedankt voor jullie sportieve invloed. Mijn laatste jaar van promoveren had geen beter jaar kunnen zijn, met jullie voor het eerst kampioen worden was fantastisch!

Alle Chimaeren en Nimearen van DRG Chimaera, bedankt voor jullie belangstelling maar vooral voor de afleiding in de vorm van activiteiten en ja inclusief het bier drinken! Chimaera Hoog, Chimaera Laag, Chimaera nooit helemaal leeg...

Beste leeeje van Peekunieja, Dagge bedankt zijt da witte. Agge Mar Leut Et!

Lieve Danielle, Francisca en Irene, mijn tijd in Nijmegen is met jullie begonnen in 2004. Van roeien was geen sprake maar van bier drinken en vooral een hechte vriendschap des te meer! Het is en blijft voor altijd HeH! (4 bier).

Lieve Heleen en Marieke, jullie namen zijn onherroepelijk aan elkaar en mij verbonden. Het is fijn te weten dat waar ik ook ben en wat ik ook doe jullie er zijn.

Ik ben zo blij en trots dat jullie mij vriendinnetjes zijn!

Familie Abbink, Lieve Bas, Bep, Esther en Gerrit bedankt voor alle relaxte weekendjes. Het is prettig om een tweede familie te hebben waar je je thuis voelt.

Oma Martens, Lieve Oma, u bent echt de allerliefste oma van de hele wereld! Als ik ook maar iets van uw geheugen had geërfd was ik een genie geworden.

Mijn broer, Lieve Daan, bedankt voor het zijn van een echte grote broer; eentje die af en toe pest, waarmee je een gezellig avond kunt hebben maar waar je ook naar toe kan voor advies. Iedereen zou een broer moeten hebben zoals jij! Ohja en na jaren van 'proefjes doen' is het met gelukt, een hogere academische titel...

Mijn ouders, Lieve papa en mama, mijn doktors titel is het bewijs van jullie steun, stimulatie en vertrouwen in mijn kunnen. Misschien wisten jullie niet precies wat ik aan het doen was, maar jullie waren (en zijn) er altijd voor mij. Het is enorm fijn om te weten dat je altijd en overal een thuis hebt!

Als laatste Wout, natuurlijk sta jij ook bij mij op deze plaats... Lieve Woutje, vaak denk ik dat ik het wel alleen kan als zelfstandige vrouw maar met jouw arm om mij heen is alles zoveel leuker, fijner en vooral mooier. Ik ben zo ontzettend gelukkig door jouw liefde en steun aan mij maar vooral ook omdat we enorm met en om elkaar kunnen lachen. Je haalt oprecht het beste in me naar boven. Ik vind je lief! X

Curriculum vitae

Floor van de Watering was born on 13 oktober 1983 in Bergen op Zoom, The Netherlands. In 1995, she attended the Mollerlyceum (HAVO) in Bergen op Zoom and graduated in 2000. A bachelor degree in Applied Science was obtained in 2004 at the Avans Hogeschool in Breda, The Netherlands. During her study she obtained a Leonardo da Vinci scholarship to conduct a research internship at University of Manchester, UK. In addition, she performed a research internship at the department of Pharmacology, MSD (before Organon NV), The Netherlands. In September 2004, she started the Master Medical Biology at the Radboud University Nijmegen, the Netherlands and graduated in April 2008. During her study she conducted research internships at the department of Cellular Animal Physiology, Radboud University Nijmegen and with the Erasmus program at the department of Cellular Biology, Physiology and Immunology, University of Cordoba, Spain. In May 2008, she started working at the Department of Biomaterials, Radboud University Nijmegen Medical Centre, the Netherlands on the PhD project 'Novel instructive scaffolds for the regeneration of bone tissue' of the TeRM Smart Mix program of the Netherlands Ministry of Economic Affairs and the Netherlands Ministry of Education, Culture and Science. The results of this study are described in this thesis, as separate publications in scientific journals and are presented at (inter)national scientific conferences. From August 2012, she is working as a postdoc at the Department of Nuclear Medicine, Radboud University Nijmegen Medical Centre, the Netherlands on the Roche Innovation Fund 'The quantitative optimization of a flexible pretargeting system for efficient targeting of tumors'.

Awards

- Jan Feijen Poster Price for best poster presentation, 12th European symposium on controlled drug delivery, April 2012, Egmond aan Zee, The Netherlands.
- Third prize for best oral presentation, NBTE annual meeting 2011, December 2011, Lunteren, The Netherlands.

List of publications

FCJ van de Watering, JDM Molkenboer-Kuenen, OC Boerman, JJJP van den Beucken, and JA Jansen, Differential loading methods for BMP-2 within injectable calcium phosphate cement, J. Control. Release, DOI: 10.1016/j.jconrel.2012.07.007

FCJ van de Watering, JJJP van den Beucken, RP Felix Lanao, JGC Wolke, JA Jansen, Biodegradation of calcium phosphate cement composites In: N. Eliaz (Ed), Degradation of Implant Materials, Springer Science + Business Media, New York, 2012 DOI:10.1007/978-1-4614-3942-4_7

FCJ van de Watering, JJJP van den Beucken, SP van der Woning, A Briest, A Eek, H Qureshi, L Winnubst, OC Boerman, JA Jansen, Non-glycosylated BMP-2 can induce ectopic bone formation at lower concentrations compared to glycosylated BMP-2, J. Control. Release 159 (2012) 69-77.

FCJ van de Watering, JJJP van den Beucken, XF Walboomers, JA Jansen, Calcium phosphate/poly(d,l-lactic-co-glycolic acid) composite bone substitute materials: evaluation of temporal degradation and bone ingrowth in a rat critical-sized cranial defect. Clin Oral Implants Res 23 (2012) 151-9.

